Institute for Circuit Theory and Signal Processing
Technische Universität München

Signal Parameter Estimation with 1-bit ADC
Performance Bounds, Methods and System Design

Manuel S. Stein

Vollständiger Abdruck der von der Fakultät für Elektrotechnik und Informationstechnik der Technischen Universität München zur Erlangung des akademischen Grades eines

Doktor-Ingenieurs

genehmigten Dissertation.

Vorsitzender: Prof. Dr. Christoph-Georg Günther
Prüfer der Dissertation:
1. Prof. Dr. Dr. h. c. Josef A. Nossek
2. Prof. Kurt Barbé, Ph.D.
   Vrije Universiteit Brussel

Die Dissertation wurde am 21.04.2016 bei der Technischen Universität München eingereicht und durch die Fakultät für Elektrotechnik und Informationstechnik am 14.07.2016 angenommen.

To Üle, for all your love, laughter and inspiration.

Para Memo, por tu gran confianza.

–MANUEL SIMÓN
(SPRING 2016)

Contents

Nomenclature

Matrices and Vectors

$\boldsymbol{a}$	column vector
$a_i, [\boldsymbol{a}]_i$	i-th element of column vector $\boldsymbol{a}$
$\boldsymbol{A}$	matrix
$a_{ij}, [\boldsymbol{A}]_{ij}$	i-th column, j-th row element of matrix $\boldsymbol{A}$
$\boldsymbol{A}^{\mathrm{T}}$	transpose of matrix $\boldsymbol{A}$
$\mathrm{Tr}\,(\boldsymbol{A})$	trace of a matrix $\boldsymbol{A}$
$\mathrm{diag}\,(\boldsymbol{A})$	diagonal matrix containing the diagonal entries of $\boldsymbol{A}$
$\mathbf{0}_M$	M-dimensional column vector with all entries equal to zero
$\boldsymbol{O}_M$	$M \times M$-dimensional zero matrix
$\mathbf{1}_M$	M-dimensional column vector with all entries equal to one
$\boldsymbol{I}_M$	$M \times M$-dimensional identity matrix
$\frac{\partial \boldsymbol{f}(\boldsymbol{a})}{\partial \boldsymbol{a}}$	derivative of $\boldsymbol{f}(\boldsymbol{a})$ with respect to $\boldsymbol{a}$, i.e., $\left[\frac{\partial \boldsymbol{f}(\boldsymbol{a})}{\partial \boldsymbol{a}}\right]_{ij} = \frac{\partial [\boldsymbol{f}(\boldsymbol{a})]_i}{\partial [\boldsymbol{a}]_j}$

Probability and Stochastics

$\boldsymbol{x}$	random variable
$\boldsymbol{\mathcal{X}}$	support of the random variable $\boldsymbol{x}$
$\boldsymbol{\theta}$	system parameter
$\boldsymbol{\Theta}$	parameter space of $\boldsymbol{\theta}$
$\hat{\boldsymbol{\theta}}(\boldsymbol{x})$	estimator of $\boldsymbol{\theta}$ based on the data $\boldsymbol{x}$
$p(\boldsymbol{x})$	probability density or mass function
$p(\boldsymbol{x}; \boldsymbol{\theta})$	parameterized probability density or mass function, likelihood function
$\tilde{p}(\boldsymbol{x}; \boldsymbol{\theta})$	likelihood function of a replacement model
$p(\boldsymbol{x} \mid \boldsymbol{\theta})$	conditional probability density or mass function
$p(\boldsymbol{x}, \boldsymbol{\theta})$	joint probability density or mass function
$\mathrm{E}_{\boldsymbol{x}}\,[\cdot]$	expectation taken with respect to $p(\boldsymbol{x})$
$\mathrm{E}_{\boldsymbol{x};\boldsymbol{\theta}}\,[\cdot]$	expectation taken with respect to $p(\boldsymbol{x}; \boldsymbol{\theta})$
$\mathrm{E}_{\tilde{\boldsymbol{x}};\boldsymbol{\theta}}\,[\cdot]$	expectation taken with respect to the replacement model $\tilde{p}(\boldsymbol{x}; \boldsymbol{\theta})$
$\mathrm{E}_{\boldsymbol{x}\mid\boldsymbol{\theta}}\,[\cdot]$	conditional expectation taken with respect to $p(\boldsymbol{x} \mid \boldsymbol{\theta})$
$\mathrm{E}_{\boldsymbol{x},\boldsymbol{\theta}}\,[\cdot]$	expectation taken with respect to $p(\boldsymbol{x}, \boldsymbol{\theta})$
$\bar{\boldsymbol{x}}$	sample-mean of $\boldsymbol{x}$
$\boldsymbol{R}_{\boldsymbol{x}}$	covariance matrix of the random variable $\boldsymbol{x}$
$\boldsymbol{F}_{\boldsymbol{x}}(\boldsymbol{\theta})$	Fisher information calculated with respect to $p(\boldsymbol{x}; \boldsymbol{\theta})$
$\tilde{\boldsymbol{F}}_{\boldsymbol{x}}(\boldsymbol{\theta})$	Fisher information calculated with respect to the replacement $\tilde{p}(\boldsymbol{x}; \boldsymbol{\theta})$

$\boldsymbol{J}_{\boldsymbol{x}}$	Bayesian information matrix
$\boldsymbol{U}_{\boldsymbol{x}}$	recursive Bayesian information matrix
$\mathcal{N}(\boldsymbol{\mu}, \boldsymbol{R})$	Gaussian distribution with mean $\boldsymbol{\mu}$ and covariance $\boldsymbol{R}$
$\tilde{\mu}_l$	l-th raw moment
μ_l	l-th central moment
$\bar{\mu}_l$	l-th normalized central moment
$w_l(\boldsymbol{\theta})$	l-th natural parameter (exponential family)
$t_l(\boldsymbol{z})$	l-th sufficient statistic (exponential family)
$\lambda(\boldsymbol{\theta})$	log-normalizer (exponential family)
$\kappa(\boldsymbol{z})$	carrier-measure (exponential family)
$\phi_l(\boldsymbol{z})$	l-th auxiliary statistic

Signals

$\breve{x}(t)$	analog signal
$x(t)$	band-limited analog signal
$\boldsymbol{y}$	digital system output (linear system)
$\boldsymbol{y}_n$	n-th digital system output sample (linear system)
$\boldsymbol{z}$	digital system output (nonlinear system)
$\boldsymbol{z}_n$	n-th digital system output sample (nonlinear system)
$\boldsymbol{s}(\boldsymbol{\theta})$	deterministic pilot-signal modulated by the parameter $\boldsymbol{\theta}$
$\boldsymbol{\eta}$	measurement noise
$\boldsymbol{c}$	chip sequence vector
w	process noise (state-space model)
υ	quantization offset (hard-limiter)

Variables

α	evolution parameter (state-space model)
a_n^k	particle weight (particle filter, k-th particle, n-th time instance)
χ	quantization loss
f_c	chip frequency
γ	receive signal strength
κ	oversampling / band-limitation factor
κ_l	model parameter (soft-limiter model)
κ_w	shape parameter (Weibull distribution)
κ_s	smoothness factor (Rapp model)
κ_r	location parameter (Rician model)
λ	steady-state quality
λ_{conv}	rate of convergence
λ_{const}	constant (convergence analysis)
ω_c	carrier frequency
ψ	phase offset (wireless channel)
ρ	power allocation (I/Q transmit signals)
τ	time-delay parameter
φ	phase offset (demodulator)
ζ	direction-of-arrival (DOA)

Numbers and Quantities

A	number of antennas
B	bandwidth
B_r	receive bandwidth
B_t	transmit bandwidth
C	carrier power
D	dimensionality of the system parameter $\boldsymbol{\theta}$
K	number of particles (particle filter)
K_{thresh}	resampling threshold (particle filter)
L	number of natural parameters / sufficient statistics
M	dimensionality of the system output, number of samples (spatial)
N	number of samples (temporal)
N_0	noise power spectral density
N_Δ	relative delay
N_λ	number of samples during the transient phase (tracking)
N_c	number of chips of a periodic BPSK signal
T_c	chip duration
T_o	observation time (duration of one observation block)

Operations

$\int_{\boldsymbol{\mathcal{X}}} \boldsymbol{f}(\boldsymbol{x})\mathrm{d}\boldsymbol{x}$	integral of $\boldsymbol{f}(\boldsymbol{x})$ over the alphabet $\boldsymbol{\mathcal{X}}$, i.e., $\int_{\mathcal{X}_1}\int_{\mathcal{X}_2}\ldots\int_{\mathcal{X}_N}\boldsymbol{f}(x_1,x_2,\ldots,x_N)\mathrm{d}x_1\mathrm{d}x_2\ldots\mathrm{d}x_N$
$\arg\max_{x\in\mathcal{X}} f(x)$	maximizer of $f(x)$
$\sum_{n=1}^{N} x_n$	sum of the elements $x_1, x_2, \ldots, x_N$
$f(x)\vert_{x=x_0}$	value of the function $f(x)$ at $x = x_0$
$\ln x$	natural logarithm (basis e)
$\log x$	logarithm (basis 10)
$\lim_{x\to a} f(x)$	value of $f(x)$ in the limit $x \to a$

Symbols

$>$	strictly greater
$\geq$	equal or greater
$\succeq$	equal or greater (matrix sense)
$=$	equal
$\triangleq$	by definition equal to
$\overset{a}{=}$	asymptotically equal
$\sim$	distributed according to the probability law
$\overset{a}{\sim}$	asymptotically distributed according to the probability law
$\overset{a}{\to}$	asymptotically converges to

Acronyms

A/D	analog-to-digital
ADC	analog-to-digital converter
AWGN	additive white Gaussian noise
BCRLB	Bayesian Cramér-Rao lower bound
BFIM	Bayesian Fisher information matrix

BPSK	binary phase-shift keying
CDF	cumulative density function
CME	conditional mean estimator
CMLE	conservative maximum-likelihood estimator
CRLB	Cramér-Rao lower bound
D/A	digital-to-analog
DAC	digital-to-analog converter
DOA	direction-of-arrival
ECRLB	expected Cramér-Rao lower bound
EFIM	expected Fisher information matrix
FIM	Fisher information matrix
GNSS	Global Navigation Satellite System
IC	integrated circuit
MAP	maximum a posterior estimator
MLE	maximum-likelihood estimator
MPF	multi-path free receive scenario
MSE	mean squared error
PCRLB	pessimistic approximation of the Cramér-Rao lower bound
PDF	probability density function
RMSE	root mean squared error
SNR	signal-to-noise ratio
ULA	uniform linear array
UWB	ultra wide-band

1. Introduction

In the last three decades wireless systems have become an accelerator for the evolution of the digital age. Today wireless communication systems provide instant access to the internet with small portable devices. Consumer-radar systems enable reliable sensing approaches for innovative applications like autonomous vehicles or smart houses. Satellite-based radio systems make wireless data transmission possible worldwide, play a crucial role for navigation in the aviation sector and allow distributed synchronization of critical infrastructure at the accuracy of atomic clocks. These examples show which impact wireless technology has onto human life today. Taking into account its importance for society and the associated security issues, it is clear that a thorough understanding of the performance limits of these pervasive systems is highly relevant.

The concept of wireless technology can be divided into four parts. Signal generation, transmission, sensing and processing. In the first step digital information is converted into an adjusted analog waveform which is then radiated by one or more transmit antennas. The electro-magnetic radio-wave propagates over the wireless medium, is sensed by the receive antennas and after analog pre-processing transformed into a digital representation. The final step, aiming at the extraction of the desired information from the noisy receive data, takes place in the digital domain where fast processing with smart algorithms can be performed.

The favorable design of such wireless systems is determined by various conflicting objectives. On the one hand, a system architecture which allows to obtain high operational performance and fast processing rates is desired. On the other hand, the wireless transmitter and receiver should exhibit low power consumption, moderate production cost, and small circuit size. Especially, the transition from the digital to the analog domain at the transmitter and the transition from the analog measurement domain to the digital processing domain at the receiver form a bottleneck with respect to the objective of obtaining a fast low-complexity wireless system [1].

Therefore, with respect to the latter notion this thesis focuses on the transformation of the continuous waveforms, acquired at the receive sensors (analog signal domain), into a representation which is discrete in time and amplitude (digital signal domain). In particular its effect on the signal parameter estimation performance of the receiver is analyzed. While an analog-to-digital (A/D) conversion with high amplitude resolution allows to perform sophisticated digital processing on dedicated hardware or with a general-purpose computer chip and to obtain high accuracy, the complexity of the analog-to-digital converter (ADC) grows exponentially $\mathcal{O}(2^b)$ with the number of bits b. Thus, while the majority of the signal processing literature focuses on digital data models with high amplitude resolution, from a hardware-aware perspective a promising system design option is to switch to data acquisition with coarse A/D resolution.

A radical approach is to use a single comparator which forwards only the sign of the analog receive signal and discards all information about the signal amplitude. This allows to obtain a cheap,

small and ultra-fast ADC device with extremely low energy consumption. As a single comparator requires small driving power, the requirements for the radio amplifier are very low and an automatic gain control (AGC) at the input of the ADC is not required. Further, the binary structure of the resulting digital receive signal allows to perform basic signal processing operations by means of efficient 1-bit arithmetic. However, despite these highly attractive properties, the nonlinear approach of using a 1-bit A/D conversion is associated with a substantial performance loss.

1.1 Outline

The following chapters consider this aspect in the context of signal parameter estimation. This specific task is a subproblem within the field of statistical signal processing [2] and is concerned with measuring signal parameters (e.g. attenuation, delay, Doppler-frequency, direction-of-arrival (DOA)) from the noisy receive data. Such estimation problems are found in various applications like wireless communication, radar, localization and GNSS positioning where the channel quality has to be determined or the distance, the velocity and the direction of a signal source is to be measured. When the noisy receive signal is passed through a hard-limiter and the amplitude information is discarded, the processing accuracy of the receiver degrades. In order to obtain a better understanding under which circumstances low-complexity 1-bit A/D conversion is an attractive system design option, the characterization of the performance gap between the 1-bit receive model and an ideal receiver with ∞-bit resolution is the focus of this thesis. Using classical estimation theoretic tools, we analyze this aspect under different setups and highlight the importance of including side-information into the estimation procedure. In order to enable the performance analysis of 1-bit receive systems with correlated noise models, we develop a pessimistic approximation for the likelihood function and the Fisher information measure. Applying these mathematical tools, we explore the performance limits of pilot-based channel estimation under 1-bit A/D conversion and an adjusted analog radio front-end. Further, we analyze the problem of DOA parameter estimation with large 1-bit sensor arrays.

1.1.1 Preliminaries

We start the discussion by reviewing the basic principles of A/D conversion and its complexity and power consumption. We also highlight the difference between a conventional Delta-sigma ADC with a single comparator and a low-complexity 1-bit ADC without feedback. Further, we review various frameworks and concepts of estimation theory which allow to formulate practical parameter estimation algorithms and enable to describe the achievable accuracy with asymptotically optimum processing rules in a compact analytic way. Applying these methods to signal models with and without coarse quantization, we analyze the estimation theoretic performance loss introduced by 1-bit ADCs in different channel parameter estimation scenarios. For the problem of channel estimation with 1-bit measurements and a state-space model, we obtain the result that the hard-limiting loss can be significantly diminished. Further, we analyze the additional loss which is introduced when signal parameter estimation with 1-bit ADC and an unknown quantization offset is performed.

When trying to extend the application of classical estimation theoretic tools to signal models with noise correlation, we identify a fundamental problem. Due to a missing compact expression for the orthant probability of a multivariate Gaussian variable, the required likelihood function at the output of the quantizer becomes intractable. This hinders the derivation of efficient processing

algorithms. Further, in the multivariate case the calculation of the Fisher information measure [3] [4] under hard-limiting exhibits exponential complexity with respect to the dimensionality of the observation model. Therefore an exact performance analysis turns out to be intractable in many relevant cases.

1.1.2 Theoretical Contributions

To overcome this obstacle, we discuss different pessimistic approximations for the Fisher information. After deriving two compact bounds for the univariate case, we show how the Fisher information matrix (FIM) can be approximated accurately through a generic lower bound after replacing the original stochastic system model by an equivalent distribution within the exponential family. We prove under which circumstances the obtained approximation for the Fisher information measure is tight. The presented information bound has the advantage that instead of an exact characterization of the model likelihood, just the mean and the covariance of a set of auxiliary statistics are required in order to approximately evaluate the estimation theoretic quality of the signal processing system. For situations where the required moments of the transformed system output are analytically intractable or unknown, the exponential replacement approach allows to access the quality of stochastic systems in a simple measurement-driven way. Further, the conservative likelihood framework resulting from the exponential replacement enables to formulate unbiased estimation algorithms which in practice achieve a performance which corresponds to the pessimistic approximation of the Fisher information measure.

In summary, under any regular probabilistic system model, these results allow to answer questions like *Which estimation performance can we at least expect from a certain measurement system?* and *Which processing rule allows us to achieve this guaranteed performance in practice?*. Such aspects are of fundamental importance for problems in engineering where in general the exact likelihood function is intractable or unknown for the technical system under investigation.

1.1.3 Practical Applications and Results

In order to demonstrate the practical impact of the obtained theoretic results, we outline the application in the context of signal parameter estimation with 1-bit quantization. First, we focus on the problem of system design for pilot-based channel parameter estimation with 1-bit ADC. For radio front-end modifications which lead to independent noise models, we analyze the behavior of the estimation accuracy. To this end, for GNSS-based synchronization, we take into consideration to change the receive bandwidth of the system and to use multiple receive antennas with 1-bit ADCs.

Then we demonstrate how to use the exponential replacement framework in order to analyze the possible estimation accuracy under 1-bit quantization with correlated noise models. By adjusting various parts of the analog processing chain prior to the 1-bit ADC, we aim at minimizing the parameter estimation error. In particular we analyze the beneficial effect of increasing the sampling rate with 1-bit ADC, optimizing the analog pre-filter or introducing signal redundancy by the technique of overdemodulation. The results show that the radio front-end of a wireless receiver can be optimized such that the performance loss with 1-bit A/D conversion can be significantly diminished. The framework of exponential replacement allows to verify this result for different signal-to-noise ratio (SNR) regimes.

Finally, we analyze the problem of blind covariance-based parameter estimation where the system parameter modulates the noise covariance structure before the hard-limiter. Such estima-

tion problems arise in applications where the direction-of-arrival (DOA) parameter of a transmit signal with unknown structure, impinging on a receive array, is to be determined. DOA parameter estimation plays a key role for technologies like wireless multi-user communication, spectrum monitoring, jammer localization and interference mitigation for satellite-based radio systems. For this class of estimation problems the pessimistic performance analysis via the derived information bound reveals the beneficial effect of using arrays with a large number of sensors. For such systems the 1-bit quantization loss becomes small and signal processing can be performed at high accuracy.

In summary, the results of this thesis show that it is possible to significantly simplify the analog complexity of signal processing systems by reducing the amplitude resolution of the ADC circuit to a single bit. Under these circumstances, an adjusted analog system design, probabilistic system modeling and advanced statistical signal processing in the digital domain allow to perform channel parameter estimation at high accuracy. Further, the results for DOA estimation with 1-bit ADC support the evolving academic discussion about shifting the design of wireless systems towards an architecture with a massive number of sensors.

1.2 Publications

1.2.1 Article under Review

While finalizing this thesis, the results on the exponential replacement and the generalized lower bound for the Fisher information matrix (Chapter 5, Section 3-5) have been pre-published (arXiv) and submitted to a peer-reviewed journal:

1) M. S. Stein, J. A. Nossek, and K. Barbé, "Fisher Information Bounds with Applications in Nonlinear Learning, Compression and Inference," online: http://arxiv.org/abs/1512.03473, arXiv timestamp: 10th December 2015.

1.2.2 List of Publications

During the preparation of this thesis, several parts and some closely related aspects have been published as articles in peer-reviewed journals or have been presented at international conferences:

2) M. S. Stein and J. A. Nossek, "A Pessimistic Approximation for the Fisher Information Measure," to appear in IEEE Transactions on Signal Processing, 2016.

3) M. Stein, J. A. Nossek, and K. Barbé, "Measurement-driven Quality Assessment of Nonlinear Systems by Exponential Replacement," IEEE Int. Instrumentation and Measurement Technology Conference (I2MTC), Taipei, Taiwan, 2016, pp. 1–5.

4) M. Stein, S. Bar, J. A. Nossek, and J. Tabrikian, "Performance Analysis for Pilot-based 1-bit Channel Estimation with Unknown Quantization Threshold," IEEE Int. Conference on Acoustics, Speech and Signal Processing (ICASSP), Shanghai, China, 2016, pp. 4353–4357.

5) L. Zhang, M. Stein, and J. A. Nossek, "Asymptotic Performance Analysis for 1-bit Bayesian Smoothing," IEEE Int. Conference on Acoustics, Speech and Signal Processing (ICASSP), Shanghai, China, 2016, pp. 4458–4462.

6) M. Stein, K. Barbé, and J. A. Nossek, "DOA Parameter Estimation with 1-bit Quantization - Bounds, Methods and the Exponential Replacement," Int. ITG Workshop on Smart Antennas (WSA), München, Germany, 2016, pp. 1–6.

7) M. Stein, A. Kürzl, A. Mezghani, and J. A. Nossek, "Asymptotic Parameter Tracking Performance with Measurement Data of 1-Bit Resolution," IEEE Transactions on Signal Processing, vol. 63, no. 22, pp. 6086–6095, 2015.

8) M. Stein, S. Theiler, and J. A. Nossek, "Overdemodulation for High-Performance Receivers with Low-Resolution ADC," IEEE Wireless Communications Letters, vol. 4, no. 2, pp. 169–172, 2015.

9) M. Stein, A. Mezghani, and J. A. Nossek, "A Lower Bound for the Fisher Information Measure," IEEE Signal Processing Letters, vol. 21, no. 7, pp. 796–799, 2014.

10) M. Stein and J. A. Nossek, "Will the 1-bit GNSS Receiver Prevail?" IEEE/ION Position, Location and Navigation Symposium (PLANS), Monterey, USA, 2014, pp. 1033–1040.

11) M. Stein, F. Wendler, A. Mezghani, and J. A. Nossek, "Quantization-Loss Reduction for Signal Parameter Estimation," IEEE Int. Conference on Acoustics, Speech and Signal Processing (ICASSP), Vancouver, Canada, 2013, pp. 5800–5804.

12) M. Stein, A. Mezghani, and J. A. Nossek, "Quantization-Loss Analysis for Array Signal-Source Localization," Int. ITG Workshop on Smart Antennas (WSA), Stuttgart, Germany, 2013, pp. 1–8.

13) F. Wendler, M. Stein, A. Mezghani, and J. A. Nossek, "Quantization-Loss Reduction for 1-bit BOC Positioning," ION Int. Technical Meeting (ITM), San Diego, USA, 2013, pp. 509–518.

1.2.3 List of Additional Publications

Several articles which are not directly related to the topic of signal processing with 1-bit ADC have been published while working on this thesis and are listed here for completeness:

14) A. Lenz, M. Stein, and J. A. Nossek, "Signal Parameter Estimation Performance under a Sampling Rate Constraint," 49th Asilomar Conference on Signals, Systems and Computers, Pacific Grove, California, USA, 2015, pp. 503–507.

15) S. Theiler, M. Stein, and J. A. Nossek, "Ranging with High Accuracy and without Ambiguities," Workshop on Positioning, Navigation and Communication (WPNC), Dresden, Germany, 2015.

16) M. Stein, M. Castañeda, A. Mezghani, and J. A. Nossek, "Information-Preserving Transformations for Signal Parameter Estimation," IEEE Signal Processing Letters, vol. 21, no. 7, pp. 866–870, 2014.

17) M. Stein, A. Lenz, A. Mezghani, and J. A. Nossek, “Optimum Analog Receive Filters for Detection and Inference under a Sampling Rate Constraint,” IEEE Int. Conference on Acoustics, Speech and Signal Processing (ICASSP), Florence, Italy, 2014, pp. 1827–1831.

18) M. Stein, M. Castañeda, and J. A. Nossek, “Information-Preserving Spatial Filtering for Direction-of-Arrival Estimation,” Int. ITG Workshop on Smart Antennas (WSA), Erlangen, Germany, 2014, pp. 1–6.

19) M. Castañeda, M. Stein, F. Antreich, E. Tasdemir, L. Kurz, T. G. Noll, and J. A. Nossek, “Joint Space-Time Interference Mitigation for Embedded Multi-Antenna GNSS Receivers,” ION GNSS+, Nashville, USA, 2013, pp. 3399–3408.

20) C. Enneking, M. Stein, M. Castañeda, F. Antreich, and J. A. Nossek, “Multi-Satellite Time-Delay Estimation for Reliable High-Resolution GNSS Receivers,” IEEE/ION Position, Location and Navigation Symposium (PLANS), Myrtle Beach, USA, 2012, pp. 488–494.

2. Analog-to-Digital Conversion

Due to the continuously increasing transistor density of integrated circuits (IC) over the last decades, today signal processing is preferably performed in the digital domain. Digital algorithms enable to execute complex operations on the available data in a fast way and can be easily extended by advanced features. Further, additional processing speed, smaller system size and lower production cost comes "for free" with every new generation of IC technology. However, as the physical world which technical systems observe and interact with is an analog entity, for the majority of modern signal processing problems it is inevitable to transform analog sensor signals into a digital representation. This process is referred to as A/D conversion. Reciprocally, the interaction of the computational domain with the physical world requires to translate digital numbers into continuous analog waveforms. This process is referred to as digital-to-analog (D/A) conversion.

2.1 Basics, Power Consumption and Complexity

This thesis focuses on the A/D interface between the physical world and the digital processing domain and analyzes the information loss associated with coarse A/D resolution when performing signal parameter estimation.

The A/D conversion process starts with the analog receive signal $y(t) \in \mathbb{R}$ of duration T_o and bandwidth B which is to be transferred into the digital sample domain (see Fig. 2.1) $\boldsymbol{z} \in \mathcal{Z}^N$,

Fig. 2.1. Analog-to-Digital Converter (ADC)

where $\mathcal{Z}$ is the set of values which each sample z_n can take. In Fig. 2.2 an exemplary analog waveform with bandwidth $B = 1.023$ MHz and duration $T_o = 5\mu s$ is depicted. Taking samples of the analog waveform $y(t)$ at discrete points in time and assuming an ideal sampler (see Fig. 2.3) with ∞-bit amplitude resolution, we obtain a discrete-time continuous-value version $\boldsymbol{y}$ of the analog sensor signal $y(t)$ like plotted in Fig. 2.4. The sampling theorem [5] states that if the sampling rate of the ideal ADC satisfies

$$f_s = \frac{1}{T_s} > 2B, \tag{2.1}$$

the samples

$$y_n = y\big((n-1)T_s\big), \quad n = 1, 2, \ldots, N \tag{2.2}$$

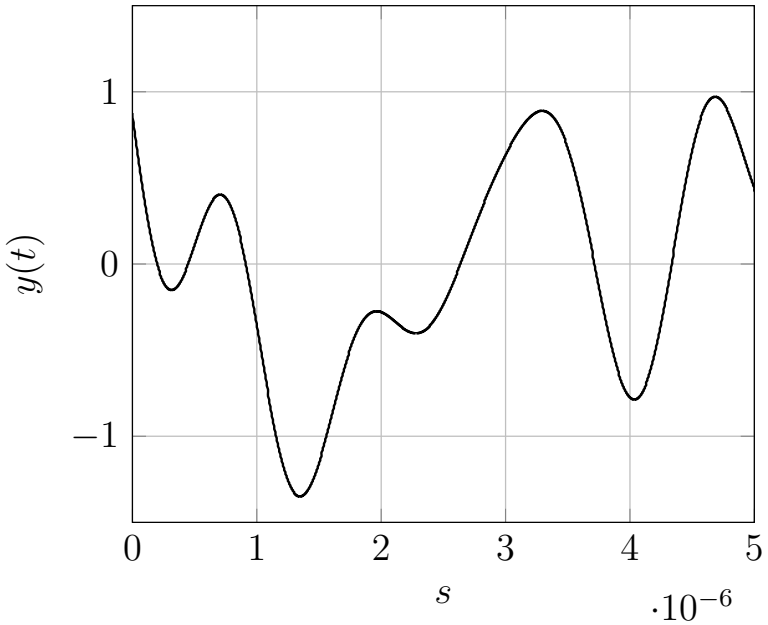

Fig. 2.2. Band-limited Analog Signal ($B = 1.023$ MHz)

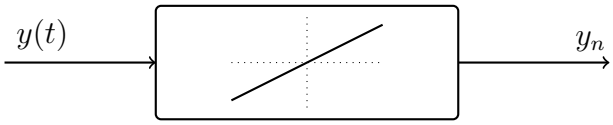

Fig. 2.3. Ideal Analog-to-Digital Converter (∞-bit ADC)

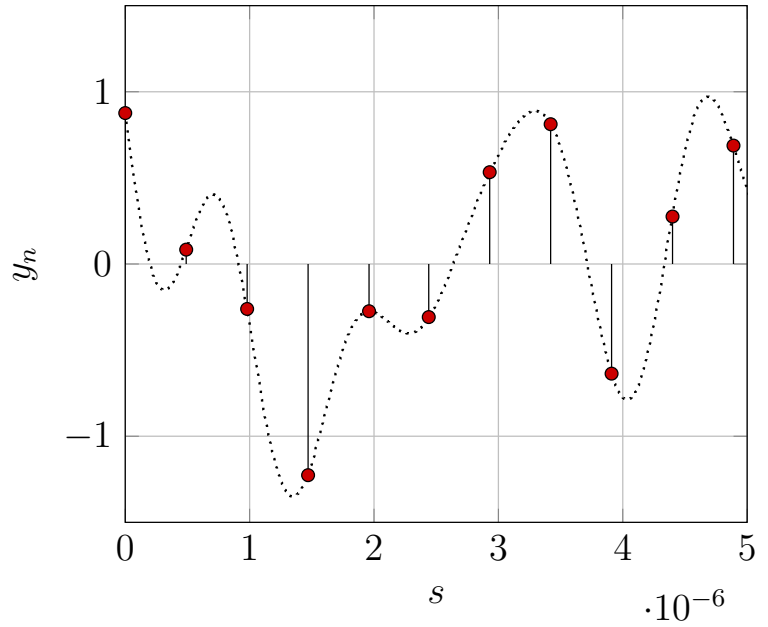

Fig. 2.4. Discrete-Time Continous-Amplitude Signal ($f_s = 2B$)

can be used to reconstruct the analog waveform $y(t)$ without error. However, in practice the resolution of the A/D conversion is limited to b bits and only a finite set of numbers $\mathcal{Z}$ can be represented at the output of the sampler. Such a realistic ADC device and a possible input-output function are

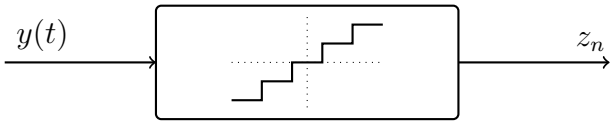

Fig. 2.5. Realistic Analog-to-Digital Converter (b-bit ADC)

shown in Fig. 2.5. Using such an ADC circuit results in discrete-time samples

$$z_n = f\Big(y\big((n-1)T_s\big)\Big), \quad n = 1, 2, \ldots, N \tag{2.3}$$

with $f(\cdot)$ being a nonlinear quantization function, restricting the output of the ADC to a finite alphabet $\mathcal{Z}$. In comparison to the exact samples y_n from the ideal ADC (Fig. 2.3), the quantized samples z_n contain errors

$$z_n = y_n + e_n \tag{2.4}$$

as depicted in Fig. 2.6. Note that in practice, due to the quantization errors e_n, perfect reconstruc-

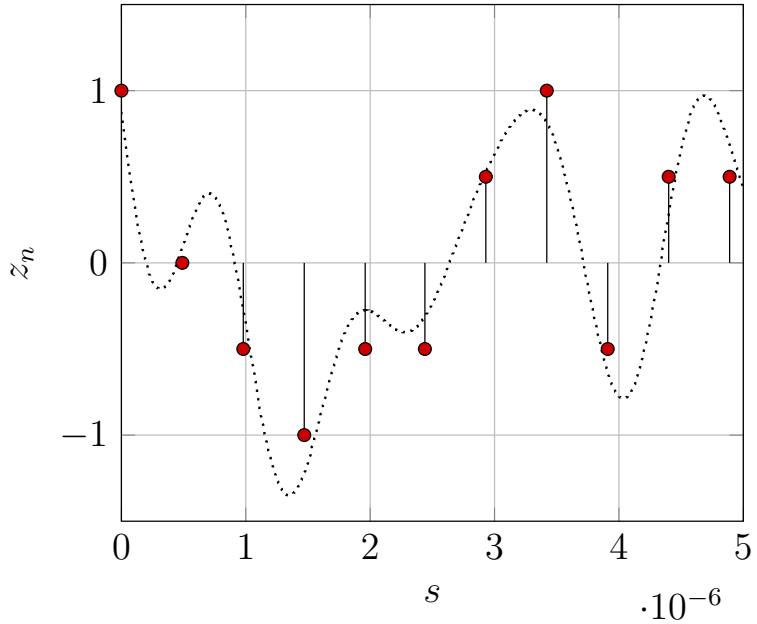

Fig. 2.6. Discrete-Time Discrete-Amplitude Signal ($f_s = 2B$)

tion of the analog sensor signal $y(t)$ from the samples $\boldsymbol{z}$ is impossible.

The circuit comprising the ADC device can be realized in different ways. The fastest architecture is to use a flash implementation where $2^b - 1$ comparators sample the input signal in parallel by comparing to individual threshold voltages. As the number of comparators grows exponentially with the number of bits b, for fast high-resolution applications it is required to use two or more ADC in a time-interleaved fashion [1]. An A/D conversion design with a single comparator is possible when using the approach of successive approximation where in each iteration the input voltage is compared to a different offset voltage in order to narrow the signal range to the desired

resolution [6]. Alternatively, a Delta-sigma converter with high oversampling factor and a subsequent digital decimation filter can be used in order to obtain an ADC circuit with a small number of comparators [7]. As a generic rule, the review of various ADC technologies and architectures in [1] shows that the power P_{ADC} dissipated by the ADC circuit scales approximately

$$P_{\text{ADC}} \approx \beta_{\text{ADC}}(2^b - 1)f_s, \tag{2.5}$$

where β_{ADC} is a constant dependent on the particular ADC technology. With (2.5) it can be observed that the number of bits b causes an exponential increase in the power consumption P_{ADC} when fixing the sampling rate f_s. Aiming at the same power dissipation P_{ADC} while increasing the number of bits b by one requires to diminish the sampling rate f_s by a factor of approximately two.

2.2 Low-Complexity 1-bit A/D Conversion

From the scaling law (2.5) it is clear that the A/D resolution b is a crucial point for the power efficiency of the receive system. Further, the resolution b forms a bottleneck when sampling at high rates or when using a high number of sensors. It is therefore an important issue to accurately determine the number of bits b which are required for the particular application of interest. While

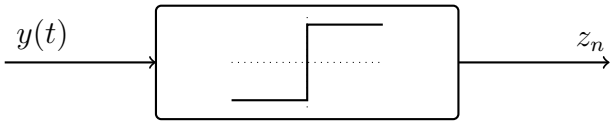

Fig. 2.7. Low-Complexity Analog-to-Digital Converter (1-bit ADC)

a large number of bits b allows to neglect quantization effects during the performance analysis and the algorithm design, the fact that most signal processing problems do not require accurate reconstruction of the analog sensor signal $y(t)$, indicates that already a few bits b can be sufficient to solve certain signal processing tasks at the required accuracy level. For example in estimation problems, the engineer is interested to implement a system which is able to measure certain signal parameters (like Doppler-frequency, time-delay, signal strength, etc.) with the noisy receive signal instead of exactly reconstructing its analog waveform $y(t)$.

In order to simplify the discussion on the appropriate number of bits b on the following pages, we focus on the simplest ADC concept. We set $b = 1$, such that the ADC circuit comprises a single comparator sampling the signal sign while discarding all information about the signal amplitude (see Fig. 2.7). This nonlinear approach has various advantages. According to (2.5), the power

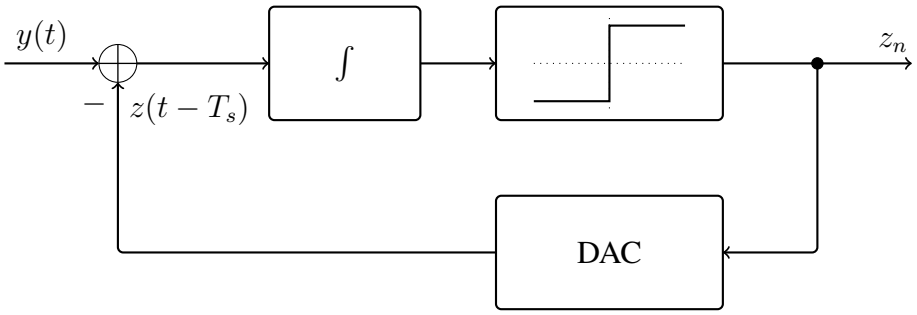

Fig. 2.8. Delta-Sigma Analog-to-Digital Converter

dissipation of the circuit is minimized for a given sampling frequency f_s or the sampling rate can

be set to the highest possible value when comparing to an ADC with b bits for a fixed power consumption. Note that for an ADC device with $b = 2$, the power dissipation under a certain sampling rate f_s is already three times higher than for the 1-bit ADC, i.e.,

$$\frac{P_{\text{ADC}}|_{b=2}}{P_{\text{ADC}}|_{b=1}} = 3. \tag{2.6}$$

Further the amplification device before the 1-bit ADC can be drastically simplified as linearity and an automatic gain control (AGC) is not required. Note that the low-complexity 1-bit ADC usually operates close to $f_s = 2B$ and is therefore distinct from the 1-bit Delta-sigma ADC depicted in Fig. 2.8. Such an ADC works in a considerably oversampled mode, i.e., $f_s = 2B\kappa$, where κ is in the range from 8 to 512 [7]. In comparison to the low-complexity 1-bit ADC (Fig. 2.7), the Delta-sigma modulator (Fig. 2.8) additionally requires a feedback loop with a DAC which can cause instability.

For the analog waveform in Fig 2.2, the signal $\boldsymbol{z} \in \{-1, 1\}^N$ from the low-complexity 1-bit ADC (Fig. 2.7) is shown in Fig. 2.9. As $\boldsymbol{z}$ consists exclusively of binary elements, basic signal processing operations (like correlation, etc.) can be performed in an efficient manner by using 1-bit arithmetic. This makes 1-bit A/D conversion an attractive approach for diminishing the digital complexity of the receiver. Note also that the data stream produced by a 1-bit ADC is of small digital size which in particular is an advantage when considering receive systems with a large number of sensors.

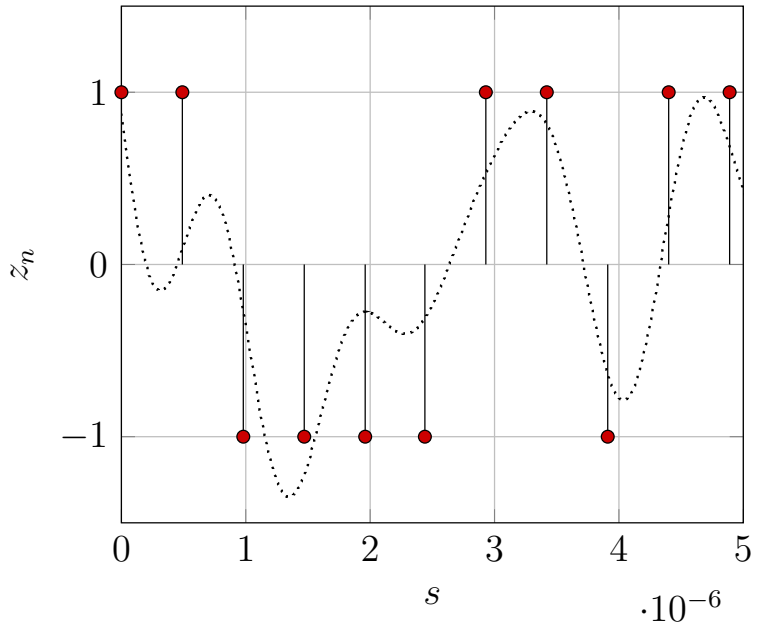

Fig. 2.9. Discrete-Time Binary-Amplitude Signal ($f_s = 2B$)

However, while it is clear that with respect to power consumption, production cost, sampling speed and circuit size it is impossible to outperform the 1-bit ADC (Fig. 2.7), it causes strong quantization errors. This leads to a substantial information loss during the A/D conversion process and affects the signal processing performance when extracting information about the analog signal $y(t)$ from the digital samples $\boldsymbol{z}$. In the next chapters we will focus on the accurate characterization of this loss by comparing the performance of receive systems using the low-complexity 1-bit ADC

(Fig. 2.7) and systems employing the ideal ∞-bit ADC (Fig. 2.3). There we elaborate on estimation problems, where the rigorous analysis of asymptotically optimum and practically feasible processing rules is possible by a compact information measure.

3. Estimation Theory and Performance Measures

In order to set the basis for the analysis of signal parameter estimation with 1-bit ADC, in this chapter we briefly review the basic concepts and methods in the context of estimation theory. For a thorough treatment we refer to [2] [8] [9].

The discipline of signal parameter estimation is concerned with the question of how to derive an accurate estimate $\hat{\boldsymbol{\theta}}(\boldsymbol{Y}) \in \mathbb{R}^D$ from N independent observations

$$\boldsymbol{Y} = \begin{bmatrix} \boldsymbol{y}_1 & \boldsymbol{y}_2 & \cdots & \boldsymbol{y}_N \end{bmatrix} \in \mathbb{R}^{M \times N} \tag{3.1}$$

of the random system output $\boldsymbol{y} \in \boldsymbol{\mathcal{Y}}$ following the parametric probability law $p(\boldsymbol{y}; \boldsymbol{\theta})$. Here $\boldsymbol{\theta} \in \boldsymbol{\Theta}$ denotes a parameter, where the parameter space is a open subset $\boldsymbol{\Theta} \subset \mathbb{R}^D$. $\boldsymbol{\mathcal{Y}}$ denotes the support of the multivariate random variable $\boldsymbol{y} \in \mathbb{R}^M$.

3.1 Regular Parametric Signal Models

For the discussion, we impose the restriction that all parametric models $p(\boldsymbol{y}; \boldsymbol{\theta})$ exhibit finite entropy and fulfill the regularity conditions. These conditions state that

$$p(\boldsymbol{y}; \boldsymbol{\theta}) > 0, \quad \forall \boldsymbol{y} \in \boldsymbol{\mathcal{Y}}, \boldsymbol{\theta} \in \boldsymbol{\Theta}, \tag{3.2}$$

which implies that the support $\boldsymbol{\mathcal{Y}}$ of the system output $\boldsymbol{y}$ is independent of the parameter $\boldsymbol{\theta}$. Further, the first derivative $\frac{\partial p(\boldsymbol{y};\boldsymbol{\theta})}{\partial \boldsymbol{\theta}}$ and the second derivative $\frac{\partial^2 p(\boldsymbol{y};\boldsymbol{\theta})}{\partial \boldsymbol{\theta}^2}$ are bounded. Due to these assumptions both derivatives are absolutely integrable and by differentiation under the integral sign

$$\begin{aligned}
\mathrm{E}_{\boldsymbol{y};\boldsymbol{\theta}} \left[\left(\frac{\partial \ln p(\boldsymbol{y}; \boldsymbol{\theta})}{\partial \boldsymbol{\theta}} \right)^{\mathrm{T}} \right] &= \int_{\boldsymbol{\mathcal{Y}}} \left(\frac{\partial \ln p(\boldsymbol{y}; \boldsymbol{\theta})}{\partial \boldsymbol{\theta}} \right)^{\mathrm{T}} p(\boldsymbol{y}; \boldsymbol{\theta}) \mathrm{d}\boldsymbol{y} \\
&= \int_{\boldsymbol{\mathcal{Y}}} \frac{1}{p(\boldsymbol{y}; \boldsymbol{\theta})} \left(\frac{\partial p(\boldsymbol{y}; \boldsymbol{\theta})}{\partial \boldsymbol{\theta}} \right)^{\mathrm{T}} p(\boldsymbol{y}; \boldsymbol{\theta}) \mathrm{d}\boldsymbol{y} \\
&= \int_{\boldsymbol{\mathcal{Y}}} \left(\frac{\partial p(\boldsymbol{y}; \boldsymbol{\theta})}{\partial \boldsymbol{\theta}} \right)^{\mathrm{T}} \mathrm{d}\boldsymbol{y} \\
&= \left(\frac{\partial}{\partial \boldsymbol{\theta}} \right)^{\mathrm{T}} \int_{\boldsymbol{\mathcal{Y}}} p(\boldsymbol{y}; \boldsymbol{\theta}) \mathrm{d}\boldsymbol{y} \\
&= \mathbf{0}.
\end{aligned} \tag{3.3}$$

Further, taking the derivative of (3.3), we find

$$\begin{aligned}
&\frac{\partial}{\partial \boldsymbol{\theta}} \int_{\boldsymbol{\mathcal{Y}}} \left(\frac{\partial \ln p(\boldsymbol{y};\boldsymbol{\theta})}{\partial \boldsymbol{\theta}} \right)^{\mathrm{T}} p(\boldsymbol{y};\boldsymbol{\theta}) \mathrm{d}\boldsymbol{y} \\
&= \int_{\boldsymbol{\mathcal{Y}}} \left(\frac{\partial^2 \ln p(\boldsymbol{y};\boldsymbol{\theta})}{\partial \boldsymbol{\theta}^2} p(\boldsymbol{y};\boldsymbol{\theta}) + \left(\frac{\partial \ln p(\boldsymbol{y};\boldsymbol{\theta})}{\partial \boldsymbol{\theta}} \right)^{\mathrm{T}} \frac{\partial p(\boldsymbol{y};\boldsymbol{\theta})}{\partial \boldsymbol{\theta}} \right) \mathrm{d}\boldsymbol{y} \\
&= \int_{\boldsymbol{\mathcal{Y}}} \left(\frac{\partial^2 \ln p(\boldsymbol{y};\boldsymbol{\theta})}{\partial \boldsymbol{\theta}^2} + \left(\frac{\partial \ln p(\boldsymbol{y};\boldsymbol{\theta})}{\partial \boldsymbol{\theta}} \right)^{\mathrm{T}} \frac{\partial \ln p(\boldsymbol{y};\boldsymbol{\theta})}{\partial \boldsymbol{\theta}} \right) p(\boldsymbol{y};\boldsymbol{\theta}) \mathrm{d}\boldsymbol{y} \\
&= \mathbf{0}, \qquad (3.4)
\end{aligned}$$

leading to a second important consequence of the regularity conditions

$$\mathrm{E}_{\boldsymbol{y};\boldsymbol{\theta}} \left[\frac{\partial^2 \ln p(\boldsymbol{y};\boldsymbol{\theta})}{\partial \boldsymbol{\theta}^2} \right] = - \mathrm{E}_{\boldsymbol{y};\boldsymbol{\theta}} \left[\left(\frac{\partial \ln p(\boldsymbol{y};\boldsymbol{\theta})}{\partial \boldsymbol{\theta}} \right)^{\mathrm{T}} \frac{\partial \ln p(\boldsymbol{y};\boldsymbol{\theta})}{\partial \boldsymbol{\theta}} \right]. \qquad (3.5)$$

Under the regularity conditions an important information measure is

$$\begin{aligned}
\boldsymbol{F}_{\boldsymbol{y}}(\boldsymbol{\theta}) &\triangleq \mathrm{E}_{\boldsymbol{y};\boldsymbol{\theta}} \left[\left(\frac{\partial \ln p(\boldsymbol{y};\boldsymbol{\theta})}{\partial \boldsymbol{\theta}} \right)^{\mathrm{T}} \frac{\partial \ln p(\boldsymbol{y};\boldsymbol{\theta})}{\partial \boldsymbol{\theta}} \right] \\
&= - \mathrm{E}_{\boldsymbol{y};\boldsymbol{\theta}} \left[\frac{\partial^2 \ln p(\boldsymbol{y};\boldsymbol{\theta})}{\partial \boldsymbol{\theta}^2} \right], \qquad (3.6)
\end{aligned}$$

the so called Fisher information measure [3] [4]. In the following sections, we review three different approaches to parameter estimation, present various processing rules $\hat{\boldsymbol{\theta}}(\boldsymbol{Y})$ and depict the available measures for analytic performance characterization.

3.2 Fisher Estimation Theory

First we discuss the problem of parameter estimation under a Fisher theoretic perspective [2]. The fundamental assumption for inference within this framework is that the parameter $\boldsymbol{\theta}$ is constant, deterministic and unknown. A common measure for the performance of the estimator $\hat{\boldsymbol{\theta}}(\boldsymbol{Y})$ is the mean squared error (MSE) matrix

$$\mathbf{MSE}_{\boldsymbol{Y}}(\boldsymbol{\theta}) \triangleq \mathrm{E}_{\boldsymbol{Y};\boldsymbol{\theta}} \left[\left(\hat{\boldsymbol{\theta}}(\boldsymbol{Y}) - \boldsymbol{\theta} \right) \left(\hat{\boldsymbol{\theta}}(\boldsymbol{Y}) - \boldsymbol{\theta} \right)^{\mathrm{T}} \right]. \qquad (3.7)$$

Note that the MSE matrix (3.7) in the Fisher estimation setting is a function of the parameter $\boldsymbol{\theta}$.

3.2.1 Maximum-Likelihood Estimator

A possible processing procedure given the data $\boldsymbol{Y}$ is the maximum-likelihood estimator (MLE)

$$\begin{aligned}
\hat{\boldsymbol{\theta}}(\boldsymbol{Y}) &\triangleq \arg \max_{\boldsymbol{\theta} \in \Theta} p(\boldsymbol{Y};\boldsymbol{\theta}) \\
&= \arg \max_{\boldsymbol{\theta} \in \Theta} \ln p(\boldsymbol{Y};\boldsymbol{\theta}) \\
&= \arg \max_{\boldsymbol{\theta} \in \Theta} \sum_{n=1}^{N} \ln p(\boldsymbol{y}_n;\boldsymbol{\theta}). \qquad (3.8)
\end{aligned}$$

The MLE aims at maximizing the log-likelihood function $\ln p(\boldsymbol{Y};\boldsymbol{\theta})$ with respect to $\boldsymbol{\theta}$ given the data $\boldsymbol{Y}$. It therefore provides the estimate $\hat{\boldsymbol{\theta}}(\boldsymbol{Y})$ of the parameter $\boldsymbol{\theta}$ which would have made the observations $\boldsymbol{Y}$ most likely. Alternately to the maximization (3.8), the solution $\hat{\boldsymbol{\theta}}(\boldsymbol{Y})$ for the MLE is found by solving for the root

$$\left(\frac{\partial \ln p(\boldsymbol{Y};\boldsymbol{\theta})}{\partial \boldsymbol{\theta}}\right)^{\mathrm{T}} = \mathbf{0}_D \tag{3.9}$$

in $\boldsymbol{\theta} \in \boldsymbol{\Theta}$.

In order to review the properties of the MLE [2], note that with the law of large numbers the log-likelihood function converges to its expectation

$$\begin{aligned}\ln p(\boldsymbol{Y};\boldsymbol{\theta}) &= \sum_{n=1}^{N} \ln p(\boldsymbol{y}_n;\boldsymbol{\theta}) \\ &\xrightarrow{a} N \int_{\boldsymbol{\mathcal{Y}}} \ln p(\boldsymbol{y};\boldsymbol{\theta}) p(\boldsymbol{y};\boldsymbol{\theta}_t) \mathrm{d}\boldsymbol{y},\end{aligned} \tag{3.10}$$

where $\boldsymbol{\theta}_t$ is the true parameter. From the non-negativity of the Kullback-Leibler divergence

$$\int_{\boldsymbol{\mathcal{Y}}} \ln\left(\frac{p(\boldsymbol{y};\boldsymbol{\theta}_t)}{p(\boldsymbol{y};\boldsymbol{\theta})}\right) p(\boldsymbol{y};\boldsymbol{\theta}_t) \mathrm{d}\boldsymbol{y} \geq 0, \tag{3.11}$$

we see that

$$\int_{\boldsymbol{\mathcal{Y}}} \ln p(\boldsymbol{y};\boldsymbol{\theta}_t) p(\boldsymbol{y};\boldsymbol{\theta}_t) \mathrm{d}\boldsymbol{y} \geq \int_{\boldsymbol{\mathcal{Y}}} \ln p(\boldsymbol{y};\boldsymbol{\theta}) p(\boldsymbol{y};\boldsymbol{\theta}_t) \mathrm{d}\boldsymbol{y}, \tag{3.12}$$

which shows that setting $\boldsymbol{\theta} = \boldsymbol{\theta}_t$ maximizes (3.10) in the asymptotic regime and therefore the MLE (3.8) is consistent, i.e.,

$$\hat{\boldsymbol{\theta}}(\boldsymbol{Y}) \xrightarrow{a} \boldsymbol{\theta}_t. \tag{3.13}$$

Let us consider the Taylor expansion of the score function (3.9) around the true parameter $\boldsymbol{\theta}_t$

$$\begin{aligned}\left(\left.\frac{\partial \ln p(\boldsymbol{Y};\boldsymbol{\theta})}{\partial \boldsymbol{\theta}}\right|_{\boldsymbol{\theta}=\hat{\boldsymbol{\theta}}(\boldsymbol{Y})}\right)^{\mathrm{T}} &= \left(\left.\frac{\partial \ln p(\boldsymbol{Y};\boldsymbol{\theta})}{\partial \boldsymbol{\theta}}\right|_{\boldsymbol{\theta}=\boldsymbol{\theta}_t}\right)^{\mathrm{T}} + \left.\frac{\partial^2 \ln p(\boldsymbol{Y};\boldsymbol{\theta})}{\partial \boldsymbol{\theta}^2}\right|_{\boldsymbol{\theta}=\bar{\boldsymbol{\theta}}} \left(\hat{\boldsymbol{\theta}}(\boldsymbol{Y}) - \boldsymbol{\theta}_t\right) \\ &= \mathbf{0}_D,\end{aligned} \tag{3.14}$$

where $\bar{\boldsymbol{\theta}}$ is a value between $\hat{\boldsymbol{\theta}}(\boldsymbol{Y})$ and $\boldsymbol{\theta}_t$. Using the MLE, (3.9) we obtain

$$\left(\left.\frac{\partial \ln p(\boldsymbol{Y};\boldsymbol{\theta})}{\partial \boldsymbol{\theta}}\right|_{\boldsymbol{\theta}=\boldsymbol{\theta}_t}\right)^{\mathrm{T}} = -\left.\frac{\partial^2 \ln p(\boldsymbol{Y};\boldsymbol{\theta})}{\partial \boldsymbol{\theta}^2}\right|_{\boldsymbol{\theta}=\bar{\boldsymbol{\theta}}} \left(\hat{\boldsymbol{\theta}}(\boldsymbol{Y}) - \boldsymbol{\theta}_t\right). \tag{3.15}$$

By rearrangement we further have

$$\sqrt{N}\left(\hat{\boldsymbol{\theta}}(\boldsymbol{Y}) - \boldsymbol{\theta}_t\right) = \left(-\frac{1}{N}\left.\frac{\partial^2 \ln p(\boldsymbol{Y};\boldsymbol{\theta})}{\partial \boldsymbol{\theta}^2}\right|_{\boldsymbol{\theta}=\boldsymbol{\theta}_t}\right)^{-1} \left(\frac{1}{\sqrt{N}}\left.\frac{\partial \ln p(\boldsymbol{Y};\boldsymbol{\theta})}{\partial \boldsymbol{\theta}}\right|_{\boldsymbol{\theta}=\boldsymbol{\theta}_t}\right)^{\mathrm{T}}. \tag{3.16}$$

From the independence of the observations $\boldsymbol{y}_n$, $n = 1, 2, \ldots, N$, and the law of large numbers it follows that

$$\begin{aligned} -\frac{1}{N} \left. \frac{\partial^2 \ln p(\boldsymbol{Y}; \boldsymbol{\theta})}{\partial \boldsymbol{\theta}^2} \right|_{\boldsymbol{\theta}=\bar{\boldsymbol{\theta}}} &= -\frac{1}{N} \sum_{n=1}^{N} \left. \frac{\partial^2 \ln p(\boldsymbol{y}_n; \boldsymbol{\theta})}{\partial \boldsymbol{\theta}^2} \right|_{\boldsymbol{\theta}=\bar{\boldsymbol{\theta}}} \\ &\overset{a}{\to} -\mathrm{E}_{\boldsymbol{y};\boldsymbol{\theta}_t} \left[\left. \frac{\partial^2 \ln p(\boldsymbol{y}; \boldsymbol{\theta})}{\partial \boldsymbol{\theta}^2} \right|_{\boldsymbol{\theta}=\boldsymbol{\theta}_t} \right] \\ &= \boldsymbol{F}_{\boldsymbol{y}}(\boldsymbol{\theta}_t), \end{aligned} \tag{3.17}$$

where we used that by the consistency of the MLE $\bar{\boldsymbol{\theta}} \overset{a}{\to} \boldsymbol{\theta}_t$ when $\hat{\boldsymbol{\theta}}(\boldsymbol{Y}) \overset{a}{\to} \boldsymbol{\theta}_t$. As the expression

$$\frac{1}{\sqrt{N}} \left. \frac{\partial \ln p(\boldsymbol{Y}; \boldsymbol{\theta})}{\partial \boldsymbol{\theta}} \right|_{\boldsymbol{\theta}=\boldsymbol{\theta}_t} = \frac{1}{\sqrt{N}} \sum_{n=1}^{N} \left. \frac{\partial \ln p(\boldsymbol{y}_n; \boldsymbol{\theta})}{\partial \boldsymbol{\theta}} \right|_{\boldsymbol{\theta}=\boldsymbol{\theta}_t} \tag{3.18}$$

is a sum of independent and identically distributed random variable with expectation

$$\begin{aligned} \mathrm{E}_{\boldsymbol{Y};\boldsymbol{\theta}_t} \left[\frac{1}{\sqrt{N}} \sum_{n=1}^{N} \left. \frac{\partial \ln p(\boldsymbol{y}_n; \boldsymbol{\theta})}{\partial \boldsymbol{\theta}} \right|_{\boldsymbol{\theta}=\boldsymbol{\theta}_t} \right] &= \frac{1}{\sqrt{N}} \sum_{n=1}^{N} \mathrm{E}_{\boldsymbol{y}_n;\boldsymbol{\theta}_t} \left[\left. \frac{\partial \ln p(\boldsymbol{y}_n; \boldsymbol{\theta})}{\partial \boldsymbol{\theta}} \right|_{\boldsymbol{\theta}=\boldsymbol{\theta}_t} \right] \\ &= \boldsymbol{0}^{\mathrm{T}} \end{aligned} \tag{3.19}$$

and covariance

$$\begin{aligned} &\mathrm{E}_{\boldsymbol{Y};\boldsymbol{\theta}_t} \left[\left(\frac{1}{\sqrt{N}} \sum_{n=1}^{N} \left. \frac{\partial \ln p(\boldsymbol{y}_n; \boldsymbol{\theta})}{\partial \boldsymbol{\theta}} \right|_{\boldsymbol{\theta}=\boldsymbol{\theta}_t} \right)^{\mathrm{T}} \left(\frac{1}{\sqrt{N}} \sum_{n=1}^{N} \left. \frac{\partial \ln p(\boldsymbol{y}_n; \boldsymbol{\theta})}{\partial \boldsymbol{\theta}} \right|_{\boldsymbol{\theta}=\boldsymbol{\theta}_t} \right) \right] \\ &= \frac{1}{N} \sum_{n=1}^{N} \mathrm{E}_{\boldsymbol{y}_n;\boldsymbol{\theta}_t} \left[\left(\left. \frac{\partial \ln p(\boldsymbol{y}_n; \boldsymbol{\theta})}{\partial \boldsymbol{\theta}} \right|_{\boldsymbol{\theta}=\boldsymbol{\theta}_t} \right)^{\mathrm{T}} \left(\left. \frac{\partial \ln p(\boldsymbol{y}_n; \boldsymbol{\theta})}{\partial \boldsymbol{\theta}} \right|_{\boldsymbol{\theta}=\boldsymbol{\theta}_t} \right) \right] \\ &= \boldsymbol{F}_{\boldsymbol{y}}(\boldsymbol{\theta}_t), \end{aligned} \tag{3.20}$$

asymptotically we have

$$\left(\frac{1}{\sqrt{N}} \left. \frac{\partial \ln p(\boldsymbol{Y}; \boldsymbol{\theta})}{\partial \boldsymbol{\theta}} \right|_{\boldsymbol{\theta}=\boldsymbol{\theta}_t} \right)^{\mathrm{T}} \overset{a}{\sim} \mathcal{N}(\boldsymbol{0}, \boldsymbol{F}_{\boldsymbol{y}}(\boldsymbol{\theta}_t)). \tag{3.21}$$

Slutsky's theorem [10] states that with two random variables $\boldsymbol{X}_1$ and $\boldsymbol{X}_2$ and a constant matrix $\boldsymbol{A}$

$$\boldsymbol{X}_1 \overset{a}{\sim} p(\boldsymbol{X}_1), \quad \boldsymbol{X}_2 \overset{a}{\to} \boldsymbol{A} \tag{3.22}$$

it holds that

$$\boldsymbol{X}_1 \boldsymbol{X}_2 \overset{a}{\to} \boldsymbol{X}_1 \boldsymbol{A}, \quad \boldsymbol{X}_2 \boldsymbol{X}_1 \overset{a}{\to} \boldsymbol{A} \boldsymbol{X}_1. \tag{3.23}$$

Therefore, with the asymptotic result (3.21) and (3.17), we have

$$\sqrt{N} \big(\hat{\boldsymbol{\theta}}(\boldsymbol{Y}) - \boldsymbol{\theta}_t \big) \overset{a}{\sim} \mathcal{N} \left(\boldsymbol{0}, \boldsymbol{F}_{\boldsymbol{y}}^{-1}(\boldsymbol{\theta}_t) \right). \tag{3.24}$$

Equivalently we can write

$$\hat{\boldsymbol{\theta}}(\boldsymbol{Y}) \overset{a}{\sim} \mathcal{N} \left(\boldsymbol{\theta}_t, \frac{1}{N} \boldsymbol{F}_{\boldsymbol{y}}^{-1}(\boldsymbol{\theta}_t) \right). \tag{3.25}$$

This means that if the number of samples N is sufficiently large, the estimates $\hat{\boldsymbol{\theta}}(\boldsymbol{Y})$ calculated by the maximum-likelihood procedure (3.8) are Gaussian distributed around the true parameter $\boldsymbol{\theta}_t$ with a covariance matrix $\frac{1}{N} \boldsymbol{F}_{\boldsymbol{y}}^{-1}(\boldsymbol{\theta}_t)$.

3.2.2 Cramér-Rao Lower Bound

In the following we are going to analyze the fundamental performance limit which is achievable within a particular class of estimation procedures. To this end, we restrict the discussion to unbiased processing rules for which

$$\mathrm{E}_{\boldsymbol{Y};\boldsymbol{\theta}}\left[\hat{\boldsymbol{\theta}}(\boldsymbol{Y})\right] = \boldsymbol{\theta}, \tag{3.26}$$

irrespective of the number of observations N contained in $\boldsymbol{Y}$. As for all considered parametric models

$$\left(\frac{\partial}{\partial\boldsymbol{\theta}}\right)^{\mathrm{T}} \int_{\mathcal{Y}} \boldsymbol{f}(\boldsymbol{y}) p(\boldsymbol{y};\boldsymbol{\theta}) \mathrm{d}\boldsymbol{y} = \int_{\mathcal{Y}} \boldsymbol{f}(\boldsymbol{y}) \left(\frac{\partial p(\boldsymbol{y};\boldsymbol{\theta})}{\partial\boldsymbol{\theta}}\right)^{\mathrm{T}} \mathrm{d}\boldsymbol{y}, \tag{3.27}$$

under any function $\boldsymbol{f}(\cdot)$ which does not present $\boldsymbol{\theta}$ as an argument, we can reformulate (3.26)

$$\int_{\mathcal{Y}^N} \hat{\boldsymbol{\theta}}(\boldsymbol{Y}) p(\boldsymbol{Y};\boldsymbol{\theta}) \mathrm{d}\boldsymbol{Y} = \boldsymbol{\theta} \tag{3.28}$$

and by differentiating on both sides obtain

$$\int_{\mathcal{Y}^N} \hat{\boldsymbol{\theta}}(\boldsymbol{Y}) \frac{\partial p(\boldsymbol{Y};\boldsymbol{\theta})}{\partial\boldsymbol{\theta}} \mathrm{d}\boldsymbol{Y} = \boldsymbol{I}_D. \tag{3.29}$$

Further, with the property

$$\begin{aligned}\int_{\mathcal{Y}^N} \boldsymbol{\theta} \frac{\partial p(\boldsymbol{Y};\boldsymbol{\theta})}{\partial\boldsymbol{\theta}} \mathrm{d}\boldsymbol{Y} &= \boldsymbol{\theta} \frac{\partial}{\partial\boldsymbol{\theta}} \int_{\mathcal{Y}^N} p(\boldsymbol{Y};\boldsymbol{\theta}) \mathrm{d}\boldsymbol{Y} \\ &= \boldsymbol{0}_D,\end{aligned} \tag{3.30}$$

the identity (3.29) can be expanded

$$\int_{\mathcal{Y}^N} \left(\hat{\boldsymbol{\theta}}(\boldsymbol{Y}) - \boldsymbol{\theta}\right) \frac{\partial p(\boldsymbol{Y};\boldsymbol{\theta})}{\partial\boldsymbol{\theta}} \mathrm{d}\boldsymbol{Y} = \boldsymbol{I}_D \tag{3.31}$$

and written as

$$\int_{\mathcal{Y}^N} \left(\hat{\boldsymbol{\theta}}(\boldsymbol{Y}) - \boldsymbol{\theta}\right) \frac{\partial \ln p(\boldsymbol{Y};\boldsymbol{\theta})}{\partial\boldsymbol{\theta}} p(\boldsymbol{Y};\boldsymbol{\theta}) \mathrm{d}\boldsymbol{Y} = \boldsymbol{I}_D, \tag{3.32}$$

where we used the property of the logarithm

$$\frac{\partial \ln p(\boldsymbol{y};\boldsymbol{\theta})}{\partial\boldsymbol{\theta}} = \frac{1}{p(\boldsymbol{y};\boldsymbol{\theta})} \frac{\partial p(\boldsymbol{y};\boldsymbol{\theta})}{\partial\boldsymbol{\theta}}. \tag{3.33}$$

Using (3.32) and the covariance inequality (see Appendix A1) we obtain the matrix inequality

$$\begin{aligned}
&\int_{\boldsymbol{\mathcal{Y}}^N} \big(\hat{\boldsymbol{\theta}}(\boldsymbol{Y}) - \boldsymbol{\theta}\big)\big(\hat{\boldsymbol{\theta}}(\boldsymbol{Y}) - \boldsymbol{\theta}\big)^{\mathrm{T}} p(\boldsymbol{Y};\boldsymbol{\theta})\mathrm{d}\boldsymbol{Y} \\
&\succeq \left(\int_{\boldsymbol{\mathcal{Y}}^N} \big(\hat{\boldsymbol{\theta}}(\boldsymbol{Y}) - \boldsymbol{\theta}\big) \frac{\partial \ln p(\boldsymbol{Y};\boldsymbol{\theta})}{\partial \boldsymbol{\theta}} p(\boldsymbol{Y};\boldsymbol{\theta})\mathrm{d}\boldsymbol{Y}\right) \\
&\quad \cdot \left(\int_{\boldsymbol{\mathcal{Y}}^N} \left(\frac{\partial \ln p(\boldsymbol{Y};\boldsymbol{\theta})}{\partial \boldsymbol{\theta}}\right)^{\mathrm{T}} \frac{\partial \ln p(\boldsymbol{Y};\boldsymbol{\theta})}{\partial \boldsymbol{\theta}} p(\boldsymbol{Y};\boldsymbol{\theta})\mathrm{d}\boldsymbol{Y}\right)^{-1} \\
&\quad \cdot \left(\int_{\boldsymbol{\mathcal{Y}}^N} \left(\frac{\partial \ln p(\boldsymbol{Y};\boldsymbol{\theta})}{\partial \boldsymbol{\theta}}\right)^{\mathrm{T}} \big(\hat{\boldsymbol{\theta}}(\boldsymbol{Y}) - \boldsymbol{\theta}\big)^{\mathrm{T}} p(\boldsymbol{Y};\boldsymbol{\theta})\mathrm{d}\boldsymbol{Y}\right) \\
&= \left(N \int_{\boldsymbol{\mathcal{Y}}} \left(\frac{\partial \ln p(\boldsymbol{y};\boldsymbol{\theta})}{\partial \boldsymbol{\theta}}\right)^{\mathrm{T}} \frac{\partial \ln p(\boldsymbol{y};\boldsymbol{\theta})}{\partial \boldsymbol{\theta}} p(\boldsymbol{y};\boldsymbol{\theta})\mathrm{d}\boldsymbol{y}\right)^{-1}. \qquad (3.34)
\end{aligned}$$

The left hand side of (3.34) is identified to be the mean squared error (MSE) matrix

$$\mathbf{MSE}_{\boldsymbol{Y}}(\boldsymbol{\theta}) \triangleq \mathrm{E}_{\boldsymbol{Y};\boldsymbol{\theta}}\left[\big(\hat{\boldsymbol{\theta}}(\boldsymbol{Y}) - \boldsymbol{\theta}\big)\big(\hat{\boldsymbol{\theta}}(\boldsymbol{Y}) - \boldsymbol{\theta}\big)^{\mathrm{T}}\right] \qquad (3.35)$$

of the estimator $\hat{\boldsymbol{\theta}}(\boldsymbol{Y})$ and the right hand side of (3.34) the Fisher information matrix

$$\boldsymbol{F}_{\boldsymbol{y}}(\boldsymbol{\theta}) \triangleq \mathrm{E}_{\boldsymbol{y};\boldsymbol{\theta}}\left[\left(\frac{\partial \ln p(\boldsymbol{y};\boldsymbol{\theta})}{\partial \boldsymbol{\theta}}\right)^{\mathrm{T}} \frac{\partial \ln p(\boldsymbol{y};\boldsymbol{\theta})}{\partial \boldsymbol{\theta}}\right]. \qquad (3.36)$$

Therefore the inequality (3.34) is equivalent to

$$\mathbf{MSE}(\boldsymbol{\theta}) \succeq \frac{1}{N}\boldsymbol{F}_{\boldsymbol{y}}^{-1}(\boldsymbol{\theta}). \qquad (3.37)$$

The equation (3.37) is known as Cramér-Rao lower bound (CRLB) [11] [12] and restricts the MSE matrix of any unbiased estimate $\hat{\boldsymbol{\theta}}(\boldsymbol{Y})$ to dominate the inverse of the Fisher information matrix. With the asymptotic unbiasedness of the MLE and its covariance (3.25) it can be concluded that the MSE of the MLE asymptotically equals the CRLB. Therefore, the MLE is said to be asymptotically efficient. This result is relevant in practice, as it allows to access the asymptotic performance of the MLE in a compact analytical way by using

$$\mathbf{MSE}_{\boldsymbol{Y}}(\boldsymbol{\theta}) \overset{a}{=} \frac{1}{N}\boldsymbol{F}_{\boldsymbol{y}}^{-1}(\boldsymbol{\theta}). \qquad (3.38)$$

As a simple example for visualization of the asymptotic equality (3.38), consider the problem

$$\begin{aligned}
\boldsymbol{y} &= \boldsymbol{s}(\theta) + \boldsymbol{\eta} \\
&= \gamma\boldsymbol{x} + \boldsymbol{\eta}, \qquad (3.39)
\end{aligned}$$

where the parameter $\theta = \gamma$ is the signal strength with which the pilot signal $\boldsymbol{x} \in \{-1, 1\}^N$ is received and $\boldsymbol{\eta} \sim \mathcal{N}\left(\boldsymbol{0}, \boldsymbol{I}_N\right)$. The MLE is given by

$$\hat{\gamma}(\boldsymbol{y}) = \frac{\boldsymbol{x}^{\mathrm{T}}\boldsymbol{y}}{\boldsymbol{x}^{\mathrm{T}}\boldsymbol{x}}, \qquad (3.40)$$

while the Fisher information measure is found to be

$$\begin{aligned} F(\theta) &= \boldsymbol{x}^{\mathrm{T}}\boldsymbol{x} \\ &= N. \end{aligned} \tag{3.41}$$

For the example (3.39), Fig. 3.1 shows the CRLB and the MSE obtained with the MLE (3.40) for

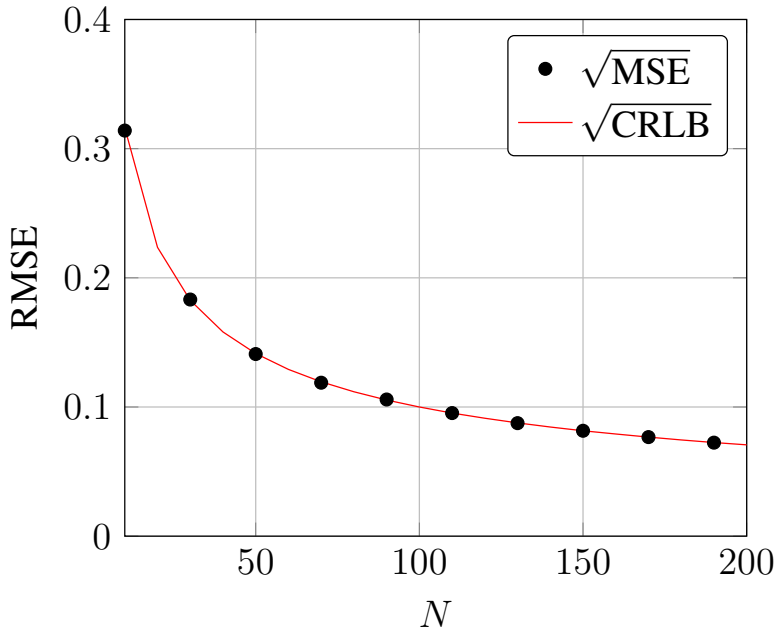

Fig. 3.1. Performance MLE $\hat{\gamma}(\boldsymbol{y})$ vs. CRLB (SNR $= 10$ dB)

different numbers of samples N when averaging over 10000 noise realizations. As predicted by (3.38), it can be observed that both measures obtain the same value. This correspondence between the MSE of the MLE and the CRLB enables us in the following chapters to discuss the quality of a certain system model $p(\boldsymbol{y};\boldsymbol{\theta})$ without having to simulate the MLE. Further, we can compare the achievable accuracy of two system designs $p(\boldsymbol{y};\boldsymbol{\theta})$ and $p(\boldsymbol{z};\boldsymbol{\theta})$ by consulting the Fisher information matrices $\boldsymbol{F}_{\boldsymbol{y}}(\boldsymbol{\theta})$ and $\boldsymbol{F}_{\boldsymbol{z}}(\boldsymbol{\theta})$.

3.3 Bayesian Estimation with Prior Information

The Bayesian perspective onto parameter estimation is fundamentally different. Here the parameter $\boldsymbol{\theta}$ is treated as a random variable which is distributed according to a probability law

$$\boldsymbol{\theta} \sim p(\boldsymbol{\theta}) \tag{3.42}$$

which is known a priori [8]. Therefore the prior knowledge $p(\boldsymbol{\theta})$ can to be incorporated into the estimation process in order to obtain higher processing performance. Note that in contrast to (3.36), the MSE matrix of a Bayesian estimator $\hat{\boldsymbol{\theta}}(\boldsymbol{Y})$

$$\begin{aligned} \mathbf{MSE}_{\boldsymbol{Y}} &\triangleq \mathrm{E}_{\boldsymbol{Y},\boldsymbol{\theta}}\left[\left(\hat{\boldsymbol{\theta}}(\boldsymbol{Y})-\boldsymbol{\theta}\right)\left(\hat{\boldsymbol{\theta}}(\boldsymbol{Y})-\boldsymbol{\theta}\right)^{\mathrm{T}}\right] \\ &= \mathrm{E}_{\boldsymbol{\theta}}\left[\mathrm{E}_{\boldsymbol{Y}|\boldsymbol{\theta}}\left[\left(\hat{\boldsymbol{\theta}}(\boldsymbol{Y})-\boldsymbol{\theta}\right)\left(\hat{\boldsymbol{\theta}}(\boldsymbol{Y})-\boldsymbol{\theta}\right)^{\mathrm{T}}\right]\right] \end{aligned} \tag{3.43}$$

is a constant matrix as the error measure is averaged with respect to $p(\boldsymbol{\theta})$.

3.3.1 Conditional Mean Estimator

In the Bayesian setting the optimum algorithm for the inference for $\boldsymbol{\theta}$ is the conditional mean estimator (CME)

$$\begin{aligned}\hat{\boldsymbol{\theta}}(\boldsymbol{Y}) \triangleq \mathrm{E}_{\boldsymbol{\theta}|\boldsymbol{Y}}\left[\boldsymbol{\theta}\right] &= \int_{\boldsymbol{\Theta}} \boldsymbol{\theta} \frac{p(\boldsymbol{Y}|\boldsymbol{\theta})p(\boldsymbol{\theta})}{p(\boldsymbol{Y})}\mathrm{d}\boldsymbol{\theta} \\ &= \frac{\int_{\boldsymbol{\Theta}} \boldsymbol{\theta} p(\boldsymbol{Y}|\boldsymbol{\theta})p(\boldsymbol{\theta})\mathrm{d}\boldsymbol{\theta}}{\int_{\boldsymbol{\Theta}} p(\boldsymbol{Y}|\boldsymbol{\theta})p(\boldsymbol{\theta})\mathrm{d}\boldsymbol{\theta}}. \end{aligned} \tag{3.44}$$

3.3.2 Bayesian Cramér-Rao Lower Bound

In order to bound the performance of (3.44) from below, note that

$$\begin{aligned}\mathrm{E}_{\boldsymbol{Y},\boldsymbol{\theta}}\left[\left(\hat{\boldsymbol{\theta}}(\boldsymbol{Y}) - \boldsymbol{\theta}\right)\frac{\partial \ln p(\boldsymbol{Y},\boldsymbol{\theta})}{\partial \boldsymbol{\theta}}\right] &= \mathrm{E}_{\boldsymbol{Y}}\left[\hat{\boldsymbol{\theta}}(\boldsymbol{Y})\,\mathrm{E}_{\boldsymbol{\theta}|\boldsymbol{Y}}\left[\frac{\partial \ln p(\boldsymbol{Y},\boldsymbol{\theta})}{\partial \boldsymbol{\theta}}\right]\right] - \mathrm{E}_{\boldsymbol{Y},\boldsymbol{\theta}}\left[\boldsymbol{\theta}\frac{\partial \ln p(\boldsymbol{Y},\boldsymbol{\theta})}{\partial \boldsymbol{\theta}}\right] \\ &= -\mathrm{E}_{\boldsymbol{Y},\boldsymbol{\theta}}\left[\boldsymbol{\theta}\frac{\partial \ln p(\boldsymbol{Y},\boldsymbol{\theta})}{\partial \boldsymbol{\theta}}\right] \end{aligned} \tag{3.45}$$

and

$$\begin{aligned}\mathrm{E}_{\boldsymbol{Y},\boldsymbol{\theta}}\left[\boldsymbol{\theta}\frac{\partial \ln p(\boldsymbol{Y},\boldsymbol{\theta})}{\partial \boldsymbol{\theta}}\right] &= \mathrm{E}_{\boldsymbol{\theta}}\left[\boldsymbol{\theta}\,\mathrm{E}_{\boldsymbol{Y}|\boldsymbol{\theta}}\left[\frac{\partial \ln p(\boldsymbol{Y},\boldsymbol{\theta})}{\partial \boldsymbol{\theta}}\right]\right] \\ &= \mathrm{E}_{\boldsymbol{\theta}}\left[\boldsymbol{\theta}\,\mathrm{E}_{\boldsymbol{Y}|\boldsymbol{\theta}}\left[\frac{\partial \ln p(\boldsymbol{Y}|\boldsymbol{\theta})}{\partial \boldsymbol{\theta}} + \frac{\partial \ln p(\boldsymbol{\theta})}{\partial \boldsymbol{\theta}}\right]\right] \\ &= \mathrm{E}_{\boldsymbol{\theta}}\left[\boldsymbol{\theta}\frac{\partial \ln p(\boldsymbol{\theta})}{\partial \boldsymbol{\theta}}\right] \\ &= \frac{\partial}{\partial \boldsymbol{\theta}}\int_{\boldsymbol{\Theta}} \boldsymbol{\theta} p(\boldsymbol{\theta})\mathrm{d}\boldsymbol{\theta} - \int_{\boldsymbol{\Theta}} \frac{\partial \boldsymbol{\theta}}{\partial \boldsymbol{\theta}} p(\boldsymbol{\theta})\mathrm{d}\boldsymbol{\theta} \\ &= -\boldsymbol{I}_D. \end{aligned} \tag{3.46}$$

Therefore, with the Bayesian version of the covariance inequality (see Appendix A2) it is possible to show that the MSE matrix (3.43) for any estimator $\hat{\boldsymbol{\theta}}(\boldsymbol{Y})$ (possibly biased) dominates

$$\begin{aligned}\mathbf{MSE}_{\boldsymbol{Y}} \succeq\ & \mathrm{E}_{\boldsymbol{Y},\boldsymbol{\theta}}\left[\left(\hat{\boldsymbol{\theta}}(\boldsymbol{Y}) - \boldsymbol{\theta}\right)\frac{\partial \ln p(\boldsymbol{Y},\boldsymbol{\theta})}{\partial \boldsymbol{\theta}}\right]\mathrm{E}_{\boldsymbol{Y},\boldsymbol{\theta}}\left[\left(\frac{\partial \ln p(\boldsymbol{Y},\boldsymbol{\theta})}{\partial \boldsymbol{\theta}}\right)^{\mathrm{T}}\frac{\partial \ln p(\boldsymbol{Y},\boldsymbol{\theta})}{\partial \boldsymbol{\theta}}\right]^{-1} \\ & \cdot \mathrm{E}_{\boldsymbol{Y},\boldsymbol{\theta}}\left[\left(\frac{\partial \ln p(\boldsymbol{Y},\boldsymbol{\theta})}{\partial \boldsymbol{\theta}}\right)^{\mathrm{T}}\left(\hat{\boldsymbol{\theta}}(\boldsymbol{Y}) - \boldsymbol{\theta}\right)^{\mathrm{T}}\right] \\ =\ & \mathrm{E}_{\boldsymbol{Y},\boldsymbol{\theta}}\left[\boldsymbol{\theta}\frac{\partial \ln p(\boldsymbol{Y},\boldsymbol{\theta})}{\partial \boldsymbol{\theta}}\right]\mathrm{E}_{\boldsymbol{Y},\boldsymbol{\theta}}\left[\left(\frac{\partial \ln p(\boldsymbol{Y},\boldsymbol{\theta})}{\partial \boldsymbol{\theta}}\right)^{\mathrm{T}}\frac{\partial \ln p(\boldsymbol{Y},\boldsymbol{\theta})}{\partial \boldsymbol{\theta}}\right]^{-1} \\ & \cdot \mathrm{E}_{\boldsymbol{Y},\boldsymbol{\theta}}\left[\left(\frac{\partial \ln p(\boldsymbol{Y},\boldsymbol{\theta})}{\partial \boldsymbol{\theta}}\right)^{\mathrm{T}}\boldsymbol{\theta}^{\mathrm{T}}\right] \\ =\ & \mathrm{E}_{\boldsymbol{Y},\boldsymbol{\theta}}\left[\left(\frac{\partial \ln p(\boldsymbol{Y},\boldsymbol{\theta})}{\partial \boldsymbol{\theta}}\right)^{\mathrm{T}}\frac{\partial \ln p(\boldsymbol{Y},\boldsymbol{\theta})}{\partial \boldsymbol{\theta}}\right]^{-1}, \end{aligned} \tag{3.47}$$

where we have used

$$\begin{aligned}
\mathrm{E}_{\boldsymbol{\theta}|\boldsymbol{Y}}\left[\frac{\partial \ln p(\boldsymbol{Y},\boldsymbol{\theta})}{\partial \boldsymbol{\theta}}\right] &= \int_{\boldsymbol{\Theta}} \frac{\partial \ln p(\boldsymbol{Y},\boldsymbol{\theta})}{\partial \boldsymbol{\theta}} p(\boldsymbol{\theta}|\boldsymbol{Y})\mathrm{d}\boldsymbol{\theta} \\
&= \int_{\boldsymbol{\Theta}} \frac{\partial \ln p(\boldsymbol{\theta}|\boldsymbol{Y})}{\partial \boldsymbol{\theta}} p(\boldsymbol{\theta}|\boldsymbol{Y})\mathrm{d}\boldsymbol{\theta} \\
&= \int_{\boldsymbol{\Theta}} \frac{\partial p(\boldsymbol{\theta}|\boldsymbol{Y})}{\partial \boldsymbol{\theta}}\mathrm{d}\boldsymbol{\theta} \\
&= \frac{\partial}{\partial \boldsymbol{\theta}} \int_{\boldsymbol{\Theta}} p(\boldsymbol{\theta}|\boldsymbol{Y})\mathrm{d}\boldsymbol{\theta} \\
&= \mathbf{0}_D. \qquad (3.48)
\end{aligned}$$

The matrix on the right hand side of inequality (3.47) is called the Bayesian Fisher information matrix (BFIM) and can be decomposed

$$\begin{aligned}
\boldsymbol{J}_{\boldsymbol{Y}} &\triangleq \mathrm{E}_{\boldsymbol{Y},\boldsymbol{\theta}}\left[\left(\frac{\partial \ln p(\boldsymbol{Y},\boldsymbol{\theta})}{\partial \boldsymbol{\theta}}\right)^{\mathrm{T}} \frac{\partial \ln p(\boldsymbol{Y},\boldsymbol{\theta})}{\partial \boldsymbol{\theta}}\right] \\
&= \mathrm{E}_{\boldsymbol{Y},\boldsymbol{\theta}}\left[\left(\frac{\partial \ln p(\boldsymbol{Y}|\boldsymbol{\theta})}{\partial \boldsymbol{\theta}} + \frac{\partial \ln p(\boldsymbol{\theta})}{\partial \boldsymbol{\theta}}\right)^{\mathrm{T}} \left(\frac{\partial \ln p(\boldsymbol{Y}|\boldsymbol{\theta})}{\partial \boldsymbol{\theta}} + \frac{\partial \ln p(\boldsymbol{\theta})}{\partial \boldsymbol{\theta}}\right)\right] \\
&= \mathrm{E}_{\boldsymbol{Y},\boldsymbol{\theta}}\left[\left(\frac{\partial \ln p(\boldsymbol{Y}|\boldsymbol{\theta})}{\partial \boldsymbol{\theta}}\right)^{\mathrm{T}} \frac{\partial \ln p(\boldsymbol{Y}|\boldsymbol{\theta})}{\partial \boldsymbol{\theta}}\right] + \mathrm{E}_{\boldsymbol{\theta}}\left[\left(\frac{\partial \ln p(\boldsymbol{\theta})}{\partial \boldsymbol{\theta}}\right)^{\mathrm{T}} \frac{\partial \ln p(\boldsymbol{\theta})}{\partial \boldsymbol{\theta}}\right] \qquad (3.49)
\end{aligned}$$

as with (3.3)

$$\begin{aligned}
\mathrm{E}_{\boldsymbol{Y},\boldsymbol{\theta}}\left[\left(\frac{\partial \ln p(\boldsymbol{Y}|\boldsymbol{\theta})}{\partial \boldsymbol{\theta}}\right)^{\mathrm{T}} \frac{\partial \ln p(\boldsymbol{\theta})}{\partial \boldsymbol{\theta}}\right] &= \mathrm{E}_{\boldsymbol{\theta}}\left[\mathrm{E}_{\boldsymbol{Y}|\boldsymbol{\theta}}\left[\left(\frac{\partial \ln p(\boldsymbol{Y}|\boldsymbol{\theta})}{\partial \boldsymbol{\theta}}\right)^{\mathrm{T}} \frac{\partial \ln p(\boldsymbol{\theta})}{\partial \boldsymbol{\theta}}\right]\right] \\
&= \mathrm{E}_{\boldsymbol{\theta}}\left[\mathrm{E}_{\boldsymbol{Y}|\boldsymbol{\theta}}\left[\left(\frac{\partial \ln p(\boldsymbol{Y}|\boldsymbol{\theta})}{\partial \boldsymbol{\theta}}\right)^{\mathrm{T}}\right] \frac{\partial \ln p(\boldsymbol{\theta})}{\partial \boldsymbol{\theta}}\right] \\
&= \mathbf{0}. \qquad (3.50)
\end{aligned}$$

Further,

$$\begin{aligned}
\boldsymbol{J}_{\boldsymbol{Y}} &= \mathrm{E}_{\boldsymbol{Y},\boldsymbol{\theta}}\left[\left(\frac{\partial \ln p(\boldsymbol{Y}|\boldsymbol{\theta})}{\partial \boldsymbol{\theta}}\right)^{\mathrm{T}} \frac{\partial \ln p(\boldsymbol{Y}|\boldsymbol{\theta})}{\partial \boldsymbol{\theta}}\right] + \mathrm{E}_{\boldsymbol{\theta}}\left[\left(\frac{\partial \ln p(\boldsymbol{\theta})}{\partial \boldsymbol{\theta}}\right)^{\mathrm{T}} \frac{\partial \ln p(\boldsymbol{\theta})}{\partial \boldsymbol{\theta}}\right] \\
&= \mathrm{E}_{\boldsymbol{\theta}}\left[\mathrm{E}_{\boldsymbol{Y}|\boldsymbol{\theta}}\left[\left(\frac{\partial \ln p(\boldsymbol{Y}|\boldsymbol{\theta})}{\partial \boldsymbol{\theta}}\right)^{\mathrm{T}} \frac{\partial \ln p(\boldsymbol{Y}|\boldsymbol{\theta})}{\partial \boldsymbol{\theta}}\right]\right] + \mathrm{E}_{\boldsymbol{\theta}}\left[\left(\frac{\partial \ln p(\boldsymbol{\theta})}{\partial \boldsymbol{\theta}}\right)^{\mathrm{T}} \frac{\partial \ln p(\boldsymbol{\theta})}{\partial \boldsymbol{\theta}}\right] \\
&= N\,\mathrm{E}_{\boldsymbol{\theta}}\left[\mathrm{E}_{\boldsymbol{y}|\boldsymbol{\theta}}\left[\left(\frac{\partial \ln p(\boldsymbol{y}|\boldsymbol{\theta})}{\partial \boldsymbol{\theta}}\right)^{\mathrm{T}} \frac{\partial \ln p(\boldsymbol{y}|\boldsymbol{\theta})}{\partial \boldsymbol{\theta}}\right]\right] + \mathrm{E}_{\boldsymbol{\theta}}\left[\left(\frac{\partial \ln p(\boldsymbol{\theta})}{\partial \boldsymbol{\theta}}\right)^{\mathrm{T}} \frac{\partial \ln p(\boldsymbol{\theta})}{\partial \boldsymbol{\theta}}\right] \\
&= N\,\mathrm{E}_{\boldsymbol{\theta}}\left[\boldsymbol{F}_{\boldsymbol{y}}(\boldsymbol{\theta})\right] + \mathrm{E}_{\boldsymbol{\theta}}\left[\left(\frac{\partial \ln p(\boldsymbol{\theta})}{\partial \boldsymbol{\theta}}\right)^{\mathrm{T}} \frac{\partial \ln p(\boldsymbol{\theta})}{\partial \boldsymbol{\theta}}\right] \\
&= N\bar{\boldsymbol{F}}_{\boldsymbol{y}} + \boldsymbol{J}_P, \qquad (3.51)
\end{aligned}$$

where the expected Fisher information matrix (EFIM)

$$\bar{\boldsymbol{F}}_{\boldsymbol{y}} \triangleq \mathrm{E}_{\boldsymbol{\theta}} \left[\boldsymbol{F}_{\boldsymbol{y}}(\boldsymbol{\theta}) \right] \tag{3.52}$$

characterizes the average contribution of the data $\boldsymbol{y}$ and $\boldsymbol{J}_P$ the contribution of the prior knowledge $p(\boldsymbol{\theta})$ to the reduction of the MSE [8]. Contrary to the result (3.25) in the Fisher framework, where the MLE asymptotically achieves the CRLB, in the Bayesian setting the CME (3.44) only attains the BCRLB

$$\mathbf{MSE} \succeq \left(N \bar{\boldsymbol{F}}_{\boldsymbol{y}} + \boldsymbol{J}_P \right)^{-1}, \tag{3.53}$$

in the special case where $p(\boldsymbol{\theta}|\boldsymbol{Y})$ is multivariate Gaussian [8].

3.3.3 Maximum A Posteriori Estimator

In many cases the evaluation of the integrals involved in the CME processing rule (3.44) is not possible in closed form. Therefore it is common to resort to the suboptimal approach of the maximum a posteriori (MAP) estimator

$$\begin{aligned} \hat{\boldsymbol{\theta}}(\boldsymbol{Y}) &\triangleq \arg \max_{\boldsymbol{\theta} \in \boldsymbol{\Theta}} \ln p(\boldsymbol{Y}, \boldsymbol{\theta}) \\ &= \arg \max_{\boldsymbol{\theta} \in \boldsymbol{\Theta}} \left(\ln p(\boldsymbol{Y}|\boldsymbol{\theta}) + \ln p(\boldsymbol{\theta}) \right). \end{aligned} \tag{3.54}$$

Due to the fact that

$$\begin{aligned} \ln p(\boldsymbol{Y}|\boldsymbol{\theta}) + \ln p(\boldsymbol{\theta}) &= \sum_{n=1}^{N} \ln p(\boldsymbol{y}_n|\boldsymbol{\theta}) + \ln p(\boldsymbol{\theta}) \\ &\overset{a}{=} \sum_{n=1}^{N} \ln p(\boldsymbol{y}_n|\boldsymbol{\theta}), \end{aligned} \tag{3.55}$$

the MAP estimator is asymptotically equivalent to the MLE. Therefore, the MSE of the MAP in the asymptotic regime is given by

$$\mathbf{MSE}_{\boldsymbol{Y}} \overset{a}{=} \frac{1}{N} \mathrm{E}_{\boldsymbol{\theta}} \left[\boldsymbol{F}_{\boldsymbol{y}}^{-1}(\boldsymbol{\theta}) \right], \tag{3.56}$$

where the right hand side of (3.56) is referred to as the expected Cramér-Rao lower bound (ECRLB).

3.4 Bayesian Estimation with State-Space Models

Estimation with state-space models makes use of the fact that in various applications the parameter $\boldsymbol{\theta}$ is not constant over the observation time T_o. While the parameter might change from sample $n-1$ to n, the two realizations of the system state $\boldsymbol{\theta}_{n-1}$ and $\boldsymbol{\theta}_n$ exhibit a stochastic relation which is expressed by a state-space model

$$\boldsymbol{\theta}_n \sim p(\boldsymbol{\theta}_n|\boldsymbol{\theta}_{n-1}) \tag{3.57}$$

with an initial distribution

$$\boldsymbol{\theta}_0 \sim p(\boldsymbol{\theta}_0). \tag{3.58}$$

Further, the measurement model can in general also dependent on the sampling time

$$\boldsymbol{y}_n \sim p(\boldsymbol{y}_n|\boldsymbol{\theta}_n). \tag{3.59}$$

3.4.1 Parameter Estimation with Tracking

The formulation of an inference problem with a state-space model allows to combine the measurement (3.59) and the process model (3.57) in order to calculate the optimum tracking filter

$$\hat{\boldsymbol{\theta}}_n(\boldsymbol{Y}_n) = \int_{\boldsymbol{\Theta}} \boldsymbol{\theta}_n p(\boldsymbol{\theta}_n|\boldsymbol{Y}_n)\,\mathrm{d}\,\boldsymbol{\theta}_n \tag{3.60}$$

of the parameter vector $\boldsymbol{\theta}_n$, where we write the receive matrix with all observations up to the n-th sampling step as

$$\boldsymbol{Y}_n = \begin{bmatrix}\boldsymbol{y}_1 & \boldsymbol{y}_2 & \dots & \boldsymbol{y}_n\end{bmatrix}. \tag{3.61}$$

The average tracking error in the n-th block is given by the tracking MSE matrix

$$\mathbf{MSE}_{\boldsymbol{Y}_n} \triangleq \mathrm{E}_{\boldsymbol{Y}_n,\boldsymbol{\theta}_n}\left[\left(\hat{\boldsymbol{\theta}}(\boldsymbol{Y}_n)-\boldsymbol{\theta}_n\right)\left(\hat{\boldsymbol{\theta}}(\boldsymbol{Y}_n)-\boldsymbol{\theta}_n\right)^{\mathrm{T}}\right]. \tag{3.62}$$

3.4.2 Recursive Bayesian Cramér-Rao Lower Bound

In order to determine the fundamental performance limit defined by the combination of a measurement (3.59) and a state-space model (3.57), it is possible to use the BCRLB (3.53) by expanding the parameter space after each observation block and consider the according entries of the growing matrix $\boldsymbol{J}_{\boldsymbol{Y}_n}$. In [13] [14] a recursive method was presented which uses the fact that the MSE matrix of the n-th step always dominates

$$\mathbf{MSE}_{\boldsymbol{Y}_n} \succeq \boldsymbol{U}_{\boldsymbol{Y}_n}^{-1}, \tag{3.63}$$

where the tracking information measure $\boldsymbol{U}_{\boldsymbol{Y}_n}$ can be calculated recursively

$$\boldsymbol{U}_{\boldsymbol{Y}_n} = \boldsymbol{U}_n^{22} - \boldsymbol{U}_n^{21}(\boldsymbol{U}_{\boldsymbol{Y}_{n-1}} + \boldsymbol{U}_n^{11})^{-1}\boldsymbol{U}_n^{12} + \mathrm{E}_{\boldsymbol{\theta}_n}\left[\boldsymbol{F}_{\boldsymbol{y}_n}(\boldsymbol{\theta}_n)\right]. \tag{3.64}$$

The first required information matrix

$$\boldsymbol{U}_n^{11} \triangleq \mathrm{E}_{\boldsymbol{\theta}_n,\boldsymbol{\theta}_{n-1}}\left[\left(\frac{\partial \ln p(\boldsymbol{\theta}_n|\boldsymbol{\theta}_{n-1})}{\partial \boldsymbol{\theta}_{n-1}}\right)^{\mathrm{T}}\left(\frac{\partial \ln p(\boldsymbol{\theta}_n|\boldsymbol{\theta}_{n-1})}{\partial \boldsymbol{\theta}_{n-1}}\right)\right] \tag{3.65}$$

can be interpreted as an information measure associated with the problem of estimating $\boldsymbol{\theta}_{n-1}$ given $\boldsymbol{\theta}_n$ by using only the state-space model (3.57). The second information matrix, connected to the problem of exclusively using the state-space model (3.57) in order to estimate $\boldsymbol{\theta}_n$ given $\boldsymbol{\theta}_{n-1}$ in the n-th sampling step, is defined as

$$\boldsymbol{U}_n^{22} \triangleq \mathrm{E}_{\boldsymbol{\theta}_n,\boldsymbol{\theta}_{n-1}}\left[\left(\frac{\partial \ln p(\boldsymbol{\theta}_n|\boldsymbol{\theta}_{n-1})}{\partial \boldsymbol{\theta}_n}\right)^{\mathrm{T}}\left(\frac{\partial \ln p(\boldsymbol{\theta}_n|\boldsymbol{\theta}_{n-1})}{\partial \boldsymbol{\theta}_n}\right)\right]. \tag{3.66}$$

An additional information matrix, associated with the interaction between the measure (3.65) and (3.66), is

$$\begin{aligned}\boldsymbol{U}_n^{12} &\triangleq \mathrm{E}_{\boldsymbol{\theta}_n,\boldsymbol{\theta}_{n-1}}\left[\left(\frac{\partial \ln p(\boldsymbol{\theta}_n|\boldsymbol{\theta}_{n-1})}{\partial \boldsymbol{\theta}_{n-1}}\right)^{\mathrm{T}}\left(\frac{\partial \ln p(\boldsymbol{\theta}_n|\boldsymbol{\theta}_{n-1})}{\partial \boldsymbol{\theta}_n}\right)\right] \\ &= \left(\boldsymbol{U}_n^{21}\right)^{\mathrm{T}}.\end{aligned} \tag{3.67}$$

The Bayesian version of the sample-based Fisher information measure $\bar{\boldsymbol{F}}_{\boldsymbol{y}_n}$ required in (3.64), is calculated under the definition

$$\boldsymbol{F}_{\boldsymbol{y}_n}(\boldsymbol{\theta}_n) \triangleq \mathrm{E}_{\boldsymbol{y}_n|\boldsymbol{\theta}_n}\left[\left(\frac{\partial \ln p(\boldsymbol{y}_n|\boldsymbol{\theta}_n)}{\partial \boldsymbol{\theta}_n}\right)^{\mathrm{T}}\left(\frac{\partial \ln p(\boldsymbol{y}_n|\boldsymbol{\theta}_n)}{\partial \boldsymbol{\theta}_n}\right)\right], \tag{3.68}$$

where the expectation is taken with respect to $\boldsymbol{\theta}_n \sim p(\boldsymbol{\theta}_n)$. Note that the required marginal is given by

$$p(\boldsymbol{\theta}_n) = \int_{\boldsymbol{\Theta}_{n-1}} \dots \int_{\boldsymbol{\Theta}_0} p(\boldsymbol{\theta}_n, \boldsymbol{\theta}_{n-1}, \dots, \boldsymbol{\theta}_0) \mathrm{d}\boldsymbol{\theta}_{n-1} \dots \mathrm{d}\boldsymbol{\theta}_0, \tag{3.69}$$

where

$$p(\boldsymbol{\theta}_n, \boldsymbol{\theta}_{n-1}, \dots, \boldsymbol{\theta}_0) = p(\boldsymbol{\theta}_0) \prod_{k=1}^{n} p(\boldsymbol{\theta}_k|\boldsymbol{\theta}_{k-1}). \tag{3.70}$$

A comprehensive derivation of the recursive bound (3.63) from the BCRLB (3.47) is found in [8, pp. 92 ff.]. Note that it is not possible to guarantee in general that the Bayesian tracking algorithm (3.60) achieves the information bound (3.63).

4. Parameter Estimation with Hard-Limited Receive Signals

Having reviewed the basics of estimation theory in the previous chapter, we start discussing the information loss associated with low-complexity 1-bit A/D conversion in the different estimation frameworks. After giving an overview on the related literature, we discuss the hard-limiting loss in the Fisher estimation and in Bayesian estimation setting. Further, we demonstrate the beneficial effect of incorporating state-space models into the problem of signal processing with 1-bit ADC. Finally, we discuss the additional loss which is introduced when the 1-bit quantizer exhibits an unknown offset.

4.1 Related Work

In the context of signal processing the analysis of nonlinear systems is a long standing problem [15] [16] [17] [18] [19] [20] [21] [22] [23] [24]. The works [25] [26] on the spectrum of quantized noise form the classical references on the particular problem of hard-limiting, while [20] is one of the first works studing statistical relations between input and output of generic nonlinear devices. The works [27] [28] [29] investigate inference of the spectral components of Gaussian random processes after hard-limiting. Estimating state-space parameters based on quantized signals is considered in the early publication [30]. A first reference for maximum-likelihood estimation with a hard-limiter is [31]. Expressions for the autocorrelation function of hard-limited Gaussian noise are derived in [32], while the estimation of autocorrelation parameters is analyzed in [33]. The benefits of oversampling hard-limited signals is discussed in [34] [35]. A survey on replacing the quantization device by a linear modeling approach is considered in [36]. More recently, [37] studies parameter estimation of sinusoidal functions in noise after hard-limiting. The paper [38] investigates quantizers with dynamically adjusted offset level. The authors of [39] elaborate on the estimation of direction-of-arrival (DOA) parameters with 1-bit signals from multiple receive sensors. Adding noise prior to the quantization operation and exploiting the effect of stochastic resonance for ADC design is proposed in [40]. The effect of a hard-limiter on the performance of moment estimators is discussed in [41], while [42] forms a popular reference on quantization-loss in the area of GNSS signal processing. An asymptotic analysis of estimation with hard-limited signals, correlated noise and randomized quantization offset is found in [43]. The work of [44] shows that a constant quantization offset maximizes the parameter estimation performance with a hard-limiter. In [45] 1-bit quantization enhanced by dithering and feedback is considered, while in [46] the estimation performance is characterized with respect to the ADC resolution. The work [47] experimentally identifies the importance of the analog pre-filter for sampling with a 1-bit ADC.

The characterization of the system performance with 1-bit ADC has recently also gained attention in the field of communication theory. The performance limits of communication systems with

1-bit ADC have been derived in [48] [49]. The benefit of oversampling the analog receive signal for communication over a noisy channel is discussed in [50] [51]. In [52] the authors analyze the adjustment of the quantizer by changing to an asymmetric hard-limiter with non-zero quantization threshold. The work [53] observes that noise correlation can increase the capacity of multiple-input multiple-output (MIMO) communication channels with coarsely quantized receive signals at low SNR.

4.2 Hard-Limiting Loss in the Fisher Estimation Framework

In the next sections we analyze the 1-bit quantization-loss under the different frameworks introduced in Chapter 3. For the discussion we assume an analog sensor signal $y(t) \in \mathbb{R}$ of the form

$$y(t) = \gamma s(t;\theta) + \eta(t). \tag{4.1}$$

The continious-time signal $y(t)$ consists of a deterministic transmit signal $s(t;\theta) \in \mathbb{R}$ which is attenuated by the factor $\gamma \in \mathbb{R}$ and modulated by the parameter $\theta \in \mathbb{R}$. White random noise $\eta(t) \in \mathbb{R}$, summarizing the effect of the analog low-noise amplifier at the receive sensor and interfering signal sources, distorts the receive signal in an additive way. The receive signal $y(t)$ is low-pass filtered to a one-sided bandwidth of B and sampled with a rate of $f_s = 2B = \frac{1}{T_s}$. Collecting N subsequent data points at the sampling device, we form the observation block

$$\boldsymbol{y} = \gamma \boldsymbol{s}(\theta) + \boldsymbol{\eta} \tag{4.2}$$

$\boldsymbol{y}, \boldsymbol{s}(\theta), \boldsymbol{\eta} \in \mathbb{R}^N$, with the individual vector entries

$$y_n = y\big((n-1)T_s\big), \tag{4.3}$$
$$s_n(\theta) = s\big((n-1)T_s;\theta\big), \tag{4.4}$$
$$\eta_n = \eta\big((n-1)T_s\big), \quad n = 1, 2, \ldots, N. \tag{4.5}$$

Due to the strict relation between the bandwidth B of the ideal low-pass filter and the sampling interval T_s, the noise observations $\boldsymbol{\eta}$ form a multivariate Gaussian random variable with

$$\mathrm{E}_{\boldsymbol{\eta}}\left[\boldsymbol{\eta}\right] = \mathbf{0}_N, \tag{4.6}$$
$$\mathrm{E}_{\boldsymbol{\eta}}\left[\boldsymbol{\eta}\boldsymbol{\eta}^{\mathrm{T}}\right] = \boldsymbol{I}_N. \tag{4.7}$$

Therefore the parametric probability density function of the receive signal $\boldsymbol{y}$ can be written

$$\begin{aligned} p(\boldsymbol{y};\theta) &= \frac{1}{(2\pi)^{\frac{N}{2}}} \exp\left(-\frac{1}{2}\big(\boldsymbol{y}-\gamma\boldsymbol{s}(\theta)\big)^{\mathrm{T}}\big(\boldsymbol{y}-\gamma\boldsymbol{s}(\theta)\big)\right) \\ &= \frac{1}{(2\pi)^{\frac{N}{2}}} \prod_{n=1}^{N} \exp\left(-\frac{1}{2}\big(y_n-\gamma s_n(\theta)\big)^2\right), \end{aligned} \tag{4.8}$$

while the noise follows a zero-mean Gaussian probability law

$$\begin{aligned} p(\boldsymbol{\eta}) &= \frac{1}{(2\pi)^{\frac{N}{2}}} \exp\left(-\frac{1}{2}\boldsymbol{\eta}^{\mathrm{T}}\boldsymbol{\eta}\right) \\ &= \frac{1}{(2\pi)^{\frac{N}{2}}} \prod_{n=1}^{N} \exp\left(-\frac{1}{2}\eta_n^2\right). \end{aligned} \tag{4.9}$$

The low-complexity receiver with 1-bit ADC has exclusively access to a hard-limited version of the receive signal

$$\boldsymbol{z} = \operatorname{sign}(\boldsymbol{y}), \tag{4.10}$$

where the element-wise signum function is defined

$$\operatorname{sign}(x) \triangleq \begin{cases} +1 & \text{if } x \geq 0 \\ -1 & \text{if } x < 0. \end{cases} \tag{4.11}$$

After this operation, the probability of the binary receive samples z_n being $+1$ or -1 is

$$\begin{aligned} p(z_n = +1; \theta) &= \int_{-\gamma s_n(\theta)}^{\infty} p(\eta_n) \mathrm{d}\eta_n \\ &= \mathrm{Q}\left(-\gamma s_n(\theta)\right) \\ &= 1 - \mathrm{Q}\left(\gamma s_n(\theta)\right) \end{aligned} \tag{4.12}$$

and

$$\begin{aligned} p(z_n = -1; \theta) &= \int_{-\infty}^{-\gamma s_n(\theta)} p(\eta_n) \mathrm{d}\eta_n \\ &= 1 - \mathrm{Q}\left(-\gamma s_n(\theta)\right) \\ &= \mathrm{Q}\left(\gamma s_n(\theta)\right), \end{aligned} \tag{4.13}$$

such that the parameterized probability mass function of the observation vector $\boldsymbol{z}$ is

$$\begin{aligned} p(\boldsymbol{z}; \theta) &= \prod_{n=1}^{N} \left(1 - \mathrm{Q}\left(\gamma z_n s_n(\theta)\right)\right) \\ &= \prod_{n=1}^{N} \mathrm{Q}\left(-\gamma z_n s_n(\theta)\right). \end{aligned} \tag{4.14}$$

Note that the Q-function is defined

$$\mathrm{Q}(x) \triangleq \frac{1}{\sqrt{2\pi}} \int_{x}^{\infty} \exp\Big(-\frac{u^2}{2}\Big) \mathrm{d}u. \tag{4.15}$$

Calculating the Fisher information measure of the hard-limiting receiver (4.10), we find that

$$\begin{aligned} F_{\boldsymbol{z}}(\theta) &= \mathrm{E}_{\boldsymbol{z};\theta}\left[\left(\frac{\partial \ln p(\boldsymbol{z}; \theta)}{\partial \theta}\right)^2\right] \\ &= \sum_{n=1}^{N} \mathrm{E}_{z_n;\theta}\left[\left(\frac{\partial \ln p(z_n; \theta)}{\partial \theta}\right)^2\right] \\ &= \sum_{n=1}^{N} \frac{\left(\frac{\partial p(z_n=+1;\theta)}{\partial \theta}\right)^2}{p(z_n = +1; \theta)} + \sum_{n=1}^{N} \frac{\left(\frac{\partial p(z_n=-1;\theta)}{\partial \theta}\right)^2}{p(z_n = -1; \theta)}. \end{aligned} \tag{4.16}$$

With the derivatives of the parametric probability mass function

$$\frac{\partial p(z_n;\theta)}{\partial \theta} = z_n \frac{\gamma}{\sqrt{2\pi}} \frac{\partial s_n(\theta)}{\partial \theta} \exp\left(-\frac{\gamma^2 s_n^2(\theta)}{2}\right), \tag{4.17}$$

the Fisher information measure is found to be given by

$$F_{\boldsymbol{z}}(\theta) = \frac{\gamma^2}{2\pi} \sum_{n=1}^{N} \frac{\frac{\partial s_n^2(\theta)}{\partial \theta} \exp\left(-\gamma^2 s_n^2(\theta)\right)}{\mathrm{Q}\left(\gamma s_n(\theta)\right) \mathrm{Q}\left(-\gamma s_n(\theta)\right)}. \tag{4.18}$$

As a performance reference for the nonlinear 1-bit system, consider the ideal receiver (4.2) which has access to the high-resolution signal $\boldsymbol{y}$. For this kind of receive system, the Fisher information measure is found to be

$$\begin{aligned} F_{\boldsymbol{y}}(\theta) &= \mathrm{E}_{\boldsymbol{y};\theta}\left[\left(\frac{\partial \ln p(\boldsymbol{y};\theta)}{\partial \theta}\right)^2\right] \\ &= \gamma^2 \left(\frac{\partial \boldsymbol{s}(\theta)}{\partial \theta}\right)^{\mathrm{T}} \frac{\partial \boldsymbol{s}(\theta)}{\partial \theta} \\ &= \gamma^2 \sum_{n=1}^{N} \frac{\partial s_n^2(\theta)}{\partial \theta}. \end{aligned} \tag{4.19}$$

In order to compare the ideal receiver (4.2) and the low-complexity 1-bit system (4.10) with respect to the achievable estimation accuracy, we define the relative performance loss by the ratio

$$\chi(\theta) \triangleq \frac{F_{\boldsymbol{z}}(\theta)}{F_{\boldsymbol{y}}(\theta)}. \tag{4.20}$$

With $\mathrm{Q}\left(0\right) = \frac{1}{2}$, we obtain in the limit

$$\lim_{\kappa \to 0} \frac{\mathrm{e}^{-\kappa^2}}{\mathrm{Q}\left(\kappa\right) \mathrm{Q}\left(-\kappa\right)} = 4, \tag{4.21}$$

such that we can analyze the hard-limiting loss (4.20) for asymptotically low SNR [26]

$$\begin{aligned} \lim_{\gamma \to 0} \chi(\theta) &= \lim_{\gamma \to 0} \frac{\frac{\gamma^2}{2\pi} \sum_{n=1}^{N} \frac{\frac{\partial s_n^2(\theta)}{\partial \theta} \exp\left(-\gamma^2 s_n^2(\theta)\right)}{\mathrm{Q}(\gamma s_n(\theta))\, \mathrm{Q}(-\gamma s_n(\theta))}}{\gamma^2 \sum_{n=1}^{N} \frac{\partial s_n^2(\theta)}{\partial \theta}} \\ &= \frac{2}{\pi}. \end{aligned} \tag{4.22}$$

Note that (4.22) is -1.96 dB when expressed as equivalent reduction in SNR.

4.3 Hard-Limiting Loss in the Bayesian Estimation Framework

From the Bayesian perspective an analysis of the 1-bit loss follows a similar approach. Here the parameter θ has to be treated as a random variable which is distributed according to a prior distri-

bution $\theta \sim p(\theta)$. The Bayesian information measure with N observations is

$$\begin{aligned} J_{\boldsymbol{z}} &= \mathrm{E}_{\boldsymbol{z},\theta}\left[\left(\frac{\partial \ln p(\boldsymbol{z},\theta)}{\partial\theta}\right)^2\right] \\ &= \mathrm{E}_{\theta}\left[\mathrm{E}_{\boldsymbol{z}|\theta}\left[\left(\frac{\partial \ln p(\boldsymbol{z}|\theta)}{\partial\theta}\right)^2\right]\right] + \mathrm{E}_{\theta}\left[\left(\frac{\partial \ln p(\theta)}{\partial\theta}\right)^2\right] \\ &= N\bar{F}_z(\theta) + J_P. \end{aligned} \tag{4.23}$$

Equivalently, for the ideal reference receiver we have

$$\begin{aligned} J_{\boldsymbol{y}} &= \mathrm{E}_{\boldsymbol{y},\theta}\left[\left(\frac{\partial \ln p(\boldsymbol{y},\theta)}{\partial\theta}\right)^2\right] \\ &= N\bar{F}_y(\theta) + J_P. \end{aligned} \tag{4.24}$$

Defining the relative performance gap in the Bayesian setting by

$$\begin{aligned} \chi &\triangleq \frac{J_{\boldsymbol{z}}}{J_{\boldsymbol{y}}} \\ &= \frac{N\bar{F}_z(\theta) + J_P}{N\bar{F}_y(\theta) + J_P}, \end{aligned} \tag{4.25}$$

allows us to compare both receive systems. For the asymptotic analysis in the low SNR regime

$$\begin{aligned} \lim_{\gamma\to 0}\lim_{N\to\infty}\chi &= \lim_{\gamma\to 0}\lim_{N\to\infty}\frac{N\bar{F}_z(\theta) + J_P}{N\bar{F}_y(\theta) + J_P} \\ &= \lim_{\gamma\to 0}\frac{\bar{F}_z(\theta)}{\bar{F}_y(\theta)} \\ &= \frac{2}{\pi}, \end{aligned} \tag{4.26}$$

we obtain the same result as in the Fisher estimation framework (4.22) by making the number of observations N sufficiently large.

4.4 Hard-Limiting Loss for Estimation with State-Space Models

Now, we assume that the parameter θ changes with each sample $\boldsymbol{y}_n$ or $\boldsymbol{z}_n$. Further, a stochastic model $p(\theta_n|\theta_{n-1})$ describing the temporal evolution of the parameter from one sample to another is available. This allows us to perform parameter estimation with tracking over subsequent blocks and to calculate the current block estimate $\hat{\theta}_n$ based on the observations of the current block and all preceding blocks (tracking). For simplicity we assume that the channel parameter θ_n evolves according to an autoregressive model of order one, i.e.,

$$\theta_n = \alpha\theta_{n-1} + w_n, \tag{4.27}$$

where $\alpha \in \mathbb{R}$. The innovation $w_n \in \mathbb{R}$ is modeled as a Gaussian random variable with

$$\mathrm{E}_{w_n}[w_n] = 0, \qquad \forall n, \tag{4.28}$$

$$\mathrm{E}_{w_n}\left[w_n^2\right] = \sigma_w^2, \qquad \forall n. \tag{4.29}$$

Under these assumptions the transition probability function of the parameter θ_n is given by

$$p(\theta_n|\theta_{n-1}) = \frac{1}{\sqrt{2\pi}\sigma_w} \exp\left(-\frac{(\theta_n - \alpha\theta_{n-1})^2}{2\sigma_w^2}\right). \tag{4.30}$$

For the first block we assume an initial prior

$$p(\theta_0) = \frac{1}{\sqrt{2\pi}\sigma_0} \mathrm{e}^{-\frac{(\theta_0-\mu_0)^2}{2\sigma_0^2}}. \tag{4.31}$$

Note that for such a state-space model, the marginal

$$p(\theta_n) = \int_{\Theta_{n-1}} \int_{\Theta_{n-2}} \dots \int_{\Theta_0} p(\theta_n|\theta_{n-1}) p(\theta_{n-1}|\theta_{n-2}) \cdot \ldots \cdot p(\theta_0) \mathrm{d}\theta_{n-1} \mathrm{d}\theta_{n-2} \cdot \ldots \cdot \mathrm{d}\theta_0 \tag{4.32}$$

follows a Gaussian distribution $\mathcal{N}(\mu_n, \sigma_n^2)$ for which the mean and the variance evolve over time according to

$$\mu_n = \mathrm{E}_{\theta_n}[\theta_n] = \alpha^n \mu_0, \tag{4.33}$$

$$\sigma_n^2 = \mathrm{E}_{\theta_n}\left[(\theta_n - \mathrm{E}_{\theta_n}[\theta_n])^2\right] = \alpha^{2n}\sigma_0^2 + \left(\sum_{i=1}^{n} \alpha^{2(n-i)}\right)\sigma_w^2. \tag{4.34}$$

In order to avoid divergence of the state-space variance (4.34), we restrict α to $0 \leq \alpha < 1$, such that in the limit

$$\lim_{n\to\infty} \mathrm{E}_{\theta_n}[\theta_n] = 0, \tag{4.35}$$

$$\lim_{n\to\infty} \mathrm{E}_{\theta_n}\left[(\theta_n - \mathrm{E}_{\theta_n}[\theta_n])^2\right] = \frac{1}{1-\alpha^2}\sigma_w^2. \tag{4.36}$$

With the state-space model (4.27), the required derivatives for the evaluation of the information measures (3.65), (3.66) and (3.67) are

$$\frac{\partial \ln p(\theta_n|\theta_{n-1})}{\partial \theta_{n-1}} = \frac{(\theta_n - \alpha\theta_{n-1})\alpha}{\sigma_w^2}, \tag{4.37}$$

$$\frac{\partial \ln p(\theta_n|\theta_{n-1})}{\partial \theta_n} = -\frac{(\theta_n - \alpha\theta_{n-1})}{\sigma_w^2}, \tag{4.38}$$

such that we obtain

$$U_n^{11} = \mathrm{E}_{\theta_{n-1}}\left[\mathrm{E}_{\theta_n|\theta_{n-1}}\left[\left(\frac{\partial \ln p(\theta_n|\theta_{n-1})}{\partial \theta_{n-1}}\right)^2\right]\right] = \frac{\alpha^2}{\sigma_w^2}, \tag{4.39}$$

$$U_n^{22} = \mathrm{E}_{\theta_{n-1}}\left[\mathrm{E}_{\theta_n|\theta_{n-1}}\left[\left(\frac{\partial \ln p(\theta_n|\theta_{n-1})}{\partial \theta_n}\right)^2\right]\right] = \frac{1}{\sigma_w^2}, \tag{4.40}$$

$$U_n^{12} = \mathrm{E}_{\theta_{n-1}}\left[\mathrm{E}_{\theta_n|\theta_{n-1}}\left[\frac{\partial \ln p(\theta_n|\theta_{n-1})}{\partial \theta_{n-1}} \frac{\partial \ln p(\theta_n|\theta_{n-1})}{\partial \theta_n}\right]\right] = -\frac{\alpha}{\sigma_w^2}. \tag{4.41}$$

Consequently, the recursive rule (3.64) for the computation of the tracking information measure $U_{\boldsymbol{z}_n}$ is given by

$$\begin{aligned} U_{\boldsymbol{z}_n} &= U_n^{22} - U_n^{21}(U_{\boldsymbol{z}_{n-1}} + U_n^{11})^{-1}U_n^{12} + \mathrm{E}_{\theta_n}\left[F_{\boldsymbol{z}}(\theta_n)\right] \\ &= \frac{1}{\sigma_w^2} - \frac{\alpha^2}{\sigma_w^4}\left(U_{\boldsymbol{z}_{n-1}} + \frac{\alpha^2}{\sigma_w^2}\right)^{-1} + \bar{F}_{\boldsymbol{z}_n} \\ &= \left(\sigma_w^2 + \frac{\alpha^2}{U_{\boldsymbol{z}_{n-1}}}\right)^{-1} + \bar{F}_{\boldsymbol{z}_n} \end{aligned} \tag{4.42}$$

and accordingly for the ideal receiver (infinite resolution)

$$U_{\boldsymbol{y}_n} = \left(\sigma_w^2 + \frac{\alpha^2}{U_{\boldsymbol{y}_{n-1}}}\right)^{-1} + \bar{F}_{\boldsymbol{y}_n}, \tag{4.43}$$

where the initial value in both cases is

$$U_{\boldsymbol{z}_0} = U_{\boldsymbol{y}_0} = \frac{1}{\sigma_0^2}. \tag{4.44}$$

4.4.1 Steady-State Tracking Performance

After an initial transient phase, the tracking algorithm reaches a steady-state such that the estimation error saturates and

$$U_{\boldsymbol{z}_n} = U_{\boldsymbol{z}_{n-1}}, \qquad \forall n > N_\lambda, \tag{4.45}$$

where N_λ defines the number of observations during the transient phase. Using the steady-state condition (4.45) in (4.42) and solving for $U_{\boldsymbol{z}}$, we obtain

$$\begin{aligned} U_{\boldsymbol{z}} &= \lim_{n\to\infty} U_{\boldsymbol{z}_n} \\ &= \frac{1-\alpha^2}{2\sigma_w^2} + \frac{\bar{F}_{\boldsymbol{z}}^{\infty}}{2} + \sqrt{\left(\frac{1-\alpha^2}{2\sigma_w^2} + \frac{\bar{F}_{\boldsymbol{z}}^{\infty}}{2}\right)^2 + \frac{\alpha^2\bar{F}_{\boldsymbol{z}}^{\infty}}{\sigma_w^2}}, \end{aligned} \tag{4.46}$$

where the expected steady-state Fisher information is

$$\begin{aligned} \bar{F}_{\boldsymbol{z}}^{\infty} &\triangleq \lim_{n\to\infty} \mathrm{E}_{\theta_n}\left[F_{\boldsymbol{z}}(\theta_n)\right] \\ &= \lim_{n\to\infty} \bar{F}_{\boldsymbol{z}_n}. \end{aligned} \tag{4.47}$$

The situation that the last term $\frac{\alpha^2\bar{F}_{\boldsymbol{z}}}{\sigma_w^2}$ in (4.46) dominates the tracking information measure $U_{\boldsymbol{z}}$ arises if the two conditions

$$\left(\frac{1-\alpha^2}{2\sigma_w^2}\right)^2 \ll \frac{\alpha^2\bar{F}_{\boldsymbol{z}}^{\infty}}{\sigma_w^2}, \tag{4.48}$$

$$\left(\frac{\bar{F}_{\boldsymbol{z}}^{\infty}}{2}\right)^2 \ll \frac{\alpha^2\bar{F}_{\boldsymbol{z}}^{\infty}}{\sigma_w^2} \tag{4.49}$$

are fulfilled. The first condition (4.48) can be reformulated

$$(1-\alpha^2)^2 \ll \alpha^2\sigma_w^2\bar{F}_{\boldsymbol{z}}^{\infty} \tag{4.50}$$

and the second condition (4.49) can be stated as

$$\bar{F}_{\boldsymbol{z}}^{\infty} \ll \frac{\alpha^2}{\sigma_w^2}. \tag{4.51}$$

Substituting (4.51) into (4.50), we get

$$1-\alpha^2 \ll \alpha^2, \tag{4.52}$$

which is satisfied if we set α close to one. Hence, if α is close to one (4.52) and the informative quality of the state-space model indicated by $\frac{\alpha^2}{\sigma_w^2}$ (4.39) is much higher than the expected steady-state Fisher information $\bar{F}_{\boldsymbol{z}}^{\infty}$ of the observation model (4.51), the steady-state tracking information measure $U_{\boldsymbol{z}}$ can be approximated by

$$U_{\boldsymbol{z}} \approx \sqrt{\frac{\alpha^2\bar{F}_{\boldsymbol{z}}^{\infty}}{\sigma_w^2}}. \tag{4.53}$$

For the comparison between the quantized receiver and the ideal system, we define the 1-bit quantization loss for parameter estimation and tracking in the n-th block as

$$\chi_n = \frac{U_{\boldsymbol{z}_n}}{U_{\boldsymbol{y}_n}}, \tag{4.54}$$

such that asymptotically

$$\begin{aligned}\chi &= \lim_{n\to\infty}\chi_n \\ &= \frac{U_{\boldsymbol{z}}}{U_{\boldsymbol{y}}},\end{aligned} \tag{4.55}$$

where the steady-state tracking information measure $U_{\boldsymbol{y}}$ for the ideal reference receiver is

$$U_{\boldsymbol{y}} = \frac{1-\alpha^2}{2\sigma_w^2} + \frac{\bar{F}_{\boldsymbol{y}}^{\infty}}{2} + \sqrt{\left(\frac{1-\alpha^2}{2\sigma_w^2} + \frac{\bar{F}_{\boldsymbol{y}}^{\infty}}{2}\right)^2 + \frac{\alpha^2\bar{F}_{\boldsymbol{y}}^{\infty}}{\sigma_w^2}}, \tag{4.56}$$

with the expected steady-state Fisher information of the ideal receiver (∞-bit)

$$\begin{aligned}\bar{F}_{\boldsymbol{y}}^{\infty} &= \lim_{n\to\infty}\mathrm{E}_{\theta_n}\left[F_{\boldsymbol{y}}(\theta)\right] \\ &= \lim_{n\to\infty}\bar{F}_{\boldsymbol{y}}(\theta).\end{aligned} \tag{4.57}$$

Under the assumption that the state-space model $p(\theta_n|\theta_{n-1})$ exhibits a much higher estimation theoretic quality than the observation models, independent of the form of the receiver, i.e.,

$$\bar{F}_{\boldsymbol{z}}^{\infty} \ll \frac{\alpha^2}{\sigma_w^2}, \tag{4.58}$$

$$\bar{F}_{\boldsymbol{y}}^{\infty} \ll \frac{\alpha^2}{\sigma_w^2}, \tag{4.59}$$

it is possible to evaluate the steady-state loss for a slow temporal state-space evolution

$$\begin{aligned}\lim_{\alpha\to 1}\lim_{n\to\infty}\chi_n &= \lim_{\alpha\to 1}\chi \\ &= \lim_{\alpha\to 1}\frac{U_{\boldsymbol{z}}}{U_{\boldsymbol{y}}} \\ &\approx \sqrt{\frac{\bar{F}_{\boldsymbol{z}}^{\infty}}{\bar{F}_{\boldsymbol{y}}^{\infty}}}.\end{aligned} \tag{4.60}$$

Note that as long as (4.58) and (4.59) are fulfilled, the result (4.60) holds in general, independent of the considered SNR regime. This implies that compared to the Fisher estimation or the Bayesian inference approach, tracking the parameter with the use of a slowly evolving state-space model leads to a 1-bit quantization loss which is potentially by a factor of two smaller when expressed in dB. With the result (4.60) and (4.26), we can make the explicit statement that for signal parameter estimation and tracking in the low SNR regime, the 1-bit quantization loss is

$$\lim_{\gamma\to 0}\lim_{\alpha\to 1}\chi \approx \sqrt{\frac{2}{\pi}}. \tag{4.61}$$

4.4.2 Convergence and Transient Phase Analysis

In order to further analyze the behavior of the 1-bit receive system, we consider the convergence of the recursive information measure (4.42). The goal is to determine the number of measurements which are required to fulfill the steady-state condition (4.45). To this end, we define a transient phase of quality $\lambda > 1$, with the duration

$$N_{\boldsymbol{z},\lambda} \triangleq \inf\left\{n \geq 1 \middle| |U_{\boldsymbol{z}_n} - U_{\boldsymbol{z}}| \leq 10^{-\lambda}|U_{\boldsymbol{z}_0} - U_{\boldsymbol{z}}|\right\}. \tag{4.62}$$

The measure $N_{\boldsymbol{z},\lambda}$ characterizes the number of observation blocks which are required from the start of the tracking procedure to the steady-state entry point of quality λ. The rate of convergence $\lambda_{\text{conv}} \in \mathbb{R}$ of recursion (4.42) is found by solving

$$\lim_{n\to\infty}\frac{|U_{\boldsymbol{z}_n} - U_{\boldsymbol{z}}|}{|U_{\boldsymbol{z}_{n-1}} - U_{\boldsymbol{z}}|^{\lambda_{\text{conv}}}} = \lambda_{\text{const}} \tag{4.63}$$

with respect to λ_{conv} under a constant $\lambda_{\text{const}} \in \mathbb{R}$, $\lambda_{\text{const}} < \infty$. As the derivative

$$\left.\frac{\partial U_{\boldsymbol{z}_n}}{\partial U_{\boldsymbol{z}_{n-1}}}\right|_{U_{\boldsymbol{z}_{n-1}}=U_{\boldsymbol{z}}} = \alpha^2(\sigma_w^2 U_{\boldsymbol{z}} + \alpha^2)^{-2} \neq 0, \tag{4.64}$$

we have $\lambda_{\text{conv}} = 1$, i.e., the order of convergence is linear and

$$\lambda_{\text{const}} = \alpha^2(\sigma_w^2 U_{\boldsymbol{z}} + \alpha^2)^{-2}. \tag{4.65}$$

With $|U_{\boldsymbol{z}_n} - U_{\boldsymbol{z}}| \approx \lambda_{\text{const}}^n |U_{\boldsymbol{z}_0} - U_{\boldsymbol{z}}|$, the duration of the transient phase $N_{\boldsymbol{z},\lambda}$ is found to be approximately

$$N_{\boldsymbol{z},\lambda} \approx -\frac{\lambda}{\log\lambda_{\text{const}}}. \tag{4.66}$$

Assuming that the conditions (4.58) and (4.59) are satisfied while α is close to one and $\sqrt{\sigma_w^2 \bar{F}_{\boldsymbol{z}}^{\infty}} + \alpha > 1$ is satisfied, it is possible to use the approximation

$$\lambda_{\text{const}} \approx \left(\sqrt{\sigma_w^2 \bar{F}_{\boldsymbol{z}}^{\infty}} + \alpha \right)^{-2}. \tag{4.67}$$

In this case, the duration of the transient phase is

$$N_{\boldsymbol{z},\lambda} \approx \frac{\lambda}{2 \log \left(\sqrt{\sigma_w^2 \bar{F}_{\boldsymbol{z}}^{\infty}} + \alpha \right)}. \tag{4.68}$$

Specifying the additional relative delay N_Δ which is introduced by 1-bit quantization

$$N_\Delta = \frac{N_{\boldsymbol{z},\lambda}}{N_{\boldsymbol{y},\lambda}}, \tag{4.69}$$

where $N_{\boldsymbol{y},\lambda}$ is the duration of the transient phase for the ideal receive system, we find that

$$\begin{aligned} N_\Delta &\approx \frac{\log \left(\sqrt{\sigma_w^2 \bar{F}_{\boldsymbol{y}}^{\infty}} + \alpha \right)}{\log \left(\sqrt{\sigma_w^2 \bar{F}_{\boldsymbol{z}}^{\infty}} + \alpha \right)} \\ &\approx \sqrt{\frac{\bar{F}_{\boldsymbol{y}}^{\infty}}{\bar{F}_{\boldsymbol{z}}^{\infty}}}, \end{aligned} \tag{4.70}$$

independent of the choice of the steady-state accuracy λ. Further, with

$$\begin{aligned} \lim_{\gamma \to 0} \sqrt{\frac{\bar{F}_{\boldsymbol{y}}^{\infty}}{\bar{F}_{\boldsymbol{z}}^{\infty}}} &= \sqrt{\frac{\pi}{2}} \\ &\approx 1.25 \end{aligned} \tag{4.71}$$

it can be concluded that with slow state-space evolution ($\alpha \to 1$) and low SNR ($\gamma \to 0$), the transient phase $N_{\boldsymbol{z},\lambda}$ with the 1-bit receiver takes approximately 25% longer than with the ideal system.

4.4.3 Satellite-Based Synchronization at Low SNR

As an application, we consider a satellite-based synchronization problem where a transmitter $x(t)$ sends a known periodic signal of the form

$$x(t) = \sum_{c=-\infty}^{\infty} [\boldsymbol{c}]_{(1+\text{mod}(c,N_c))} g(t - cT_c). \tag{4.72}$$

The vector $\boldsymbol{c} \in \{-1, 1\}_c^N$ is a binary sequence with N_c symbols. Each symbol has a duration T_c and $g(t)$ is a band-limited rectangular transmit pulse. A Doppler-compensated receiver observes an attenuated and delayed copy of the transmit signal

$$\begin{aligned} y(t) &= \gamma s(t; \theta(t)) + \eta(t) \\ &= \gamma x(t - \tau(t)) + \eta(t) \end{aligned} \tag{4.73}$$

with AWGN $\eta(t)$ and time-delay $\tau(t)$. By band-limiting and sampling the analog signal (4.73) according to the sampling theorem, the ideal receiver obtains the digital receive signal

$$\boldsymbol{y}_n = \gamma \boldsymbol{s}(\tau_n) + \boldsymbol{\eta}_n, \tag{4.74}$$

while a low-cost 1-bit version of the receiver operates exclusively on the basis of the signal sign

$$\begin{aligned} \boldsymbol{z}_n &= \operatorname{sign}(\boldsymbol{y}_n) \\ &= \operatorname{sign}(\gamma \boldsymbol{s}(\tau_n) + \boldsymbol{\eta}_n). \end{aligned} \tag{4.75}$$

The temporal evolution of the time-delay parameter $\theta_n = \tau_n$ can be approximated by

$$\theta_n = \alpha \theta_{n-1} + w_n. \tag{4.76}$$

Note, that in this radio-based ranging example, α is related to the movement of transmitter and receiver. For simplicity, we assume that the state-space parameter α is constant over the considered amount of blocks and is known at the receiver. The receivers task is to estimate the distance to the transmitter in each observation block n by measuring the time-delay parameter $\hat{\tau}_n$.

Because the optimum estimator (3.60) is difficult to calculate in this situation we use a suboptimal nonlinear filter [54] for simulations. The particle filter is based on approximating the posterior probability of the parameter θ_n given all available data $\boldsymbol{Z}_n$

$$\begin{aligned} p(\theta_n|\boldsymbol{Z}_n) &\approx \sum_{k=1}^{K} a_n^k \delta(\theta_n - \theta_n^k) \\ &= \tilde{p}(\theta_n|\boldsymbol{Z}_n) \end{aligned} \tag{4.77}$$

by K particles θ_n^k. The particle weights $a_n^k \geq 0$ satisfy

$$\sum_{k=1}^{K} a_n^k = 1, \tag{4.78}$$

such that a sample-wise estimate $\hat{\theta}_n$ can be calculated by

$$\hat{\theta}_n = \sum_{k=1}^{K} a_n^k \theta_n^k. \tag{4.79}$$

Using the transition probability function $p(\theta_n|\theta_{n-1})$ as the importance density, the particle weights are updated recursively

$$\tilde{a}_n^k = a_{n-1}^k p(\boldsymbol{z}_n|\theta_n^k) \tag{4.80}$$

and normalized

$$a_n^k = \frac{\tilde{a}_n^k}{\sum_{k=1}^{K} \tilde{a}_n^k}, \tag{4.81}$$

in order to fulfill (4.78). If the effective number of particles

$$K_{\text{eff}} = \frac{1}{\sum_{k=1}^{K} (a_n^k)^2} \tag{4.82}$$

falls below a certain threshold K_{thresh}, i.e.,

$$K_{\text{eff}} \leq K_{\text{thresh}}, \tag{4.83}$$

a resampling step is performed, which replaces the particles by sampling K times from $\tilde{p}(\theta_n|\boldsymbol{Z}_n)$.

For simulations, we use the signal of the 5-th GPS satellite with $N_c = 1023$, $T_c = (1.023\,\text{MHz})^{-1}$ and a rectangular transmit pulse $g(t)$ [55]. According to the chip rate, the one-sided bandwidth of the receiver is set to $B = 1.023$ MHz. The sampling rate is set to $f_s = 2B$ and each observation has the duration $MT_s = 1$ ms, i.e., an observation vector contains $M = 2046$ data samples. The SNR is set to $\text{SNR} = -15.0$ dB. For the state-space model, we choose $\alpha = 1 - 10^{-3}$ and $\sigma_w = 10^{-3}$ and the initialization setup (4.31) is $\mu_0 = 398.7342 \cdot T_c$ and $\sigma_0 = 0.1 \cdot T_c$. For $N = 250$ blocks, we generate 100 delay processes and run the nonlinear filters with $K = 100$ particles for each delay process 1000 times with independent noise realizations while the resampling threshold is set to $K_{\text{thresh}} = 0.66K$. The results depicted in Fig. 4.1 show that the analytic range

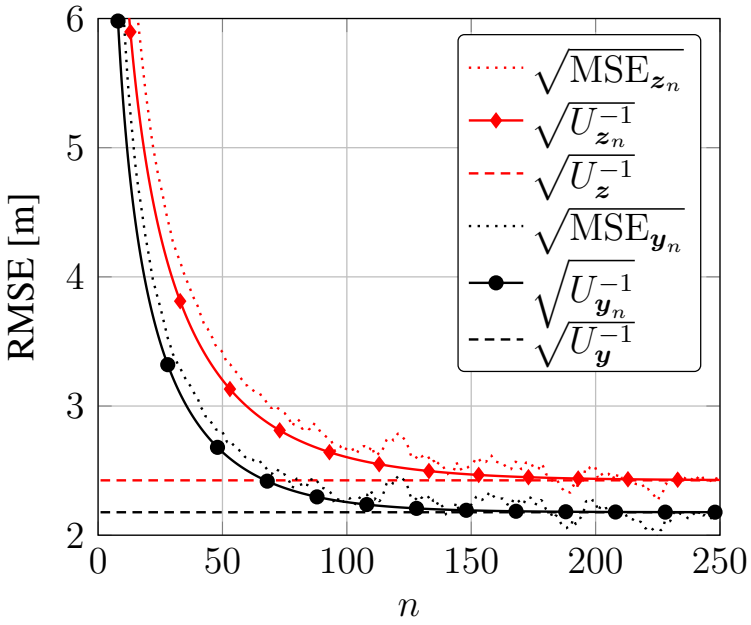

Fig. 4.1. Tracking Error - Ranging

tracking errors $U^{-1}_{\boldsymbol{z}_n}$ and $U^{-1}_{\boldsymbol{y}_n}$ in meter approach the asymptotic steady-state errors $U^{-1}_{\boldsymbol{z}}$ and $U^{-1}_{\boldsymbol{y}}$. Further, it can be observed that both nonlinear filters are efficient, such that the errors $\text{MSE}_{\boldsymbol{z}_n}$ and $\text{MSE}_{\boldsymbol{y}_n}$ reach the theoretic tracking bounds $U^{-1}_{\boldsymbol{z}_n}$ and $U^{-1}_{\boldsymbol{y}_n}$. Therefore, in Fig. 4.2, the quantization loss χ_n defined in (4.54) is visualized. It is observed that at the beginning of the tracking process, the performance gap between both receivers is moderate ($\chi_n = -1.38$ dB at $n = 1$), due to the same initial state-space uncertainty σ_0^2. In the transient phase, the quantization loss becomes quite pronounced ($\chi_n = -1.90$ dB at $n = 15$). While reaching the steady-state phase ($n > 250$), the loss converges to $\chi = -0.93$ dB.

4.4.4 UWB Channel Estimation at Low SNR

As a second application we consider the estimation of the channel quality in the context of ultra wide-band (UWB) communication. Similar to the satellite-based ranging problem, the receive

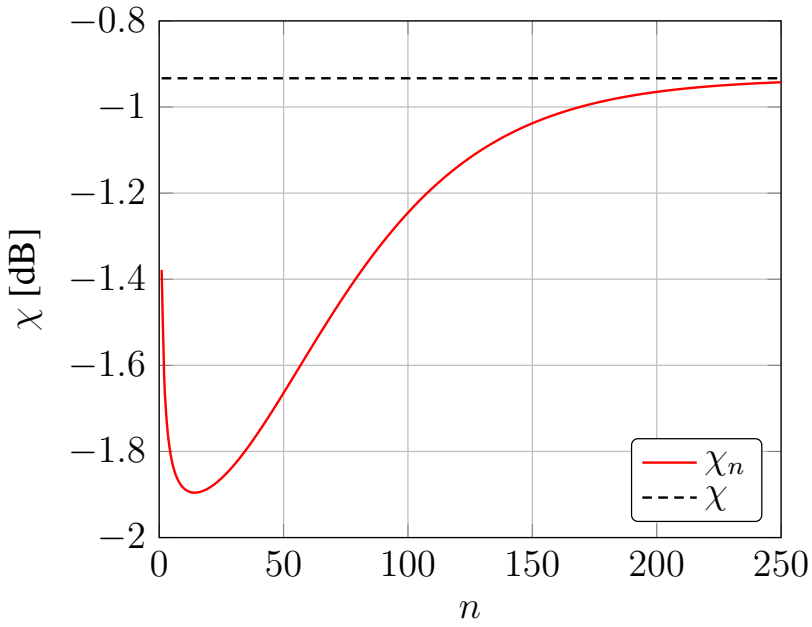

Fig. 4.2. 1-bit Tracking Loss - Ranging

signal of a synchronized receiver during a pilot phase can be modeled

$$\begin{aligned} \boldsymbol{y}_n &= \boldsymbol{s}(\theta_n) + \boldsymbol{\eta}_n \\ &= \gamma_n \boldsymbol{x}_n + \boldsymbol{\eta}_n, \end{aligned} \tag{4.84}$$

where $\boldsymbol{x}_n$ is the discrete-time form of a known pilot signal with analog structure as in (4.72) and γ_n is the signal receive strength. Note, that in contrast to the ranging problem, the parameter $\theta_n = \gamma_n$ in the ideal receive model (4.84) shows up in a linear form. The task of a low-cost 1-bit UWB receiver

$$\begin{aligned} \boldsymbol{z}_n &= \operatorname{sign}(\boldsymbol{y}) \\ &= \operatorname{sign}(\gamma_n \boldsymbol{x}_n + \boldsymbol{\eta}_n) \end{aligned} \tag{4.85}$$

is to estimate the signal attenuation $\hat{\gamma}_n$ for each pilot block, while the channel coefficient $\gamma_n = \theta_n$ follows the temporal evolution model (4.27). In contrast to the ranging application, we assume $B = 528$ MHz, a Nyquist transmit pulse $g(t)$ of bandwidth B and $N_c = 10$ symbols with $\mathrm{SNR}_{\mathrm{dB}} = -15.0$ dB. The state-space model parameters are $\alpha = 1 - 10^{-4}$ and $\sigma_w = \sqrt{(1-\alpha^2)\,\mathrm{SNR}}$. The initialization setup is $\mu_0 = \sqrt{\mathrm{SNR}}$ and $\sigma_0 = 0.05$. In Fig. 4.3 it can be seen that, like in the ranging application, the nonlinear filters, simulated with 1000 channel coefficient processes and 100 independent noise realizations, perform efficiently and therefore close to the tracking bounds $U_{\boldsymbol{z}_n}^{-1}$ or $U_{\boldsymbol{y}_n}^{-1}$. These bounds asymptotically equal the analytic steady-state errors $U_{\boldsymbol{z}}^{-1}$ and $U_{\boldsymbol{y}}^{-1}$. In Fig. 4.4, the performance loss χ_n is depicted in dB. As in the ranging problem, it is observed that the loss after the initial transient phase recovers and approaches $\chi_n = -1.02$ dB. Note that for both of the considered applications, the asymptotic loss is slightly different from $\chi = -0.98$ dB, as the low SNR and the slow channel evolution assumption are not fully valid for the chosen simulation setups.

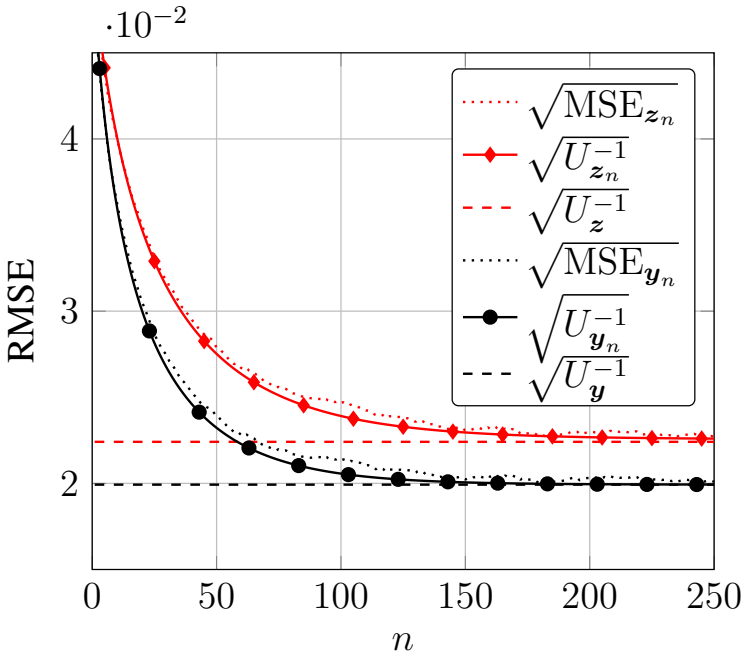

Fig. 4.3. Tracking Error - UWB Channel Estimation

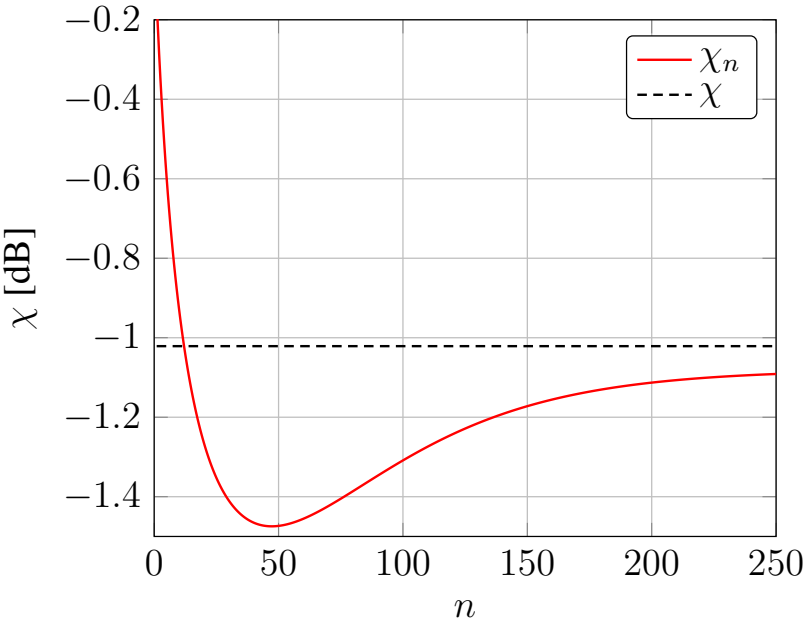

Fig. 4.4. 1-bit Tracking Loss - UWB Channel Estimation

4.5 Hard-Limiting Loss with Unknown Quantization Threshold

Up to this point, we have considered receive systems with 1-bit ADC which can be modeled by a symmetric hard-limiting operation (4.11). However in practice the ADC will exhibit a quantization offset which is different from zero. One could argue that in such a case the threshold can be adjusted during runtime. However, a problem that arises when the quantization level of a 1-bit ADC is to be controlled, is the fact that a high resolution digital-to-analog converter (DAC) is required in order to set an analog offset voltage source. As the complexity of DACs scales $\mathcal{O}(2^b)$ with the number of bits b, this stands in contradiction with the main motivation behind 1-bit ADC technology, which is an energy and hardware efficient radio front-end. Therefore, low-complexity 1-bit ADCs will lack the feature of an accurately adjustable quantization level. Rather, a low-cost sampling device will be constructed such that the hard-limiting level is fixed to a constant value. Inevitable mismatches of the circuit parts during the production process and external effects will lead to an unknown quantization level of the sampler, such that calibration or a method which estimates and compensates the unknown threshold during runtime is required.

Therefore in this section, the performance loss associated with 1-bit quantization and an unknown threshold is analyzed for the application of pilot-based channel estimation. The problem is studied under the assumption that the channel parameter and the quantization level are deterministic unknown. We characterize the optimal performance in the asymptotic regime, which is associated with the maximum likelihood estimator (MLE) for the deterministic setup and analyze the 1-bit loss with unknown quantization level.

For the discussion we consider the problem of pilot-based receive strength estimation. Therefore, the digital signal model of the ideal receive system with infinite resolution is given by

$$\begin{aligned} \boldsymbol{y} &= \boldsymbol{s}(\theta) + \boldsymbol{\eta} \\ &= \gamma \boldsymbol{x} + \boldsymbol{\eta}, \end{aligned} \tag{4.86}$$

where $\boldsymbol{x} \in \mathbb{R}^N$ is a pilot signal of known structure, $\gamma \in \mathbb{R}$ characterizes the signal receive strength and $\boldsymbol{\eta} \in \mathbb{R}^N$ is AWGN with elements of unit variance. For simplicity, we assume a phase-shift keying (BPSK) transmitter and a synchronized receiver such that $\boldsymbol{x} \in \{-1, 1\}^N$, where

$$\frac{1}{N} \sum_{n=1}^{N} x_n = 0. \tag{4.87}$$

The low-complexity receiver is equipped with a 1-bit ADC which provides the digital signal

$$\begin{aligned} \boldsymbol{z} &= \operatorname{sign}\left(\boldsymbol{y} - \upsilon \mathbf{1}_N\right) \\ &= \operatorname{sign}\left(\gamma \boldsymbol{x} + \boldsymbol{\eta} - \upsilon \mathbf{1}_N\right), \end{aligned} \tag{4.88}$$

where $\mathbf{1}_N \in \mathbb{R}^N$ denotes the all-ones vector and $\upsilon \in \mathbb{R}$ forms an unknown threshold level. With $\theta = \gamma$ the conditional probability density function of the resulting binary received signal is

$$p(\boldsymbol{z}; \theta, \upsilon) = \prod_{n=1}^{N} \mathrm{Q}\left(z_n(\upsilon - \theta x_n)\right). \tag{4.89}$$

Under the assumption that the ideal receiver treats θ as deterministic unknown, the asymptotically optimum unbiased estimator is the maximum likelihood estimator (MLE)

$$\begin{aligned}\hat{\theta}(\boldsymbol{y}) &\triangleq \arg\max_{\theta\in\Theta} p(\boldsymbol{y};\theta)\\ &= \arg\max_{\theta\in\Theta} \sum_{n=1}^{N} \ln p(y_n;\theta),\end{aligned} \tag{4.90}$$

with the corresponding MSE

$$\mathrm{MSE}_{\boldsymbol{y}}(\theta) \triangleq \mathrm{E}_{\boldsymbol{y};\theta}\left[\left(\hat{\theta}(\boldsymbol{y})-\theta\right)^2\right]. \tag{4.91}$$

The 1-bit receiver considers the signal strength parameter θ and the threshold υ as deterministic unknown. The MLE is therefore based on joint estimation of the parameter θ and the threshold υ, such that

$$\begin{aligned}\begin{bmatrix}\hat{\theta}(\boldsymbol{z}) & \hat{\upsilon}(\boldsymbol{z})\end{bmatrix}^{\mathrm{T}} &\triangleq \arg\max_{\theta\in\Theta,\upsilon\in\mathbb{R}} p(\boldsymbol{z};\theta,\upsilon)\\ &= \arg\max_{\theta\in\Theta,\upsilon\in\mathbb{R}} \sum_{n=1}^{N} \ln p(z_n;\theta,\upsilon),\end{aligned} \tag{4.92}$$

with the corresponding error

$$\mathrm{MSE}_{\boldsymbol{z}}(\theta,\upsilon) \triangleq \mathrm{E}_{\boldsymbol{z};\theta,\upsilon}\left[\left(\hat{\theta}(\boldsymbol{z})-\theta\right)^2\right]. \tag{4.93}$$

For the ideal receiver and estimation with the MLE, the MSE can be approximated asymptotically by the CRLB

$$\mathrm{MSE}_{\boldsymbol{y}}(\theta) \overset{\mathrm{a}}{=} F_{\boldsymbol{y}}^{-1}(\theta), \tag{4.94}$$

where with (4.86) the Fisher information measure is found to be

$$\begin{aligned}F_{\boldsymbol{y}}(\theta) &= \mathrm{E}_{\boldsymbol{y};\theta}\left[\left(\frac{\partial \ln p(\boldsymbol{y};\theta)}{\partial\theta}\right)^2\right]\\ &= \sum_{n=1}^{N} x_n^2\\ &= N.\end{aligned} \tag{4.95}$$

For the 1-bit receiver, the estimation of the threshold $\hat{\upsilon}(\boldsymbol{z})$ has an effect onto the inference of the attenuation parameter $\hat{\theta}(\boldsymbol{z})$. The corresponding CRLB for the estimator $\hat{\theta}(\boldsymbol{z})$ is

$$\mathrm{MSE}_{\boldsymbol{z}}(\theta,\upsilon) \overset{\mathrm{a}}{=} \frac{F_{\boldsymbol{z},\upsilon\upsilon}(\theta,\upsilon)}{F_{\boldsymbol{z},\theta\theta}(\theta,\upsilon)F_{\boldsymbol{z},\upsilon\upsilon}(\theta,\upsilon) - F_{\boldsymbol{z},\theta\upsilon}^2(\theta,\upsilon)}. \tag{4.96}$$

The required individual Fisher information measures are given by

$$\begin{aligned} F_{\boldsymbol{z},\theta\theta}(\theta,\upsilon) &= \mathrm{E}_{\boldsymbol{z};\theta,\upsilon}\left[\left(\frac{\partial \ln p(\boldsymbol{z};\theta,\upsilon)}{\partial\theta}\right)^2\right] \\ &= \sum_{n=1}^{N} \mathrm{E}_{z_n;\theta,\upsilon}\left[\frac{x_n^2 \exp\left(-(\upsilon-\theta x_n)^2\right)}{2\pi\,\mathrm{Q}^2\left(z_n(\upsilon-\theta x_n)\right)}\right] \\ &= \sum_{n=1}^{N} \frac{x_n^2 \exp\left(-(\upsilon-\theta x_n)^2\right)}{2\pi\big(\,\mathrm{Q}\left(\upsilon-\theta x_n\right)-\mathrm{Q}^2\left(\upsilon-\theta x_n\right)\big)} \\ &= \frac{N}{2}\big(\psi_+(\theta,\upsilon)+\psi_-(\theta,\upsilon)\big), \end{aligned} \tag{4.97}$$

where the third equality is due to the fact that with (4.89)

$$\begin{aligned} \mathrm{E}_{z_n;\theta,\upsilon}\left[\frac{1}{\mathrm{Q}^2\left(z_n(\upsilon-\theta x_n)\right)}\right] &= \sum_{z_n=\pm 1} \frac{\mathrm{Q}\left(z_n(\upsilon-\theta x_n)\right)}{\mathrm{Q}^2\left(z_n(\upsilon-\theta x_n)\right)} \\ &= \frac{1}{\mathrm{Q}\left(\upsilon-\theta x_n\right)-\mathrm{Q}^2\left(\upsilon-\theta x_n\right)} \end{aligned} \tag{4.98}$$

and the last equality in (4.97) stems from the BPSK modulation of $\boldsymbol{x}$ and the definition

$$\psi_\pm(\theta,\upsilon) \triangleq \frac{\exp\left(-(\upsilon\pm\theta)^2\right)}{2\pi\big(\,\mathrm{Q}\left(\upsilon\pm\theta\right)-\mathrm{Q}^2\left(\upsilon\pm\theta\right)\big)}. \tag{4.99}$$

Along the same lines, we have

$$\begin{aligned} F_{\boldsymbol{z},\upsilon\upsilon}(\theta,\upsilon) &= \mathrm{E}_{\boldsymbol{z};\theta,\upsilon}\left[\left(\frac{\partial \ln p(\boldsymbol{z};\theta,\upsilon)}{\partial\upsilon}\right)^2\right] \\ &= \sum_{n=1}^{N} \mathrm{E}_{z_n;\theta,\upsilon}\left[\frac{\exp\left(-(\upsilon-\theta x_n)^2\right)}{2\pi\,\mathrm{Q}^2\left(z_n(\upsilon-\theta x_n)\right)}\right] \\ &= \frac{M}{2}\big(\psi_+(\theta,\upsilon)+\psi_-(\theta,\upsilon)\big) \end{aligned} \tag{4.100}$$

and

$$\begin{aligned} F_{\boldsymbol{z},\theta\alpha}(\theta,\upsilon) &= \mathrm{E}_{\boldsymbol{z};\theta,\upsilon}\left[\frac{\partial \ln p(\boldsymbol{z};\theta,\upsilon)}{\partial\theta}\frac{\partial \ln p(\boldsymbol{z};\theta,\upsilon)}{\partial\upsilon}\right] \\ &= -\sum_{n=1}^{N} \mathrm{E}_{z_n;\theta,\upsilon}\left[\frac{x_n \exp\left(-(\upsilon-\theta x_n)^2\right)}{2\pi\,\mathrm{Q}^2\left(z_n(\upsilon-\theta x_n)\right)}\right] \\ &= \frac{N}{2}\big(\psi_+(\theta,\upsilon)-\psi_-(\theta,\upsilon)\big). \end{aligned} \tag{4.101}$$

Note that if the quantization level υ is known to the 1-bit receiver, the asymptotic performance is

$$\mathrm{MSE}^{\star}_{\boldsymbol{z}}(\theta,\upsilon) \overset{\mathrm{a}}{=} F^{-1}_{\boldsymbol{z},\theta\theta}(\theta,\upsilon). \tag{4.102}$$

To characterize the information loss introduced by the hard-limiter, we define the quantization loss via the two MSE ratios

$$\begin{aligned}\chi(\theta,\upsilon) &\triangleq \frac{\mathrm{MSE}_{\boldsymbol{y}}(\theta)}{\mathrm{MSE}_{\boldsymbol{z}}(\theta,\upsilon)} \\ &\overset{\text{a}}{=} \frac{F_{\boldsymbol{z},\theta\theta}(\theta,\upsilon)F_{\boldsymbol{z},\upsilon\upsilon}(\theta,\upsilon) - F^2_{\boldsymbol{z},\theta\upsilon}(\theta,\upsilon)}{F_{\boldsymbol{z},\upsilon\upsilon}(\theta,\upsilon)F_{\boldsymbol{y},\theta\theta}(\theta)} \\ &= 2\frac{\psi_+(\theta,\upsilon)\psi_-(\theta,\upsilon)}{\psi_+(\theta,\upsilon)+\psi_-(\theta,\upsilon)}\end{aligned} \tag{4.103}$$

and

$$\begin{aligned}\chi^\star(\theta,\upsilon) &\triangleq \frac{\mathrm{MSE}_{\boldsymbol{y}}(\theta)}{\mathrm{MSE}^\star_{\boldsymbol{z}}(\theta,\upsilon)} \\ &\overset{\text{a}}{=} \frac{F_{\boldsymbol{z},\theta\theta}(\theta,\upsilon)}{F_{\boldsymbol{y},\theta\theta}(\theta)} \\ &= \frac{1}{2}\big(\psi_+(\theta,\upsilon)+\psi_-(\theta,\upsilon)\big).\end{aligned} \tag{4.104}$$

Fig. 4.5 shows the performance loss (4.103) for different SNR levels in solid lines, where we use the convention SNR $= \gamma^2$. Note that the loss is symmetric for negative thresholds υ. The

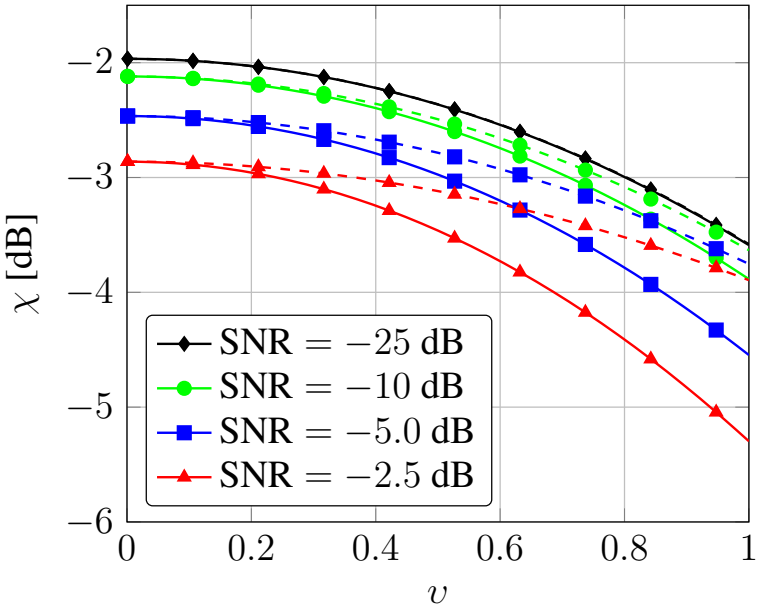

Fig. 4.5. Quantization Loss - χ (solid) and $\chi^\star$ (dashed)

results show that for the considered application, a quantization level υ close to zero is in general preferable and that the performance gap increases with the SNR. Additionally, with dashed lines, Fig. 4.5 shows the alternative loss (4.104) with known quantization level. While in the low SNR regime the estimation of υ has no effect onto the estimation of θ, the situation changes within the medium SNR regime. Here the fact that the threshold is known can have a beneficial effect, in particular when υ is far from zero.

The discussion shows that in the low SNR regime the negative effect of the unknown offset υ onto the performance of $\hat{\theta}(\boldsymbol{z})$ vanishes. This confirms that 1-bit ADCs are an interesting option for low SNR applications. For signal processing with 1-bit ADCs in the medium SNR regime careful hardware design is required such that the threshold υ is close to the symmetric case.

4.6 Hard-Limiting Loss with Correlated Noise Models

On the last pages, we have restricted the discussion to the characterization of the hard-limiting loss for system models of the form

$$\boldsymbol{y} = \boldsymbol{s}(\boldsymbol{\theta}) + \boldsymbol{\eta}, \tag{4.105}$$

where the noise covariance matrix exhibits a diagonal structure

$$\mathrm{E}_{\boldsymbol{\eta}}\left[\boldsymbol{\eta}\boldsymbol{\eta}^{\mathrm{T}}\right] = \boldsymbol{I}_M. \tag{4.106}$$

When taking into consideration a more general class of problems, where the covariance has a generic structure

$$\mathrm{E}_{\boldsymbol{\eta}}\left[\boldsymbol{\eta}\boldsymbol{\eta}^{\mathrm{T}}\right] = \boldsymbol{R}_{\boldsymbol{\eta}}, \tag{4.107}$$

for the ideal receiver we obtain the measurement model with correlated noise

$$p(\boldsymbol{y};\boldsymbol{\theta}) = \frac{1}{(2\pi)^{\frac{N}{2}}\sqrt{\det \boldsymbol{R}_{\boldsymbol{\eta}}}} \exp\left(-\frac{1}{2}\big(\boldsymbol{y}-\boldsymbol{s}(\boldsymbol{\theta})\big)^{\mathrm{T}}\boldsymbol{R}_{\boldsymbol{\eta}}^{-1}\big(\boldsymbol{y}-\boldsymbol{s}(\boldsymbol{\theta})\big)\right). \tag{4.108}$$

With N observation blocks, for such a model we find the MLE by solving

$$\begin{aligned}\hat{\theta}(\boldsymbol{Y}) &= \arg\max_{\boldsymbol{\theta}\in\boldsymbol{\Theta}} \ln p(\boldsymbol{Y};\boldsymbol{\theta}) \\ &= \arg\max_{\boldsymbol{\theta}\in\boldsymbol{\Theta}} \sum_{n=1}^{N} \ln p(\boldsymbol{y}_n;\boldsymbol{\theta}) \\ &= \arg\min_{\boldsymbol{\theta}\in\boldsymbol{\Theta}} \sum_{n=1}^{N} \big(\boldsymbol{y}_n-\boldsymbol{s}(\boldsymbol{\theta})\big)^{\mathrm{T}}\boldsymbol{R}_{\boldsymbol{\eta}}^{-1}\big(\boldsymbol{y}_n-\boldsymbol{s}(\boldsymbol{\theta})\big).\end{aligned} \tag{4.109}$$

With the property of the Gaussian score

$$\left(\frac{\partial \ln p(\boldsymbol{y};\boldsymbol{\theta})}{\partial \boldsymbol{\theta}}\right)^{\mathrm{T}} = \left(\frac{\partial \boldsymbol{s}(\boldsymbol{\theta})}{\partial \boldsymbol{\theta}}\right)^{\mathrm{T}} \boldsymbol{R}_{\boldsymbol{\eta}}^{-1}\big(\boldsymbol{y}-\boldsymbol{s}(\boldsymbol{\theta})\big), \tag{4.110}$$

the problem of solving the MLE optimization problem (4.109) with respect to $\boldsymbol{\theta}$ can be formulated equivalently as finding the root

$$\sum_{n=1}^{N}\left(\frac{\partial \boldsymbol{s}(\boldsymbol{\theta})}{\partial \boldsymbol{\theta}}\right)^{\mathrm{T}} \boldsymbol{R}_{\boldsymbol{\eta}}^{-1}\big(\boldsymbol{y}_n-\boldsymbol{s}(\boldsymbol{\theta})\big) = \boldsymbol{0} \tag{4.111}$$

or

$$\left(\frac{\partial \boldsymbol{s}(\boldsymbol{\theta})}{\partial \boldsymbol{\theta}}\right)^{\mathrm{T}} \boldsymbol{R}_{\boldsymbol{\eta}}^{-1}\big(\bar{\boldsymbol{y}}-\boldsymbol{s}(\boldsymbol{\theta})\big) = \boldsymbol{0}, \tag{4.112}$$

where we denote the sample mean by

$$\bar{\boldsymbol{y}} = \frac{1}{N}\sum_{n=1}^{N} \boldsymbol{y}_n. \tag{4.113}$$

Note, that with (4.110) the Fisher information measure of the multivariate model (4.108) is directly available by

$$\begin{aligned}
\boldsymbol{F}_{\boldsymbol{y}}(\boldsymbol{\theta}) &= \mathrm{E}_{\boldsymbol{y};\boldsymbol{\theta}}\left[\left(\frac{\partial \ln p(\boldsymbol{y};\boldsymbol{\theta})}{\partial \boldsymbol{\theta}}\right)^{\mathrm{T}} \frac{\partial \ln p(\boldsymbol{y};\boldsymbol{\theta})}{\partial \boldsymbol{\theta}}\right] \\
&= \mathrm{E}_{\boldsymbol{y};\boldsymbol{\theta}}\left[\left(\frac{\partial \boldsymbol{s}(\boldsymbol{\theta})}{\partial \boldsymbol{\theta}}\right)^{\mathrm{T}} \boldsymbol{R}_{\boldsymbol{\eta}}^{-1}\big(\boldsymbol{y}-\boldsymbol{s}(\boldsymbol{\theta})\big)\big(\boldsymbol{y}-\boldsymbol{s}(\boldsymbol{\theta})\big)^{\mathrm{T}} \boldsymbol{R}_{\boldsymbol{\eta}}^{-1} \frac{\partial \boldsymbol{s}(\boldsymbol{\theta})}{\partial \boldsymbol{\theta}}\right] \\
&= \left(\frac{\partial \boldsymbol{s}(\boldsymbol{\theta})}{\partial \boldsymbol{\theta}}\right)^{\mathrm{T}} \boldsymbol{R}_{\boldsymbol{\eta}}^{-1}\, \mathrm{E}_{\boldsymbol{y};\boldsymbol{\theta}}\left[\big(\boldsymbol{y}-\boldsymbol{s}(\boldsymbol{\theta})\big)\big(\boldsymbol{y}-\boldsymbol{s}(\boldsymbol{\theta})\big)^{\mathrm{T}}\right] \boldsymbol{R}_{\boldsymbol{\eta}}^{-1} \frac{\partial \boldsymbol{s}(\boldsymbol{\theta})}{\partial \boldsymbol{\theta}} \\
&= \left(\frac{\partial \boldsymbol{s}(\boldsymbol{\theta})}{\partial \boldsymbol{\theta}}\right)^{\mathrm{T}} \boldsymbol{R}_{\boldsymbol{\eta}}^{-1} \frac{\partial \boldsymbol{s}(\boldsymbol{\theta})}{\partial \boldsymbol{\theta}}.
\end{aligned} \tag{4.114}$$

A second important multivariate model in statistical signal processing is a multivariate Gaussian distribution with zero-mean and parametric covariance

$$\boldsymbol{R}_{\boldsymbol{y}}(\boldsymbol{\theta}) = \mathrm{E}_{\boldsymbol{y};\boldsymbol{\theta}}\left[\boldsymbol{y}\boldsymbol{y}^{\mathrm{T}}\right], \tag{4.115}$$

such that the parametric probability density function of the receive signal is given by

$$p(\boldsymbol{y};\boldsymbol{\theta}) = \frac{1}{(2\pi)^{\frac{N}{2}}\sqrt{\det \boldsymbol{R}_{\boldsymbol{y}}(\boldsymbol{\theta})}} \exp\left(-\frac{1}{2}\boldsymbol{y}^{\mathrm{T}}\boldsymbol{R}_{\boldsymbol{y}}^{-1}(\boldsymbol{\theta})\boldsymbol{y}\right). \tag{4.116}$$

Given N independent data snapshots $\boldsymbol{y}$, maximizing the likelihood is performed by calculating

$$\begin{aligned}
\hat{\boldsymbol{\theta}}(\boldsymbol{Y}) &= \arg\max_{\boldsymbol{\theta}\in\Theta} \ln p(\boldsymbol{Y};\boldsymbol{\theta}) \\
&= \arg\max_{\boldsymbol{\theta}\in\Theta} \sum_{n=1}^{N} \ln p(\boldsymbol{y}_n;\boldsymbol{\theta}) \\
&= \arg\min_{\boldsymbol{\theta}\in\Theta} \ln\big(\det \boldsymbol{R}_{\boldsymbol{y}}(\boldsymbol{\theta})\big) + \mathrm{Tr}\left(\bar{\boldsymbol{R}}_{\boldsymbol{y}}(\boldsymbol{Y})\boldsymbol{R}_{\boldsymbol{y}}^{-1}(\boldsymbol{\theta})\right),
\end{aligned} \tag{4.117}$$

where the sample mean covariance matrix is given by

$$\bar{\boldsymbol{R}}_{\boldsymbol{y}}(\boldsymbol{Y}) = \frac{1}{N}\sum_{n=1}^{N} \boldsymbol{y}_n\boldsymbol{y}_n^{\mathrm{T}}. \tag{4.118}$$

For the case of a single parameter θ, we obtain the Fisher information of (4.116) by [2, p. 47]

$$F_{\boldsymbol{y}}(\theta) = \frac{1}{2}\,\mathrm{Tr}\left(\boldsymbol{R}_{\boldsymbol{y}}^{-1}(\theta)\frac{\partial \boldsymbol{R}_{\boldsymbol{y}}(\theta)}{\partial \theta}\boldsymbol{R}_{\boldsymbol{y}}^{-1}(\theta)\frac{\partial \boldsymbol{R}_{\boldsymbol{y}}(\theta)}{\partial \theta}\right). \tag{4.119}$$

4.6.1 Likelihood Representation with Hard-Limiting and Correlated Noise

The situation changes fundamentally if a nonlinear transformation

$$\boldsymbol{z} = \boldsymbol{f}(\boldsymbol{y}) \tag{4.120}$$

is involved. In the case where we wish to process the output data $\boldsymbol{z}$ with the efficient approach of maximizing the likelihood (3.8), an exact representation of the parametric output model $p(\boldsymbol{z};\boldsymbol{\theta})$ is required. In general the likelihood of the transformed output (4.120) is found by evaluating an integral of the form

$$p(\boldsymbol{z};\boldsymbol{\theta}) = \int_{\boldsymbol{\mathcal{Y}}(\boldsymbol{z})} p(\boldsymbol{y};\boldsymbol{\theta})\mathrm{d}\boldsymbol{y}, \tag{4.121}$$

where $\boldsymbol{\mathcal{Y}}(\boldsymbol{z})$ is the subset of $\boldsymbol{\mathcal{Y}}$ which is mapped by $\boldsymbol{f}(\cdot)$ to the output signal $\boldsymbol{z}$. In the case of a element-wise hard-limiter

$$\boldsymbol{z} = \operatorname{sign}(\boldsymbol{y}), \tag{4.122}$$

computation of such an integral requires the orthant probability of a multivariate Gaussian variable (multivariate version of the Q-function (4.15)). Unfortunately, a general compact expression for the orthant probability is an open mathematical problem. Only for the cases $M \leq 4$ solutions are provided in literature [56] [57]. The problem becomes even worse, if one is interested in analytically evaluating the estimation performance of the 1-bit receive system. The associated Fisher information matrix

$$\begin{aligned}\boldsymbol{F}_{\boldsymbol{z}}(\boldsymbol{\theta}) &= \int_{\boldsymbol{\mathcal{Z}}} \left(\frac{\partial \ln p(\boldsymbol{z};\boldsymbol{\theta})}{\partial \boldsymbol{\theta}}\right)^{\mathrm{T}} \frac{\partial \ln p(\boldsymbol{z};\boldsymbol{\theta})}{\partial \boldsymbol{\theta}} \mathrm{d}\boldsymbol{z} \\ &= \sum_{\boldsymbol{\mathcal{Z}}} \left(\frac{\partial \ln p(\boldsymbol{z};\boldsymbol{\theta})}{\partial \boldsymbol{\theta}}\right)^{\mathrm{T}} \frac{\partial \ln p(\boldsymbol{z};\boldsymbol{\theta})}{\partial \boldsymbol{\theta}}\end{aligned} \tag{4.123}$$

is computed by summing the outer product of the score function over the discrete support of $\boldsymbol{z}$. As $\boldsymbol{\mathcal{Z}}$ contains 2^M possible receive constellations, direct computation of $F_{\boldsymbol{z}}(\boldsymbol{\theta})$ is prohibitively complex when the dimensionality M of the model (4.122) is large.

4.6.2 Bussgang Decomposition for Hard-Limited Noisy Signals

In the context of communication theory, [53] [58] show that for

$$\boldsymbol{x} \sim \mathcal{N}(\boldsymbol{0}, \boldsymbol{R}_{\boldsymbol{x}}), \quad \boldsymbol{\eta} \sim \mathcal{N}(\boldsymbol{0}, \boldsymbol{R}_{\boldsymbol{\eta}}), \tag{4.124}$$

the transmission line

$$\begin{aligned}\boldsymbol{z} &= \operatorname{sign}(\boldsymbol{y}) \\ &= \operatorname{sign}(\boldsymbol{x} + \boldsymbol{\eta})\end{aligned} \tag{4.125}$$

can be approximated through a Bussgang decomposition

$$\boldsymbol{z} \approx \boldsymbol{x}' + \boldsymbol{\eta}', \tag{4.126}$$

where the random variables follow Gaussian probability laws

$$\boldsymbol{x}' \sim \mathcal{N}\left(\mathbf{0}, \boldsymbol{R}_{\boldsymbol{x}'}\right), \tag{4.127}$$

$$\boldsymbol{\eta}' \sim \mathcal{N}\left(\mathbf{0}, \boldsymbol{R}_{\boldsymbol{\eta}'}\right). \tag{4.128}$$

The corresponding covariance matrices of the Bussgang model (4.126) are

$$\boldsymbol{R}_{\boldsymbol{x}'} = \frac{2}{\pi} \operatorname{diag}\left(\boldsymbol{R}_{\boldsymbol{y}}\right)^{-\frac{1}{2}} \boldsymbol{R}_{\boldsymbol{x}} \operatorname{diag}\left(\boldsymbol{R}_{\boldsymbol{y}}\right)^{-\frac{1}{2}} \tag{4.129}$$

and

$$\begin{aligned} \boldsymbol{R}_{\boldsymbol{\eta}'} = & \frac{2}{\pi}\Big(\arcsin\big(\operatorname{diag}\left(\boldsymbol{R}_{\boldsymbol{y}}\right)^{-\frac{1}{2}} \boldsymbol{R}_{\boldsymbol{y}} \operatorname{diag}\left(\boldsymbol{R}_{\boldsymbol{y}}\right)^{-\frac{1}{2}} \big) \Big) \\ & - \frac{2}{\pi} \operatorname{diag}\left(\boldsymbol{R}_{\boldsymbol{y}}\right)^{-\frac{1}{2}} \boldsymbol{R}_{\boldsymbol{y}} \operatorname{diag}\left(\boldsymbol{R}_{\boldsymbol{y}}\right)^{-\frac{1}{2}} \\ & + \frac{2}{\pi} \operatorname{diag}\left(\boldsymbol{R}_{\boldsymbol{y}}\right)^{-\frac{1}{2}} \boldsymbol{R}_{\boldsymbol{\eta}} \operatorname{diag}\left(\boldsymbol{R}_{\boldsymbol{y}}\right)^{-\frac{1}{2}} \end{aligned} \tag{4.130}$$

with

$$\boldsymbol{R}_{\boldsymbol{y}} = \boldsymbol{R}_{\boldsymbol{x}} + \boldsymbol{R}_{\boldsymbol{\eta}}. \tag{4.131}$$

It can be shown that the model (4.126) provides a pessimistic equivalent system (in an information theoretic sense). To this end, it was proven in [53] [58] that the coding capacity of the transmission line (4.125) is in general lower bounded by

$$\max_{p(\boldsymbol{x})} I(\boldsymbol{x}; \boldsymbol{z}) \geq \frac{1}{2} \log_2 \det\left(\mathbf{1}_M + \boldsymbol{R}_{\boldsymbol{\eta}'}^{-1} \boldsymbol{R}_{\boldsymbol{x}'}\right), \tag{4.132}$$

where the right hand side of (4.132) is the capacity of the Bussgang model (4.126). For the problem of signal parameter estimation with a model (4.108), the decomposition (4.126) can not be applied as the input to the quantizer $\boldsymbol{y}$ is not zero-mean. While this is the case for models like (4.116), by the result (4.132) it is not guaranteed that the Bussgang approach (4.126) forms an equivalent pessimistic replacement model with respect to Fisher information (estimation theoretic sense).

5. Fisher Information and the Exponential Replacement

In the preceding chapters, it has become evident that the Fisher information measure [3] [4] is a strong estimation theoretic tool which provides access to the fundamental quality of a parametric system with respect to the inference of its unknown parameters. In particular for Gaussian models (4.108) (4.116), the information measure forms a method to characterize the capability of the system with respect to the estimation problem in a compact way (4.114) (4.119). However, as demonstrated with the simple example of a hard-limited multivariate Gaussian system (4.122), the calculation of the Fisher information can become intractable already for simple nonlinear transformations of the receive signal. Further, in the situation where the system model $p(\boldsymbol{z};\boldsymbol{\theta})$ is not available in an analytical form, the Fisher information measure can not be determined. This forms a fundamental problem for the analysis of real-world signal processing systems which exhibit nonlinear effects like saturation, phase distortion and quantization. After such nonlinear transformations of the sensor signals the characterization of the likelihood function $p(\boldsymbol{z};\boldsymbol{\theta})$ and the assessment of the estimation theoretic quality of the resulting output model becomes challenging. Taking into account all nonlinear effects and internal noise sources usually results in a situation where the output model $p(\boldsymbol{z};\boldsymbol{\theta})$ is mathematically intractable such that it can only be determined in a measurement-driven way.

In this chapter we will show that compact pessimistic approximations for the Fisher information measure can be obtained [59] [60]. These lower bounds are based on the parametric characterization of the moments of the system output $\boldsymbol{z}$ (or a transformed version of it) which usually are better tractable then the likelihood function $p(\boldsymbol{z};\boldsymbol{\theta})$ itself. We generalize these results by replacing the actual system model by an equivalent distribution in the exponential family and show how to obtain a practical algorithm which achieves the performance guaranteed by the inverse of the pessimistic Fisher information measure. Finally, we discuss the connection between the concept of maximum likelihood and the generalized method of moments which can be established by the exponential replacement. With various examples we try to outline some practical and estimation theoretic problems where the presented results turn out useful and provide interesting insights.

5.1 First-Order Fisher Information Lower Bound

For the initial discussion, consider an univariate parametric system, characterized by a probability distribution function $p(z;\theta)$, with a single parameter $\theta \in \Theta$ and a random output $z \in \mathcal{Z}$, where $\mathcal{Z}$ denotes the support of z. Further, we assume that $p(z;\theta)$ takes a complicated or intractable analytic form. In order to determine the fundamental estimation theoretic performance of $p(z;\theta)$, we follow

the idea of approximating the true information measure

$$F_z(\theta) \triangleq \int_{\mathcal{Z}} \left(\frac{\partial \ln p(z;\theta)}{\partial \theta} \right)^2 p(z;\theta) \mathrm{d}z \tag{5.1}$$

from below [59], i.e.,

$$F_z(\theta) \geq \tilde{F}_z(\theta), \tag{5.2}$$

where $\tilde{F}_z(\theta)$ is a pessimistic version of the Fisher information measure.

5.1.1 Derivation of the Fisher Information Lower Bound

To this end, we use the Cauchy-Schwarz inequality [61] which states that for two real-valued functions $f(\cdot)$ and $g(\cdot)$

$$\int_{\boldsymbol{\mathcal{X}}} f^2(\boldsymbol{x}) p(\boldsymbol{x}) \mathrm{d}\boldsymbol{x} \int_{\boldsymbol{\mathcal{X}}} g^2(\boldsymbol{x}) p(\boldsymbol{x}) \mathrm{d}\boldsymbol{x} \geq \left(\int_{\boldsymbol{\mathcal{X}}} f(\boldsymbol{x}) g(\boldsymbol{x}) p(\boldsymbol{x}) \mathrm{d}\boldsymbol{x} \right)^2. \tag{5.3}$$

Applying the inequality (5.3) with

$$f(z;\theta) = \frac{\partial \ln p(z;\theta)}{\partial \theta} \tag{5.4}$$

and a generic function $g(z;\theta)$ in order to lower bound the Fisher information

$$F_z(\theta) = \int_{\mathcal{Z}} f^2(z;\theta) p(z;\theta) \mathrm{d}z, \tag{5.5}$$

we obtain the generic pessimistic approximation

$$\begin{aligned} F_z(\theta) &= \int_{\mathcal{Z}} \left(\frac{\partial \log p(z;\theta)}{\partial \theta} \right)^2 p(z;\theta) \mathrm{d}z \\ &\geq \frac{\left(\int_{\mathcal{Z}} g(z;\theta) \frac{\partial \log p(z;\theta)}{\partial \theta} p(z;\theta) \mathrm{d}z \right)^2}{\int_{\mathcal{Z}} g^2(z;\theta) p(z;\theta) \mathrm{d}z} \\ &= \tilde{F}_z(\theta). \end{aligned} \tag{5.6}$$

In the following we discuss two different choices for the function $g(z;\theta)$. For

$$g(z;\theta) = z - \mu_1(\theta), \tag{5.7}$$

where the output mean $\mu_1(\theta)$ is given by

$$\mu_1(\theta) \triangleq \int_{\mathcal{Z}} z p(z;\theta) \mathrm{d}z, \tag{5.8}$$

it follows that

$$\begin{aligned}\int_{\mathcal{Z}} g(z;\theta)\frac{\partial \log p(z;\theta)}{\partial\theta}p(z;\theta)\mathrm{d}z &= \int_{\mathcal{Z}} \big(z-\mu_1(\theta)\big)\frac{\partial \log p(z;\theta)}{\partial\theta}p(z;\theta)\mathrm{d}z\\ &= \int_{\mathcal{Z}} \big(z-\mu_1(\theta)\big)\frac{\partial p(z;\theta)}{\partial\theta}\mathrm{d}z\\ &= \int_{\mathcal{Z}} z\frac{\partial p(z;\theta)}{\partial\theta}\mathrm{d}z - \int_{\mathcal{Z}} \mu_1(\theta)\frac{\partial p(z;\theta)}{\partial\theta}\mathrm{d}z\\ &= \frac{\partial}{\partial\theta}\int_{\mathcal{Z}} zp(z;\theta)\mathrm{d}z - \mu_1(\theta)\frac{\partial}{\partial\theta}\int_{\mathcal{Z}} p(z;\theta)\mathrm{d}z\\ &= \frac{\partial\mu_1(\theta)}{\partial\theta}. \end{aligned} \tag{5.9}$$

With the definition of the variance

$$\mu_2(\theta) \triangleq \int_{\mathcal{Z}} \big(z-\mu_1(\theta)\big)^2 p(z;\theta)\mathrm{d}z, \tag{5.10}$$

we find

$$\int_{\mathcal{Z}} g^2(z;\theta)p(z;\theta)\mathrm{d}z = \mu_2(\theta), \tag{5.11}$$

such that with (5.6) we obtain a first lower bound for the Fisher information measure

$$\begin{aligned} F_z(\theta) &\geq \frac{1}{\mu_2(\theta)}\left(\frac{\partial\mu_1(\theta)}{\partial\theta}\right)^2\\ &= \tilde{F}_z(\theta). \end{aligned} \tag{5.12}$$

Note that this information bound was derived as a side result in an early paper [59] by rearranging the Cramér-Rao inequality [11] [12], but did not find attention in the signal processing literature as its practical relevance was not emphasized.

5.1.2 Interpretation of the Fisher Information Lower Bound

For an interpretation of the bounding result (5.12), consider instead of the original model $p(z;\theta)$ a Gaussian parametric model of the form

$$q(z;\theta) = \frac{1}{\sqrt{2\pi\mu_2(\theta)}}\exp\left(-\frac{\big(z-\mu_1(\theta)\big)^2}{2\mu_2(\theta)}\right), \tag{5.13}$$

with mean $\mu_1(\theta)$ and variance $\mu_2(\theta)$. If the dependency between $\mu_2(\theta)$ and the parameter θ is ignored and

$$\frac{\partial\mu_2(\theta)}{\partial\theta} = 0, \qquad \forall\theta\in\Theta \tag{5.14}$$

is postulated for the model (5.13), the Gaussian Fisher information measure is

$$\begin{aligned} F_G(\theta) &= \int_{\mathcal{Z}} \left(\frac{\partial \log q(z;\theta)}{\partial \theta} \right)^2 q(z;\theta) \mathrm{d}z \\ &= \int_{\mathcal{Z}} \left(\frac{\big(z - \mu_1(\theta)\big)}{\mu_2(\theta)} \frac{\partial \mu_1(\theta)}{\partial \theta} \right)^2 q(z;\theta) \mathrm{d}z \\ &= \frac{1}{\mu_2^2(\theta)} \int_{\mathcal{Z}} \big(z - \mu_1(\theta)\big)^2 q(z;\theta) \mathrm{d}z \left(\frac{\partial \mu_1(\theta)}{\partial \theta} \right)^2 \\ &= \frac{1}{\mu_2(\theta)} \left(\frac{\partial \mu_1(\theta)}{\partial \theta} \right)^2 \end{aligned} \tag{5.15}$$

and matches the pessimistic approximation (5.12) for the original model $p(z;\theta)$

$$\tilde{F}_z(\theta) = \frac{1}{\mu_2(\theta)} \left(\frac{\partial \mu_1(\theta)}{\partial \theta} \right)^2. \tag{5.16}$$

This shows that the bounding approach (5.12) can be interpreted as a replacement of the original system $p(z;\theta)$ by an Gaussian parametric system (5.13) with equivalent mean and variance, for which the inequality

$$F_z(\theta) \geq F_G(\theta) = \tilde{F}_z(\theta) \tag{5.17}$$

holds. So the Fisher information $F_z(\theta)$ of the original system $p(z;\theta)$ always dominates the information measure $F_G(\theta)$ calculated for the equivalent Gaussian system (5.13). Note that while for the special case of an additive system this observation is a well-discussed result [63] [64], with (5.12) this illustrative interpretation can be extended to non-additive systems $p(z;\theta)$.

5.1.3 Quality of the Information Bound - Hard-Limiter

In order to show, that already the simple bound (5.12) has the potential to approximate the Fisher information measure of certain system models in an accurate way, we consider a hard-limiting example

$$z = \mathrm{sign}(\theta + \eta - \upsilon), \tag{5.18}$$

where the 1-bit quantizer with offset υ processes a Gaussian input signal with mean $\theta \in \mathbb{R}$ and unit variance, i.e., $\eta \sim \mathcal{N}(0,1)$. In this case the conditional probabilities for the two output constellations are

$$\begin{aligned} p(z=+1;\theta) &= \int_{-\theta+\upsilon}^{\infty} p_\eta(\eta) \mathrm{d}\eta \\ &= \mathrm{Q}\left(-\theta + \upsilon\right) \\ &= 1 - \mathrm{Q}\left(\theta - \upsilon\right), \end{aligned} \tag{5.19}$$

$$\begin{aligned} p(z=-1;\theta) &= \int_{-\infty}^{-\theta+\upsilon} p_\eta(\eta) \mathrm{d}\eta \\ &= 1 - \mathrm{Q}\left(-\theta + \upsilon\right) \\ &= \mathrm{Q}\left(\theta - \upsilon\right) \end{aligned} \tag{5.20}$$

and the corresponding derivatives are

$$\frac{\partial p(z=+1;\theta)}{\partial\theta} = \frac{1}{\sqrt{2\pi}}\exp\left(-\frac{(\theta-\upsilon)^2}{2}\right), \tag{5.21}$$

$$\frac{\partial p(z=-1;\theta)}{\partial\theta} = -\frac{1}{\sqrt{2\pi}}\exp\left(-\frac{(\theta-\upsilon)^2}{2}\right). \tag{5.22}$$

Therefore, the exact Fisher information of the system (5.18) is

$$\begin{aligned} F(\theta) &= \int_{\mathcal{Z}} \frac{1}{p(z;\theta)}\left(\frac{\partial p(z;\theta)}{\partial\theta}\right)^2 \mathrm{d}z \\ &= \left(\frac{\exp\left(-\frac{(\theta-\upsilon)^2}{2}\right)}{\sqrt{2\pi}}\right)^2 \left(\frac{1}{\mathrm{Q}\left(-\theta+\upsilon\right)} + \frac{1}{\mathrm{Q}\left(\theta-\upsilon\right)}\right) \\ &= \frac{1}{2\pi}\frac{\exp\left(-(\theta-\upsilon)^2\right)}{\mathrm{Q}\left(\theta-\upsilon\right)\mathrm{Q}\left(-\theta+\upsilon\right)}. \end{aligned} \tag{5.23}$$

In order to apply the information bound (5.12), the mean of the output (5.18) is required

$$\begin{aligned} \mu_1(\theta) &= \int_{\mathcal{Z}} z p(z;\theta)\mathrm{d}z \\ &= 1 - 2\,\mathrm{Q}\left(\theta-\upsilon\right) \end{aligned} \tag{5.24}$$

together with the variance

$$\begin{aligned} \mu_2(\theta) &= \int_{\mathcal{Z}} \big(z-\mu_1(\theta)\big)^2 p(z;\theta)\mathrm{d}z \\ &= 4\,\mathrm{Q}^2\left(\theta-\upsilon\right)\big(1-\mathrm{Q}\left(\theta-\upsilon\right)\big) + \big(2\,\mathrm{Q}\left(\theta-\upsilon\right)-2\big)^2\,\mathrm{Q}\left(\theta-\upsilon\right) \\ &= 4\big(\,\mathrm{Q}\left(\theta-\upsilon\right) - \mathrm{Q}^2\left(\theta-\upsilon\right)\big) \\ &= 4\,\mathrm{Q}\left(\theta-\upsilon\right)\big(1-\mathrm{Q}\left(\theta-\upsilon\right)\big). \end{aligned} \tag{5.25}$$

With the derivative of the mean (5.24) being

$$\frac{\partial\mu_1(\theta)}{\partial\theta} = \sqrt{\frac{2}{\pi}}\exp\left(-\frac{(\theta-\upsilon)^2}{2}\right), \tag{5.26}$$

the pessimistic approximation of the Fisher information measure

$$\begin{aligned} \tilde{F}(\theta) &= \frac{1}{\mu_2(\theta)}\left(\frac{\partial\mu_1(\theta)}{\partial\theta}\right)^2 \\ &= \frac{1}{2\pi}\frac{\exp\left(-(\theta-\upsilon)^2\right)}{\mathrm{Q}\left(\theta-\upsilon\right)\mathrm{Q}\left(-\theta+\upsilon\right)} \end{aligned} \tag{5.27}$$

matches the exact result (5.23).

5.2 Second-Order Fisher Information Lower Bound

However, a simple counter example, where expression (5.12) obtains a loose result, is immediately constructed. To this end, consider a generic parametric Gaussian probability law

$$p(z;\theta) = \frac{1}{\sqrt{2\pi\mu_2(\theta)}} \mathrm{e}^{-\frac{(z-\mu_1(\theta))^2}{2\mu_2(\theta)}}. \tag{5.28}$$

The exact Fisher information of model (5.28) is [2, pp. 47]

$$F_z(\theta) = \frac{1}{\mu_2(\theta)} \left(\frac{\partial \mu_1(\theta)}{\partial \theta} \right)^2 + \frac{1}{2\mu_2^2(\theta)} \left(\frac{\partial \mu_2(\theta)}{\partial \theta} \right)^2, \tag{5.29}$$

and is equal to the right hand side of (5.12) only for the case where the variance is constant, i.e.,

$$\frac{\partial \mu_2(\theta)}{\partial \theta} = 0, \qquad \forall \theta \in \Theta. \tag{5.30}$$

Obviously the inequality (5.12) does in general not take into account the variation of the variance $\mu_2(\theta)$ in the parameter θ and the resulting contribution to the Fisher information measure $F_z(\theta)$.

5.2.1 Derivation of the Fisher Information Lower Bound

Due to this insight, we aim at an improvement of (5.12) by utilizing the Cauchy-Schwarz inequality (5.3) under a more general approach. To this end, in (5.6) we choose

$$f(z;\theta) = \frac{\partial \ln p(z;\theta)}{\partial \theta} \tag{5.31}$$

and

$$g(z;\theta) = \left(\frac{z-\mu_1(\theta)}{\sqrt{\mu_2(\theta)}} \right) + \beta(\theta) \left(\frac{z-\mu_1(\theta)}{\sqrt{\mu_2(\theta)}} \right)^2 - \beta(\theta), \tag{5.32}$$

where $\beta(\theta) \in \mathbb{R}$ is a variable to be determined later. With the manipulations

$$\begin{aligned}
\int_{\mathcal{Z}} \left(\frac{z-\mu_1(\theta)}{\sqrt{\mu_2(\theta)}} \right) \frac{\partial \ln p(z;\theta)}{\partial \theta} p(z;\theta) \mathrm{d}z &= \int_{\mathcal{Z}} \left(\frac{z-\mu_1(\theta)}{\sqrt{\mu_2(\theta)}} \right) \frac{\partial p(z;\theta)}{\partial \theta} \mathrm{d}z \\
&= \frac{1}{\sqrt{\mu_2(\theta)}} \left(\int_{\mathcal{Z}} z \frac{\partial p(z;\theta)}{\partial \theta} \mathrm{d}z - \mu_1(\theta) \int_{\mathcal{Z}} \frac{\partial p(z;\theta)}{\partial \theta} \mathrm{d}z \right) \\
&= \frac{1}{\sqrt{\mu_2(\theta)}} \left(\frac{\partial}{\partial \theta} \int_{\mathcal{Z}} z p(z;\theta) \mathrm{d}z - \mu_1(\theta) \frac{\partial}{\partial \theta} \int_{\mathcal{Z}} p(z;\theta) \mathrm{d}z \right) \\
&= \frac{1}{\sqrt{\mu_2(\theta)}} \frac{\partial \mu_1(\theta)}{\partial \theta},
\end{aligned} \tag{5.33}$$

$$\begin{aligned}\int_{\mathcal{Z}} \left(\frac{z-\mu_1(\theta)}{\sqrt{\mu_2(\theta)}}\right)^2 \frac{\partial \ln p(z;\theta)}{\partial\theta} p(z;\theta)\mathrm{d}z &= \int_{\mathcal{Z}} \left(\frac{z-\mu_1(\theta)}{\sqrt{\mu_2(\theta)}}\right)^2 \frac{\partial p(z;\theta)}{\partial\theta}\mathrm{d}z \\ &= \frac{1}{\mu_2(\theta)}\left(\int_{\mathcal{Z}} z^2 \frac{\partial p(z;\theta)}{\partial\theta}\mathrm{d}z - 2\mu_1(\theta)\int_{\mathcal{Z}} z\frac{\partial p(z;\theta)}{\partial\theta}\mathrm{d}z \right. \\ &\quad \left. + \mu_1^2(\theta)\int_{\mathcal{Z}} \frac{\partial p(z;\theta)}{\partial\theta}\mathrm{d}z\right) \\ &= \frac{1}{\mu_2(\theta)}\left(\frac{\partial}{\partial\theta}\int_{\mathcal{Z}} z^2 p(z;\theta)\mathrm{d}z - 2\mu_1(\theta)\frac{\partial}{\partial\theta}\int_{\mathcal{Z}} z p(z;\theta)\mathrm{d}z\right) \\ &= \frac{1}{\mu_2(\theta)}\left(\frac{\partial}{\partial\theta}\big(\mu_2(\theta)+\mu_1^2(\theta)\big) - 2\mu_1(\theta)\frac{\partial\mu_1(\theta)}{\partial\theta}\right) \\ &= \frac{1}{\mu_2(\theta)}\frac{\partial\mu_2(\theta)}{\partial\theta}, \end{aligned} \tag{5.34}$$

where we have used the fact that

$$\int_{\mathcal{Z}} z^2 p(z;\theta)\mathrm{d}z = \mu_2(\theta) + \mu_1^2(\theta), \tag{5.35}$$

and

$$\begin{aligned}\int_{\mathcal{Z}} \beta(\theta)\frac{\partial \ln p(z;\theta)}{\partial\theta} p(z;\theta)\mathrm{d}z &= \beta(\theta)\int_{\mathcal{Z}} \frac{\partial \ln p(z;\theta)}{\partial\theta} p(z;\theta)\mathrm{d}z \\ &= \beta(\theta)\frac{\partial}{\partial\theta}\int_{\mathcal{Z}} p(z;\theta)\mathrm{d}z \\ &= 0, \end{aligned} \tag{5.36}$$

the identity

$$\begin{aligned}\int_{\mathcal{Z}} g(z;\theta)\frac{\partial \ln p(z;\theta)}{\partial\theta} p(z;\theta)\mathrm{d}z &= \int_{\mathcal{Z}} \left(\frac{z-\mu_1(\theta)}{\sqrt{\mu_2(\theta)}}\right)\frac{\partial \ln p(z;\theta)}{\partial\theta} p(z;\theta)\mathrm{d}z \\ &\quad + \beta(\theta)\int_{\mathcal{Z}} \left(\frac{z-\mu_1(\theta)}{\sqrt{\mu_2(\theta)}}\right)^2 \frac{\partial \ln p(z;\theta)}{\partial\theta} p(z;\theta)\mathrm{d}z \\ &\quad - \int_{\mathcal{Z}} \beta(\theta)\frac{\partial \ln p(z;\theta)}{\partial\theta} p(z;\theta)\mathrm{d}z \\ &= \frac{1}{\sqrt{\mu_2(\theta)}}\frac{\partial\mu_1(\theta)}{\partial\theta} + \frac{\beta(\theta)}{\mu_2(\theta)}\frac{\partial\mu_2(\theta)}{\partial\theta} \end{aligned} \tag{5.37}$$

is found. For further discussion, we additionally require

$$\mu_3(\theta) \triangleq \int_{\mathcal{Z}} \big(z-\mu_1(\theta)\big)^3 p(z;\theta)\mathrm{d}z, \tag{5.38}$$

$$\mu_4(\theta) \triangleq \int_{\mathcal{Z}} \big(z-\mu_1(\theta)\big)^4 p(z;\theta)\mathrm{d}z \tag{5.39}$$

and their normalized versions

$$\begin{aligned}\bar{\mu}_3(\theta) &\triangleq \int_{\mathcal{Z}} \left(\frac{z-\mu_1(\theta)}{\sqrt{\mu_2(\theta)}}\right)^3 p(z;\theta)\mathrm{d}z \\ &= \mu_3(\theta)\mu_2^{-\frac{3}{2}}(\theta), \qquad (5.40)\\ \bar{\mu}_4(\theta) &\triangleq \int_{\mathcal{Z}} \left(\frac{z-\mu_1(\theta)}{\sqrt{\mu_2(\theta)}}\right)^4 p(z;\theta)\mathrm{d}z \\ &= \mu_4(\theta)\mu_2^{-2}(\theta). \qquad (5.41)\end{aligned}$$

Note that $\bar{\mu}_3(\theta)$ is referred to as the skewness, an indicator for the asymmetry of the output distribution $p(z;\theta)$, while $\bar{\mu}_4(\theta)$ is called the kurtosis, a characterization for the shape of the output distribution $p(z;\theta)$. Both moments stand in relation through Pearson's inequality [65]

$$\bar{\mu}_4(\theta) \geq \bar{\mu}_3^2(\theta) + 1. \qquad (5.42)$$

A compact and elegant proof on (5.42) can be found in [66]. For the denominator which is required to form (5.6), with the function (5.32) we get

$$\begin{aligned}\int_{\mathcal{Z}} g^2(z;\theta)p(z;\theta)\mathrm{d}z &= \int_{\mathcal{Z}} \left(\left(\frac{z-\mu_1(\theta)}{\sqrt{\mu_2(\theta)}}\right) + \beta(\theta)\left(\frac{z-\mu_1(\theta)}{\sqrt{\mu_2(\theta)}}\right)^2 - \beta(\theta)\right)^2 p(z;\theta)\mathrm{d}z \\ &= \int_{\mathcal{Z}} \left(\frac{z-\mu_1(\theta)}{\sqrt{\mu_2(\theta)}}\right)^2 p(z;\theta)\mathrm{d}z + \beta^2(\theta)\int_{\mathcal{Z}} \left(\frac{z-\mu_1(\theta)}{\sqrt{\mu_2(\theta)}}\right)^4 p(z;\theta)\mathrm{d}z \\ &\quad + \beta^2(\theta)\int_{\mathcal{Z}} p(z;\theta)\mathrm{d}z + 2\beta(\theta)\int_{\mathcal{Z}} \left(\frac{z-\mu_1(\theta)}{\sqrt{\mu_2(\theta)}}\right)^3 p(z;\theta)\mathrm{d}z \\ &\quad + \beta(\theta)\int_{\mathcal{Z}} \left(\frac{z-\mu_1(\theta)}{\sqrt{\mu_2(\theta)}}\right) p(z;\theta)\mathrm{d}z - \beta^2(\theta)\int_{\mathcal{Z}} \left(\frac{z-\mu_1(\theta)}{\sqrt{\mu_2(\theta)}}\right)^2 p(z;\theta)\mathrm{d}z \\ &= 1 + 2\beta(\theta)\bar{\mu}_3(\theta) + \beta^2(\theta)\bar{\mu}_4(\theta) - \beta^2(\theta), \qquad (5.43)\end{aligned}$$

by taking into account that

$$\int_{\mathcal{Z}} \left(\frac{z-\mu_1(\theta)}{\sqrt{\mu_2(\theta)}}\right)^2 p(z;\theta)\mathrm{d}z = 1 \qquad (5.44)$$

and

$$\int_{\mathcal{Z}} \left(\frac{z-\mu_1(\theta)}{\sqrt{\mu_2(\theta)}}\right) p(z;\theta)\mathrm{d}z = 0. \qquad (5.45)$$

Therefore, with (5.6), (5.37) and (5.43) it can be shown, that the Fisher information can in general not fall below

$$\begin{aligned}F_z(\theta) = \int_{\mathcal{Z}} \left(\frac{\partial \log p(z;\theta)}{\partial\theta}\right)^2 p(z;\theta)\mathrm{d}z &\geq \frac{\left(\int_{\mathcal{Z}} g(z;\theta)\frac{\partial \log p(z;\theta)}{\partial\theta} p(z;\theta)\mathrm{d}z\right)^2}{\int_{\mathcal{Z}} g^2(z;\theta)p(z;\theta)\mathrm{d}z} \\ &= \frac{1}{\mu_2(\theta)} \frac{\left(\frac{\partial\mu_1(\theta)}{\partial\theta} + \frac{\beta(\theta)}{\sqrt{\mu_2(\theta)}}\frac{\partial\mu_2(\theta)}{\partial\theta}\right)^2}{1 + 2\beta(\theta)\bar{\mu}_3(\theta) + \beta^2(\theta)(\bar{\mu}_4(\theta) - 1)}. \qquad (5.46)\end{aligned}$$

Note, that an alternative bound based on raw moments and cumulants is found in [60, eq. 2.5].

5.2.2 Optimization of the Fisher Information Lower Bound

The expression (5.46) contains the factor $\beta(\theta)$, which can be used to optimize the Fisher information lower bound (5.46). For the trivial choice of $\beta(\theta) = 0$, the expression becomes

$$F_z(\theta) \geq \frac{1}{\mu_2(\theta)} \left(\frac{\partial \mu_1(\theta)}{\partial \theta} \right)^2, \tag{5.47}$$

which turns out to be the first-order bound (5.12). To improve this result, take into consideration that the problem

$$x^\star = \arg\max_{x \in \mathbb{R}} h(x) \tag{5.48}$$

with

$$h(x) = \frac{(a + xb)^2}{1 + 2xc + x^2 d} \tag{5.49}$$

and

$$bc - ad \neq 0, \tag{5.50}$$

has a unique maximizing solution

$$x^\star = \frac{ac - b}{bc - ad}. \tag{5.51}$$

Consequently, the tightest form of (5.46) is given by

$$\begin{aligned} F_z(\theta) &\geq \frac{1}{\mu_2(\theta)} \frac{\left(\frac{\partial \mu_1(\theta)}{\partial \theta} + \frac{\beta^\star(\theta)}{\sqrt{\mu_2(\theta)}} \frac{\partial \mu_2(\theta)}{\partial \theta} \right)^2}{1 + 2\beta^\star(\theta)\bar{\mu}_3(\theta) + \beta^{\star 2}(\theta)(\bar{\mu}_4(\theta) - 1)} \\ &= \tilde{F}_z(\theta), \end{aligned} \tag{5.52}$$

with the optimization factor

$$\begin{aligned} \beta^\star(\theta) &= \frac{\frac{\partial \mu_1(\theta)}{\partial \theta} \bar{\mu}_3(\theta) - \frac{1}{\sqrt{\mu_2(\theta)}} \frac{\partial \mu_2(\theta)}{\partial \theta}}{\frac{1}{\sqrt{\mu_2(\theta)}} \frac{\partial \mu_2(\theta)}{\partial \theta} \bar{\mu}_3(\theta) - \frac{\partial \mu_1(\theta)}{\partial \theta} (\bar{\mu}_4(\theta) - 1)} \\ &= \frac{\frac{\partial \mu_1(\theta)}{\partial \theta} \sqrt{\mu_2(\theta)} \bar{\mu}_3(\theta) - \frac{\partial \mu_2(\theta)}{\partial \theta}}{\frac{\partial \mu_2(\theta)}{\partial \theta} \bar{\mu}_3(\theta) - \frac{\partial \mu_1(\theta)}{\partial \theta} \sqrt{\mu_2(\theta)} (\bar{\mu}_4(\theta) - 1)}. \end{aligned} \tag{5.53}$$

Note that the Fisher information $F_z(\theta)$ requires to integrate the squared score function $\left(\frac{\partial \ln p(z;\theta)}{\partial \theta} \right)^2$ over the whole support $\mathcal{Z}$. In contrast, the alternative measure $\tilde{F}_z(\theta)$ exclusively requires the mean $\mu_1(\theta)$, the variance $\mu_2(\theta)$, the skewness $\bar{\mu}_3(\theta)$ and the kurtosis $\bar{\mu}_4(\theta)$ in parametric form.

Also note that for the case where the identity

$$\frac{\partial \mu_1(\theta)}{\partial \theta} \sqrt{\mu_2(\theta)} \bar{\mu}_3(\theta) = \frac{\partial \mu_2(\theta)}{\partial \theta}, \qquad \forall \theta \in \Theta, \tag{5.54}$$

holds, the optimization of (5.52) results in

$$\beta^{\star}(\theta) = 0 \tag{5.55}$$

and the approximation (5.52) obtains the compact form of the first-order bound (5.12).

To ensure that the approximation (5.52) is always positive, it has to hold that

$$1 + 2\beta(\theta)\bar{\mu}_3(\theta) + \beta^2(\theta)(\bar{\mu}_4(\theta) - 1) \geq 0, \qquad \forall \beta(\theta), \theta. \tag{5.56}$$

In order to demonstrate that this is the case, consider the fact that by construction

$$\begin{aligned}(1 + \beta(\theta)\sqrt{\bar{\mu}_4(\theta) - 1})^2 &= 1 + 2\beta(\theta)\sqrt{\bar{\mu}_4(\theta) - 1} + \beta^2(\theta)(\bar{\mu}_4(\theta) - 1) \\ &\geq 0, \qquad \forall \beta(\theta), \theta.\end{aligned} \tag{5.57}$$

With Pearson's inequality (5.42) we have

$$\sqrt{\bar{\mu}_4(\theta) - 1} \geq |\bar{\mu}_3(\theta)|, \qquad \forall \theta, \tag{5.58}$$

such that

$$1 + 2\beta(\theta)\,|\bar{\mu}_3(\theta)| + \beta^2(\theta)(\bar{\mu}_4(\theta) - 1) \geq 0, \qquad \forall \beta(\theta), \theta. \tag{5.59}$$

As the inequality (5.59) holds irrespectively if $\beta(\theta)$ is positive or negative, we equivalently have

$$1 + 2\beta(\theta)\bar{\mu}_3(\theta) + \beta^2(\theta)(\bar{\mu}_4(\theta) - 1) \geq 0, \qquad \forall \beta(\theta), \theta. \tag{5.60}$$

5.2.3 Special Cases of the Fisher Information Lower Bound

In order to derive simplified forms of the conservative information measure $\tilde{F}_z(\theta)$, let us consider some special cases. For the situation where the first moment $\mu_1(\theta)$ does not vary with the system parameter θ, i.e.,

$$\frac{\partial \mu_1(\theta)}{\partial \theta} = 0, \qquad \forall \theta \in \Theta, \tag{5.61}$$

we obtain

$$\beta^{\star}(\theta) = -\frac{1}{\bar{\mu}_3(\theta)}, \tag{5.62}$$

such that a pessimistic approximation $\tilde{F}_z(\theta)$ for the information measure $F_z(\theta)$ is given by

$$\begin{aligned}\tilde{F}_z(\theta) &= \frac{1}{\mu_2(\theta)} \frac{\Big(-\frac{1}{\bar{\mu}_3(\theta)\sqrt{\mu_2(\theta)}} \frac{\partial \mu_2(\theta)}{\partial \theta}\Big)^2}{1 - 2 + \frac{(\bar{\mu}_4(\theta) - 1)}{\bar{\mu}_3^2(\theta)}} \\ &= \frac{1}{\mu_2^2(\theta)} \frac{\big(\frac{\partial \mu_2(\theta)}{\partial \theta}\big)^2}{\bar{\mu}_4(\theta) - \bar{\mu}_3^2(\theta) - 1}.\end{aligned} \tag{5.63}$$

When the variance $\mu_2(\theta)$ is constant within θ, i.e.,

$$\frac{\partial \mu_2(\theta)}{\partial \theta} = 0, \qquad \forall \theta \in \Theta, \tag{5.64}$$

it holds that

$$\beta^{\star}(\theta) = -\frac{\bar{\mu}_3(\theta)}{(\bar{\mu}_4(\theta)-1)}. \tag{5.65}$$

In this situation we obtain the pessimistic Fisher information measure

$$\begin{aligned}\tilde{F}_z(\theta) &= \frac{1}{\mu_2(\theta)} \frac{\left(\frac{\partial \mu_1(\theta)}{\partial \theta}\right)^2}{1 - 2\frac{\bar{\mu}_3^2(\theta)}{(\bar{\mu}_4(\theta)-1)} + \frac{\bar{\mu}_3^2(\theta)}{(\bar{\mu}_4(\theta)-1)}} \\ &= \frac{1}{\mu_2(\theta)} \frac{\left(\frac{\partial \mu_1(\theta)}{\partial \theta}\right)^2}{1 - \frac{\bar{\mu}_3^2(\theta)}{(\bar{\mu}_4(\theta)-1)}}.\end{aligned} \tag{5.66}$$

Note that (5.66) equals the expression in (5.12) whenever the skewness $\bar{\mu}_3$ vanishes. In general the relation (5.42) makes (5.66) larger than the first-order bound (5.12).

For symmetric output distributions with zero skewness, i.e.,

$$\bar{\mu}_3(\theta) = 0, \tag{5.67}$$

we verify that the optimization of the information bound derived in (5.52) results in

$$\beta^{\star}(\theta) = \frac{\frac{\partial \mu_2(\theta)}{\partial \theta}}{\frac{\partial \mu_1(\theta)}{\partial \theta}\sqrt{\mu_2(\theta)}(\bar{\mu}_4(\theta)-1)}, \tag{5.68}$$

such that

$$\begin{aligned}\tilde{F}(\theta) &= \frac{1}{\mu_2(\theta)} \frac{\left(\frac{\partial \mu_1(\theta)}{\partial \theta} + \frac{\left(\frac{\partial \mu_2(\theta)}{\partial \theta}\right)^2}{\frac{\partial \mu_1(\theta)}{\partial \theta}\mu_2(\theta)(\bar{\mu}_4(\theta)-1)}\right)^2}{1 + \left(\frac{\frac{\partial \mu_2(\theta)}{\partial \theta}}{\frac{\partial \mu_1(\theta)}{\partial \theta}\sqrt{\mu_2(\theta)(\bar{\mu}_4(\theta)-1)}}\right)^2 (\bar{\mu}_4(\theta)-1)} \\ &= \frac{\left(\frac{\partial \mu_1(\theta)}{\partial \theta}\right)^2 \mu_2(\theta)(\bar{\mu}_4(\theta)-1) + \left(\frac{\partial \mu_2(\theta)}{\partial \theta}\right)^2}{\mu_2^2(\theta)(\bar{\mu}_4(\theta)-1)} \\ &= \frac{1}{\mu_2(\theta)}\left(\frac{\partial \mu_1(\theta)}{\partial \theta}\right)^2 + \frac{1}{\mu_2^2(\theta)(\bar{\mu}_4(\theta)-1)}\left(\frac{\partial \mu_2(\theta)}{\partial \theta}\right)^2.\end{aligned} \tag{5.69}$$

5.2.4 Quality of the Information Bound - Models with Continuous Support

In order to analyze the tightness of the derived lower bound $\tilde{F}_z(\theta)$, we consider different examples where the exact Fisher information measure $F_z(\theta)$ can be derived in compact form. First we discuss several well-studied distributions with continuous support $\mathcal{Z}$.

5.2.4.1 Gaussian System Output

Consider the system output z to follow a generic Gaussian distribution in parametric form

$$p(z;\theta) = \frac{1}{\sqrt{2\pi\nu_2(\theta)}} \mathrm{e}^{-\frac{(z-\nu_1(\theta))^2}{2\nu_2(\theta)}}. \tag{5.70}$$

The exact Fisher information measure is given by

$$F(\theta) = \frac{1}{\nu_2(\theta)}\left(\frac{\partial \nu_1(\theta)}{\partial \theta}\right)^2 + \frac{1}{2\nu_2^2(\theta)}\left(\frac{\partial \nu_2(\theta)}{\partial \theta}\right)^2. \tag{5.71}$$

As for this case the output mean and variance are

$$\mu_1(\theta) = \nu_1(\theta), \tag{5.72}$$
$$\mu_2(\theta) = \nu_2(\theta) \tag{5.73}$$

and the skewness and the kurtosis are

$$\bar{\mu}_3(\theta) = 0, \tag{5.74}$$
$$\bar{\mu}_4(\theta) = 3, \tag{5.75}$$

with (5.69) we get the approximation

$$\begin{aligned}\tilde{F}_z(\theta) = &= \frac{1}{\mu_2(\theta)}\left(\frac{\partial \mu_1(\theta)}{\partial \theta}\right)^2 + \frac{1}{\mu_2^2(\theta)(\bar{\mu}_4(\theta)-1)}\left(\frac{\partial \mu_2(\theta)}{\partial \theta}\right)^2 \\ &= \frac{1}{\nu_2(\theta)}\left(\frac{\partial \nu_1(\theta)}{\partial \theta}\right)^2 + \frac{1}{2\nu_2^2(\theta)}\left(\frac{\partial \nu_2(\theta)}{\partial \theta}\right)^2,\end{aligned} \tag{5.76}$$

which obviously is an exact approximation for the original information measure (5.71).

5.2.4.2 Exponential System Output

As another example we analyze the case where samples from a parametric exponential distribution

$$p(z;\theta) = \nu(\theta)\mathrm{e}^{-\nu(\theta)z}, \tag{5.77}$$

with $\nu(\theta) \geq 0$ and $z \geq 0$, can be collected at the system output. The score function under this model is

$$\frac{\partial \ln p(z;\theta)}{\partial \theta} = \frac{1}{\nu(\theta)}\frac{\partial \nu(\theta)}{\partial \theta} - z\frac{\partial \nu(\theta)}{\partial \theta}, \tag{5.78}$$

such that the exact Fisher information is given by

$$\begin{aligned}F_z(\theta) &= \int_{\mathcal{Z}}\left(\frac{\partial \ln p(z;\theta)}{\partial \theta}\right)^2 p(z;\theta)\mathrm{d}z \\ &= \int_{\mathcal{Z}}\left(\frac{1}{\nu(\theta)}\frac{\partial \nu(\theta)}{\partial \theta} - z\frac{\partial \nu(\theta)}{\partial \theta}\right)^2 p(z;\theta)\mathrm{d}z \\ &= \frac{1}{\nu^2(\theta)}\left(\frac{\partial \nu(\theta)}{\partial \theta}\right)^2 + \left(\frac{\partial \nu(\theta)}{\partial \theta}\right)^2 \int_{\mathcal{Z}} z^2 p(z;\theta)\mathrm{d}z - 2\frac{1}{\nu(\theta)}\left(\frac{\partial \nu(\theta)}{\partial \theta}\right)^2 \int_{\mathcal{Z}} z p(z;\theta)\mathrm{d}z \\ &= \frac{1}{\nu^2(\theta)}\left(\frac{\partial \nu(\theta)}{\partial \theta}\right)^2,\end{aligned} \tag{5.79}$$

where we used the fact that for an exponential distribution

$$\int_{\mathcal{Z}} zp(z;\theta)\mathrm{d}z = \frac{1}{\nu(\theta)}, \tag{5.80}$$

$$\int_{\mathcal{Z}} z^2 p(z;\theta)\mathrm{d}z = \frac{2}{\nu^2(\theta)}. \tag{5.81}$$

For the approximation $\tilde{F}_z(\theta)$ the required mean and variance are

$$\mu_1(\theta) = \frac{1}{\nu(\theta)}, \tag{5.82}$$

$$\mu_2(\theta) = \frac{1}{\nu^2(\theta)} \tag{5.83}$$

and the skewness and kurtosis are

$$\bar{\mu}_3(\theta) = 2, \tag{5.84}$$

$$\bar{\mu}_4(\theta) = 3, \tag{5.85}$$

such that we obtain

$$\begin{aligned}\frac{\partial\mu_1(\theta)}{\partial\theta}\sqrt{\mu_2(\theta)}\bar{\mu}_3(\theta) &= -\frac{2}{\nu^3(\theta)}\frac{\partial\nu(\theta)}{\partial\theta} \\ &= \frac{\partial\mu_2(\theta)}{\partial\theta},\end{aligned} \tag{5.86}$$

producing $\beta^\star(\theta) = 0$ as noted in (5.55). We therefore arrive at the inequality discussed in (5.12)

$$\begin{aligned}\tilde{F}_z(\theta) &= \frac{1}{\mu_2(\theta)}\left(\frac{\partial\mu_1(\theta)}{\partial\theta}\right)^2 \\ &= \nu^2(\theta)\left(-\frac{1}{\nu^2(\theta)}\frac{\partial\nu(\theta)}{\partial\theta}\right)^2 \\ &= \frac{1}{\nu^2(\theta)}\left(\frac{\partial\nu(\theta)}{\partial\theta}\right)^2,\end{aligned} \tag{5.87}$$

which obviously matches the exact Fisher information of the exponential system model (5.79).

5.2.4.3 Laplacian System Output

For a third example, we assume that the output z follows a parametric Laplace distribution with zero mean, i.e.,

$$p(z;\theta) = \frac{1}{2\nu(\theta)}\mathrm{e}^{-\frac{|z|}{\nu(\theta)}}. \tag{5.88}$$

The score function is then given by

$$\frac{\partial\ln p(z;\theta)}{\partial\theta} = -\frac{1}{\nu(\theta)}\frac{\partial\nu(\theta)}{\partial\theta} + \frac{|z|}{\nu^2(\theta)}\frac{\partial\nu(\theta)}{\partial\theta} \tag{5.89}$$

and the exact Fisher information is found to be

$$\begin{aligned} F_z(\theta) &= \int_{\mathcal{Z}} \left(\frac{\partial \ln p(z;\theta)}{\partial \theta} \right)^2 p(z;\theta) \mathrm{d}z \\ &= \frac{1}{\nu^2(\theta)} \left(\frac{\partial \nu(\theta)}{\partial \theta} \right)^2 + \frac{1}{\nu^4(\theta)} \left(\frac{\partial \nu(\theta)}{\partial \theta} \right)^2 \int_{\mathcal{Z}} |z|^2 \, p(z;\theta) \mathrm{d}z \\ &\quad - 2 \frac{1}{\nu^3(\theta)} \left(\frac{\partial \nu(\theta)}{\partial \theta} \right)^2 \int_{\mathcal{Z}} |z| \, p(z;\theta) \mathrm{d}z \\ &= \frac{1}{\nu^2(\theta)} \left(\frac{\partial \nu(\theta)}{\partial \theta} \right)^2, \end{aligned} \tag{5.90}$$

where we have used

$$\int_{-\infty}^{\infty} |z|^2 \, \frac{1}{2\nu(\theta)} \mathrm{e}^{-\frac{|z|}{\nu(\theta)}} \mathrm{d}z = 2\nu^2(\theta) \tag{5.91}$$

and

$$\begin{aligned} \int_{-\infty}^{\infty} |z| \, \frac{1}{2\nu(\theta)} \mathrm{e}^{-\frac{|z|}{\nu(\theta)}} \mathrm{d}z &= 2 \int_0^{\infty} z \frac{1}{2\nu(\theta)} \mathrm{e}^{-\frac{z}{\nu(\theta)}} \mathrm{d}z \\ &= \nu(\theta). \end{aligned} \tag{5.92}$$

The mean and variance of the system output are

$$\mu_1(\theta) = 0, \tag{5.93}$$

$$\mu_2(\theta) = 2\nu^2(\theta) \tag{5.94}$$

and the skewness and kurtosis are

$$\bar{\mu}_3(\theta) = 0, \tag{5.95}$$

$$\bar{\mu}_4(\theta) = 6. \tag{5.96}$$

As the first moment is constant with respect to the system parameter θ, the approximation takes the form (5.63) and we obtain

$$\begin{aligned} \tilde{F}_z(\theta) &= \frac{1}{\mu_2^2(\theta)} \frac{\left(\frac{\partial \mu_2(\theta)}{\partial \theta} \right)^2}{(\bar{\mu}_4(\theta) - 1)} \\ &= \frac{1}{4\nu^4(\theta)} \frac{\left(4\nu(\theta) \frac{\partial \nu(\theta)}{\partial \theta} \right)^2}{5} \\ &= \frac{4}{5} \frac{1}{\nu^2(\theta)} \left(\frac{\partial \nu(\theta)}{\partial \theta} \right)^2. \end{aligned} \tag{5.97}$$

In contrast to the other examples, the information bound $\tilde{F}_z(\theta)$ is not tight under the Laplacian system model (5.88). However, note that $\tilde{F}_z(\theta)$ still allows to obtain a pessimistic characterization for the exact Fisher information measure $F_z(\theta)$ of the Laplacian model.

5.2.5 Quality of the Information Bound - Models with Discrete Support

In the following we extend the discussion about the tightness of the approximation $\tilde{F}_z(\theta)$ to the case where the system output z takes values from a discrete alphabet $\mathcal{Z}$.

5.2.5.1 Bernoulli System Output

As a first example for such kind of system outputs, observations from a parametric Bernoulli distribution with

$$\begin{aligned} p(z=1;\theta) &= 1 - p(z=0;\theta) \\ &= \nu(\theta) \end{aligned} \tag{5.98}$$

are considered, where

$$0 < \nu(\theta) < 1, \qquad \forall \theta \in \Theta. \tag{5.99}$$

The Fisher information measure under this model is

$$\begin{aligned} F_z(\theta) &= \int_{\mathcal{Z}} \left(\frac{\partial \ln p(z;\theta)}{\partial \theta} \right)^2 p(z;\theta) \mathrm{d}z \\ &= \sum_{\mathcal{Z}} \left(\frac{\partial p(z;\theta)}{\partial \theta} \right)^2 \frac{1}{p(z;\theta)} \\ &= \frac{\left(\frac{\partial p(z=1;\theta)}{\partial \theta}\right)^2}{p(z=1;\theta)} + \frac{\left(\frac{\partial p(z=0;\theta)}{\partial \theta}\right)^2}{p(z=0;\theta)} \\ &= \frac{1}{\nu(\theta)(1-\nu(\theta))} \left(\frac{\partial \nu(\theta)}{\partial \theta} \right)^2. \end{aligned} \tag{5.100}$$

The mean and the variance are

$$\mu_1(\theta) = \nu(\theta), \tag{5.101}$$

$$\mu_2(\theta) = \nu(\theta)(1-\nu(\theta)), \tag{5.102}$$

with derivatives

$$\frac{\partial \mu_1(\theta)}{\partial \theta} = \frac{\partial \nu(\theta)}{\partial \theta}, \tag{5.103}$$

$$\frac{\partial \mu_2(\theta)}{\partial \theta} = \big(1 - 2\nu(\theta)\big) \frac{\partial \nu(\theta)}{\partial \theta}. \tag{5.104}$$

The skewness is

$$\begin{aligned} \bar{\mu}_3(\theta) &= \sum_{\mathcal{Z}} \left(\frac{z - \mu_1(\theta)}{\sqrt{\mu_2(\theta)}} \right)^3 p(z;\theta) \\ &= \left(\frac{1-\nu(\theta)}{\sqrt{\nu(\theta)(1-\nu(\theta))}} \right)^3 \nu(\theta) + \left(\frac{-\nu(\theta)}{\sqrt{\nu(\theta)(1-\nu(\theta))}} \right)^3 (1-\nu(\theta)) \\ &= \frac{1-2\nu(\theta)}{\sqrt{\nu(\theta)(1-\nu(\theta))}} \end{aligned} \tag{5.105}$$

and the kurtosis is given by

$$\begin{aligned}\bar{\mu}_4(\theta) &= \sum_{\mathcal{Z}} \left(\frac{z - \mu_1(\theta)}{\sqrt{\mu_2(\theta)}} \right)^4 p(z;\theta) \\ &= \left(\frac{1-\nu(\theta)}{\sqrt{\nu(\theta)(1-\nu(\theta))}} \right)^4 \nu(\theta) + \left(\frac{-\nu(\theta)}{\sqrt{\nu(\theta)(1-\nu(\theta))}} \right)^4 (1-\nu(\theta)) \\ &= \frac{1}{\nu(\theta)(1-\nu(\theta))} - 3. \end{aligned} \tag{5.106}$$

As

$$\begin{aligned}\frac{\partial \mu_1(\theta)}{\partial \theta} \sqrt{\mu_2(\theta)} \bar{\mu}_3(\theta) &= \big(1 - 2\nu(\theta)\big) \frac{\partial \nu(\theta)}{\partial \theta} \\ &= \frac{\partial \mu_2(\theta)}{\partial \theta} \end{aligned} \tag{5.107}$$

and consequently $\beta^\star(\theta) = 0$, the approximation takes the simplified form (5.12)

$$\begin{aligned}\tilde{F}_z(\theta) &= \frac{1}{\mu_2(\theta)} \left(\frac{\partial \mu_1(\theta)}{\partial \theta} \right)^2 \\ &= \frac{1}{\nu(\theta)(1-\nu(\theta))} \left(\frac{\partial \nu(\theta)}{\partial \theta} \right)^2. \end{aligned} \tag{5.108}$$

It becomes clear that also for a binary system output z, following a parametric Bernoulli distribution (5.98), the derived expression (5.108) is a tight approximation for the original inference capability (5.100).

5.2.5.2 Poisson System Output

As a second example with discrete output, we consider the Poisson distribution. The samples at the output z are distributed according to the model

$$p(z;\theta) = \frac{\nu^z(\theta)}{z!} \mathrm{e}^{-\nu(\theta)}, \tag{5.109}$$

with

$$\mathcal{Z} = \{0, 1, 2, \ldots\} \tag{5.110}$$

and

$$\nu(\theta) > 0, \qquad \forall \theta \in \Theta. \tag{5.111}$$

The derivative of the log-likelihood is given by

$$\frac{\partial \ln p(z;\theta)}{\partial \theta} = \frac{z}{\nu(\theta)} \frac{\partial \nu(\theta)}{\partial \theta} - \frac{\partial \nu(\theta)}{\partial \theta}, \tag{5.112}$$

such that we calculate

$$\begin{aligned} F_z(\theta) &= \int_{\mathcal{Z}} \left(\frac{\partial \ln p(z;\theta)}{\partial \theta} \right)^2 p(z;\theta) \mathrm{d}z \\ &= \int_{\mathcal{Z}} \left(\frac{z}{\nu(\theta)} \frac{\partial \nu(\theta)}{\partial \theta} - \frac{\partial \nu(\theta)}{\partial \theta} \right)^2 p(z;\theta) \mathrm{d}z \\ &= \frac{1}{\nu^2(\theta)} \left(\frac{\partial \nu(\theta)}{\partial \theta} \right)^2 \int_{\mathcal{Z}} z^2 p(z;\theta) \mathrm{d}z - \frac{2}{\nu(\theta)} \left(\frac{\partial \nu(\theta)}{\partial \theta} \right)^2 \int_{\mathcal{Z}} z p(z;\theta) \mathrm{d}z + \left(\frac{\partial \nu(\theta)}{\partial \theta} \right)^2 \\ &= \frac{1}{\nu(\theta)} \left(\frac{\partial \nu(\theta)}{\partial \theta} \right)^2, \end{aligned} \tag{5.113}$$

where we have used that

$$\int_{\mathcal{Z}} z p(z;\theta) \mathrm{d}z = \sum_{z=0}^{\infty} z \frac{\nu^z(\theta)}{z!} \mathrm{e}^{-\nu(\theta)} = \nu(\theta), \tag{5.114}$$

$$\int_{\mathcal{Z}} z^2 p(z;\theta) \mathrm{d}z = \sum_{z=0}^{\infty} z^2 \frac{\nu^z(\theta)}{z!} \mathrm{e}^{-\nu(\theta)} = \nu(\theta) + \nu^2(\theta). \tag{5.115}$$

In order to apply the approximation (5.52), we require mean and variance which are given by

$$\mu_1(\theta) = \nu(\theta), \tag{5.116}$$

$$\mu_2(\theta) = \nu(\theta), \tag{5.117}$$

together with the skewness and the kurtosis

$$\bar{\mu}_3(\theta) = \frac{1}{\sqrt{\nu(\theta)}}, \tag{5.118}$$

$$\bar{\mu}_4(\theta) = \frac{1}{\nu(\theta)} + 3. \tag{5.119}$$

As these quantities exhibit the property

$$\begin{aligned} \frac{\partial \mu_1(\theta)}{\partial \theta} \sqrt{\mu_2(\theta)} \bar{\mu}_3(\theta) &= \frac{\partial \nu(\theta)}{\partial \theta} \\ &= \frac{\partial \mu_2(\theta)}{\partial \theta}, \end{aligned} \tag{5.120}$$

we obtain $\beta^\star(\theta) = 0$ and the approximation is given by the first-order bound (5.12)

$$\begin{aligned} \tilde{F}(\theta) &= \frac{1}{\mu_2(\theta)} \Big(\frac{\partial \mu_1(\theta)}{\partial \theta} \Big)^2 \\ &= \frac{1}{\nu(\theta)} \Big(\frac{\partial \nu(\theta)}{\partial \theta} \Big)^2 \end{aligned} \tag{5.121}$$

which is tight with respect to the exact information measure (5.113).

5.2.6 Applications

Within this section, we outline possible applications of the presented information bound (5.52). To this end, we present three problems for which $\tilde{F}(\theta)$ provides interesting and useful insights. The discussed problems cover theoretic as well as practical aspects in statistical signal processing.

5.2.6.1 Minimum Fisher Information

A common assumption in the field of signal processing is that noise affects technical receive systems in an additive way. Therefore a system characterization of high practical relevance is a signal model with independent additive noise

$$y = s(\theta) + \eta, \tag{5.122}$$

where $s(\theta)$ is a deterministic pilot signal modulated by the unknown parameter θ (for example attenuation, time-delay, frequency-offset, etc.) and η is additive independent random noise with fixed variance σ^2. Within this framework, the question which distribution $p(\eta)$ provides the smallest Fisher information has received attention [63] [64] [67] [68] [69] [70] [71] [72]. In order to see that our approach allows to analyze this relevant special case, note that with (5.12) for the system model (5.122)

$$\begin{aligned} F_y(\theta) &\geq \frac{1}{\mu_2(\theta)} \left(\frac{\partial \mu_1(\theta)}{\partial \theta} \right)^2 \\ &= \frac{1}{\sigma^2} \left(\frac{\partial s(\theta)}{\partial \theta} \right)^2, \end{aligned} \tag{5.123}$$

where equality is obtained if $p(\eta)$ is a Gaussian distribution with constant variance σ^2. This shows that for additive noisy systems like (5.122) with fixed variance σ^2, a Gaussian assumption provides the worst-case scenario from an estimation theoretic perspective [63] [64].

The presented second-order bounding approach (5.52) allows us to generalize this statement. If for any system $p(z;\theta)$ (including non-additive systems) the output z exhibits the characteristic

$$\begin{aligned} \mu_1(\theta) &= \mathrm{E}_{z;\theta}\left[z\right] \\ &= s(\theta), \end{aligned} \tag{5.124}$$

$$\begin{aligned} \mu_2 &= \mathrm{E}_{z;\theta}\left[\left(z - \mu_1(\theta) \right)^2 \right] \\ &= \sigma^2, \end{aligned} \tag{5.125}$$

the result (5.66) shows that the Fisher information measure can not violate

$$F_z(\theta) \geq \frac{1}{\mu_2} \frac{\left(\frac{\partial \mu_1(\theta)}{\partial \theta} \right)^2}{1 - \frac{\bar{\mu}_3^2(\theta)}{(\bar{\mu}_4(\theta) - 1)}}. \tag{5.126}$$

This lower bound is minimized by a symmetric distribution $\bar{\mu}_3(\theta) = 0$. The resulting expression

$$F_z(\theta) \geq \frac{1}{\mu_2} \left(\frac{\partial \mu_1(\theta)}{\partial \theta} \right)^2, \tag{5.127}$$

reaches equality under the assumption that $p(z;\theta)$ follows an additive Gaussian system model

$$p(z;\theta) = \frac{1}{\sqrt{2\pi\sigma^2}} \mathrm{e}^{-\frac{(z-s(\theta))^2}{2\sigma^2}}, \tag{5.128}$$

such that the worst-case model assumption with respect to Fisher information $F_z(\theta)$ under the considered restrictions (5.124) and (5.125) is in general additive and Gaussian.

In the more general setting, where also the output variance exhibits a dependency on the system parameter θ,

$$\begin{aligned} \mu_1(\theta) &= \mathrm{E}_{z;\theta}\left[z\right] \\ &= s(\theta), \end{aligned} \tag{5.129}$$

$$\begin{aligned} \mu_2(\theta) &= \mathrm{E}_{z;\theta}\left[(z-\mu_1(\theta))^2\right] \\ &= \sigma^2(\theta) \end{aligned} \tag{5.130}$$

and additionally the output distribution is symmetric, i.e.,

$$\bar{\mu}_3(\theta) = 0, \tag{5.131}$$

the result (5.69) allows to conclude, that the Fisher information is in general bounded below

$$F_z(\theta) \geq \frac{1}{\sigma^2(\theta)} \left(\frac{\partial s(\theta)}{\partial \theta}\right)^2 + \frac{1}{\sigma^4(\theta)(\bar{\mu}_4(\theta)-1)} \left(\frac{\partial \sigma^2(\theta)}{\partial \theta}\right)^2. \tag{5.132}$$

As the system model

$$p(z;\theta) = \frac{1}{\sqrt{2\pi\sigma^2(\theta)}} \mathrm{e}^{-\frac{(z-s(\theta))^2}{2\sigma^2(\theta)}} \tag{5.133}$$

exhibits the inference capability

$$F_z(\theta) = \frac{1}{\sigma^2(\theta)} \left(\frac{\partial s(\theta)}{\partial \theta}\right)^2 + \frac{1}{2\sigma^2(\theta)} \left(\frac{\partial \sigma^4(\theta)}{\partial \theta}\right)^2, \tag{5.134}$$

by comparing (5.132) and (5.134) it can be concluded that for all cases where the kurtosis fulfills

$$\bar{\mu}_4(\theta) \leq 3, \tag{5.135}$$

from an estimation theoretic perspective the parametric Gaussian model (5.133) forms a conservative assumption.

5.2.6.2 Information Loss of the Squaring Device

Another interesting problem in statistical signal processing is to characterize the estimation theoretic quality of nonlinear receive and measurement systems. The Fisher information measure $F_z(\theta)$ is a rigorous mathematical tool which allows to draw precise conclusions with respect to this question. However, depending on the nature of the nonlinearity, the exact calculation of the information measure $F_z(\theta)$ can become complicated. As an univariate example for such a scenario

consider the problem of analyzing the intrinsic estimation theoretic capability of a system with a squaring sensor output

$$z = y^2 \tag{5.136}$$

with respect to the inference of the mean $\theta > 0$ of a Gaussian input

$$p(y;\theta) = \frac{1}{\sqrt{2\pi}} \mathrm{e}^{-\frac{(y-\theta)^2}{2}} \tag{5.137}$$

with unit variance. In such a case the system output z follows a non-central chi-square distribution parameterized by θ. As the analytical description of the associated likelihood function $p(z;\theta)$ includes a Bessel function, the characterization of the Fisher information $F_z(\theta)$ in compact analytical form is non-trivial. We short-cut the derivation by using the presented approximation $\tilde{F}_z(\theta)$ instead of $F_z(\theta)$. The first two output moments are found to be given by

$$\begin{aligned} \mathrm{E}_{z;\theta}\left[z\right] &= \mathrm{E}_\eta\left[\theta^2 + 2\theta\eta + \eta^2\right] \\ &= \theta^2 + 1 \\ &= \mu_1(\theta), \end{aligned} \tag{5.138}$$

$$\begin{aligned} \mathrm{E}_{z;\theta}\left[\left(z - \mu_1(\theta)\right)^2\right] &= \mathrm{E}_\eta\left[(\theta^2 + 2\theta\eta + \eta^2 - \theta^2 - 1)^2\right] \\ &= \mathrm{E}_\eta\left[\eta^4 + 4\eta^3\theta + 4\eta^2\theta^2 - 2\eta^2 - 4\eta\theta + 1\right] \\ &= \mathrm{E}_\eta\left[\eta^4 + (4\theta^2 - 2)\eta^2 + 1\right] \\ &= 3 + 4\theta^2 - 2 + 1 \\ &= 2(2\theta^2 + 1) \\ &= \mu_2(\theta), \end{aligned} \tag{5.139}$$

where we have introduced the auxiliary random variable

$$\eta = y - \theta. \tag{5.140}$$

The third central output moment is

$$\begin{aligned} \mathrm{E}_{z;\theta}\left[\left(z - \mu_1(\theta)\right)^3\right] &= \mathrm{E}_\eta\left[(\theta^2 + 2\theta\eta + \eta^2 - \theta^2 - 1)^3\right] \\ &= \mathrm{E}_\eta\left[\eta^6 + 6\eta^5\theta + 12\theta^2\eta^4 - 3\eta^4 + 8\eta^3\theta^3 - 12\eta^3\theta - 12\eta^2\theta^2 + 3\eta^2\right. \\ &\quad \left. +6\eta\theta - 1\right] \\ &= \mathrm{E}_\eta\left[\eta^6 + (12\theta^2 - 3)\eta^4 - (12\theta^2 - 3)\eta^2\right] - 1 \\ &= 15 + 3(12\theta^2 - 3) - (12\theta^2 - 3) - 1 \\ &= 24\theta^2 + 8 \\ &= 8(3\theta^2 + 1) \\ &= \mu_3(\theta), \end{aligned} \tag{5.141}$$

while the fourth central moment is given by

$$\begin{aligned}
\mathrm{E}_{z;\theta}\left[(z-\mu_1(\theta))^4\right] &= \mathrm{E}_\eta\left[(\theta^2+2\theta\eta+\eta^2-\theta^2-1)^4\right] \\
&= \mathrm{E}_\eta\left[\eta^8+8\eta^7\theta+24\eta^6\theta^2-4\eta^6+32\eta^5\theta^3\right. \\
&\quad -24\eta^5\theta+16\eta^4\theta^4-48\eta^4\theta^2+6\eta^4-32\eta^3\theta^3 \\
&\quad \left.+24\eta^3\theta+24\eta^2\theta^2-4\eta^2-8\eta\theta+1\right] \\
&= \mathrm{E}_\eta\left[\eta^8+(24\theta^2-4)\eta^6+(16\theta^4-48\theta^2+6)\eta^4+(24\theta^2-4)\eta^2+1\right] \\
&= 105+15(24\theta^2-4)+3(16\theta^4-48\theta^2+6)+24\theta^2-4+1 \\
&= 12(4\theta^4+20\theta^2+5) \\
&= 12\big((2\theta^2+1)^2+16\theta^2+4\big) \\
&= 12\big((2\theta^2+1)^2+4(4\theta^2+1)\big) \\
&= \mu_4(\theta). \qquad (5.142)
\end{aligned}$$

The skewness and the kurtosis of the system output are therefore

$$\begin{aligned}
\bar{\mu}_3(\theta) &= \mu_3(\theta)\mu_2^{-\frac{3}{2}}(\theta) \\
&= \frac{8(3\theta^2+1)}{2\sqrt{2}(2\theta^2+1)^{\frac{3}{2}}} \\
&= \frac{2\sqrt{2}(3\theta^2+1)}{(2\theta^2+1)^{\frac{3}{2}}}, \qquad (5.143) \\
\bar{\mu}_4(\theta) &= \mu_4(\theta)\mu_2^{-2}(\theta) \\
&= \frac{12\big((2\theta^2+1)^2+4(4\theta^2+1)\big)}{4(2\theta^2+1)^2} \\
&= \frac{12(4\theta^2+1)}{(2\theta^2+1)^2}+3. \qquad (5.144)
\end{aligned}$$

With the two derivatives

$$\begin{aligned}
\frac{\partial\mu_1(\theta)}{\partial\theta} &= 2\theta, \\
\frac{\partial\mu_2(\theta)}{\partial\theta} &= 8\theta, \qquad (5.145)
\end{aligned}$$

we obtain

$$\begin{aligned}
\beta^\star(\theta) &= \frac{\frac{\partial\mu_1(\theta)}{\partial\theta}\sqrt{\mu_2(\theta)}\bar{\mu}_3(\theta) - \frac{\partial\mu_2(\theta)}{\partial\theta}}{\frac{\partial\mu_2(\theta)}{\partial\theta}\bar{\mu}_3(\theta) - \frac{\partial\mu_1(\theta)}{\partial\theta}\sqrt{\mu_2(\theta)}(\bar{\mu}_4(\theta)-1)} \\
&= \frac{2\theta\sqrt{2}\sqrt{2\theta^2+1}\frac{2\sqrt{2}(3\theta^2+1)}{(2\theta^2+1)^{\frac{3}{2}}} - 8\theta}{8\theta\frac{2\sqrt{2}(3\theta^2+1)}{(2\theta^2+1)^{\frac{3}{2}}} - 2\theta\sqrt{2}\sqrt{2\theta^2+1}\Big(\frac{12(4\theta^2+1)}{(2\theta^2+1)^2}+2\Big)} \\
&= \frac{8(3\theta^2+1)(2^2+1) - 8(2\theta^2+1)^2}{16\sqrt{2}\sqrt{(2\theta^2+1)}(3\theta^2+1) - 4\sqrt{2}\sqrt{2\theta^2+1}\big(6(4\theta^2+1)+(2\theta^2+1)^2\big)} \\
&= \frac{(2\theta^2+1)}{\sqrt{2}\sqrt{(2\theta^2+1)}}\frac{2(3\theta^2+1)-2(2\theta^2+1)}{4(3\theta^2+1)-\big(6(4\theta^2+1)+(2\theta^2+1)^2\big)} \\
&= \frac{\sqrt{(2\theta^2+1)}}{\sqrt{2}}\frac{2\theta^2}{(12\theta^2+4)-\big((24\theta^2+6)+(4\theta^4+4\theta^2+1)\big)} \\
&= -\frac{\theta^2\sqrt{2}\sqrt{(2\theta^2+1)}}{(4\theta^4+16\theta^2+3)}
\end{aligned} \tag{5.146}$$

and the approximation of the Fisher information measure (5.52) is finally given by

$$\begin{aligned}
\tilde{F}_z(\theta) &= \frac{1}{\mu_2(\theta)}\frac{\Big(\frac{\partial\mu_1(\theta)}{\partial\theta}+\frac{\beta^\star(\theta)}{\sqrt{\mu_2(\theta)}}\frac{\partial\mu_2(\theta)}{\partial\theta}\Big)^2}{1+2\beta^\star(\theta)\bar{\mu}_3(\theta)+\beta^{\star 2}(\theta)(\bar{\mu}_4(\theta)-1)} \\
&= \frac{1}{2(2\theta^2+1)}\frac{\Big(2\theta-\frac{8\theta^3}{(4\theta^4+16\theta^2+3)}\Big)^2}{1-\frac{2\theta^2\sqrt{2}\sqrt{(2\theta^2+1)}}{(4\theta^4+16\theta^2+3)}\frac{2\sqrt{2}(3\theta^2+1)}{(2\theta^2+1)^{\frac{3}{2}}}+\Big(\frac{\theta^2\sqrt{2}\sqrt{(2\theta^2+1)}}{(4\theta^4+16\theta^2+3)}\Big)^2\Big(\frac{12(4\theta^2+1)}{(2\theta^2+1)^2}+2\Big)} \\
&= \frac{2\theta^2\Big(1-\frac{4\theta^2}{(4\theta^4+16\theta^2+3)}\Big)^2}{(2\theta^2+1)-\frac{2\theta^2\sqrt{2}}{(4\theta^4+16\theta^2+3)}\frac{2\sqrt{2}(3\theta^2+1)}{1}+\frac{4\theta^4}{(4\theta^4+16\theta^2+3)^2}\Big(6(4\theta^2+1)+(2\theta^2+1)^2\Big)} \\
&= \frac{2\theta^2\Big(1-\frac{4\theta^2}{(4\theta^4+16\theta^2+3)}\Big)^2}{(2\theta^2+1)-\frac{8\theta^2(3\theta^2+1)}{(4\theta^4+16\theta^2+3)}+\frac{4\theta^4(6(4\theta^2+1)+(2\theta^2+1)^2)}{(4\theta^4+16\theta^2+3)^2}} \\
&= \frac{2\theta^2\Big((4\theta^4+16\theta^2+3)-4\theta^2\Big)^2}{(2\theta^2+1)(4\theta^4+16\theta^2+3)^2-8\theta^2(3\theta^2+1)(4\theta^4+16\theta^2+3)+4\theta^4(4\theta^4+28\theta^2+7)} \\
&= \frac{2\theta^2\big(4\theta^4+12\theta^2+3\big)^2}{\big(4\theta^4+12\theta^2+3\big)\big(8\theta^6+24\theta^4+18\theta^2+3\big)} \\
&= \frac{2\theta^2\big(4\theta^4+12\theta^2+3\big)}{\big(8\theta^6+24\theta^4+18\theta^2+3\big)}.
\end{aligned} \tag{5.147}$$

Fig. 5.1 depicts the approximative information loss

$$\tilde{\chi}(\theta) = \frac{\tilde{F}_z(\theta)}{F_y(\theta)}, \tag{5.148}$$

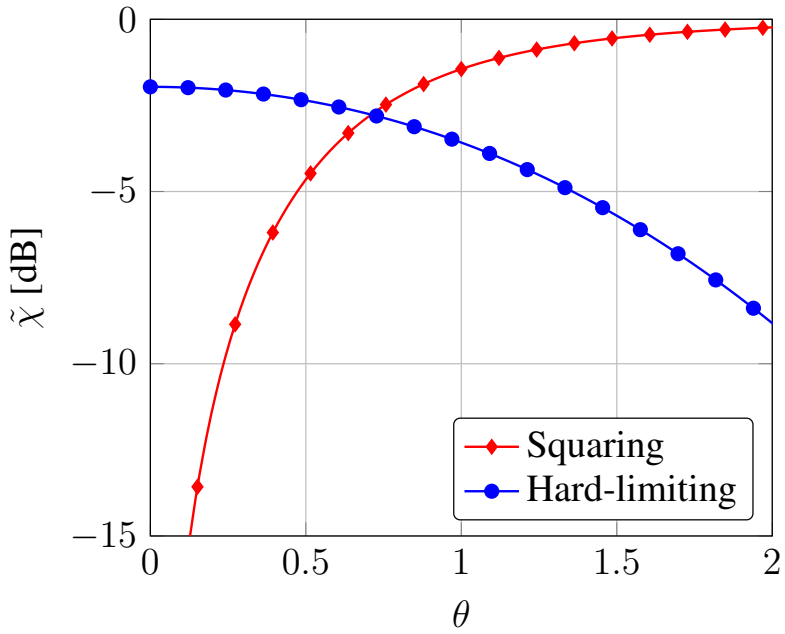

Fig. 5.1. Performance Loss - Squaring Device

when squaring the random input variable y. As a comparison also the corresponding loss for a symmetric hard-limiter (5.18 with $\upsilon = 0$) is visualized. It can be observed that for small values of θ the information about the sign (hard-limiting) of the system input y conveys much more information about the input mean θ than the amplitude (squaring). For $\theta \geq 0.75$ the situation changes and the squaring receiver outperforms the hard-limiter when it comes to estimating the mean θ of the input y from samples of the system output z. Note that for the squaring device the pessimistic approximation (5.52) allows us to assess the crossing point $\theta = 0.75$ in a conservative way.

5.2.6.3 Measuring Inference Capability after Soft-Limiting

A situation that can be encountered in practice is that the analytical characterization of the system model $p(z;\theta)$ or its moments is difficult. If the appropriate parametric system model $p(z;\theta)$ is unknown, the direct consultation of an analytical tool like the Fisher information measure $F_z(\theta)$ becomes impossible [62]. However, in such a situation the presented approach of the information bound $\tilde{F}_z(\theta)$ allows to numerically approximate the Fisher information measure $F_z(\theta)$ at low complexity. To this end, the moments of the system output z are measured in a calibrated setup, where the parameter θ can be controlled or determined by Monte-Carlo simulations. We demonstrate this validation technique by using a soft-limiter model, i.e., the system input y is transformed by

$$\begin{aligned} z &= \sqrt{\frac{2}{\pi {\kappa_l}^2}} \int_0^y \exp\left(-\frac{u^2}{2{\kappa_l}^2}\right) \mathrm{d}u \\ &= \operatorname{erf}\left(\frac{y}{\sqrt{2{\kappa_l}^2}}\right), \end{aligned} \tag{5.149}$$

where $\kappa_l \in \mathbb{R}$ is a constant model parameter and

$$\operatorname{erf}(x) \triangleq \frac{2}{\sqrt{\pi}} \int_0^x \exp\left(-u^2\right) \mathrm{d}u \tag{5.150}$$

is the error function. This nonlinear model can for example be used in order to characterize saturation effects in analog system components. In Fig. 5.2 the input-to-output mapping of the model

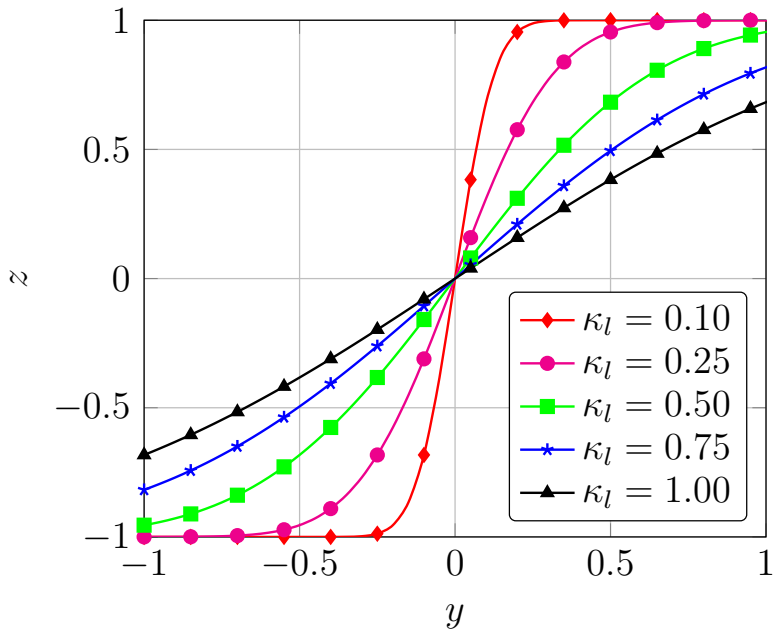

Fig. 5.2. Input-to-Output - Soft Limiter Model

(5.149) is depicted for different setups κ_l. As input we consider a Gaussian distribution with unit variance like in (5.137). The output mean $\mu_1(\theta)$, the variance $\mu_2(\theta)$, the skewness $\bar{\mu}_3(\theta)$ and the kurtosis $\bar{\mu}_4(\theta)$ are measured by simulating the nonlinear system output with 10^9 independent realizations for each considered value of the input mean θ. The result is shown in Fig. 5.3. After

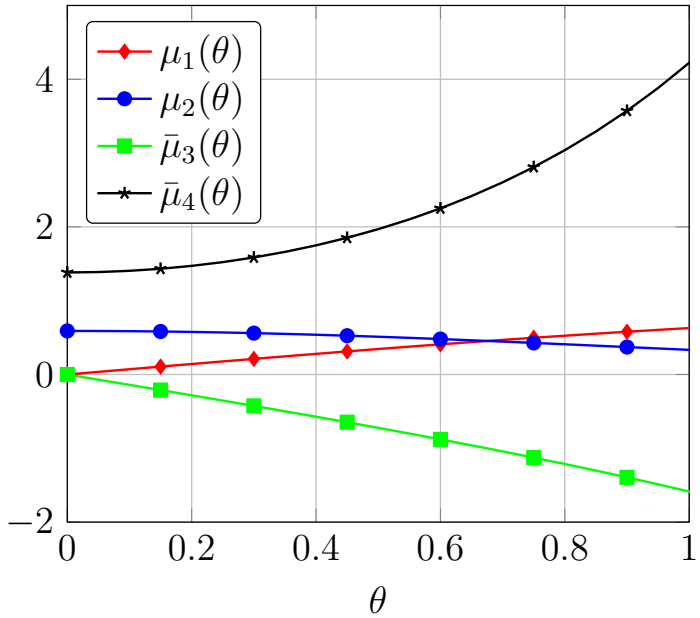

Fig. 5.3. Measured Moments - Soft-Limiter Model ($\kappa_l = 0.5$)

numerically approximating the required derivatives $\frac{\partial \mu_1(\theta)}{\partial \theta}$, $\frac{\partial \mu_2(\theta)}{\partial \theta}$, which are depicted in Fig. 5.4,

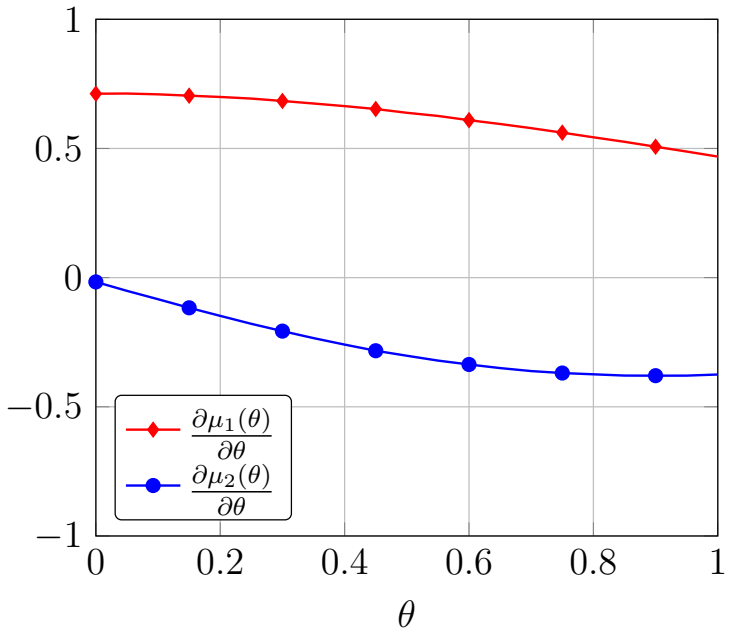

Fig. 5.4. Measured Derivatives - Soft-Limiter Model ($\kappa_l = 0.5$)

the approximation (5.52) is calculated. In Fig. 5.5 the measured information loss $\tilde{\chi}(\theta)$ of the soft-limiter model is shown, where the dotted line indicates the exact information loss $\chi(\theta)$ with a symmetric hard-limiter (5.18) which is equivalent to a soft-limiter with $\kappa_l \to 0$.

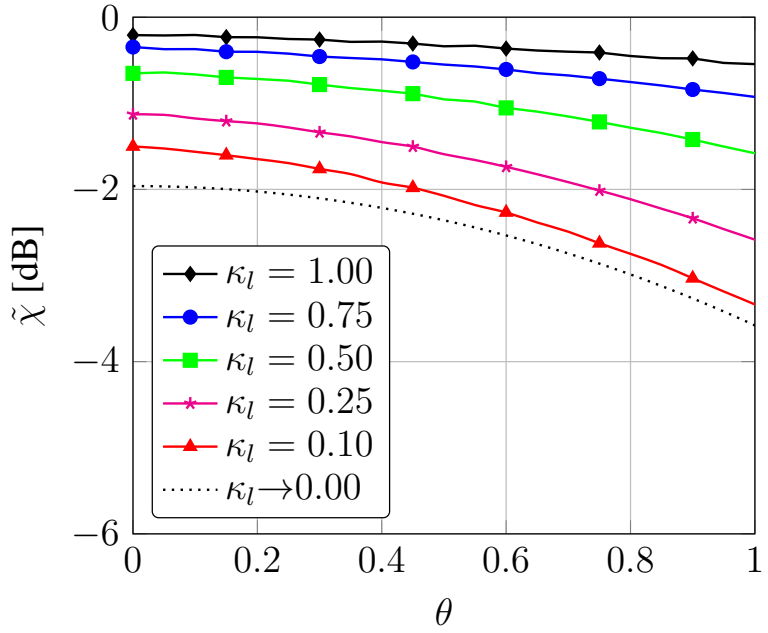

Fig. 5.5. Performance Loss - Soft-Limiter Model

5.3 Generalized Fisher Information Lower Bound

While the second-order approach on bounding the Fisher information measure (5.52) turns out to provide tight results for various cases (Bernoulli, exponential, Gaussian or Poisson distribution), we have also identified an example where the information bound is loose (Laplace distribution). Looking at the properties of these example distributions, it becomes obvious that for the tight cases the sufficient statistics are z (exponential, Bernoulli, Poisson) or z and z^2 (Gaussian). In contrast, the zero-mean Laplace distribution has the sufficient statistic $|z|$. Such a statistic is not well captured by z and z^2, which we have used in centralized and normalized form for the construction of the second-order bound (5.52). Might this be the reason why the approximation (5.52) fails to generate a tight bound under the Laplacian distribution?

5.3.1 Fisher Information Lower Bounds and Sufficient Statistics

Addressing this question, in the following we pick the log-normal distribution with known scale parameter σ and the Weibull distribution with known shape parameter κ_w as additional examples. Like the Laplace distribution, the log-normal distribution has sufficient statistics which are distinct from z and z^2, i.e., $\ln z$ and $\ln^2 z$. The Weibull distribution has the property that its sufficient statistic is z^{κ_w}. Therefore, the second-order Fisher information bound (5.52) should be tight for the Weibull distribution when $\kappa_w = 1$ and $\kappa_w = 2$ and loose in any other configuration, including the log-normal distribution, in order to confirm an existing connection between the construction of the information bound and the sufficient statistics of the model $p(z;\theta)$.

5.3.1.1 Log-normal Distribution

The log-normal distribution with known scale parameter $\sigma > 0$ is characterized by the probability density function

$$p(z;\theta) = \frac{1}{\sqrt{2\pi\sigma^2}z} \exp\left(-\frac{(\log z - \theta)^2}{2\sigma^2}\right) \tag{5.151}$$

with $z > 0$. The log-likelihood function is given by

$$\ln p(z;\theta) = -\frac{1}{2}\ln 2\pi\sigma^2 - \ln z - \frac{1}{2\sigma^2}(\log z - \theta)^2. \tag{5.152}$$

The score function is

$$\frac{\partial \ln p(z;\theta)}{\partial\theta} = \frac{1}{\sigma^2}(\log z - \theta), \tag{5.153}$$

with its derivative

$$\frac{\partial^2 \ln p(z;\theta)}{\partial\theta^2} = -\frac{1}{\sigma^2}. \tag{5.154}$$

Therefore, the Fisher information measure with respect to the parameter θ is given by

$$\begin{aligned} F_z(\theta) &= \mathrm{E}_{z;\theta}\left[\left(\frac{\partial \ln p(z;\theta)}{\partial\theta}\right)^2\right] \\ &= -\mathrm{E}_{z;\theta}\left[\frac{\partial^2 \ln p(z;\theta)}{\partial\theta^2}\right] = \frac{1}{\sigma^2}. \end{aligned} \tag{5.155}$$

For the evaluation of the mean and the variance we use the fact that the l-th raw moment of the log-normal distribution is

$$\begin{aligned} \mathrm{E}_{z;\theta}\left[z^l\right] &= \tilde{\mu}_l(\theta) \\ &= \mathrm{e}^{l\theta+\frac{1}{2}l^2\sigma^2}. \end{aligned} \tag{5.156}$$

Accordingly, the mean and its derivative are given by

$$\begin{aligned} \mu_1(\theta) &= \mathrm{E}_{z;\theta}\left[z\right] \\ &= \mathrm{e}^{\theta+\frac{1}{2}\sigma^2}, \end{aligned} \tag{5.157}$$

$$\frac{\partial \mu_1(\theta)}{\partial \theta} = \mathrm{e}^{\theta+\frac{1}{2}\sigma^2}. \tag{5.158}$$

The variance and its derivative are

$$\begin{aligned} \mu_2(\theta) &= \mathrm{E}_{z;\theta}\left[\big(z-\mu_1(\theta)\big)^2\right] \\ &= \tilde{\mu}_2(\theta) - \mu_1^2(\theta) \\ &= \mathrm{e}^{2\theta+\sigma^2}(\mathrm{e}^{\sigma^2}-1), \end{aligned} \tag{5.159}$$

$$\frac{\partial \mu_2(\theta)}{\partial \theta} = 2\,\mathrm{e}^{2\theta+\sigma^2}(\mathrm{e}^{\sigma^2}-1). \tag{5.160}$$

The skewness of the log-normal system model is obtained by

$$\begin{aligned} \bar{\mu}_3(\theta) &= \mathrm{E}_{z;\theta}\left[\left(\frac{z-\mu_1(\theta)}{\sqrt{\mu_2(\theta)}}\right)^3\right] \\ &= \frac{\tilde{\mu}_3 - 3\mu_1(\theta)\tilde{\mu}_2(\theta) + 2\mu_1^3(\theta)}{\mu_2^{\frac{3}{2}}(\theta)} \\ &= \frac{\mathrm{e}^{3\theta+\frac{9}{2}\sigma^2} - 3\,\mathrm{e}^{\theta+\frac{1}{2}\sigma^2}\,\mathrm{e}^{2\theta+2\sigma^2} + 2\,\mathrm{e}^{3\theta+\frac{3}{2}\sigma^2}}{(\mathrm{e}^{2\theta+\sigma^2}(\mathrm{e}^{\sigma^2}-1))^{\frac{3}{2}}} \\ &= \frac{\mathrm{e}^{3\theta+\frac{9}{2}\sigma^2} - 3\,\mathrm{e}^{3\theta+\frac{5}{2}\sigma^2} + 2\,\mathrm{e}^{3\theta+\frac{3}{2}\sigma^2}}{\mathrm{e}^{3\theta+\frac{3}{2}\sigma^2}(\mathrm{e}^{\sigma^2}-1)^{\frac{3}{2}}} \\ &= \frac{\mathrm{e}^{3\sigma^2} - 3\,\mathrm{e}^{\sigma^2} + 2}{(\mathrm{e}^{\sigma^2}-1)^{\frac{3}{2}}} \\ &= \frac{(\mathrm{e}^{\sigma^2}-1)^2(\mathrm{e}^{\sigma^2}+2)}{(\mathrm{e}^{\sigma^2}-1)^{\frac{3}{2}}} \\ &= \sqrt{(\mathrm{e}^{\sigma^2}-1)}(\mathrm{e}^{\sigma^2}+2) \end{aligned} \tag{5.161}$$

and the kurtosis is found to be

$$\begin{aligned}
\bar{\mu}_4(\theta) &= \mathrm{E}_{z;\theta}\left[\left(\frac{z-\mu_1(\theta)}{\sqrt{\mu_2(\theta)}}\right)^4\right] \\
&= \frac{\tilde{\mu}_4 - 4\mu_1(\theta)\tilde{\mu}_3(\theta) + 6\mu_1^2(\theta)\tilde{\mu}_2(\theta) - 3\mu_1^4(\theta)}{\mu_2^2(\theta)} \\
&= \frac{\mathrm{e}^{4\theta+8\sigma^2} - 4\,\mathrm{e}^{\theta+\frac{1}{2}\sigma^2}\,\mathrm{e}^{3\theta+\frac{9}{2}\sigma^2} + 6\,\mathrm{e}^{2\theta+\sigma^2}\,\mathrm{e}^{2\theta+2\sigma^2} - 3\,\mathrm{e}^{4\theta+2\sigma^2}}{(\mathrm{e}^{2\theta+\sigma^2}(\mathrm{e}^{\sigma^2}-1))^2} \\
&= \frac{\mathrm{e}^{4\theta+8\sigma^2} - 4\,\mathrm{e}^{4\theta+5\sigma^2} + 6\,\mathrm{e}^{4\theta+3\sigma^2} - 3\,\mathrm{e}^{4\theta+2\sigma^2}}{\mathrm{e}^{4\theta+2\sigma^2}(\mathrm{e}^{\sigma^2}-1)^2} \\
&= \frac{\mathrm{e}^{6\sigma^2} - 4\,\mathrm{e}^{3\sigma^2} + 6\,\mathrm{e}^{\sigma^2} - 3}{(\mathrm{e}^{\sigma^2}-1)^2} \\
&= \frac{(\mathrm{e}^{\sigma^2}-1)^2(3\,\mathrm{e}^{2\sigma^2} + 2\,\mathrm{e}^{3\sigma^2} + \mathrm{e}^{4\sigma^2} - 3)}{(\mathrm{e}^{\sigma^2}-1)^2} \\
&= 3\,\mathrm{e}^{2\sigma^2} + 2\,\mathrm{e}^{3\sigma^2} + \mathrm{e}^{4\sigma^2} - 3.
\end{aligned} \tag{5.162}$$

For the assessment of the quality of the information bound (5.52) we define the ratio between the approximation (5.52) and the exact information measure (5.155)

$$\chi(\theta) \triangleq \frac{\tilde{F}_z(\theta)}{F_z(\theta)}. \tag{5.163}$$

As the gap (5.163) is independent of θ, in Fig. 5.6, we depict $\chi(\theta)$ for different values of the known scale parameter σ. It can be observed that for a scale parameter $\sigma > 1$ the difference between $\tilde{F}_z(\theta)$ and the exact Fisher information $F_z(\theta)$ becomes large.

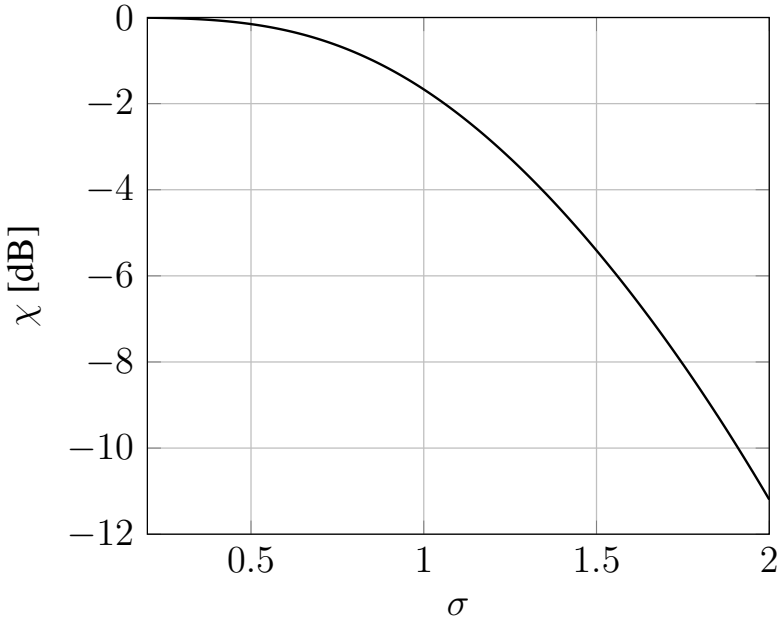

Fig. 5.6. Bounding Gap - Log-Normal Distribution

5.3.1.2 Weibull Distribution

As a second example, we study the quality of the Fisher information bound $\tilde{F}(\theta)$ for the case of the Weibull distribution. The Weibull distribution with known shape parameter κ_w is characterized by the probability density function

$$p(z;\theta) = \frac{\kappa_w}{\theta}\left(\frac{z}{\theta}\right)^{\kappa_w - 1} \mathrm{e}^{-(\frac{z}{\theta})^{\kappa_w}} \tag{5.164}$$

with $z, \theta, \kappa_w > 0$. The log-likelihood of the distribution is

$$\ln p(z;\theta) = \ln \kappa_w - \ln \theta + (\kappa_w - 1)\ln z - (\kappa_w - 1)\ln \theta - \left(\frac{z}{\theta}\right)^{\kappa_w} \tag{5.165}$$

and the score function is given by

$$\begin{aligned}\frac{\partial \ln p(z;\theta)}{\partial \theta} &= -\frac{1}{\theta} - (\kappa_w - 1)\frac{1}{\theta} + \kappa_w\left(\frac{z}{\theta}\right)^{\kappa_w - 1}\frac{z}{\theta^2} \\ &= -\frac{\kappa_w}{\theta} + \frac{\kappa_w}{\theta}\left(\frac{z}{\theta}\right)^{\kappa_w} \\ &= \frac{\kappa_w}{\theta}\left(\left(\frac{z}{\theta}\right)^{\kappa_w} - 1\right).\end{aligned} \tag{5.166}$$

The derivative of the score function has the form

$$\begin{aligned}\frac{\partial^2 \ln p(z;\theta)}{\partial \theta^2} &= -\frac{\kappa_w}{\theta^2}\left(\left(\frac{z}{\theta}\right)^{\kappa_w} - 1\right) + \frac{\kappa_w}{\theta}\left(-\kappa_w\left(\frac{z}{\theta}\right)^{\kappa_w - 1}\frac{z}{\theta^2}\right) \\ &= -\frac{\kappa_w}{\theta^2}\left(\left(\frac{z}{\theta}\right)^{\kappa_w} - 1\right) - \frac{\kappa_w^2}{\theta^2}\left(\frac{z}{\theta}\right)^{\kappa_w} \\ &= -\frac{\kappa_w(\kappa_w + 1)}{\theta^2}\left(\frac{z}{\theta}\right)^{\kappa_w} + \frac{\kappa_w}{\theta^2}.\end{aligned} \tag{5.167}$$

Consequently, the Fisher information measure is given by

$$\begin{aligned}F_z(\theta) &= \mathrm{E}_{z;\theta}\left[\left(\frac{\partial \ln p(z;\theta)}{\partial \theta}\right)^2\right] \\ &= -\mathrm{E}_{z;\theta}\left[\frac{\partial^2 \ln p(z;\theta)}{\partial \theta^2}\right] \\ &= \frac{\kappa_w(\kappa_w + 1)}{\theta^{\kappa_w + 2}}\mathrm{E}_{z;\theta}\left[z^{\kappa_w}\right] - \frac{\kappa_w}{\theta^2} \\ &= \frac{\kappa_w}{\theta^2}\left(\frac{(\kappa_w + 1)}{\theta^{\kappa_w}}\mathrm{E}_{z;\theta}\left[z^{\kappa_w}\right] - 1\right) \\ &= \frac{\kappa_w}{\theta^2}\Big((\kappa_w + 1)\Gamma(2) - 1\Big) \\ &= \left(\frac{\kappa_w}{\theta}\right)^2,\end{aligned} \tag{5.168}$$

where we used the property that the l-th raw moment of the Weibull distribution is

$$\begin{aligned}\tilde{\mu}_l &= \mathrm{E}_{z;\theta}\left[z^l\right] \\ &= \theta^l \Gamma_l,\end{aligned} \tag{5.169}$$

with the shorthand notational convention

$$\Gamma_l \triangleq \Gamma\Big(1+\frac{l}{\kappa_w}\Big) \tag{5.170}$$

for the Gamma function

$$\Gamma(x) \triangleq \int_0^\infty u^{x-1}\exp\left(-u\right)\mathrm{d}u. \tag{5.171}$$

For the information bound (5.52) we require the first moment

$$\begin{aligned}\mu_1(\theta) &= \mathrm{E}_{z;\theta}\left[z\right]\\ &= \theta\Gamma_1,\end{aligned} \tag{5.172}$$

its derivative

$$\frac{\partial\mu_1(\theta)}{\partial\theta} = \Gamma_1, \tag{5.173}$$

the second central moment

$$\begin{aligned}\mu_2(\theta) &= \mathrm{E}_{z;\theta}\left[\big(z-\mu_1(\theta)\big)^2\right]\\ &= \tilde{\mu}_2(\theta) - \mu_1^2(\theta)\\ &= \theta^2\big(\Gamma_2-\Gamma_1^2\big),\end{aligned} \tag{5.174}$$

its derivative

$$\frac{\partial\mu_2(\theta)}{\partial\theta} = 2\theta\big(\Gamma_2-\Gamma_1^2\big), \tag{5.175}$$

the skewness of the Weibull system model

$$\begin{aligned}\bar{\mu}_3(\theta) &= \mathrm{E}_{z;\theta}\left[\left(\frac{z-\mu_1(\theta)}{\sqrt{\mu_2(\theta)}}\right)^3\right]\\ &= \frac{\tilde{\mu}_3 - 3\mu_1(\theta)\tilde{\mu}_2(\theta) + 2\mu_1^3(\theta)}{\mu_2^{\frac{3}{2}}(\theta)}\\ &= \frac{\theta^3\Gamma_3 - 3\theta^3\Gamma_1\Gamma_2 + 2\theta^3\Gamma_1^3}{\theta^3\Big(\Gamma_2-\Gamma_1^2\Big)^{\frac{3}{2}}}\\ &= \frac{\Gamma_3 - 3\Gamma_1\Gamma_2 + 2\Gamma_1^3}{\big(\Gamma_2-\Gamma_1^2\big)^{\frac{3}{2}}},\end{aligned} \tag{5.176}$$

and the kurtosis

$$\begin{aligned}\bar{\mu}_4(\theta) &= \mathrm{E}_{z;\theta}\left[\left(\frac{z-\mu_1(\theta)}{\sqrt{\mu_2(\theta)}}\right)^4\right]\\ &= \frac{\tilde{\mu}_4 - 4\mu_1(\theta)\tilde{\mu}_3(\theta) + 6\mu_1^2(\theta)\tilde{\mu}_2(\theta) - 3\mu_1^4(\theta)}{\mu_2^2(\theta)}\\ &= \frac{\Gamma_4 - 4\Gamma_1\Gamma_3 + 6\Gamma_1^2\Gamma_2 - 3\Gamma_1^4}{\big(\Gamma_2-\Gamma_1^2\big)^2}.\end{aligned} \tag{5.177}$$

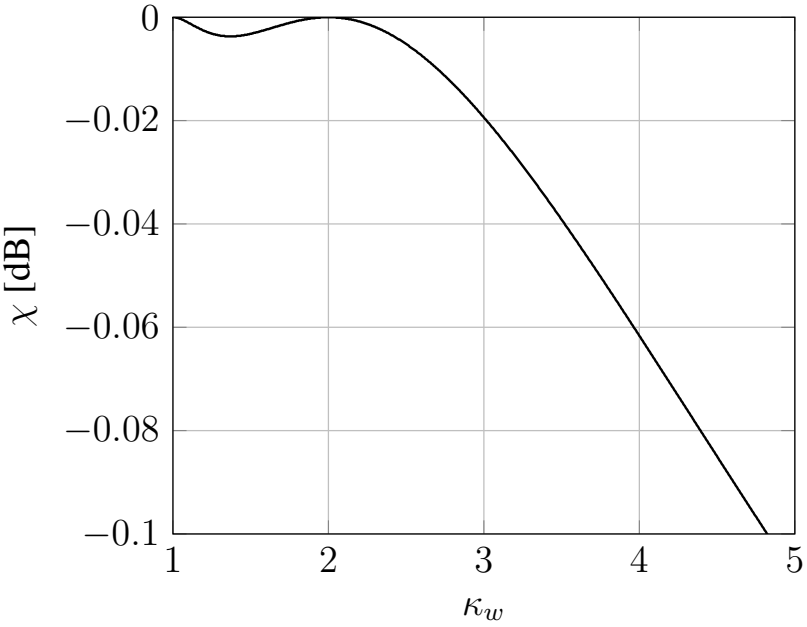

Fig. 5.7. Bounding Gap - Weibull Distribution

In Fig. 5.7 we plot the information loss $\chi(\theta)$ for different shape values $\kappa_w = 1, \ldots, 5$. Note, that in this example the loss $\chi(\theta)$ is independent of the parameter θ. It can be observed that the information bound $\tilde{F}_z(\theta)$ is tight for the cases where the shape of the distribution is $\kappa_w = 1$ and $\kappa_w = 2$ while the quality of $\tilde{F}_z(\theta)$ degrades significantly for the cases where $\kappa_w > 2$.

The Weibull example is of special interest for the analysis of the quality of the approximation (5.52) as it contains cases where the Fisher information lower bound is tight and cases where it is not. We have verified that (5.52) is tight for the Bernoulli, exponential, Gaussian and Poisson distributions. These distributions have in common that their sufficient statistics are z or z and z^2. Interestingly, for the Weibull distribution the sufficient statistic is given by z^{κ_w} and the information bound (5.52) is only tight for $\kappa_w = 1$ and $\kappa_w = 2$. Additionally, the approximation of the Fisher information (5.52) is loose for the log-normal distribution and the Laplacian distribution, both cases where the sufficient statistics are distinct from z or z^2. This indicates a connection between the sufficient statistics and the quality of lower bounds for the Fisher information bound. Note, that the information bound (5.52) was constructed through the Cauchy-Schwarz inequality

$$\int_{\mathcal{Z}} f^2(z;\theta)p(z;\theta)\mathrm{d}z \geq \frac{\left(\int_{\mathcal{Z}} f(z;\theta)g(z;\theta)p(z;\theta)\mathrm{d}z\right)^2}{\int_{\mathcal{Z}} g^2(z;\theta)p(z;\theta)\mathrm{d}z} \tag{5.178}$$

by using the functions

$$f(z;\theta) = \frac{\partial \ln p(z;\theta)}{\partial \theta} \tag{5.179}$$

and

$$g(z;\theta) = \left(\frac{z-\mu_1(\theta)}{\sqrt{\mu_2(\theta)}}\right) + \beta(\theta)\left(\frac{z-\mu_1(\theta)}{\sqrt{\mu_2(\theta)}}\right)^2 - \beta(\theta). \tag{5.180}$$

The latter contains the statistics z and z^2 in normalized central form. This corresponds to the sufficient statistics of the distributions where (5.52) provides tight results.

5.3.2 Fisher Information and the Exponential Family

Another interesting observation is the fact that all example distributions discussed so far belong to the exponential family. Therefore, in order to obtain a better understanding on Fisher information and possible lower bounds, we adapt our level of abstraction and study the properties of the Fisher information measure for distributions of the exponential family. Restricting to such a class of distributions allows to provide an identity connecting Fisher information and a weighted sum of the derivatives of the expected sufficient statistics. The weight of each statistic within this sum is the derivative of the associated natural parameter. In order to provide the main results in a general form in the following we focus on the multivariate case $p(\boldsymbol{z};\boldsymbol{\theta})$ with output variable $\boldsymbol{z} \in \mathbb{R}^M$ and a multi-dimensional parameter $\boldsymbol{\theta} \in \mathbb{R}^D$.

5.3.2.1 The Exponential Family

The multivariate exponential family with a parameter $\boldsymbol{\theta} \in \mathbb{R}^D$ is the set of probability density or mass functions, which can be factorized

$$p(\boldsymbol{z};\boldsymbol{\theta}) = \exp\left(\sum_{l=1}^{L} w_l(\boldsymbol{\theta}) t_l(\boldsymbol{z}) - \lambda(\boldsymbol{\theta}) + \kappa(\boldsymbol{z})\right), \tag{5.181}$$

where $w_l(\boldsymbol{\theta}) \in \mathbb{R}$ is the l-th natural parameter, $t_l(\boldsymbol{z}) \in \mathbb{R}$ is the associated sufficient statistic, $\lambda(\boldsymbol{\theta}) \in \mathbb{R}$ is the log-normalizer and $\kappa(\boldsymbol{z}) \in \mathbb{R}$ is the so-called carrier measure. The log-likelihood function of the exponential family (5.181) is given by

$$\ln p(\boldsymbol{z};\boldsymbol{\theta}) = \sum_{l=1}^{L} w_l(\boldsymbol{\theta}) t_l(\boldsymbol{z}) - \lambda(\boldsymbol{\theta}) + \kappa(\boldsymbol{z}), \tag{5.182}$$

while the score function is

$$\frac{\partial \ln p(\boldsymbol{z};\boldsymbol{\theta})}{\partial \boldsymbol{\theta}} = \sum_{l=1}^{L} \frac{\partial w_l(\boldsymbol{\theta})}{\partial \boldsymbol{\theta}} t_l(\boldsymbol{z}) - \frac{\partial \lambda(\boldsymbol{\theta})}{\partial \boldsymbol{\theta}}. \tag{5.183}$$

As discussed in (3.3), an essential property of the score function (5.183) is that its expected value vanishes, i.e.,

$$\mathrm{E}_{\boldsymbol{z};\boldsymbol{\theta}}\left[\frac{\partial \ln p(\boldsymbol{z};\boldsymbol{\theta})}{\partial \boldsymbol{\theta}}\right] = \mathbf{0}^{\mathrm{T}}. \tag{5.184}$$

Therefore, with (5.183) it holds that for the exponential family

$$\sum_{l=1}^{L} \frac{\partial w_l(\boldsymbol{\theta})}{\partial \boldsymbol{\theta}} \mathrm{E}_{\boldsymbol{z};\boldsymbol{\theta}}\left[t_l(\boldsymbol{z})\right] = \frac{\partial \lambda(\boldsymbol{\theta})}{\partial \boldsymbol{\theta}}. \tag{5.185}$$

5.3.2.2 Fisher Information within the Exponential Family

With the definition of the Fisher information we obtain

$$\begin{aligned}\boldsymbol{F}(\boldsymbol{\theta}) &= \int_{\mathcal{Z}} \left(\frac{\partial \ln p(\boldsymbol{z};\boldsymbol{\theta})}{\partial \boldsymbol{\theta}}\right)^{\mathrm{T}} \left(\frac{\partial \ln p(\boldsymbol{z};\boldsymbol{\theta})}{\partial \boldsymbol{\theta}}\right) p(\boldsymbol{z};\boldsymbol{\theta}) \mathrm{d}\boldsymbol{z} \\ &= \int_{\mathcal{Z}} \left(\frac{\partial \ln p(\boldsymbol{z};\boldsymbol{\theta})}{\partial \boldsymbol{\theta}}\right)^{\mathrm{T}} \left(\sum_{l=1}^{L} \frac{\partial w_l(\boldsymbol{\theta})}{\partial \boldsymbol{\theta}} t_l(\boldsymbol{z})\right) p(\boldsymbol{z};\boldsymbol{\theta}) \mathrm{d}\boldsymbol{z} \\ &\quad - \int_{\mathcal{Z}} \left(\frac{\partial \ln p(\boldsymbol{z};\boldsymbol{\theta})}{\partial \boldsymbol{\theta}}\right)^{\mathrm{T}} \frac{\partial \lambda(\boldsymbol{\theta})}{\partial \boldsymbol{\theta}} p(\boldsymbol{z};\boldsymbol{\theta}) \mathrm{d}\boldsymbol{z}, \end{aligned} \tag{5.186}$$

where we have used (5.183) in the second step to substitute one of the involved score functions. Using (5.184), we obtain

$$\begin{aligned}\boldsymbol{F}(\boldsymbol{\theta}) &= \sum_{l=1}^{L} \left(\int_{\mathcal{Z}} \frac{\partial \ln p(\boldsymbol{z};\boldsymbol{\theta})}{\partial \boldsymbol{\theta}} t_l(\boldsymbol{z}) p(\boldsymbol{z};\boldsymbol{\theta}) \mathrm{d}\boldsymbol{z}\right)^{\mathrm{T}} \frac{\partial w_l(\boldsymbol{\theta})}{\partial \boldsymbol{\theta}} \\ &\quad - \left(\int_{\mathcal{Z}} \left(\frac{\partial \ln p(\boldsymbol{z};\boldsymbol{\theta})}{\partial \boldsymbol{\theta}}\right)^{\mathrm{T}} p(\boldsymbol{z};\boldsymbol{\theta}) \mathrm{d}\boldsymbol{z}\right) \frac{\partial \lambda(\boldsymbol{\theta})}{\partial \boldsymbol{\theta}} \\ &= \sum_{l=1}^{L} \left(\int_{\mathcal{Z}} \frac{\partial p(\boldsymbol{z};\boldsymbol{\theta})}{\partial \boldsymbol{\theta}} t_l(\boldsymbol{z}) \mathrm{d}\boldsymbol{z}\right)^{\mathrm{T}} \frac{\partial w_l(\boldsymbol{\theta})}{\partial \boldsymbol{\theta}} - \left(\int_{\mathcal{Z}} \frac{\partial p(\boldsymbol{z};\boldsymbol{\theta})}{\partial \boldsymbol{\theta}} \mathrm{d}\boldsymbol{z}\right)^{\mathrm{T}} \frac{\partial \lambda(\boldsymbol{\theta})}{\partial \boldsymbol{\theta}} \\ &= \sum_{l=1}^{L} \left(\frac{\partial}{\partial \boldsymbol{\theta}} \int_{\mathcal{Z}} p(\boldsymbol{z};\boldsymbol{\theta}) t_l(\boldsymbol{z}) \mathrm{d}\boldsymbol{z}\right)^{\mathrm{T}} \frac{\partial w_l(\boldsymbol{\theta})}{\partial \boldsymbol{\theta}} \\ &= \sum_{l=1}^{L} \left(\frac{\partial \, \mathrm{E}_{\boldsymbol{z};\boldsymbol{\theta}}\left[t_l(\boldsymbol{z})\right]}{\partial \boldsymbol{\theta}}\right)^{\mathrm{T}} \frac{\partial w_l(\boldsymbol{\theta})}{\partial \boldsymbol{\theta}}. \end{aligned} \tag{5.187}$$

Defining the vector of sufficient statistics

$$\boldsymbol{t}(\boldsymbol{z}) = \begin{bmatrix} t_1(\boldsymbol{z}) & t_2(\boldsymbol{z}) & \ldots & t_L(\boldsymbol{z}) \end{bmatrix}^{\mathrm{T}}, \tag{5.188}$$

its expected value

$$\boldsymbol{\mu}_{\boldsymbol{t}}(\boldsymbol{\theta}) = \mathrm{E}_{\boldsymbol{z};\boldsymbol{\theta}}\left[\boldsymbol{t}(\boldsymbol{z})\right], \tag{5.189}$$

and the vector of natural parameters

$$\boldsymbol{w}(\boldsymbol{\theta}) = \begin{bmatrix} w_1(\boldsymbol{\theta}) & w_2(\boldsymbol{\theta}) & \ldots & w_L(\boldsymbol{\theta}) \end{bmatrix}^{\mathrm{T}}, \tag{5.190}$$

we can reformulate the identity (5.187) in a compact form

$$\boldsymbol{F}(\boldsymbol{\theta}) = \left(\frac{\partial \boldsymbol{\mu}_{\boldsymbol{t}}(\boldsymbol{\theta})}{\partial \boldsymbol{\theta}}\right)^{\mathrm{T}} \frac{\partial \boldsymbol{w}(\boldsymbol{\theta})}{\partial \boldsymbol{\theta}}. \tag{5.191}$$

5.3.2.3 Univariate Gaussian Model with a Single Parameter

As an example for the identity (5.191), consider the univariate parametric Gaussian distribution

$$p(z;\theta) = \frac{1}{\sqrt{2\pi\sigma^2(\theta)}} \exp\left(-\frac{\big(z - s(\theta)\big)^2}{2\sigma^2(\theta)}\right) \tag{5.192}$$

with $z \in \mathbb{R}$ and parameter $\theta \in \mathbb{R}$. The natural parameters are

$$w_1(\theta) = \frac{s(\theta)}{\sigma^2(\theta)}, \tag{5.193}$$

$$w_2(\theta) = -\frac{1}{2\sigma^2(\theta)} \tag{5.194}$$

and the two corresponding sufficient statistics are

$$t_1(z) = z, \tag{5.195}$$

$$t_2(z) = z^2. \tag{5.196}$$

Therefore, the expectations of the sufficient statistics are

$$\mathrm{E}_{z;\theta}\left[t_1(z)\right] = \mu(\theta), \tag{5.197}$$

$$\mathrm{E}_{z;\theta}\left[t_2(z)\right] = \sigma^2(\theta) + s^2(\theta). \tag{5.198}$$

With the derivatives of the natural parameters

$$\frac{\partial w_1(\theta)}{\partial\theta} = \frac{1}{\sigma^2(\theta)}\frac{\partial s(\theta)}{\partial\theta} - \frac{s(\theta)}{\sigma^4(\theta)}\frac{\partial\sigma^2(\theta)}{\partial\theta}, \tag{5.199}$$

$$\frac{\partial w_2(\theta)}{\partial\theta} = \frac{1}{2\sigma^4(\theta)}\frac{\partial\sigma^2(\theta)}{\partial\theta} \tag{5.200}$$

and the derivatives of the expected sufficient statistics

$$\begin{aligned}\frac{\partial\,\mathrm{E}_{z;\theta}\left[t_1(z)\right]}{\partial\theta} &= \frac{\partial s(\theta)}{\partial\theta},\\ \frac{\partial\,\mathrm{E}_{z;\theta}\left[t_2(z)\right]}{\partial\theta} &= \frac{\partial\sigma^2(\theta)}{\partial\theta} + 2s(\theta)\frac{\partial s(\theta)}{\partial\theta},\end{aligned} \tag{5.201}$$

using the identity for the exponential family (5.187) we obtain

$$\begin{aligned}F(\theta) &= \frac{\partial w_1(\theta)}{\partial\theta}\frac{\partial\,\mathrm{E}_{z;\theta}\left[t_1(z)\right]}{\partial\theta} + \frac{\partial w_2(\theta)}{\partial\theta}\frac{\partial\,\mathrm{E}_{z;\theta}\left[t_2(z)\right]}{\partial\theta}\\ &= \frac{1}{\sigma^2(\theta)}\Big(\frac{\partial s(\theta)}{\partial\theta}\Big)^2 + \frac{1}{2\sigma^4(\theta)}\Big(\frac{\partial\sigma^2(\theta)}{\partial\theta}\Big)^2.\end{aligned} \tag{5.202}$$

It can be verified [2, pp. 47] that (5.202) is the actual Fisher information measure for the parametric Gaussian model (5.192).

5.3.3 The Exponential Replacement

If the parametric model $p(\boldsymbol{z};\boldsymbol{\theta})$ belongs to the exponential family, the natural parameters $\boldsymbol{w}(\boldsymbol{\theta})$ and the associated expected values of the sufficient statistics $\boldsymbol{\mu}_{\boldsymbol{t}}(\boldsymbol{\theta})$ are known, the identity (5.191) shows that the Fisher information measure can be computed by evaluating a sum instead of integrating the squared score function. In the inconvenient situation where it is unclear if the model $p(\boldsymbol{z};\boldsymbol{\theta})$ belongs to the exponential family and the sufficient statistics $\boldsymbol{t}(\boldsymbol{z})$ or the natural parameters $\boldsymbol{w}(\boldsymbol{\theta})$ are unknown, the identity (5.191) can not be applied in order to derive the Fisher information measure. However, the Fisher identity of the exponential family (5.191) provides a guideline for the construction of strong Fisher information lower bounds for any kind of stochastic system.

To this end, the original system $p(\boldsymbol{z};\boldsymbol{\theta})$ is replaced by a counterpart in the exponential family $\tilde{p}(\boldsymbol{z};\boldsymbol{\theta})$, which is equivalent with respect to a set of L auxiliary statistics

$$\phi_l(\boldsymbol{z}) : \mathbb{R}^M \to \mathbb{R}, \quad l = 1, 2, \ldots, L. \tag{5.203}$$

After selecting (5.203), with the definition

$$\boldsymbol{\phi}(\boldsymbol{z}) = \begin{bmatrix} \phi_1(\boldsymbol{z}) & \phi_2(\boldsymbol{z}) & \ldots & \phi_L(\boldsymbol{z}) \end{bmatrix}^{\mathrm{T}}, \tag{5.204}$$

we determine the expected values

$$\begin{aligned} \boldsymbol{\mu}_{\boldsymbol{\phi}}(\boldsymbol{\theta}) &= \mathrm{E}_{\boldsymbol{z};\boldsymbol{\theta}}\left[\boldsymbol{\phi}(\boldsymbol{z})\right] \\ &= \int_{\boldsymbol{\mathcal{Z}}} \boldsymbol{\phi}(\boldsymbol{z}) p(\boldsymbol{z};\boldsymbol{\theta}) \mathrm{d}\boldsymbol{z}, \end{aligned} \tag{5.205}$$

$$\begin{aligned} \boldsymbol{R}_{\boldsymbol{\phi}}(\boldsymbol{\theta}) &= \mathrm{E}_{\boldsymbol{z};\boldsymbol{\theta}}\left[\big(\boldsymbol{\phi}(\boldsymbol{z}) - \boldsymbol{\mu}_{\boldsymbol{\phi}}(\boldsymbol{\theta})\big)^{\mathrm{T}}\big(\boldsymbol{\phi}(\boldsymbol{z}) - \boldsymbol{\mu}_{\boldsymbol{\phi}}(\boldsymbol{\theta})\big)\right] \\ &= \int_{\boldsymbol{\mathcal{Z}}} \boldsymbol{\phi}(\boldsymbol{z})\boldsymbol{\phi}^{\mathrm{T}}(\boldsymbol{z}) p(\boldsymbol{z};\boldsymbol{\theta}) \mathrm{d}\boldsymbol{z} - \boldsymbol{\mu}_{\boldsymbol{\phi}}(\boldsymbol{\theta})\boldsymbol{\mu}_{\boldsymbol{\phi}}^{\mathrm{T}}(\boldsymbol{\theta}) \end{aligned} \tag{5.206}$$

under the original probability law $p(\boldsymbol{z};\boldsymbol{\theta})$ and choose the exponential family distribution $\tilde{p}(\boldsymbol{z};\boldsymbol{\theta})$ with sufficient statistics $\boldsymbol{t}(\boldsymbol{z}) = \boldsymbol{\phi}(\boldsymbol{z})$ and equivalent expected values

$$\begin{aligned} \boldsymbol{\mu}_{\boldsymbol{\phi}}(\boldsymbol{\theta}) &= \mathrm{E}_{\tilde{\boldsymbol{z}};\boldsymbol{\theta}}\left[\boldsymbol{\phi}(\boldsymbol{z})\right] \\ &= \int_{\boldsymbol{\mathcal{Z}}} \boldsymbol{\phi}(\boldsymbol{z}) \tilde{p}(\boldsymbol{z};\boldsymbol{\theta}) \mathrm{d}\boldsymbol{z}, \end{aligned} \tag{5.207}$$

$$\begin{aligned} \boldsymbol{R}_{\boldsymbol{\phi}}(\boldsymbol{\theta}) &= \mathrm{E}_{\tilde{\boldsymbol{z}};\boldsymbol{\theta}}\left[\big(\boldsymbol{\phi}(\boldsymbol{z}) - \boldsymbol{\mu}_{\boldsymbol{\phi}}(\boldsymbol{\theta})\big)^{\mathrm{T}}\big(\boldsymbol{\phi}(\boldsymbol{z}) - \boldsymbol{\mu}_{\boldsymbol{\phi}}(\boldsymbol{\theta})\big)\right] \\ &= \int_{\boldsymbol{\mathcal{Z}}} \boldsymbol{\phi}(\boldsymbol{z})\boldsymbol{\phi}^{\mathrm{T}}(\boldsymbol{z}) \tilde{p}(\boldsymbol{z};\boldsymbol{\theta}) \mathrm{d}\boldsymbol{z} - \boldsymbol{\mu}_{\boldsymbol{\phi}}(\boldsymbol{\theta})\boldsymbol{\mu}_{\boldsymbol{\phi}}^{\mathrm{T}}(\boldsymbol{\theta}) \end{aligned} \tag{5.208}$$

as replacement model. By $\tilde{p}(\boldsymbol{z};\boldsymbol{\theta})$ being of the form (5.181), with L weighting vectors $\boldsymbol{b}_l(\boldsymbol{\theta}) \in \mathbb{R}^D$ summarized in the matrix

$$\boldsymbol{B}(\boldsymbol{\theta}) = \begin{bmatrix} \boldsymbol{b}_1(\boldsymbol{\theta}) & \boldsymbol{b}_2(\boldsymbol{\theta}) & \ldots & \boldsymbol{b}_L(\boldsymbol{\theta}) \end{bmatrix}^{\mathrm{T}}, \tag{5.209}$$

the score function of the exponential replacement factorizes

$$\frac{\partial \ln \tilde{p}(\boldsymbol{z};\boldsymbol{\theta})}{\partial \boldsymbol{\theta}} = \boldsymbol{\phi}^{\mathrm{T}}(\boldsymbol{z})\boldsymbol{B}(\boldsymbol{\theta}) - \boldsymbol{\alpha}^{\mathrm{T}}(\boldsymbol{\theta}) \tag{5.210}$$

where the normalizer $\boldsymbol{\alpha}(\boldsymbol{\theta}) \in \mathbb{R}^D$.

Through the covariance inequality it is possible to show that the Fisher information matrix

$$\tilde{\boldsymbol{F}}(\boldsymbol{\theta}) = \int_{\mathcal{Z}} \left(\frac{\partial \ln \tilde{p}(\boldsymbol{z};\boldsymbol{\theta})}{\partial \boldsymbol{\theta}} \right)^{\mathrm{T}} \frac{\partial \ln \tilde{p}(\boldsymbol{z};\boldsymbol{\theta})}{\partial \boldsymbol{\theta}} \tilde{p}(\boldsymbol{z};\boldsymbol{\theta}) \mathrm{d}\boldsymbol{z} \tag{5.211}$$

of the equivalent exponential replacement is always dominated by the information measure

$$\boldsymbol{F}(\boldsymbol{\theta}) = \int_{\mathcal{Z}} \left(\frac{\partial \ln p(\boldsymbol{z};\boldsymbol{\theta})}{\partial \boldsymbol{\theta}} \right)^{\mathrm{T}} \frac{\partial \ln p(\boldsymbol{z};\boldsymbol{\theta})}{\partial \boldsymbol{\theta}} p(\boldsymbol{z};\boldsymbol{\theta}) \mathrm{d}\boldsymbol{z} \tag{5.212}$$

of the original system. To this end, note that

$$\begin{aligned}
\mathrm{E}_{\boldsymbol{z};\boldsymbol{\theta}} \left[\left(\frac{\partial \ln p(\boldsymbol{z};\boldsymbol{\theta})}{\partial \boldsymbol{\theta}} \right)^{\mathrm{T}} \frac{\partial \ln \tilde{p}(\boldsymbol{z};\boldsymbol{\theta})}{\partial \boldsymbol{\theta}} \right] &= \int_{\mathcal{Z}} \left(\frac{\partial \ln p(\boldsymbol{z};\boldsymbol{\theta})}{\partial \boldsymbol{\theta}} \right)^{\mathrm{T}} \Big(\boldsymbol{\phi}^{\mathrm{T}}(\boldsymbol{z}) \boldsymbol{B}(\boldsymbol{\theta}) - \boldsymbol{\alpha}^{\mathrm{T}}(\boldsymbol{\theta}) \Big) p(\boldsymbol{z};\boldsymbol{\theta}) \mathrm{d}\boldsymbol{z} \\
&= \left(\int_{\mathcal{Z}} \boldsymbol{\phi}(\boldsymbol{z}) \frac{\partial p(\boldsymbol{z};\boldsymbol{\theta})}{\partial \boldsymbol{\theta}} \mathrm{d}\boldsymbol{z} \right)^{\mathrm{T}} \boldsymbol{B}(\boldsymbol{\theta}) \\
&= \left(\frac{\partial \boldsymbol{\mu}_{\boldsymbol{\phi}}(\boldsymbol{\theta})}{\partial \boldsymbol{\theta}} \right)^{\mathrm{T}} \boldsymbol{B}(\boldsymbol{\theta}) \\
&= \tilde{\boldsymbol{F}}(\boldsymbol{\theta}),
\end{aligned} \tag{5.213}$$

where we have used the identity (5.191) in the last step. Further, under the equivalences (5.207) and (5.208)

$$\begin{aligned}
&\mathrm{E}_{\boldsymbol{z};\boldsymbol{\theta}} \left[\left(\frac{\partial \ln \tilde{p}(\boldsymbol{z};\boldsymbol{\theta})}{\partial \boldsymbol{\theta}} \right)^{\mathrm{T}} \frac{\partial \ln \tilde{p}(\boldsymbol{z};\boldsymbol{\theta})}{\partial \boldsymbol{\theta}} \right] \\
&= \mathrm{E}_{\boldsymbol{z};\boldsymbol{\theta}} \left[\Big(\boldsymbol{\phi}^{\mathrm{T}}(\boldsymbol{z}) \boldsymbol{B}(\boldsymbol{\theta}) - \boldsymbol{\alpha}^{\mathrm{T}}(\boldsymbol{\theta}) \Big)^{\mathrm{T}} \Big(\boldsymbol{\phi}^{\mathrm{T}}(\boldsymbol{z}) \boldsymbol{B}(\boldsymbol{\theta}) - \boldsymbol{\alpha}^{\mathrm{T}}(\boldsymbol{\theta}) \Big) \right] \\
&= \mathrm{E}_{\tilde{\boldsymbol{z}};\boldsymbol{\theta}} \left[\Big(\boldsymbol{\phi}^{\mathrm{T}}(\boldsymbol{z}) \boldsymbol{B}(\boldsymbol{\theta}) - \boldsymbol{\alpha}^{\mathrm{T}}(\boldsymbol{\theta}) \Big)^{\mathrm{T}} \Big(\boldsymbol{\phi}^{\mathrm{T}}(\boldsymbol{z}) \boldsymbol{B}(\boldsymbol{\theta}) - \boldsymbol{\alpha}^{\mathrm{T}}(\boldsymbol{\theta}) \Big) \right] \\
&= \mathrm{E}_{\tilde{\boldsymbol{z}};\boldsymbol{\theta}} \left[\left(\frac{\partial \ln \tilde{p}(\boldsymbol{z};\boldsymbol{\theta})}{\partial \boldsymbol{\theta}} \right)^{\mathrm{T}} \frac{\partial \ln \tilde{p}(\boldsymbol{z};\boldsymbol{\theta})}{\partial \boldsymbol{\theta}} \right] \\
&= \tilde{\boldsymbol{F}}(\boldsymbol{\theta}).
\end{aligned} \tag{5.214}$$

Therefore, with the covariance inequality (Appendix A1), (5.213) and (5.214)

$$\begin{aligned}
\boldsymbol{F}(\boldsymbol{\theta}) \succeq\ & \mathrm{E}_{\boldsymbol{z};\boldsymbol{\theta}} \left[\left(\frac{\partial \ln p(\boldsymbol{z};\boldsymbol{\theta})}{\partial \boldsymbol{\theta}} \right)^{\mathrm{T}} \frac{\partial \ln \tilde{p}(\boldsymbol{z};\boldsymbol{\theta})}{\partial \boldsymbol{\theta}} \right] \mathrm{E}_{\boldsymbol{z};\boldsymbol{\theta}} \left[\left(\frac{\partial \ln \tilde{p}(\boldsymbol{z};\boldsymbol{\theta})}{\partial \boldsymbol{\theta}} \right)^{\mathrm{T}} \frac{\partial \ln \tilde{p}(\boldsymbol{z};\boldsymbol{\theta})}{\partial \boldsymbol{\theta}} \right]^{-1} \\
&\cdot \mathrm{E}_{\boldsymbol{z};\boldsymbol{\theta}} \left[\left(\frac{\partial \ln \tilde{p}(\boldsymbol{z};\boldsymbol{\theta})}{\partial \boldsymbol{\theta}} \right)^{\mathrm{T}} \frac{\partial \ln p(\boldsymbol{z};\boldsymbol{\theta})}{\partial \boldsymbol{\theta}} \right] \\
=\ & \tilde{\boldsymbol{F}}(\boldsymbol{\theta}) \tilde{\boldsymbol{F}}^{-1}(\boldsymbol{\theta}) \tilde{\boldsymbol{F}}^{\mathrm{T}}(\boldsymbol{\theta}) \\
=\ & \tilde{\boldsymbol{F}}(\boldsymbol{\theta}).
\end{aligned} \tag{5.215}$$

5.3.4 Generalized Lower Bound for the Fisher Information Matrix

We use the property (5.215) of the exponential replacement in order to establish a generic lower bound on the FIM (5.212) of the original system $p(\boldsymbol{z};\boldsymbol{\theta})$. Therefore, let us assume that a good choice for the normalizer is

$$\boldsymbol{\alpha}(\boldsymbol{\theta}) = \boldsymbol{B}^{\mathrm{T}}(\boldsymbol{\theta})\boldsymbol{\mu}_{\boldsymbol{\phi}}(\boldsymbol{\theta}). \tag{5.216}$$

Then it holds that

$$\begin{aligned}
\tilde{\boldsymbol{F}}(\boldsymbol{\theta}) &= \mathrm{E}_{\tilde{\boldsymbol{z}};\boldsymbol{\theta}}\left[\left(\frac{\partial \ln \tilde{p}(\boldsymbol{z};\boldsymbol{\theta})}{\partial \boldsymbol{\theta}}\right)^{\mathrm{T}} \frac{\partial \ln \tilde{p}(\boldsymbol{z};\boldsymbol{\theta})}{\partial \boldsymbol{\theta}}\right] \\
&= \mathrm{E}_{\tilde{\boldsymbol{z}};\boldsymbol{\theta}}\left[\Big(\boldsymbol{\phi}^{\mathrm{T}}(\boldsymbol{z})\boldsymbol{B}(\boldsymbol{\theta}) - \boldsymbol{\alpha}^{\mathrm{T}}(\boldsymbol{\theta})\Big)^{\mathrm{T}}\Big(\boldsymbol{\phi}^{\mathrm{T}}(\boldsymbol{z})\boldsymbol{B}(\boldsymbol{\theta}) - \boldsymbol{\alpha}^{\mathrm{T}}(\boldsymbol{\theta})\Big)\right] \\
&= \boldsymbol{B}^{\mathrm{T}}(\boldsymbol{\theta})\Big(\mathrm{E}_{\tilde{\boldsymbol{z}};\boldsymbol{\theta}}\left[\boldsymbol{\phi}(\boldsymbol{z})\boldsymbol{\phi}^{\mathrm{T}}(\boldsymbol{z})\right] - \boldsymbol{\mu}_{\boldsymbol{\phi}}(\boldsymbol{\theta})\boldsymbol{\mu}_{\boldsymbol{\phi}}^{\mathrm{T}}(\boldsymbol{\theta})\Big)\boldsymbol{B}(\boldsymbol{\theta}) \\
&= \boldsymbol{B}^{\mathrm{T}}(\boldsymbol{\theta})\boldsymbol{R}_{\boldsymbol{\phi}}(\boldsymbol{\theta})\boldsymbol{B}(\boldsymbol{\theta}),
\end{aligned} \tag{5.217}$$

such that with (5.213) and (5.215) we obtain

$$\begin{aligned}
\boldsymbol{F}(\boldsymbol{\theta}) &\succeq \tilde{\boldsymbol{F}}(\boldsymbol{\theta})\tilde{\boldsymbol{F}}^{-1}(\boldsymbol{\theta})\tilde{\boldsymbol{F}}(\boldsymbol{\theta}) \\
&= \left(\frac{\partial \boldsymbol{\mu}_{\boldsymbol{\phi}}(\boldsymbol{\theta})}{\partial \boldsymbol{\theta}}\right)^{\mathrm{T}} \boldsymbol{B}(\boldsymbol{\theta})\big(\boldsymbol{B}^{\mathrm{T}}(\boldsymbol{\theta})\boldsymbol{R}_{\boldsymbol{\phi}}(\boldsymbol{\theta})\boldsymbol{B}(\boldsymbol{\theta})\big)^{-1}\boldsymbol{B}^{\mathrm{T}}(\boldsymbol{\theta})\frac{\partial \boldsymbol{\mu}_{\boldsymbol{\phi}}(\boldsymbol{\theta})}{\partial \boldsymbol{\theta}}.
\end{aligned} \tag{5.218}$$

The question is now how to choose $\boldsymbol{\phi}(\boldsymbol{z})$ and optimize $\boldsymbol{B}(\boldsymbol{\theta})$ such that the right hand side of (5.218) is maximized in matrix sense?

If the underlying statistical model $p(\boldsymbol{z};\boldsymbol{\theta})$ is from the exponential family type (5.181) and the sufficient statistics $\boldsymbol{\phi}(\boldsymbol{z}) = \boldsymbol{t}(\boldsymbol{z})$ are used for the approximation $\tilde{p}(\boldsymbol{z};\boldsymbol{\theta})$, it is possible to obtain a tight bound (5.218). To see this, note that with $\boldsymbol{\phi}(\boldsymbol{\theta}) = \boldsymbol{t}(\boldsymbol{\theta})$ and optimized weightings $\boldsymbol{B}^{\star}(\boldsymbol{\theta})$, due to the definition (5.206), we have

$$\boldsymbol{B}^{\star\,\mathrm{T}}(\boldsymbol{\theta})\boldsymbol{R}_{\boldsymbol{\phi}}(\boldsymbol{\theta})\boldsymbol{B}^{\star}(\boldsymbol{\theta}) = \mathrm{E}_{\boldsymbol{z};\boldsymbol{\theta}}\left[\boldsymbol{B}^{\star\,\mathrm{T}}(\boldsymbol{\theta})\boldsymbol{t}(\boldsymbol{\theta})\boldsymbol{t}^{\mathrm{T}}(\boldsymbol{\theta})\boldsymbol{B}^{\star}(\boldsymbol{\theta})\right] - \boldsymbol{B}^{\star\,\mathrm{T}}(\boldsymbol{\theta})\boldsymbol{\mu}_{\boldsymbol{t}}(\boldsymbol{\theta})\boldsymbol{\mu}_{\boldsymbol{t}}^{\mathrm{T}}(\boldsymbol{\theta})\boldsymbol{B}^{\star}(\boldsymbol{\theta}). \tag{5.219}$$

Now let us assume that a possible optimizer is

$$\boldsymbol{B}^{\star}(\boldsymbol{\theta}) = \frac{\partial \boldsymbol{w}(\boldsymbol{\theta})}{\partial \boldsymbol{\theta}}, \tag{5.220}$$

where $\boldsymbol{w}(\boldsymbol{\theta})$ are the natural parameters of the original system $p(\boldsymbol{z};\boldsymbol{\theta})$. Then with (5.219)

$$\begin{aligned}
\boldsymbol{B}^{\star\,\mathrm{T}}(\boldsymbol{\theta})\boldsymbol{R}_{\boldsymbol{\phi}}(\boldsymbol{\theta})\boldsymbol{B}^{\star}(\boldsymbol{\theta}) = \mathrm{E}_{\boldsymbol{z};\boldsymbol{\theta}}&\left[\left(\frac{\partial \boldsymbol{w}(\boldsymbol{\theta})}{\partial \boldsymbol{\theta}}\right)^{\mathrm{T}} \boldsymbol{t}(\boldsymbol{\theta})\boldsymbol{t}^{\mathrm{T}}(\boldsymbol{\theta})\frac{\partial \boldsymbol{w}(\boldsymbol{\theta})}{\partial \boldsymbol{\theta}}\right] \\
&- \left(\frac{\partial \boldsymbol{w}(\boldsymbol{\theta})}{\partial \boldsymbol{\theta}}\right)^{\mathrm{T}} \boldsymbol{\mu}_{\boldsymbol{t}}(\boldsymbol{\theta})\boldsymbol{\mu}_{\boldsymbol{t}}^{\mathrm{T}}(\boldsymbol{\theta})\frac{\partial \boldsymbol{w}(\boldsymbol{\theta})}{\partial \boldsymbol{\theta}}.
\end{aligned} \tag{5.221}$$

Substituting

$$\frac{\partial \ln p(\boldsymbol{z};\boldsymbol{\theta})}{\partial \boldsymbol{\theta}} = \boldsymbol{t}^{\mathrm{T}}(\boldsymbol{z})\frac{\partial \boldsymbol{w}(\boldsymbol{\theta})}{\partial \boldsymbol{\theta}} - \frac{\partial \lambda(\boldsymbol{\theta})}{\partial \boldsymbol{\theta}} \tag{5.222}$$

and

$$\mathrm{E}_{\boldsymbol{z};\boldsymbol{\theta}}\left[\frac{\partial \ln p(\boldsymbol{z};\boldsymbol{\theta})}{\partial \boldsymbol{\theta}}\right] = \boldsymbol{\mu}_{\boldsymbol{t}}^{\mathrm{T}}(\boldsymbol{\theta})\frac{\partial \boldsymbol{w}(\boldsymbol{\theta})}{\partial \boldsymbol{\theta}} - \frac{\partial \lambda(\boldsymbol{\theta})}{\partial \boldsymbol{\theta}} = \boldsymbol{0}^{\mathrm{T}}, \tag{5.223}$$

in (5.221), we obtain

$$\begin{aligned}\boldsymbol{B}^{\star\,\mathrm{T}}(\boldsymbol{\theta})\boldsymbol{R}_{\boldsymbol{\phi}}(\boldsymbol{\theta})\boldsymbol{B}^{\star}(\boldsymbol{\theta}) &= \mathrm{E}\left[\left(\frac{\partial \ln p(\boldsymbol{z};\boldsymbol{\theta})}{\partial \boldsymbol{\theta}} + \frac{\partial \lambda(\boldsymbol{\theta})}{\partial \boldsymbol{\theta}}\right)^{\mathrm{T}}\left(\frac{\partial \ln p(\boldsymbol{z};\boldsymbol{\theta})}{\partial \boldsymbol{\theta}} + \frac{\partial \lambda(\boldsymbol{\theta})}{\partial \boldsymbol{\theta}}\right)\right] \\ &\quad - \left(\frac{\partial \lambda(\boldsymbol{\theta})}{\partial \boldsymbol{\theta}}\right)^{\mathrm{T}}\left(\frac{\partial \lambda(\boldsymbol{\theta})}{\partial \boldsymbol{\theta}}\right) \\ &= \mathrm{E}_{\boldsymbol{z};\boldsymbol{\theta}}\left[\left(\frac{\partial \ln p(\boldsymbol{z};\boldsymbol{\theta})}{\partial \boldsymbol{\theta}}\right)^{\mathrm{T}}\left(\frac{\partial \ln p(\boldsymbol{z};\boldsymbol{\theta})}{\partial \boldsymbol{\theta}}\right)\right] \\ &= \left(\frac{\partial \boldsymbol{\mu}_{\boldsymbol{t}}(\boldsymbol{\theta})}{\partial \boldsymbol{\theta}}\right)^{\mathrm{T}}\frac{\partial \boldsymbol{w}(\boldsymbol{\theta})}{\partial \boldsymbol{\theta}}.\end{aligned} \tag{5.224}$$

Using (5.220) and (5.224) in (5.218) we finally arrive at

$$\boldsymbol{F}(\boldsymbol{\theta}) \succeq \left(\frac{\partial \boldsymbol{\mu}_{\boldsymbol{t}}(\boldsymbol{\theta})}{\partial \boldsymbol{\theta}}\right)^{\mathrm{T}}\frac{\partial \boldsymbol{w}(\boldsymbol{\theta})}{\partial \boldsymbol{\theta}}, \tag{5.225}$$

which, due to the identity (5.191), holds with equality for the exponential family.

5.3.5 Optimization of the Generalized Fisher Information Lower Bound

In the following we discuss how to perform the optimization of the right hand side of (5.218) when the sufficient statistics $\boldsymbol{t}(\boldsymbol{z})$ are unknown and we have to resort to a set of auxiliary statistics $\boldsymbol{\phi}(\boldsymbol{z})$. Substituting

$$\boldsymbol{B}(\boldsymbol{\theta}) = \boldsymbol{R}_{\boldsymbol{\phi}}^{-\frac{1}{2}}(\boldsymbol{\theta})\boldsymbol{B}'(\boldsymbol{\theta}) \tag{5.226}$$

in (5.218) under the constraint that

$$\boldsymbol{B}'^{\,\mathrm{T}}(\boldsymbol{\theta})\boldsymbol{B}'(\boldsymbol{\theta}) = \boldsymbol{I}, \tag{5.227}$$

we obtain a modified bound

$$\boldsymbol{F}(\boldsymbol{\theta}) \succeq \left(\frac{\partial \boldsymbol{\mu}_{\boldsymbol{\phi}}(\boldsymbol{\theta})}{\partial \boldsymbol{\theta}}\right)^{\mathrm{T}}\boldsymbol{R}_{\boldsymbol{\phi}}^{-\frac{1}{2}}(\boldsymbol{\theta})\boldsymbol{B}'(\boldsymbol{\theta})\boldsymbol{B}'^{\,\mathrm{T}}(\boldsymbol{\theta})\boldsymbol{R}_{\boldsymbol{\phi}}^{-\frac{1}{2}}(\boldsymbol{\theta})\frac{\partial \boldsymbol{\mu}_{\boldsymbol{\phi}}(\boldsymbol{\theta})}{\partial \boldsymbol{\theta}}. \tag{5.228}$$

The right hand side of (5.228) is maximized in the matrix sense under the constraint (5.227) with

$$\boldsymbol{B}'(\boldsymbol{\theta}) = \boldsymbol{R}_{\boldsymbol{\phi}}^{-\frac{1}{2}}(\boldsymbol{\theta})\frac{\partial \boldsymbol{\mu}_{\boldsymbol{\phi}}(\boldsymbol{\theta})}{\partial \boldsymbol{\theta}}\left(\left(\frac{\partial \boldsymbol{\mu}_{\boldsymbol{\phi}}(\boldsymbol{\theta})}{\partial \boldsymbol{\theta}}\right)^{\mathrm{T}}\boldsymbol{R}_{\boldsymbol{\phi}}^{-1}(\boldsymbol{\theta})\frac{\partial \boldsymbol{\mu}_{\boldsymbol{\phi}}(\boldsymbol{\theta})}{\partial \boldsymbol{\theta}}\right)^{-\frac{1}{2}}. \tag{5.229}$$

Using (5.229) and (5.226) in (5.218), we obtain the result that for any parameterized probability distribution $p(\boldsymbol{z};\boldsymbol{\theta})$ and any set of L auxiliary statistics $\boldsymbol{\phi}(\boldsymbol{z})$, with the definitions (5.205) and (5.206), the Fisher information matrix $\boldsymbol{F}(\boldsymbol{\theta})$ dominates

$$\boldsymbol{F}(\boldsymbol{\theta}) \succeq \left(\frac{\partial \boldsymbol{\mu}_{\boldsymbol{\phi}}(\boldsymbol{\theta})}{\partial \boldsymbol{\theta}}\right)^{\mathrm{T}} \boldsymbol{R}_{\boldsymbol{\phi}}^{-1}(\boldsymbol{\theta}) \frac{\partial \boldsymbol{\mu}_{\boldsymbol{\phi}}(\boldsymbol{\theta})}{\partial \boldsymbol{\theta}}. \tag{5.230}$$

Note that due to the tightness of the bound (5.230) for exponential family models (5.181), besides (5.191) we have an additional identity

$$\boldsymbol{F}(\boldsymbol{\theta}) = \left(\frac{\partial \boldsymbol{\mu}_{\boldsymbol{t}}(\boldsymbol{\theta})}{\partial \boldsymbol{\theta}}\right)^{\mathrm{T}} \boldsymbol{R}_{\boldsymbol{t}}^{-1}(\boldsymbol{\theta}) \frac{\partial \boldsymbol{\mu}_{\boldsymbol{t}}(\boldsymbol{\theta})}{\partial \boldsymbol{\theta}} \tag{5.231}$$

for such kind of system models.

5.4 Applications

In the following we will demonstrate applications of the presented main result (5.230). For simplicity, we focus on univariate problems $z \in \mathbb{R}$ with a single parameter $\theta \in \mathbb{R}$. We utilize the generic result (5.230) in order to formulate a specific information bound involving the derivatives of the first L raw moments [60]. For the initial example of a log-normal and a Weibull distribution, we test the quality of this approximation of the Fisher information. By constructing a second bound which takes into consideration raw moments, the expected absolute value and the expected log-value, we show how to use the information bound (5.230) in order to learn informative statistics of a parametric system with unknown output model and how to determine the minimum guaranteed interference capability of the model by calibrated measurements. In order to emphasize the practical impact, we demonstrate this aspect with the Rapp model [73], which is popular for modeling the saturation effect of solid-state power amplifiers.

5.4.1 Fisher Information Lower Bound with L Moments

In order to test a generalization of the approach (5.52) with the derivatives of L raw moments, we use the obtained result (5.230) under the convention

$$\phi_l(z) = z^l \tag{5.232}$$

and apply the resulting information bound to the log-normal (5.151) and the Weilbull model (5.164). The required expectations (5.205) and (5.206) of the auxiliary statistics $\phi_l(z)$ are directly available by the fact that for the log-normal distribution (5.151) the l-th raw moment is given by

$$\mathrm{E}_{z;\theta}\left[z^l\right] = \mathrm{e}^{l\theta + \frac{1}{2}l^2\sigma^2} \tag{5.233}$$

and therefore its derivative is

$$\frac{\partial\, \mathrm{E}_{z;\theta}\left[z^l\right]}{\partial \theta} = l\, \mathrm{e}^{l\theta + \frac{1}{2}l^2\sigma^2}. \tag{5.234}$$

Accordingly, for the Weibull distribution (5.164) we have

$$\mathrm{E}_{z;\theta}\left[z^l\right] = \theta^l \Gamma_l, \tag{5.235}$$

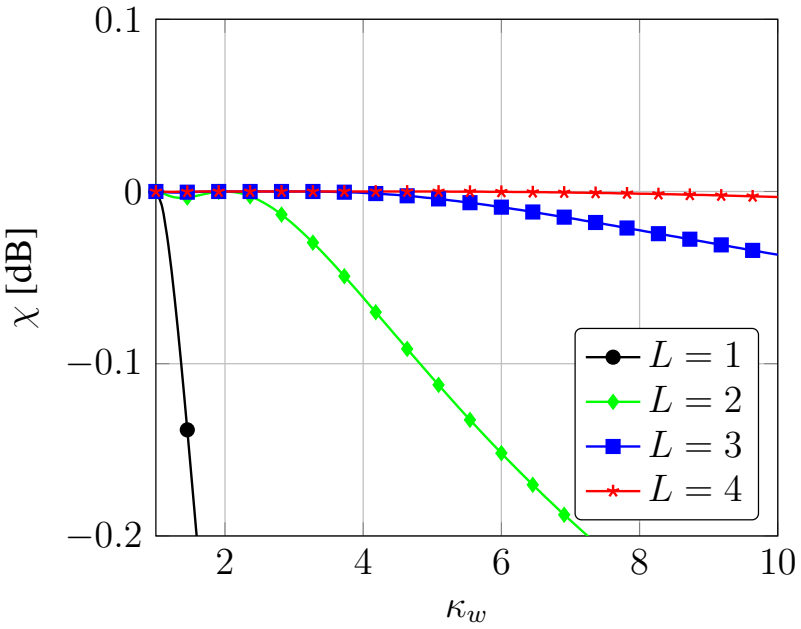

Fig. 5.8. Bounding Gap (L Moment Bound) - Weibull Distribution

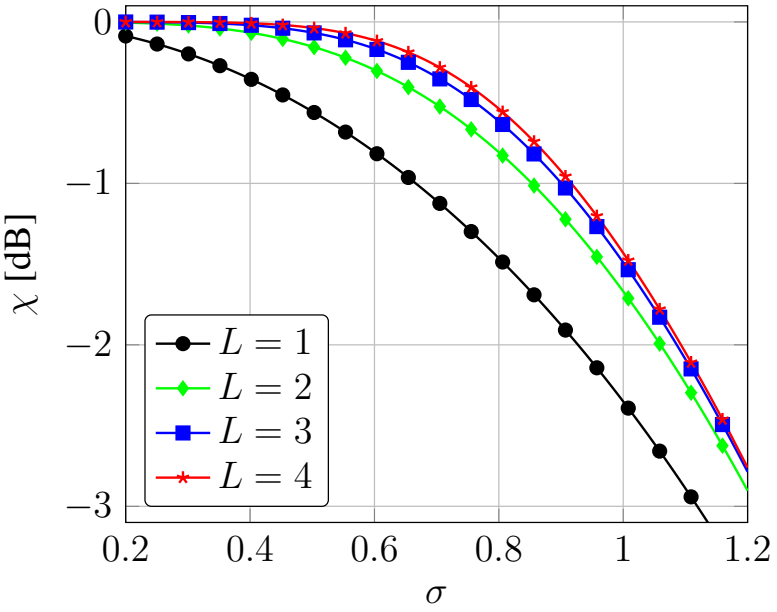

Fig. 5.9. Bounding Gap (L Moment Bound) - Log-normal Distribution

and

$$\frac{\partial \, \mathrm{E}_{z;\theta}\left[z^l\right]}{\partial \theta} = l\theta^{l-1}\Gamma_l. \tag{5.236}$$

In Fig. 5.8 and Fig. 5.9 the approximation accuracy

$$\chi(\theta) = \frac{\tilde{F}_z(\theta)}{F_z(\theta)} = \frac{\left(\frac{\partial \boldsymbol{\mu}_{\boldsymbol{\phi}}(\theta)}{\partial \theta}\right)^{\mathrm{T}} \boldsymbol{R}_{\boldsymbol{\phi}}^{-1}(\theta) \frac{\partial \boldsymbol{\mu}_{\boldsymbol{\phi}}(\theta)}{\partial \theta}}{F_z(\theta)} \tag{5.237}$$

for different values L is depicted. For the Weibull distribution (5.164), for which the result is depicted in Fig. 5.8, we observe, that the bound with $L = 1$ (5.12) and $L = 2$ (5.52) can be significantly improved by incorporating the derivatives of the third and the fourth moment. In contrast for the log-normal distribution (5.151) taking into account more than the first two raw moments results only in a slight performance improvement (see Fig. 5.9). In order to visualize the result of the optimization of the bound (5.218), in Fig. 5.10 the normalized absolute weights

$$\bar{b}_l^\star(\theta) = \frac{|b_l^\star(\theta)|}{\sum_{l=1}^{L} |b_l^\star(\theta)|} \tag{5.238}$$

are plotted for the Weibull example, where with (5.226) and (5.229)

$$b_l^\star(\theta) = \frac{\left[\boldsymbol{R}_{\boldsymbol{\phi}}^{-1}(\theta) \frac{\partial \boldsymbol{\mu}_{\boldsymbol{\phi}}(\theta)}{\partial \theta}\right]_l}{\sqrt{\left(\frac{\partial \boldsymbol{\mu}_{\boldsymbol{\phi}}(\theta)}{\partial \theta}\right)^{\mathrm{T}} \boldsymbol{R}_{\boldsymbol{\phi}}^{-1}(\theta) \frac{\partial \boldsymbol{\mu}_{\boldsymbol{\phi}}(\theta)}{\partial \theta}}}. \tag{5.239}$$

The individual normalized weights $\bar{b}_l^\star(\theta)$ indicate the importance of the corresponding auxiliary statistic $\phi_l(\theta) = z^l$ in the approximation of the Fisher information. It can be seen, that for the Weibull distribution the sufficient statistic z^{κ_w} attains the full weight in the cases $\kappa_w = 1, 2, 3, 4$. In

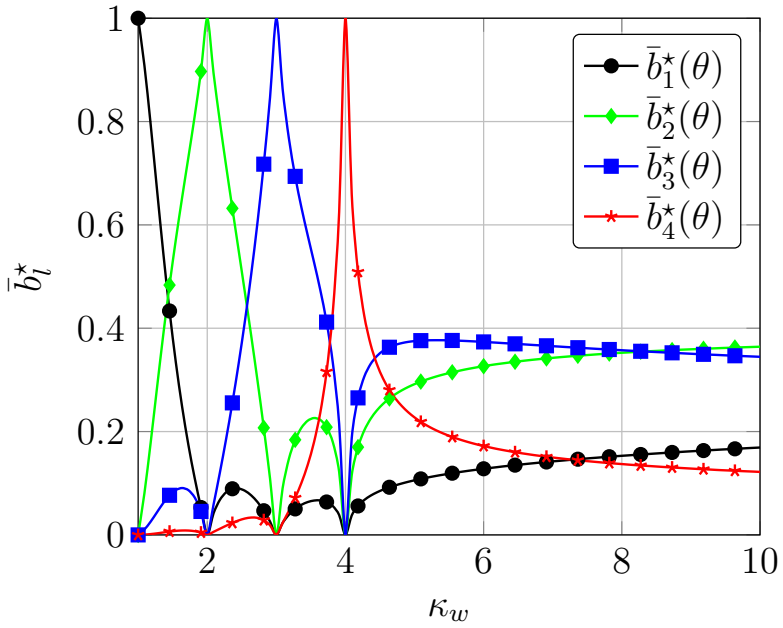

Fig. 5.10. Optimized Weights - Weibull Distribution ($L = 4$)

contrast for the log-normal distribution it is observed in Fig. 5.11 that none of the moments obtains full weight. However, the first moment plays a dominant role, in particular when $\sigma > 0.6$. Note, that for the log-normal distribution with known scale parameter σ, $\ln z$ is a sufficient statistic. Incorporating it into the approximation by using $\phi_1(z) = \ln z$ would change the situation and provide a tight approximation for $F_z(\theta)$.

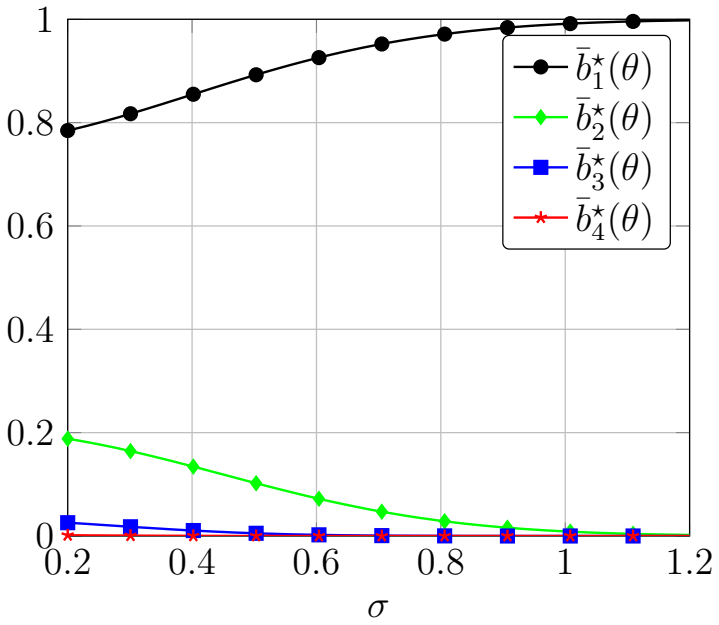

Fig. 5.11. Optimized Weights - Log-normal Distribution ($L = 4$)

5.4.2 Measurement-Driven Learning of Nonlinear Statistical Models

The previous section indicates an interesting application of the presented result (5.230). Being able to describe the expectations (5.205) and (5.206) for an arbitrary statistical model $p(z;\theta)$ with an arbitrary set of auxiliary functions $\boldsymbol{\phi}(z)$, the optimization result (5.229) can be used in order to identify, among the auxiliary statistics $\boldsymbol{\phi}(z)$, candidates for the sufficient statistics of the system model. Further, together with (5.205) and (5.206), the information bound (5.230) allows to specify the minimum inference capability that can be guaranteed to be achievable for the model of interest. This has high practical relevance as in real-world applications technical systems are subject to various random and nonlinear effects. Under such circumstances an accurate analytical description of the probability density or mass function $p(z;\theta)$ is usually hard to obtain. Nevertheless, to be able to identify transformations of the data exhibiting high information content is attractive in such a situation. Such functions can be used for applications like efficient data compression and for the formulation of high-resolution estimation algorithms. Further, a conservative approximation of the Fisher information measure like (5.230) allows to benchmark the performance of estimation algorithms on the system under investigation or to identify system layouts of high estimation theoretic quality. If the system parameter θ can be controlled in a calibrated setup, the entities (5.205) and (5.206) and therefore an exponential replacement $\tilde{p}(z;\theta)$ can be determined for any system $p(z;\theta)$ by measurements at the system output z.

5.4.2.1 Nonlinear Amplification Device

We demonstrate such a measurement-driven learning approach for the exponential replacement $\tilde{p}(z;\theta)$ in a calibrated setup with the example of a solid-state power amplifier. The system parameter θ of interest is assumed to be the direct-current offset (the mean) at the input of the nonlinear device. For the mapping from the input x to the output y of the amplifier, we apply the Rapp model

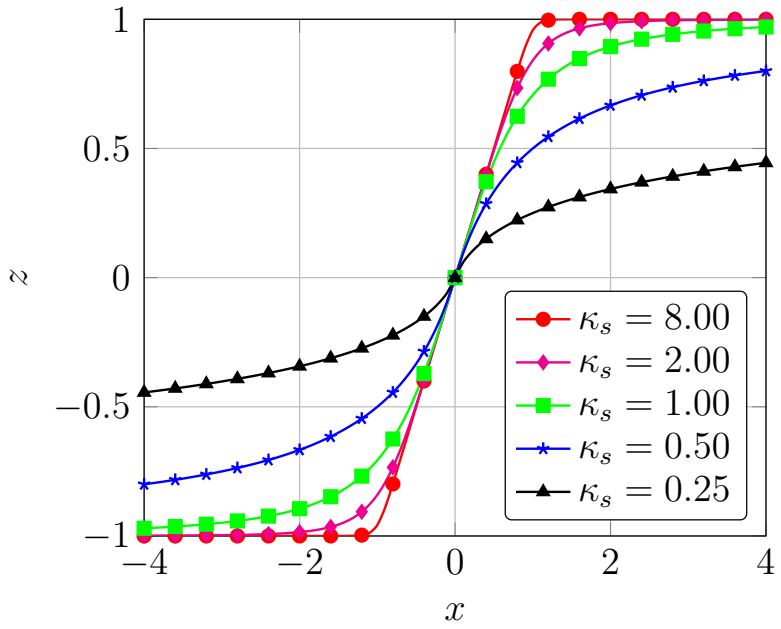

Fig. 5.12. Input-to-Output - Rapp Model

[73]

$$z = \frac{x}{(1 + |x|^{2\kappa_s})^{\frac{1}{2\kappa_s}}}, \tag{5.240}$$

where here κ_s is a smoothness factor. Fig. 5.12 depicts the input-to-output relation of this nonlinear system model for different values of κ_s. We apply a Gaussian input

$$x = \theta + \eta \tag{5.241}$$

with $\eta \sim \mathcal{N}(0, 1)$ to the nonlinear system (5.240), set

$$\boldsymbol{\phi}(z) = \begin{bmatrix} z & z^2 & z^3 & z^4 & |z| & \ln|z| \end{bmatrix}^{\mathrm{T}} \tag{5.242}$$

and for each value of θ approximate the expectations (5.205) and (5.206), with 10^8 independent realizations of the system output, by their sample mean. Fig. 5.13 shows the approximated loss

$$\chi(\theta) = \frac{\left(\frac{\partial \boldsymbol{\mu}_{\boldsymbol{\phi}}(\theta)}{\partial \theta}\right)^{\mathrm{T}} \boldsymbol{R}_{\boldsymbol{\phi}}^{-1}(\theta) \frac{\partial \boldsymbol{\mu}_{\boldsymbol{\phi}}(\theta)}{\partial \theta}}{F_x(\theta)} \tag{5.243}$$

which is introduced by the nonlinear Rapp model with smoothness factor $\kappa_s = 2.0$. Note, that $F_x(\theta)$ is the Fisher information with respect to θ at the input x of the nonlinear Rapp model. It is observed that for an input mean $\theta > 2.0$, the saturation of the nonlinear Rapp model introduces a significant information loss. Fig. 5.14 shows the normalized absolute weights $\bar{b}_l^\star$ associated with each statistic, which have been attained by the optimization (5.229). It can be seen that here the second moment and the expected absolute value play a dominant role in the approximation of the Fisher information measure.

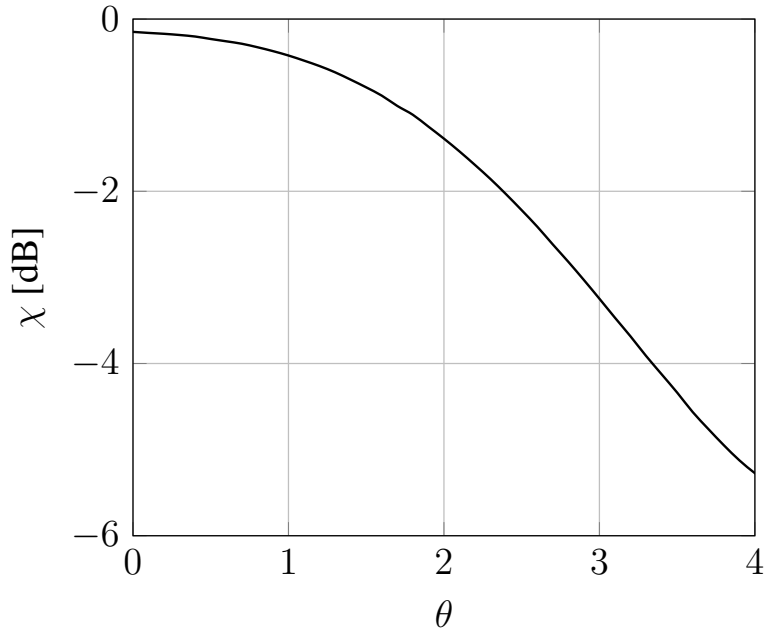

Fig. 5.13. Performance Loss - Rapp Model ($\kappa_s = 2.0$)

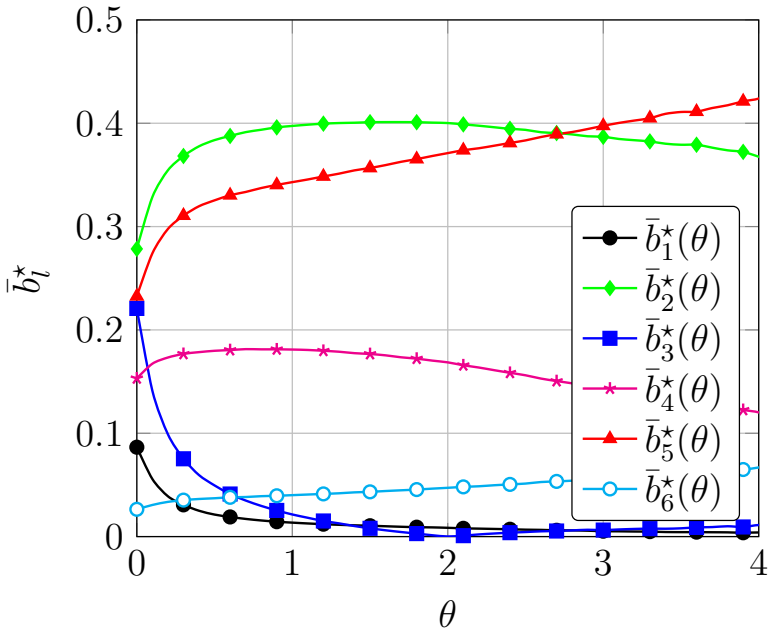

Fig. 5.14. Optimized Weights - Rapp Model ($\kappa_s = 2.0$)

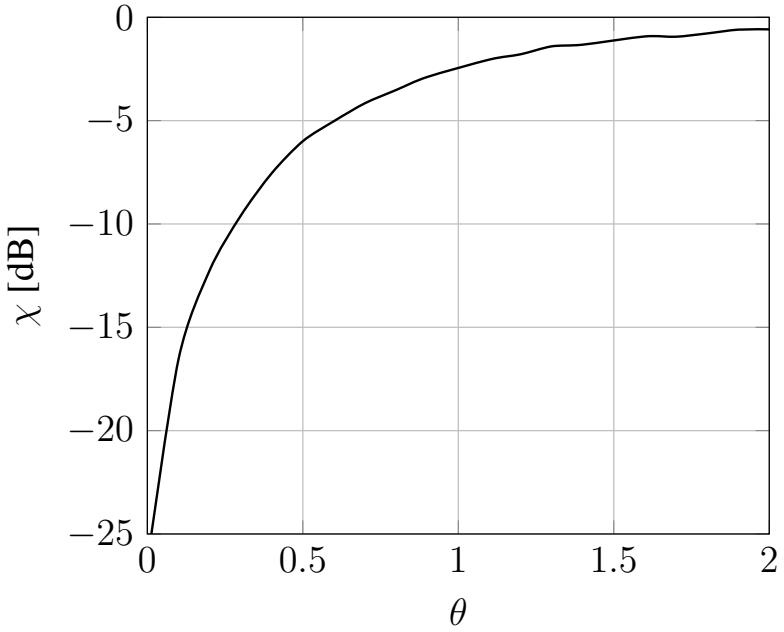

Fig. 5.15. Performance Loss - Rician Model

5.4.2.2 Rician System Model

As a second example we investigate a Rician model

$$z = \sqrt{x_1^2 + x_2^2}, \tag{5.244}$$

where $x_1 \sim \mathcal{N}(\theta\cos(\kappa_r), 1)$ and $x_2 \sim \mathcal{N}(\theta\sin(\kappa_r), 1)$. Such a model is popular in wireless communications in order to describe the strength of the line-of-sight (LOS) propagation in relation to the multi-path channels [74] [75]. Further, one finds such models in biomedical signal processing for the characterization of brain scan images with fMRI [76]. Fig. 5.15 shows the information loss of the Rician system

$$\chi(\theta) = \frac{1}{F_x(\theta)} \left(\frac{\partial \boldsymbol{\mu}_{\boldsymbol{\phi}}(\theta)}{\partial \theta} \right)^{\mathrm{T}} \boldsymbol{R}_{\boldsymbol{\phi}}^{-1}(\theta) \frac{\partial \boldsymbol{\mu}_{\boldsymbol{\phi}}(\theta)}{\partial \theta} \tag{5.245}$$

in dB. Note, that the Fisher information measure with respect to θ under direct access to both inputs x_1 and x_2 is $F_x(\theta) = 1$ and that (5.245) is independent of κ_r. It becomes visible that phase information is extremely important for small values of the distance parameter θ. This kind of information is discarded by the Rician model (5.244).

5.5 Signal Processing under the Exponential Replacement

Finally, we address the question how to perform estimation of the system parameter θ under an unknown statistical system model $p(z;\theta)$ after having learned the properties $\boldsymbol{\mu}_{\boldsymbol{\phi}}(\theta)$ and $\boldsymbol{R}_{\boldsymbol{\phi}}(\theta)$ with an arbitrary set of L auxiliary statistics $\boldsymbol{\phi}(z)$ by calibrated measurements or by analytical derivations. To this end, we show that consistent estimators can be obtained from compressed observations of the system output which achieve a performance equivalent to the inverse of our pessimistic approximation for the Fisher information measure (5.230).

5.5.1 Conservative Maximum-Likelihood Estimation

To this end, we assume that N independent output samples of the system $p(z;\theta)$ have been observed, such that the data vector $\boldsymbol{z} \in \mathbb{R}^N$ is available. First we apply a data compression step by using the auxiliary statistics $\boldsymbol{\phi}(z)$ to form the sample mean

$$\tilde{\boldsymbol{\phi}} = \frac{1}{N}\sum_{n=1}^{N} \boldsymbol{\phi}(z_n) \tag{5.246}$$

and subsequently discarding the original data $\boldsymbol{z}$. Note that this reduces the size of the data by a factor of $\frac{N}{L}$. In the situation where the analytic characterization of the data-generating model $p(z;\theta)$ is available, given the observations $\boldsymbol{z}$ one would resort to the maximization of the log-likelihood

$$\begin{aligned}\hat{\theta}(\boldsymbol{z}) &= \arg\max_{\theta\in\Theta} \ln p(\boldsymbol{z};\theta) \\ &= \arg\max_{\theta\in\Theta} \sum_{n=1}^{N} \ln p(z_n;\theta).\end{aligned} \tag{5.247}$$

In the situation where no description of the model $p(z;\theta)$ is available this is not possible. Therefore here we follow the idea of replacing the original system $p(z;\theta)$ by a distribution in the exponential family (5.181) with log-likelihood function

$$\ln \tilde{p}(z;\theta) = \boldsymbol{\beta}^{\mathrm{T}}(\theta)\boldsymbol{\phi}(z) - \lambda(\theta) + \kappa(z) \tag{5.248}$$

and the equivalent behavior of the first and second moment of $\boldsymbol{\phi}(\theta)$

$$\int_{\mathcal{Z}} \boldsymbol{\phi}(z)\tilde{p}(z;\theta)\mathrm{d}z = \int_{\mathcal{Z}} \boldsymbol{\phi}(z)p(z;\theta)\mathrm{d}z, \tag{5.249}$$

$$\int_{\mathcal{Z}} \boldsymbol{\phi}(z)\boldsymbol{\phi}^{\mathrm{T}}(z)\tilde{p}(z;\theta)\mathrm{d}z = \int_{\mathcal{Z}} \boldsymbol{\phi}(z)\boldsymbol{\phi}^{\mathrm{T}}(z)p(z;\theta)\mathrm{d}z. \tag{5.250}$$

The estimation is then perform by a conservative maximum-likelihood estimate (CMLE)

$$\begin{aligned}\hat{\theta}(\boldsymbol{z}) &= \arg\max_{\theta\in\Theta} \ln \tilde{p}(\boldsymbol{z};\theta) \\ &= \arg\max_{\theta\in\Theta} \sum_{n=1}^{N} \ln \tilde{p}(z_n;\theta).\end{aligned} \tag{5.251}$$

Note, that $\boldsymbol{\beta}(\theta)$ are the natural parameters and $\boldsymbol{\phi}(z)$ the sufficient statistics of the exponential replacement $\tilde{p}(z;\theta)$. Therefore, the score function takes the form

$$\frac{\partial \ln \tilde{p}(z;\theta)}{\partial\theta} = \frac{\partial\boldsymbol{\beta}^{\mathrm{T}}(\theta)}{\partial\theta}\boldsymbol{\phi}(z) - \frac{\partial\lambda(\theta)}{\partial\theta}. \tag{5.252}$$

By setting

$$\boldsymbol{b}(\theta) = \frac{\partial\boldsymbol{\beta}(\theta)}{\partial\theta} \tag{5.253}$$

and using the fact that for the exponential family

$$\frac{\partial \lambda(\theta)}{\partial \theta} = \boldsymbol{\mu}_{\boldsymbol{\phi}}^{\mathrm{T}}(\theta) \frac{\partial \boldsymbol{\beta}(\theta)}{\partial \theta}, \tag{5.254}$$

it is possible to write the score function (5.252)

$$\frac{\partial \ln \tilde{p}(z;\theta)}{\partial \theta} = \boldsymbol{b}^{\mathrm{T}}(\theta)\big(\boldsymbol{\phi}(z) - \boldsymbol{\mu}_{\boldsymbol{\phi}}(\theta)\big). \tag{5.255}$$

The CMLE (5.251) is found by setting the replacement score of the observed data $\boldsymbol{z}$ to zero, i.e.,

$$\left.\frac{\partial \ln \tilde{p}(\boldsymbol{z};\theta)}{\partial \theta}\right|_{\theta=\hat{\theta}} = 0. \tag{5.256}$$

For independent samples, the receive score can be written

$$\begin{aligned}\frac{\partial \ln \tilde{p}(\boldsymbol{z};\theta)}{\partial \theta} &= \sum_{n=1}^{N} \frac{\partial \ln \tilde{p}(z_n;\theta)}{\partial \theta} \\ &= \boldsymbol{b}^{\mathrm{T}}(\theta) \sum_{n=1}^{N} \big(\boldsymbol{\phi}(z_n) - \boldsymbol{\mu}_{\boldsymbol{\phi}}(\theta)\big) \\ &= N\boldsymbol{b}^{\mathrm{T}}(\theta)\big(\tilde{\boldsymbol{\phi}} - \boldsymbol{\mu}_{\boldsymbol{\phi}}(\theta)\big),\end{aligned} \tag{5.257}$$

such that the CMLE $\hat{\theta}(\tilde{\boldsymbol{\phi}})$ is found by solving

$$\boldsymbol{b}^{\mathrm{T}}(\theta)\big(\tilde{\boldsymbol{\phi}} - \boldsymbol{\mu}_{\boldsymbol{\phi}}(\theta)\big) = 0 \tag{5.258}$$

with respect to θ. Note, that for the calculation of the CMLE (5.258), access to the original data $\boldsymbol{z}$ is not required. The CMLE can be found by having exclusively access to the compressed data $\tilde{\boldsymbol{\phi}}$.

Note that by the law of large numbers in the asymptotic regime we obtain

$$\begin{aligned}\frac{1}{N}\sum_{n=1}^{N} \ln \tilde{p}(z_n;\theta) &\xrightarrow{a} \int_{\mathcal{Z}} \ln \tilde{p}(z;\theta) p(z;\theta_t) \mathrm{d}z \\ &= \boldsymbol{\beta}^{\mathrm{T}}(\theta)\boldsymbol{\mu}_{\boldsymbol{\phi}}(\theta_t) - \lambda(\theta) + \bar{\kappa}\end{aligned} \tag{5.259}$$

where θ_t is the true parameter. Therefore (5.259) is maximized when

$$\begin{aligned}\frac{\partial \boldsymbol{\beta}^{\mathrm{T}}(\theta)}{\partial \theta}\boldsymbol{\mu}_{\boldsymbol{\phi}}(\theta_t) - \frac{\partial \lambda(\theta)}{\partial \theta} &= \frac{\partial \boldsymbol{\beta}^{\mathrm{T}}(\theta)}{\partial \theta}\boldsymbol{\mu}_{\boldsymbol{\phi}}(\theta_t) - \frac{\partial \boldsymbol{\beta}^{\mathrm{T}}(\theta)}{\partial \theta}\boldsymbol{\mu}_{\boldsymbol{\phi}}(\theta) \\ &= 0,\end{aligned} \tag{5.260}$$

i.e., $\theta = \theta_t$, where we have used (5.185). This shows that the CMLE (5.251) is consistent, i.e.,

$$\hat{\theta}(\boldsymbol{z}) \xrightarrow{a} \theta_t. \tag{5.261}$$

In order to analyze the performance of the CMLE, we proceed according to [2, p. 212] and use a Taylor expansion of the replacement score function around the true parameter θ_t

$$\left.\frac{\partial \ln \tilde{p}(\boldsymbol{z};\theta)}{\partial \theta}\right|_{\theta=\hat{\theta}} = \left.\frac{\partial \ln \tilde{p}(\boldsymbol{z};\theta)}{\partial \theta}\right|_{\theta=\theta_t} + \left.\frac{\partial^2 \ln \tilde{p}(\boldsymbol{z};\theta)}{\partial \theta^2}\right|_{\theta=\bar{\theta}} (\hat{\theta} - \theta_t) \tag{5.262}$$

in conjunction with the mean value theorem, such that $\bar{\theta}$ lies between $\hat{\theta}$ and θ_t. Due to (5.256)

$$\left.\frac{\partial \ln \tilde{p}(\boldsymbol{z};\theta)}{\partial\theta}\right|_{\theta=\theta_t} = -\left.\frac{\partial^2 \ln \tilde{p}(\boldsymbol{z};\theta)}{\partial\theta^2}\right|_{\theta=\bar{\theta}} (\hat{\theta}-\theta_t), \tag{5.263}$$

such that

$$\sqrt{N}(\hat{\theta}-\theta_t) = \frac{\left.\frac{1}{\sqrt{N}}\,\frac{\partial \ln \tilde{p}(\boldsymbol{z};\theta)}{\partial\theta}\right|_{\theta=\theta_t}}{\left.-\frac{1}{N}\,\frac{\partial^2 \ln \tilde{p}(\boldsymbol{z};\theta)}{\partial\theta^2}\right|_{\theta=\bar{\theta}}}. \tag{5.264}$$

With (5.261) the denominator of (5.264)

$$-\frac{1}{N}\left.\frac{\partial^2 \ln \tilde{p}(\boldsymbol{z};\theta)}{\partial\theta^2}\right|_{\theta=\bar{\theta}} = -\frac{1}{N}\sum_{n=1}^{N}\left.\frac{\partial^2 \ln \tilde{p}(z_n;\theta)}{\partial\theta^2}\right|_{\theta=\bar{\theta}} \tag{5.265}$$

converges towards the constant value

$$-\,\mathrm{E}_{z;\theta_t}\left[\left.\frac{\partial^2 \ln \tilde{p}(z;\theta)}{\partial\theta^2}\right|_{\theta=\theta_t}\right] = \boldsymbol{b}^{\mathrm{T}}(\theta_t)\frac{\partial \boldsymbol{\mu}_{\boldsymbol{\phi}}(\theta_t)}{\partial\theta}, \tag{5.266}$$

where we have used the derivative of the replacement score

$$\frac{\partial^2 \ln \tilde{p}(z;\theta)}{\partial\theta^2} = \left(\frac{\partial \boldsymbol{b}(\theta)}{\partial\theta}\right)^{\mathrm{T}}\big(\boldsymbol{\phi}(z)-\boldsymbol{\mu}_{\boldsymbol{\phi}}(\theta)\big) - \boldsymbol{b}^{\mathrm{T}}(\theta_t)\frac{\partial \boldsymbol{\mu}_{\boldsymbol{\phi}}(\theta_t)}{\partial\theta} \tag{5.267}$$

and the property

$$\mathrm{E}_{z;\theta}\left[\frac{\partial^2 \ln \tilde{p}(z;\theta)}{\partial\theta^2}\right] = -\boldsymbol{b}^{\mathrm{T}}(\theta_t)\frac{\partial \boldsymbol{\mu}_{\boldsymbol{\phi}}(\theta_t)}{\partial\theta}. \tag{5.268}$$

Due to the central limit theorem and the property

$$\mathrm{E}_{z;\theta}\left[\frac{\partial \ln \tilde{p}(z;\theta)}{\partial\theta}\right] = 0, \tag{5.269}$$

the nominator of (5.264)

$$\frac{1}{\sqrt{N}}\left.\frac{\partial \ln \tilde{p}(\boldsymbol{z};\theta)}{\partial\theta}\right|_{\theta=\theta_t} = \frac{1}{\sqrt{N}}\sum_{n=1}^{N}\left.\frac{\partial \ln \tilde{p}(z_n;\theta)}{\partial\theta}\right|_{\theta=\theta_t} \tag{5.270}$$

converges to a Gaussian random variable with zero mean

$$\mathrm{E}_{\boldsymbol{z};\theta_t}\left[\frac{1}{\sqrt{N}}\sum_{n=1}^{N}\left.\frac{\partial \ln \tilde{p}(z_n;\theta)}{\partial\theta}\right|_{\theta=\theta_t}\right] = \sqrt{N}\,\mathrm{E}_{z;\theta_t}\left[\left.\frac{\partial \ln \tilde{p}(z;\theta)}{\partial\theta}\right|_{\theta=\theta_t}\right] = 0 \tag{5.271}$$

and variance

$$\begin{aligned}\mathrm{E}_{\boldsymbol{z};\theta_t}\left[\left(\frac{1}{\sqrt{N}}\sum_{n=1}^{N}\left.\frac{\partial \ln \tilde{p}(z_n;\theta)}{\partial\theta}\right|_{\theta=\theta_t}\right)^2\right] &= \mathrm{E}_{z;\theta_t}\left[\left.\left(\frac{\partial \ln \tilde{p}(z;\theta)}{\partial\theta}\right)^2\right|_{\theta=\theta_t}\right] \\ &= \mathrm{E}_{z;\theta_t}\left[\left(\boldsymbol{b}^{\mathrm{T}}(\theta_t)\big(\boldsymbol{\phi}(z)-\boldsymbol{\mu}_{\boldsymbol{\phi}}(\theta_t)\big)\right)^2\right] \\ &= \boldsymbol{b}^{\mathrm{T}}(\theta_t)\boldsymbol{R}_{\boldsymbol{\phi}}(\theta_t)\boldsymbol{b}(\theta_t).\end{aligned} \tag{5.272}$$

With Slutsky's theorem [12, pp. 255], it follows that asymptotically

$$\sqrt{N}(\hat{\theta} - \theta_t) \sim \mathcal{N}\left(0, \frac{\boldsymbol{b}^{\mathrm{T}}(\theta_t)\boldsymbol{R}_{\boldsymbol{\phi}}(\theta_t)\boldsymbol{b}(\theta_t)}{\left(\frac{\partial \boldsymbol{\mu}_{\boldsymbol{\phi}}(\theta_t)}{\partial \theta}\right)^{\mathrm{T}} \boldsymbol{b}(\theta_t)\boldsymbol{b}^{\mathrm{T}}(\theta_t)\frac{\partial \boldsymbol{\mu}_{\boldsymbol{\phi}}(\theta_t)}{\partial \theta}}\right). \tag{5.273}$$

Therefore, if $p(z;\theta)$ is the data-generating model, the CMLE $\hat{\theta}(\tilde{\boldsymbol{\phi}})$, asymptotically in N, produces estimates which are Gaussian distributed

$$\hat{\theta} \sim \mathcal{N}\left(\theta, \frac{1}{N}\frac{\boldsymbol{b}^{\mathrm{T}}(\theta)\boldsymbol{R}_{\boldsymbol{\phi}}(\theta)\boldsymbol{b}(\theta)}{\left(\frac{\partial \boldsymbol{\mu}_{\boldsymbol{\phi}}(\theta)}{\partial \theta}\right)^{\mathrm{T}} \boldsymbol{b}(\theta)\boldsymbol{b}^{\mathrm{T}}(\theta)\frac{\partial \boldsymbol{\mu}_{\boldsymbol{\phi}}(\theta)}{\partial \theta}}\right). \tag{5.274}$$

Using the best weighting

$$\boldsymbol{b}^{\star}(\theta) = \boldsymbol{R}_{\boldsymbol{\phi}}^{-1}(\theta)\frac{\partial \boldsymbol{\mu}_{\boldsymbol{\phi}}(\theta)}{\partial \theta}\left(\left(\frac{\partial \boldsymbol{\mu}_{\boldsymbol{\phi}}(\theta)}{\partial \theta}\right)^{\mathrm{T}} \boldsymbol{R}_{\boldsymbol{\phi}}^{-1}(\theta)\frac{\partial \boldsymbol{\mu}_{\boldsymbol{\phi}}(\theta)}{\partial \theta}\right)^{-\frac{1}{2}} \tag{5.275}$$

for the auxiliary statistics, the CMLE is found by solving

$$\frac{\left(\frac{\partial \boldsymbol{\mu}_{\boldsymbol{\phi}}(\theta)}{\partial \theta}\right)^{\mathrm{T}} \boldsymbol{R}_{\boldsymbol{\phi}}^{-1}(\theta)}{\sqrt{\left(\left(\frac{\partial \boldsymbol{\mu}_{\boldsymbol{\phi}}(\theta)}{\partial \theta}\right)^{\mathrm{T}} \boldsymbol{R}_{\boldsymbol{\phi}}^{-1}(\theta)\frac{\partial \boldsymbol{\mu}_{\boldsymbol{\phi}}(\theta)}{\partial \theta}\right)}}\left(\tilde{\boldsymbol{\phi}} - \boldsymbol{\mu}_{\boldsymbol{\phi}}(\theta)\right) = 0. \tag{5.276}$$

As

$$\frac{\boldsymbol{b}^{\star\,\mathrm{T}}(\theta)\boldsymbol{R}_{\boldsymbol{\phi}}(\theta)\boldsymbol{b}^{\star}(\theta)}{\left(\frac{\partial \boldsymbol{\mu}_{\boldsymbol{\phi}}(\theta)}{\partial \theta}\right)^{\mathrm{T}} \boldsymbol{b}^{\star}(\theta)\boldsymbol{b}^{\star\,\mathrm{T}}(\theta)\frac{\partial \boldsymbol{\mu}_{\boldsymbol{\phi}}(\theta)}{\partial \theta}} = \frac{1}{\left(\frac{\partial \boldsymbol{\mu}_{\boldsymbol{\phi}}(\boldsymbol{\theta})}{\partial \boldsymbol{\theta}}\right)^{\mathrm{T}} \boldsymbol{R}_{\boldsymbol{\phi}}^{-1}(\boldsymbol{\theta})\frac{\partial \boldsymbol{\mu}_{\boldsymbol{\phi}}(\boldsymbol{\theta})}{\partial \boldsymbol{\theta}}}, \tag{5.277}$$

the CMLE estimator then achieves a performance equivalent to the inverse of the approximation (5.230) for the Fisher information measure by producing estimates

$$\hat{\theta} \sim \mathcal{N}\left(\theta, \frac{1}{N}\frac{1}{\left(\frac{\partial \boldsymbol{\mu}_{\boldsymbol{\phi}}(\theta)}{\partial \theta}\right)^{\mathrm{T}} \boldsymbol{R}_{\boldsymbol{\phi}}^{-1}(\theta)\frac{\partial \boldsymbol{\mu}_{\boldsymbol{\phi}}(\theta)}{\partial \theta}}\right). \tag{5.278}$$

5.5.2 Connection to the Generalized Method of Moments

By squaring the CMLE (5.258) can be reformulated

$$\hat{\theta}(\tilde{\boldsymbol{\phi}}) = \arg\min_{\theta \in \Theta} \left(\tilde{\boldsymbol{\phi}} - \boldsymbol{\mu}_{\boldsymbol{\phi}}(\theta)\right)^{\mathrm{T}} \boldsymbol{b}(\theta)\boldsymbol{b}^{\mathrm{T}}(\theta)\left(\tilde{\boldsymbol{\phi}} - \boldsymbol{\mu}_{\boldsymbol{\phi}}(\theta)\right), \tag{5.279}$$

which is identified as a special case of Hansen's estimator [77]

$$\hat{\theta}(\boldsymbol{z}) = \arg\min_{\theta \in \Theta} \left(\frac{1}{N}\sum_{n=1}^{N} \boldsymbol{f}(z_n;\theta)\right)^{\mathrm{T}} \boldsymbol{D}(\theta)\left(\frac{1}{N}\sum_{n=1}^{N} \boldsymbol{f}(z_n;\theta)\right) \tag{5.280}$$

with the moment condition

$$\boldsymbol{f}(z;\theta) = \boldsymbol{\phi}(z) - \boldsymbol{\mu}_{\boldsymbol{\phi}}(\theta) \tag{5.281}$$

and an optimized weighting matrix

$$\boldsymbol{D}^{\star}(\theta) = \frac{\boldsymbol{R}_{\boldsymbol{\phi}}^{-1}(\theta)\frac{\partial \boldsymbol{\mu}_{\boldsymbol{\phi}}(\theta)}{\partial \theta}\left(\frac{\partial \boldsymbol{\mu}_{\boldsymbol{\phi}}(\theta)}{\partial \theta}\right)^{\mathrm{T}}\boldsymbol{R}_{\boldsymbol{\phi}}^{-1}(\theta)}{\left(\left(\frac{\partial \boldsymbol{\mu}_{\boldsymbol{\phi}}(\theta)}{\partial \theta}\right)^{\mathrm{T}}\boldsymbol{R}_{\boldsymbol{\phi}}^{-1}(\theta)\frac{\partial \boldsymbol{\mu}_{\boldsymbol{\phi}}(\theta)}{\partial \theta}\right)}. \tag{5.282}$$

The generalized method of moments (5.280) is an extension of the classical method of moments [78], derived by considering orthogonality conditions [77]

$$\mathrm{E}_{z;\theta_t}\left[\boldsymbol{f}(z;\theta_t)\right] = \boldsymbol{0} \tag{5.283}$$

under the true parameter θ_t. It is interesting to observe, that we obtain the method (5.280) as a straightforward maximum-likelihood estimator after approximating the original system model $p(z;\theta)$ through a set of auxiliary statistics $\boldsymbol{\phi}(z)$ by the closest (in the sense of the Fisher information measure) equivalent distribution $\tilde{p}(z;\theta)$ within the exponential family. Therefore the equivalent exponential replacement provides a potential unifying link, like subtly requested by [79], between Pearson's method of moments [78] and Fisher's competing concept of likelihood [3].

6. System Design for Pilot-Based Estimation with 1-bit ADC

While the approach of using 1-bit ADCs is highly attractive with respect to hardware complexity and energy efficiency, it has a strong impact on the channel parameter estimation performance of the receiver. As discussed in Chapter 4, for applications with low SNR the relative performance gap between a 1-bit system and an ideal receiver with infinite A/D resolution is moderate with $2/\pi$ (-1.96 dB) [26]. In contrast, for the medium to high SNR regime the loss is much more pronounced. However, switching to an A/D conversion with coarse resolution allows to exploit other system design options like increasing the bandwidth of the receiver or using a sensor array with multiple antennas. The generic Fisher information lower bound (5.230) and the concept of exponential replacement (5.248) enables us to discuss the estimation theoretic performance limits of hard-limited signal models with correlated noise. This makes it possible to analyze the hard-limiting loss for wireless channel estimation with oversampling or with an adjusted analog pre-filter and to examine if it is possible to push the 1-bit performance loss below the classical benchmark of $2/\pi$.

Therefore, in this chapter we discuss the estimation performance with 1-bit ADC and a modified wireless radio front-end. After deriving the required expressions for the performance analysis of signal parameter estimation with 1-bit quantization under the exponential replacement framework, by the example of a Global Navigation Satellite System (GNSS) receiver, we discuss the behavior of the estimation performance when extending the bandwidth of the receiver or when increasing the number of receive antennas in different receive scenarios. Then we analyze the influence of the sampling rate by oversampling the analog receive signal, i.e., choosing the sampling rate f_s higher than twice the bandwidth B_r of the analog receive pre-filter. Further we show that for a fixed sampling rate the analog pre-filter can be adjusted in order to maximize the Fisher information measure at the output of the 1-bit ADC. Finally, we discuss the demodulation operation and demonstrate that using more than two mixing channels (quadrature demodulator) when sampling with 1-bit ADCs can result in significant performance improvements. Like oversampling, the approach of overdemodulation creates redundancy before the hard-limiting operation and therefore allows to partially compensate the 1-bit performance loss for the task of channel estimation.

6.1 Performance of Pilot-Based Estimation with 1-bit ADC

During the discussion in this chapter we focus on pilot-based estimation where the structure of the transmit signal $\boldsymbol{s}(\boldsymbol{\theta})$ is known to the receiver. Therfore we can assume the signal model

$$p(\boldsymbol{y};\boldsymbol{\theta}) = \frac{1}{(2\pi)^{\frac{N}{2}}\sqrt{\det \boldsymbol{R}_{\boldsymbol{\eta}}}} \exp\left(-\frac{1}{2}\big(\boldsymbol{y}-\boldsymbol{s}(\boldsymbol{\theta})\big)^{\mathrm{T}}\boldsymbol{R}_{\boldsymbol{\eta}}^{-1}\big(\boldsymbol{y}-\boldsymbol{s}(\boldsymbol{\theta})\big)\right) \tag{6.1}$$

with a fixed covariance matrix $\boldsymbol{R}_{\boldsymbol{\eta}}$ prior to the hard-limiting operation which is performed on the noisy receive data

$$\boldsymbol{z} = \operatorname{sign}(\boldsymbol{y}). \tag{6.2}$$

6.1.1 Fisher Information Bound for Pilot-Based Estimation under 1-bit ADC

To circumvent calculation of the exact likelihood function (4.121) and the exact Fisher information (4.123) in the cases where the noise covariance $\boldsymbol{R}_{\boldsymbol{\eta}}$ does not exhibit a diagonal structure, we use the bounding approach (5.230) presented in Chapter 5 in order to approximate the Fisher information in a pessimistic way. To this end, here we use identity to form the required auxiliary statistics

$$\boldsymbol{\phi}(\boldsymbol{z}) = \boldsymbol{z}, \tag{6.3}$$

such that the mean

$$\begin{aligned} \boldsymbol{\mu}_{\boldsymbol{\phi}}(\boldsymbol{\theta}) &= \mathrm{E}_{\boldsymbol{z};\boldsymbol{\theta}}\left[\boldsymbol{\phi}(\boldsymbol{z})\right] \\ &= \mathrm{E}_{\boldsymbol{z};\boldsymbol{\theta}}\left[\boldsymbol{z}\right] \\ &= \boldsymbol{\mu}_{\boldsymbol{z}}(\boldsymbol{\theta}) \end{aligned} \tag{6.4}$$

and the covariance matrix

$$\begin{aligned} \boldsymbol{R}_{\boldsymbol{\phi}}(\boldsymbol{\theta}) &= \mathrm{E}_{\boldsymbol{z};\boldsymbol{\theta}}\left[\boldsymbol{\phi}(\boldsymbol{z})\boldsymbol{\phi}^{\mathrm{T}}(\boldsymbol{z})\right] - \boldsymbol{\mu}_{\boldsymbol{\phi}}(\boldsymbol{\theta})\boldsymbol{\mu}_{\boldsymbol{\phi}}^{\mathrm{T}}(\boldsymbol{\theta}) \\ &= \mathrm{E}_{\boldsymbol{z};\boldsymbol{\theta}}\left[\big(\boldsymbol{z} - \boldsymbol{\mu}_{\boldsymbol{z}}(\boldsymbol{\theta})\big)\big(\boldsymbol{z} - \boldsymbol{\mu}_{\boldsymbol{z}}(\boldsymbol{\theta})\big)^{\mathrm{T}}\right] \\ &= \boldsymbol{R}_{\boldsymbol{z}}(\boldsymbol{\theta}) \end{aligned} \tag{6.5}$$

are required in order to calculate a lower bound (5.230) for the Fisher information measure

$$\begin{aligned} \boldsymbol{F}(\boldsymbol{\theta}) &\succeq \left(\frac{\partial \boldsymbol{\mu}_{\boldsymbol{\phi}}(\boldsymbol{\theta})}{\partial \boldsymbol{\theta}}\right)^{\mathrm{T}} \boldsymbol{R}_{\boldsymbol{\phi}}^{-1}(\boldsymbol{\theta}) \frac{\partial \boldsymbol{\mu}_{\boldsymbol{\phi}}(\boldsymbol{\theta})}{\partial \boldsymbol{\theta}} \\ &= \left(\frac{\partial \boldsymbol{\mu}_{\boldsymbol{z}}(\boldsymbol{\theta})}{\partial \boldsymbol{\theta}}\right)^{\mathrm{T}} \boldsymbol{R}_{\boldsymbol{z}}^{-1}(\boldsymbol{\theta}) \frac{\partial \boldsymbol{\mu}_{\boldsymbol{z}}(\boldsymbol{\theta})}{\partial \boldsymbol{\theta}}. \end{aligned} \tag{6.6}$$

The first moment (6.4) can be determined element-wise by

$$\begin{aligned} \mu_{\boldsymbol{z},m}(\boldsymbol{\theta}) &= p\big(z_m = 1;\boldsymbol{\theta}\big) - p\big(z_m = -1;\boldsymbol{\theta}\big) \\ &= 1 - 2\,\mathrm{Q}\left(\frac{s_m(\boldsymbol{\theta})}{\sqrt{[\boldsymbol{R}_{\boldsymbol{\eta}}]_{mm}}}\right). \end{aligned} \tag{6.7}$$

For the second moment (6.5) the diagonal elements are given by

$$[\boldsymbol{R}_{\boldsymbol{z}}(\boldsymbol{\theta})]_{mm} = 1 - \mu_{\boldsymbol{z},m}^2(\boldsymbol{\theta}), \tag{6.8}$$

while the off-diagonal entries are calculated

$$[\boldsymbol{R}_{\boldsymbol{z}}(\boldsymbol{\theta})]_{ij} = 4\Psi_{ij}(\boldsymbol{\theta}) - \big(1 - \mu_{\boldsymbol{z},i}(\boldsymbol{\theta})\big)\big(1 - \mu_{\boldsymbol{z},j}(\boldsymbol{\theta})\big), \tag{6.9}$$

where $\Psi_{ij}(\boldsymbol{\theta})$ is the cumulative density function (CDF) of the bivariate Gaussian distribution

$$p(y_i - s_i(\boldsymbol{\theta}), y_j - s_j(\boldsymbol{\theta}); \boldsymbol{\theta}) \sim \mathcal{N}\left(\begin{bmatrix} 0 \\ 0 \end{bmatrix}, \begin{bmatrix} [\boldsymbol{R}_{\boldsymbol{\eta}}]_{ii} & [\boldsymbol{R}_{\boldsymbol{\eta}}]_{ij} \\ [\boldsymbol{R}_{\boldsymbol{\eta}}]_{ji} & [\boldsymbol{R}_{\boldsymbol{\eta}}]_{jj} \end{bmatrix} \right) \tag{6.10}$$

with upper integration border $\left[-s_i(\boldsymbol{\theta}) - s_j(\boldsymbol{\theta})\right]^{\mathrm{T}}$. The required derivative of the first moment is found by the element-wise rule

$$\left[\frac{\partial \boldsymbol{\mu}_{\boldsymbol{z}}(\boldsymbol{\theta})}{\partial \boldsymbol{\theta}}\right]_{ij} = \frac{2 \exp\left(-\frac{s_i^2(\boldsymbol{\theta})}{2[\boldsymbol{R}_{\boldsymbol{\eta}}]_{ii}}\right)}{\sqrt{2\pi[\boldsymbol{R}_{\boldsymbol{\eta}}]_{ii}}} \left[\frac{\partial \boldsymbol{s}(\boldsymbol{\theta})}{\partial \boldsymbol{\theta}}\right]_{ij}. \tag{6.11}$$

Note that the particular choice of the auxiliary statistics $\boldsymbol{\phi}(\boldsymbol{z}) = \boldsymbol{z}$ used here results in a multivariate and multiple parameter version (6.6) of the first-order information bound (5.12).

6.2 Uncorrelated Noise - System Design for 1-bit GNSS Synchronization

As an application of low resolution A/D conversion with an adjusted system design, the problem of range estimation in the context of satellite-based positioning is considered. While 1-bit ADCs degrade the positioning performance of Global Navigation Satellite System (GNSS) receivers, their simplicity allows to realize sampling at high spatial and temporal rates in an energy and hardware efficient way. This is of practical interest due to the fact that the development of high-performance GNSS receive systems becomes challenging if one imposes strict constraints on the available power, chip size or money budget. As the operation of critical infrastructure like mobile communication systems, electric distribution networks or financial trading systems depends on correct time synchronization attained through GNSS receive systems, robustness against interference and multi-path propagation is another important requirement that must be met by the receiver design without violating the technical limitations defined by the available hardware. Under the assumption that the receive system operates on the basis of an efficient estimation algorithm, two fundamental design options exist in order to obtain high positioning accuracy and robustness against channel imperfections like multi-path propagation. One is to extend the amount of receive antennas, the other is to implement a higher receive bandwidth through fast temporal sampling rates. In the following we analyze the estimation theoretic performance limits of 1-bit GNSS receive systems which exploit these design options.

6.2.1 System Model

To this end, we assume a GNSS receiver with an uniform linear array (ULA) which consists of A antennas. The antennas are placed with a spacing corresponding to half the carrier wavelength. Each antenna, $a = 1, 2, \ldots, A$, has an analog in-phase output $y_{I,a}(t) \in \mathbb{R}$ and an analog quadrature output $y_{Q,a}(t) \in \mathbb{R}$. The overall analog GNSS receive signal from all sensors can be written in vector notation by

$$\boldsymbol{y}(t) = \begin{bmatrix} \boldsymbol{y}_I^{\mathrm{T}}(t) & \boldsymbol{y}_Q^{\mathrm{T}}(t) \end{bmatrix}^{\mathrm{T}} \in \mathbb{R}^{2A}, \tag{6.12}$$

with $\boldsymbol{y}_I(t), \boldsymbol{y}_Q(t) \in \mathbb{R}^A$ and

$$\boldsymbol{y}_{I/Q}(t) = \begin{bmatrix} y_{I/Q,1}(t) & y_{I/Q,2}(t) & \ldots & y_{I/Q,A}(t) \end{bmatrix}^{\mathrm{T}}. \tag{6.13}$$

The coherent and Doppler-compensated receive model

$$\boldsymbol{y}(t) = \gamma_S \boldsymbol{A}(\zeta_S)\boldsymbol{x}(t-\tau_S) + \gamma_P \boldsymbol{A}(\zeta_P)\boldsymbol{\Phi}(\psi_P)\boldsymbol{x}(t-\tau_P) + \boldsymbol{\eta}(t) \tag{6.14}$$

is assumed to comprise a line-of-sight satellite signal $\boldsymbol{x}(t-\tau_S) \in \mathbb{R}^2$, a multi-path component $\boldsymbol{x}(t-\tau_P) \in \mathbb{R}^2$ and sensor noise $\boldsymbol{\eta}(t) \in \mathbb{R}^{2A}$. The line-of-sight satellite signal $\boldsymbol{x}(t-\tau_S)$ impinges on the array attenuated by $\gamma_S \in \mathbb{R}$ under the angle $\zeta_S \in \mathbb{R}$ and with time-shift $\tau_S \in \mathbb{R}$, while the multi-path component $\boldsymbol{x}(t-\tau_P)$ arrives attenuated by $\gamma_P \in \mathbb{R}$ with a time-delay $\tau_P \in \mathbb{R}$, angle $\zeta_P \in \mathbb{R}$ and phase-offset $\psi_P \in \mathbb{R}$. The receive setup is depicted in Fig. 6.1. The steering matrix of

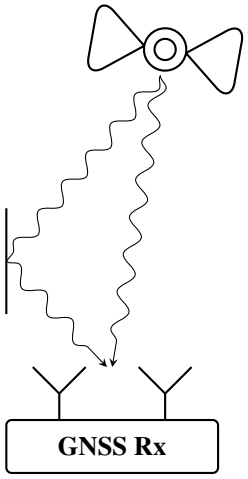

Fig. 6.1. GNSS Receive Setup with Multi-Path Propagation

the receive array as a function of the angle-of-arrival parameter ζ

$$\boldsymbol{A}(\zeta) = \begin{bmatrix} \boldsymbol{A}_I^{\mathrm{T}}(\zeta) & \boldsymbol{A}_Q^{\mathrm{T}}(\zeta) \end{bmatrix}^{\mathrm{T}} \in \mathbb{R}^{2A\times 2}, \tag{6.15}$$

is determined by the steering matrix corresponding to the in-phase sensor outputs

$$\boldsymbol{A}_I(\zeta) = \begin{bmatrix} \alpha_1(\zeta) & \beta_1(\zeta) \\ \alpha_2(\zeta) & \beta_2(\zeta) \\ \vdots & \vdots \\ \alpha_A(\zeta) & \beta_A(\zeta) \end{bmatrix} \in \mathbb{R}^{A\times 2} \tag{6.16}$$

and the steering matrix associated with the quadrature outputs

$$\boldsymbol{A}_Q(\zeta) = \begin{bmatrix} -\beta_1(\zeta) & \alpha_1(\zeta) \\ -\beta_2(\zeta) & \alpha_2(\zeta) \\ \vdots & \vdots \\ -\beta_A(\zeta) & \alpha_A(\zeta) \end{bmatrix} \in \mathbb{R}^{A\times 2}, \tag{6.17}$$

where for both matrices the single entries are given by

$$\alpha_a(\zeta) = \cos\big((a-1)\pi \sin(\zeta)\big), \tag{6.18}$$

$$\beta_a(\zeta) = \sin\big((a-1)\pi \sin(\zeta)\big). \tag{6.19}$$

The channel phase-offset is modeled by the rotation matrix

$$\boldsymbol{\Phi}(\psi) = \begin{bmatrix} \cos(\psi) & -\sin(\psi) \\ \sin(\psi) & \cos(\psi) \end{bmatrix} \in \mathbb{R}^{2\times 2}. \tag{6.20}$$

The transmit signal of the GNSS satellite consists of an in-phase and a quadrature transmit component

$$\boldsymbol{x}(t) = \left[\sqrt{\rho C}x_I(t) \quad \sqrt{(1-\rho)C}x_Q(t)\right]^T \in \mathbb{R}^2, \tag{6.21}$$

where C is the carrier power in Watts and $0 \leq \rho \leq 1$ determines the power allocation between the in-phase and quadrature component. The sensor noise

$$\boldsymbol{\eta}(t) = \left[\boldsymbol{\eta}_I^{\mathrm{T}}(t) \quad \boldsymbol{\eta}_Q^{\mathrm{T}}(t)\right]^{\mathrm{T}} \in \mathbb{R}^{2A} \tag{6.22}$$

consists of $2A$ independent and wide-sense stationary Gaussian random processes

$$\boldsymbol{\eta}_{I/Q}(t) = \left[\eta_{I/Q,1}(t) \quad \eta_{I/Q,2}(t) \quad \dots \quad \eta_{I/Q,A}(t)\right]^{\mathrm{T}} \in \mathbb{R}^{A}, \tag{6.23}$$

with flat power spectral density of $\frac{N_0}{2}$ Watts per Hertz. Band-limiting the $2A$ analog receive signals (6.12) by ideal low-pass filters with one-sided bandwidth B_r and sampling at a rate of $f_s = \frac{1}{T_s}$ with $f_s = 2B_r$ for a duration of $T_o = NT_s$, results in a digital receive signal of the form

$$\begin{aligned} \boldsymbol{y} &= \gamma_S(\boldsymbol{A}(\zeta_S) \otimes \boldsymbol{I}_N)\boldsymbol{x}(\tau_S) + \gamma_P(\boldsymbol{A}(\zeta_P)\boldsymbol{\Phi}(\psi_P) \otimes \boldsymbol{I}_N)\boldsymbol{x}(\tau_P) + \boldsymbol{\eta} \\ &= \boldsymbol{s}(\boldsymbol{\theta}) + \boldsymbol{\eta}, \end{aligned} \tag{6.24}$$

where we summarize the channel parameters in the vector

$$\boldsymbol{\theta} = \left[\zeta_S \quad \tau_S \quad \zeta_P \quad \psi_P \quad \tau_P\right]^{\mathrm{T}} \in \mathbb{R}^5 \tag{6.25}$$

and for notational convenience use

$$\boldsymbol{s}(\boldsymbol{\theta}) = \gamma_S(\boldsymbol{A}(\zeta_S) \otimes \boldsymbol{I}_N)\boldsymbol{x}(\tau_S) + \gamma_P(\boldsymbol{A}(\zeta_P)\boldsymbol{\Phi}(\psi_P) \otimes \boldsymbol{I}_N)\boldsymbol{x}(\tau_P). \tag{6.26}$$

The entries of the signal vectors in (6.24) are given by

$$\boldsymbol{x}(\tau) = \left[\boldsymbol{x}_I^{\mathrm{T}}(\tau) \quad \boldsymbol{x}_Q^{\mathrm{T}}(\tau)\right]^{\mathrm{T}} \in \mathbb{R}^{2N}, \tag{6.27}$$

$$\boldsymbol{\eta} = \left[\boldsymbol{\eta}_I^{\mathrm{T}} \quad \boldsymbol{\eta}_Q^{\mathrm{T}}\right]^{\mathrm{T}} \in \mathbb{R}^{2AN}, \tag{6.28}$$

$$\boldsymbol{\eta}_{I/Q} = \left[\boldsymbol{\eta}_{I/Q,1}^{\mathrm{T}} \quad \boldsymbol{\eta}_{I/Q,2}^{\mathrm{T}} \quad \cdots \quad \boldsymbol{\eta}_{I/Q,M}^{\mathrm{T}}\right]^{\mathrm{T}} \in \mathbb{R}^{AN}, \tag{6.29}$$

with

$$\boldsymbol{x}_I(\tau) = \left[x_I(-\tau) \quad \dots \quad x_I((N-1)T_s - \tau)\right]^{\mathrm{T}}, \tag{6.30}$$

$$\boldsymbol{x}_Q(\tau) = \left[x_Q(-\tau) \quad \dots \quad x_Q((N-1)T_s - \tau)\right]^{\mathrm{T}}, \tag{6.31}$$

$$\boldsymbol{\eta}_{I/Q,m}(\tau) = \left[\eta_{I/Q,m}(0) \quad \dots \quad \eta_{I/Q,m}((N-1)T_s)\right]^{\mathrm{T}}. \tag{6.32}$$

Due to the antenna spacing and the strict relation between bandwidth and sampling rate $f_s = 2B_r$, the covariance matrix of the sensor noise is

$$\boldsymbol{R}_{\boldsymbol{\eta}} = \mathrm{E}\left[\boldsymbol{\eta}\boldsymbol{\eta}^{\mathrm{T}}\right] = \boldsymbol{I}_{2AN}. \tag{6.33}$$

In the following we assume that the ADC for each of the $M = 2A$ output channels is a symmetric hard-limiter, such that the final digital receive data $\boldsymbol{z} \in \{-1, 1\}^{2AN}$ is given by

$$\boldsymbol{z} = \operatorname{sign}\big(\boldsymbol{y}\big). \tag{6.34}$$

6.2.2 Performance Analysis

In order to discuss the performance of the receiver in a compact analytical way, it is assumed that the maximum-likelihood estimator (MLE)

$$\hat{\boldsymbol{\theta}}(\boldsymbol{z}) = \arg\max_{\boldsymbol{\theta}} \ln p(\boldsymbol{z};\boldsymbol{\theta}) \tag{6.35}$$

is used for the estimation of the channel parameters $\boldsymbol{\theta}$. As shown in (3.38)

$$\mathbf{MSE}(\boldsymbol{\theta}) \overset{a}{=} \frac{1}{N}\boldsymbol{F}_{\boldsymbol{z}}^{-1}(\boldsymbol{\theta}) \tag{6.36}$$

holds in the asymptotic regime, such that with a pessimistic version of the FIM

$$\boldsymbol{F}_{\boldsymbol{z}}(\boldsymbol{\theta}) \succeq \tilde{\boldsymbol{F}}_{\boldsymbol{z}},(\boldsymbol{\theta}) \tag{6.37}$$

we can bound the resulting asymptotic estimation error of the MLE from above

$$\frac{1}{N}\tilde{\boldsymbol{F}}_{\boldsymbol{z}}^{-1}(\boldsymbol{\theta}) \succeq \mathbf{MSE}(\boldsymbol{\theta}). \tag{6.38}$$

For the conservative approximation of the FIM (6.6), the derivatives

$$\frac{\partial \boldsymbol{s}(\boldsymbol{\theta})}{\partial \boldsymbol{\theta}} = \begin{bmatrix} \frac{\partial \boldsymbol{s}(\boldsymbol{\theta})}{\partial \zeta_S} & \frac{\partial \boldsymbol{s}(\boldsymbol{\theta})}{\partial \tau_S} & \frac{\partial \boldsymbol{s}(\boldsymbol{\theta})}{\partial \zeta_P} & \frac{\partial \boldsymbol{s}(\boldsymbol{\theta})}{\partial \psi_P} & \frac{\partial \boldsymbol{s}(\boldsymbol{\theta})}{\partial \tau_P} \end{bmatrix} \tag{6.39}$$

with

$$\frac{\partial \boldsymbol{s}(\boldsymbol{\theta})}{\partial \zeta_S} = \gamma_S \Big(\frac{\partial \boldsymbol{A}(\zeta_S)}{\partial \zeta_S} \otimes \mathbf{1}_N \Big) \boldsymbol{x}(\tau_S), \tag{6.40}$$

$$\frac{\partial \boldsymbol{s}(\boldsymbol{\theta})}{\partial \tau_S} = \gamma_S \big(\boldsymbol{A}(\zeta_S) \otimes \mathbf{1}_N \big) \frac{\partial \boldsymbol{x}(\tau_S)}{\partial \tau_S}, \tag{6.41}$$

$$\frac{\partial \boldsymbol{s}(\boldsymbol{\theta})}{\partial \zeta_P} = \gamma_P \Big(\frac{\partial \boldsymbol{A}(\zeta_P)}{\partial \zeta_P} \boldsymbol{\Phi}(\psi_P) \otimes \mathbf{1}_N \Big) \boldsymbol{x}(\tau_P), \tag{6.42}$$

$$\frac{\partial \boldsymbol{s}(\boldsymbol{\theta})}{\partial \psi_P} = \gamma_P \Big(\boldsymbol{A}(\zeta_P) \frac{\partial \boldsymbol{\Phi}(\psi_P)}{\partial \psi_P} \otimes \mathbf{1}_N \Big) \boldsymbol{x}(\tau_P), \tag{6.43}$$

$$\frac{\partial \boldsymbol{s}(\boldsymbol{\theta})}{\partial \tau_P} = \gamma_P \big(\boldsymbol{A}(\zeta_P) \boldsymbol{\Phi}(\psi_P) \otimes \mathbf{1}_N \big) \frac{\partial \boldsymbol{x}(\tau_P)}{\partial \tau_P} \tag{6.44}$$

and

$$\frac{\partial \boldsymbol{\Phi}(\psi)}{\partial \psi} = \begin{bmatrix} -\sin(\psi) & \cos(\psi) \\ -\cos(\psi) & -\sin(\psi) \end{bmatrix} \tag{6.45}$$

are required, where the derivatives of the transmit signal with respect to the time-delay are

$$\frac{\partial \boldsymbol{x}(\tau)}{\partial \tau} = \begin{bmatrix} \frac{\partial \boldsymbol{x}_I^{\mathrm{T}}(\tau)}{\partial \tau} & \frac{\partial \boldsymbol{x}_Q^{\mathrm{T}}(\tau)}{\partial \tau} \end{bmatrix}^{\mathrm{T}}, \tag{6.46}$$

$$\left[\frac{\partial \boldsymbol{x}_{I/Q}(\tau)}{\partial \tau} \right]_i = -\frac{\mathrm{d}x_{I/Q}(t)}{\mathrm{d}t}\Big|_{t=(i-1)T_s-\tau} \tag{6.47}$$

and the derivative of the steering matrix is

$$\frac{\partial \boldsymbol{A}(\zeta)}{\partial \zeta} = \begin{bmatrix} \frac{\partial \boldsymbol{A}_I^{\mathrm{T}}(\zeta)}{\partial \zeta} & \frac{\partial \boldsymbol{A}_Q^{\mathrm{T}}(\zeta)}{\partial \zeta} \end{bmatrix}^{\mathrm{T}}, \tag{6.48}$$

with the in-phase component

$$\frac{\partial \boldsymbol{A}_I(\zeta)}{\partial \zeta} = \begin{bmatrix} \frac{\partial \alpha_1(\zeta)}{\partial \zeta} & \frac{\partial \beta_1(\zeta)}{\partial \zeta} \\ \frac{\partial \alpha_2(\zeta)}{\partial \zeta} & \frac{\partial \beta_2(\zeta)}{\partial \zeta} \\ \vdots & \vdots \\ \frac{\partial \alpha_A(\zeta)}{\partial \zeta} & \frac{\partial \beta_A(\zeta)}{\partial \zeta} \end{bmatrix} \tag{6.49}$$

and a quadrature component

$$\frac{\partial \boldsymbol{A}_Q(\zeta)}{\partial \zeta} = \begin{bmatrix} -\frac{\partial \beta_1(\zeta)}{\partial \zeta} & \frac{\partial \alpha_1(\zeta)}{\partial \zeta} \\ -\frac{\partial \beta_2(\zeta)}{\partial \zeta} & \frac{\partial \alpha_2(\zeta)}{\partial \zeta} \\ \vdots & \vdots \\ -\frac{\partial \beta_A(\zeta)}{\partial \zeta} & \frac{\partial \alpha_A(\zeta)}{\partial \zeta} \end{bmatrix}, \tag{6.50}$$

while the individual entries are

$$\frac{\partial \alpha_a(\zeta)}{\partial \zeta} = -(a-1)\pi \cos(\zeta) \sin\big((a-1)\pi \sin(\zeta)\big), \tag{6.51}$$

$$\frac{\partial \beta_a(\zeta)}{\partial \zeta} = (a-1)\pi \cos(\zeta) \cos\big((a-1)\pi \sin(\zeta)\big). \tag{6.52}$$

In order to analyze the potential of 1-bit GNSS receivers with multiple antennas and high temporal sampling rates, we will compare the achievable ranging accuracy of different receive setups to an ideal reference system with infinite ADC resolution. To this end we focus on the accuracy of the range measurement obtained by estimating the line-of-sight propagation delay $\hat{\tau}_S$ which is given by

$$\mathrm{MSE}(\tau_S) = \big[\boldsymbol{F}_{\boldsymbol{z}}^{-1}(\boldsymbol{\theta})\big]_{22} \tag{6.53}$$

and is directly related to the accuracy of the final positioning solution of the GNSS system. In order to compare different receive systems with infinite A/D resolution to a reference system, we introduce the relative performance measure

$$\chi_{\infty}(\boldsymbol{\theta}) = \frac{\big[\boldsymbol{F}_{\mathrm{REF}}^{-1}(\boldsymbol{\theta})\big]_{22}}{\big[\boldsymbol{F}_{\boldsymbol{y}}^{-1}(\boldsymbol{\theta})\big]_{22}}, \tag{6.54}$$

where the FIM for an ideal receiver which has access to the unquantized receive signal $\boldsymbol{y}$ is

$$\boldsymbol{F}_{\boldsymbol{y}}(\boldsymbol{\theta}) = \left(\frac{\partial \boldsymbol{s}(\boldsymbol{\theta})}{\partial \boldsymbol{\theta}}\right)^{T} \frac{\partial \boldsymbol{s}(\boldsymbol{\theta})}{\partial \boldsymbol{\theta}}. \tag{6.55}$$

For a comparison of the 1-bit receive system with the reference system the relative performance measure

$$\chi_{\text{1-bit}}(\boldsymbol{\theta}) = \frac{\big[\boldsymbol{F}_{\mathrm{REF}}^{-1}(\boldsymbol{\theta})\big]_{22}}{\big[\tilde{\boldsymbol{F}}_{\boldsymbol{z}}^{-1}(\boldsymbol{\theta})\big]_{22}}, \tag{6.56}$$

is used, where the pessimistic FIM for the quantized receiver is

$$\tilde{\boldsymbol{F}}_{\boldsymbol{z}}(\boldsymbol{\theta}) = \left(\frac{\partial \boldsymbol{\mu}_{\boldsymbol{z}}(\boldsymbol{\theta})}{\partial \boldsymbol{\theta}}\right)^{\mathrm{T}} \boldsymbol{R}_{\boldsymbol{z}}^{-1}(\boldsymbol{\theta}) \frac{\partial \boldsymbol{\mu}_{\boldsymbol{z}}(\boldsymbol{\theta})}{\partial \boldsymbol{\theta}}. \tag{6.57}$$

The relative performance measures (6.54) and (6.56) allow to characterize the gain or loss in estimation accuracy in terms of an equivalent change in SNR. For example, a system which exhibits $\chi = 3.0$ dB attains the same performance as the reference system with the satellite using the double amount of transmit power. Note that in such a case the root mean squared error of the estimation solution is diminished accordingly by a factor of $\frac{1}{\sqrt{2}}$. Also note that (6.56) is in general a pessimistic measure for the quantization loss, i.e., the 1-bit performance gap can be smaller than indicated by (6.56). For the special case of uncorrelated noise, (6.56) forms an exact measure due to the result (5.27).

In all discussed GNSS scenarios we assume the transmitter to be a satellite of the American GPS system sending C/A - L1 signals [55] with a symbol duration of $T_c = \frac{1}{f_c}$ at a carrier frequency of $2\pi\omega_c = 1575.42$ MHz. The reference frequency of the system is $f_c = 1.023$MHz. The transmit signal is limited to a one-sided bandwidth of $B_t = 11.253$ MHz (main-lobe and 5 side-lobes) at the satellite, an civil I/Q power allocation of $\rho = 1$ is assumed and the receive strength is $C/N_0 = 45.0$ dB-Hz at each sensor. After demodulation to baseband, the receiver restricts the receive signal of each antenna to a one-sided bandwidth of $B_r = \kappa f_c$, $\kappa \geq 1$ by using an ideal low-pass filter and samples at a rate of $f_s = 2B_r$ for a duration of $T_o = 1$ ms. For the reference receive system with infinite ADC resolution, we assume $A = 2$ antennas and $\kappa = 1$, such that

$$\boldsymbol{F}_{\text{REF}}(\boldsymbol{\theta}) = \left(\frac{\partial \boldsymbol{s}(\boldsymbol{\theta})}{\partial \boldsymbol{\theta}}\right)^{\mathrm{T}} \frac{\partial \boldsymbol{s}(\boldsymbol{\theta})}{\partial \boldsymbol{\theta}}\bigg|_{A=2,\kappa=1}. \tag{6.58}$$

6.2.2.1 Line-of-Sight GNSS Channel Synchronization

The first scenario we discuss is a simple line-of-sight receive situation without multi-path (see Fig. 6.2). In this case, the receive signal model (6.24) simplifies to

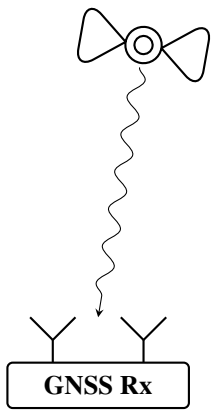

Fig. 6.2. Line-of-Sight GNSS Receive Setup

$$\begin{aligned} \boldsymbol{y} &= \gamma_S(\boldsymbol{A}(\zeta_S) \otimes \boldsymbol{I}_N)\boldsymbol{x}(\tau_S) + \boldsymbol{\eta} \\ &= \boldsymbol{s}(\boldsymbol{\theta}) + \boldsymbol{\eta}, \end{aligned} \tag{6.59}$$

where the channel parameters are

$$\boldsymbol{\theta} = \begin{bmatrix} \zeta_S & \tau_S \end{bmatrix}^{\mathrm{T}}. \tag{6.60}$$

For the performance analysis, we set the angle of the direct path to $\zeta_S = 0$. In order to visualize the behavior of the estimation error in correspondence to the number of receive antennas A, Fig. 6.3 depicts the relative performance χ_∞, where an ideal receive system with A antennas operating at a bandwidth $\kappa = 1$ is compared to the reference system with $A = 2$ antennas and $\kappa = 1$. It

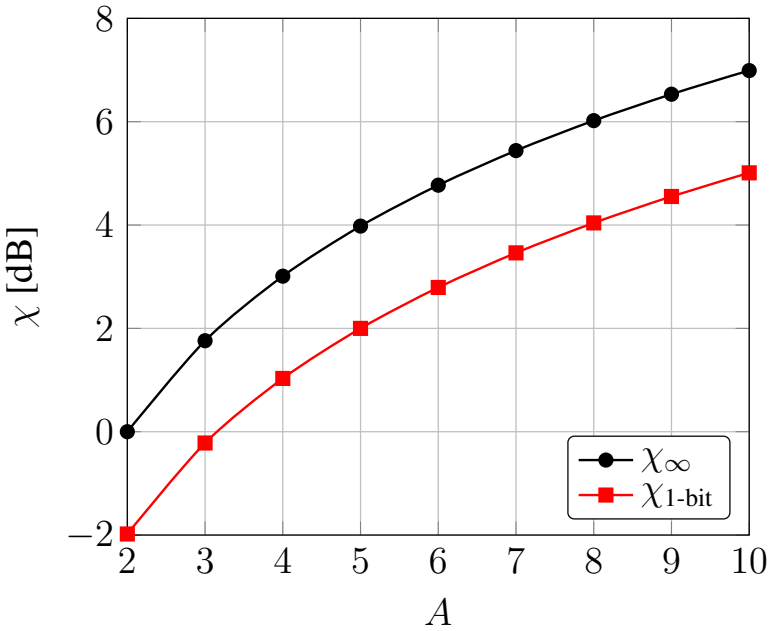

Fig. 6.3. Performance vs. Number of Antennas A

can be observed that doubling the number of receive antennas results in a gain of $\chi_\infty = 3.0$ dB. This is also the case for systems with 1-bit ADC, which in general show a performance $\chi_{\text{1-bit}}$ that lies -2.0 dB below the performance of receivers with infinite ADC resolution. The result indicates that using a 1-bit GNSS receiver with $A = 3$ antennas allows to approximately obtain the same performance as with the ideal reference system with $A = 2$ antennas. Taking into consideration that a 2-bit receive system would require 3 times more comparators for the realization of the ADC circuit than a 1-bit receiver, it becomes clear that using $A = 6$ antennas with 1-bit resolution instead of $A = 2$ and 2-bit ADC resolution will lead to a system design which is at least 3 dB better with respect to the problem of channel synchronization in the low SNR regime under the same number of comparator operations per sample.

In contrast Fig. 6.4 shows the behavior of the estimation performance χ as a function of the receive bandwidth κ. Therefore, under the relative performance measure χ_∞ an ideal receive system with infinite ADC resolution, $A = 2$ antennas and receive bandwidth $\kappa \geq 1$ is compared to the reference system operating at $\kappa = 1$. In parallel the figure of merit $\chi_{\text{1-bit}}$ is depicted in Fig. 6.4 in order to show the relative performance of a system with 1-bit ADC. It is observed that the receive bandwidth κ is a crucial design criterion for high-performance GNSS systems as it allows to significantly increase the channel synchronization performance. This is due to the fact that for the Fisher information of the time-delay parameter τ_S the SNR per Hz exhibits a quadratic weight with respect to the frequency offset from the carrier frequency f_c. As the spectral power density

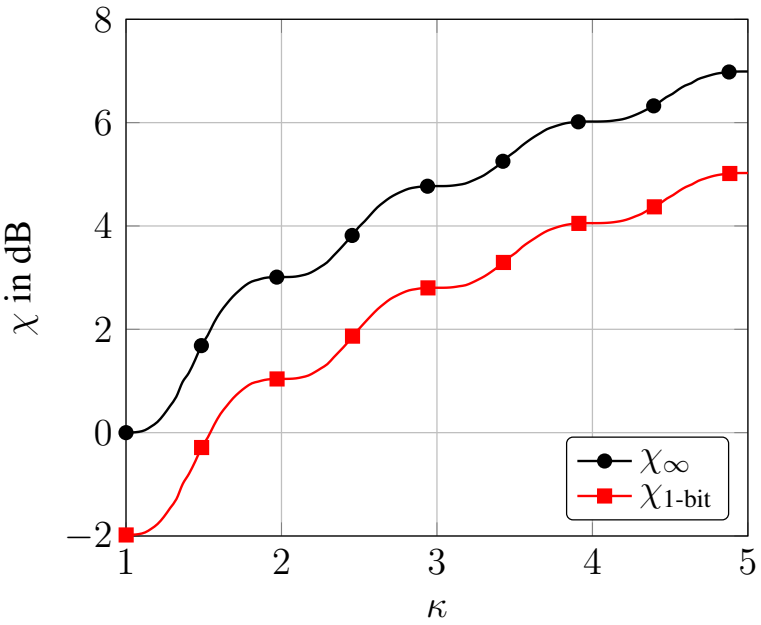

Fig. 6.4. Performance vs. Receive Bandwidth κ

of the satellite signal, and consequently the SNR per Hz decays quadratically with frequency, a linear growth of the accuracy, similar to the case with A antennas, is observed. The 1-bit GNSS receive systems benefit from the same effect while their relative performance $\chi_{\text{1-bit}}$ in this scenario lies constantly -2.0 dB below the performance of the receivers with a high-resolution ADC. Consequently, a receiver with 1-bit A/D conversion, sampling at a temporal rate of approximately $\kappa = 1.5$, is sufficient to outperform the ideal reference system with $\kappa = 1.0$. Recalling from Chapter 3 that the 1-bit system can be operated at least at $\kappa = 3$ under the same power consumption (2.5) as a 2-bit receiver, it becomes clear that from a performance-oriented perspective the ADC resolution plays a minor role in this low SNR application. For the GNSS synchronization problem, the receive bandwidth is the dominating design. This leads to the result that with a fixed number of comparator operations per time instance, a 1-bit ADC with $\kappa \geq 3$ outperforms any other system with higher A/D resolution and $\kappa = 1$.

6.2.2.2 GNSS Channel Synchronization under Multi-Path Propagation

For the second scenario, we assume that the GNSS satellite signal is received through the line-of-sight path with an additional multi-path component (see Fig. 6.5). The receive signal model therefore is as derived in (6.24)

$$\begin{aligned}\boldsymbol{y} &= \gamma_S(\boldsymbol{A}(\zeta_S) \otimes \boldsymbol{I}_N)\boldsymbol{x}(\tau_S) + \gamma_P(\boldsymbol{A}(\zeta_P)\boldsymbol{\Phi}(\psi_P) \otimes \boldsymbol{I}_N)\boldsymbol{x}(\tau_P) + \boldsymbol{\eta} \\ &= \boldsymbol{s}(\boldsymbol{\theta}) + \boldsymbol{\eta}\end{aligned} \tag{6.61}$$

with the channel parameter vector

$$\boldsymbol{\theta} = \begin{bmatrix}\zeta_S & \tau_S & \zeta_P & \psi_P & \tau_P\end{bmatrix}. \tag{6.62}$$

The time-delays of the direct path and the multi-path component are chosen such that $\Delta\tau = \tau_P - \tau_S = 0.1T_c$ while the angles are $\zeta_S = 0$ and $\zeta_P = \frac{\pi}{16}$. The multi-path attenuation is set to $\gamma_P = \sqrt{0.5}\gamma_S$, i.e., -3.0 dB in comparison to the direct path, and the phase offset is $\psi_P = 0$.

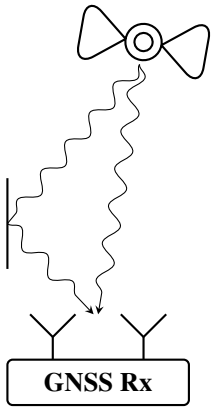

Fig. 6.5. GNSS Receive Setup with Multi-Path Propagation

In order to investigate the behavior of the GNSS synchronization performance under multi-path propagation in correspondence with the number of antennas A, Fig. 6.6 visualizes the relative performance χ_∞ with respect to an ideal receive system with infinite ADC resolution, $A = 2$ antennas and $\kappa = 1$. It becomes clear that the positioning performance is substantially increased

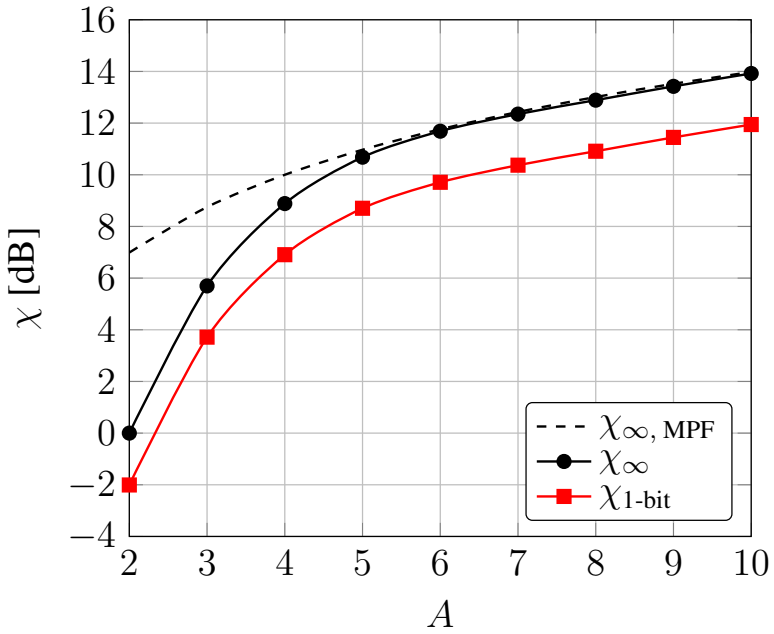

Fig. 6.6. Estimation Performance vs. Number of Antennas A

if a higher number of antennas A is used. In this specific GNSS scenario using $A = 6$ instead of $A = 2$ antennas with ideal ADCs allows to attain the same performance as in a multi-path free (MPF) scenario ($\chi_{\infty,\,\mathrm{MPF}}$, dashed line). The 1-bit GNSS system with $A = 3$ antennas already outperforms the ideal reference system with $A = 2$ by $\chi_{\text{1-bit}} = 3.71$ dB under the chosen multi-path propagation setup. Fig. 6.7 shows a similar comparison where the performance scaling is visualized as a function of the receive bandwidth κ. With the performance measure χ_∞ an ideal receive system with infinite ADC resolution, $A = 2$ antennas and a receive bandwidth of $\kappa \geq 1$ is compared to the reference system with $A = 2$ operating at $\kappa = 1$. It can be observed that also the receive bandwidth κ is an effective design option in order to mitigate the effect of multi-path

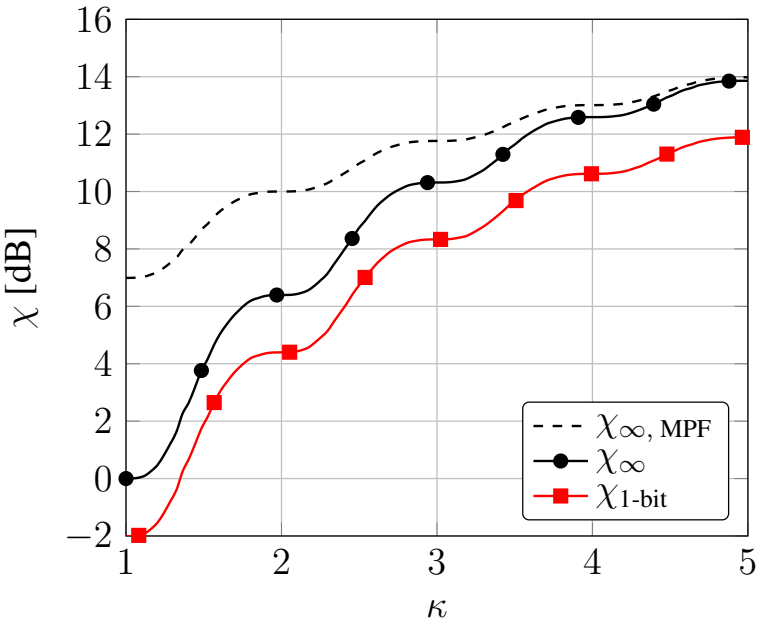

Fig. 6.7. Estimation Performance vs. Receive Bandwidth κ

propagation. Increasing the receive bandwidth by factor $\kappa = 5$ with an ideal ADC allows to obtain the same performance as in a multi-path free scenario ($\chi_{\infty,\,\mathrm{MPF}}$, dashed line). Fig. 6.7 shows that in the considered case already with a bandwidth of $\kappa = 1.35$ the 1-bit system outperforms the ideal reference receiver with $\kappa = 1$.

We have carried out a performance analysis of GNSS receive systems with ideal ADC and 1-bit ADC with respect to the achievable synchronization accuracy. The investigation under different numbers of receive antennas and receive bandwidths shows that these two design parameters are key for the development of robust high-performance GNSS receive systems. The resolution of the ADC only plays a secondary role. If a very simple symmetric 1-bit ADC is used, high receive bandwidth and multiple antennas can be realized in an energy and hardware-efficient way. The achievable performance gain clearly outweighs the loss that has to be taken into account due to the nonlinearity of the 1-bit ADCs. Already increasing the number of antennas or the receive bandwidth by a factor of 2 allows to attain a positioning accuracy with 1-bit ADC which is higher than with any other A/D resolution. This shows that the energy and hardware budget of GNSS receive systems should not be invested into the resolution of the ADCs but into the number of receive sensors and the receive bandwidth. This will allow to build efficient and reliable high-performance receivers capable of coping with challenging GNSS receive situations.

6.3 Correlated Noise - System Design for Channel Estimation with 1-bit ADC

While in the last section, we have focused on system design modifications which result in receive signal models without noise correlation, on the next pages we consider adjustments of the analog radio front-end which introduce noise correlation. As with hard-limiting these models are challenging to analyze by means of the Fisher information measure (see Section 4.6), we make use of the approximation (5.230) in order to explore possible information gain. In particular, we discuss oversampling the analog receive signal without changing the analog receive filter. Further, for a fixed sampling rate we verify the impact of the analog pre-filter onto the estimation performance of the

channel parameters. Then we discuss the demodulation operation and analyze the estimation performance which is achieved with $M > 2$ demodulation output channels (overdemodulation) which are sampled with 1-bit ADCs.

6.3.1 Impact of the Sampling Rate and the Analog Pre-filter

For the discussion of oversampling and pre-filter adjustment, we assume a real-valued receive signal of the form

$$\breve{y}(t) = \sqrt{C}\breve{x}(t-\tau) + \breve{\eta}(t), \tag{6.63}$$

with $C \in \mathbb{R}$ being the carrier power and $\tau \in \mathbb{R}$ a time-delay. The signal is filtered by an ideal low-pass filter

$$H(\omega) = \begin{cases} 1 & \text{if } |\omega| \leq 2\pi B_r \\ 0 & \text{else} \end{cases} \tag{6.64}$$

with bandwidth B_r, such that the analog receive signal is given by

$$\begin{aligned} y(t) &= \breve{y}(t) * h(t) \\ &= \sqrt{C}x(t-\tau) + \eta(t). \end{aligned} \tag{6.65}$$

The received pilot signal has the form

$$x(t) = \sum_{c=-\infty}^{+\infty} [\boldsymbol{c}]_{(1+\mathrm{mod}(c,N_c))} g(t - cT_c), \tag{6.66}$$

with $\boldsymbol{c} \in \{-1, 1\}^{N_c}$ being a binary chip sequence with $N_c = 1023$ elements and a chip frequency $f_c = \frac{1}{T_c} = 1.023$ MHz, such that the chip-duration is $T_c = 977.52$ ns and the signal $x(t)$ is periodic with $T_o = 1$ ms. The received pilot pulse

$$g(t) = \frac{1}{\pi\sqrt{T_c}} \left[\mathrm{Si}\left(2\pi B_r\Big(t + \frac{T_c}{2}\Big)\right) - \mathrm{Si}\left(2\pi B_r\Big(t - \frac{T_c}{2}\Big)\right) \right]$$

is the band-limited version of a rectangular pulse $\breve{g}(t)$, where we use the definition

$$\mathrm{Si}(t) = \int_0^t \frac{\sin(x)}{x} dx. \tag{6.67}$$

Assuming AWGN $\breve{\eta}(t)$ with constant power spectral density $\frac{N_0}{2}$, the temporal auto-correlation function of the additive noise after low-pass filtering

$$r(t) = \int_{-\infty}^{\infty} \eta(\alpha)\eta(\alpha - t)\mathrm{d}\alpha, \tag{6.68}$$

can be characterized by the inverse Fourier transform of the auto-correlation function in the frequency domain

$$\begin{aligned} r(t) &= \frac{1}{2\pi} \int_{-\infty}^{\infty} \frac{N_0}{2} \left|H(\omega)\right|^2 e^{-\mathrm{j}\omega t} \mathrm{d}\omega \\ &= B_r N_0 \,\mathrm{sinc}\,(2B_r t), \end{aligned} \tag{6.69}$$

where

$$\operatorname{sinc}(x) = \frac{\sin(\pi x)}{\pi x}. \tag{6.70}$$

The analog signal $y(t)$ is sampled with a sampling frequency of $f_s = \frac{1}{T_s}$ such that the digital receive signal

$$\boldsymbol{y} = \sqrt{C}\boldsymbol{x}(\tau) + \boldsymbol{\eta} \tag{6.71}$$

with vector entries

$$y_m = y\big((m-1)T_s\big), \tag{6.72}$$
$$x_m(\tau) = x\big((m-1)T_s - \tau\big), \tag{6.73}$$
$$\eta_m = \eta\big((m-1)T_s\big) \tag{6.74}$$

is obtained. Due to the form of the auto-correlation function (6.69) of the noise the temporal covariance matrix

$$\boldsymbol{R}_{\boldsymbol{\eta}} = \mathrm{E}\left[\boldsymbol{\eta}\boldsymbol{\eta}^{\mathrm{T}}\right] \tag{6.75}$$

is given by

$$[\boldsymbol{R}_{\boldsymbol{\eta}}]_{ij} = B_r N_0 \operatorname{sinc}\left(2B_r T_s \left|i-j\right|\right). \tag{6.76}$$

It is observed that temporally white noise, i.e.,

$$\boldsymbol{R}_{\boldsymbol{\eta}} = B_r N_0 \boldsymbol{I}_N \tag{6.77}$$

is obtained only if the relation between the sampling rate f_s and the low-pass filter bandwidth $f_s = 2B_r$ is exactly satisfied. Note, that the carrier-to-noise ratio $\frac{C}{N_0}$ is a measure for the available receive power at the antenna which is independent of the filter bandwidth B_r. This is important in order to obtain a fair comparison in the following when changing the analog receive filter. For consistency with prior sections, we rewrite the digital signal model

$$\begin{aligned}\boldsymbol{y} &= \gamma\boldsymbol{x}(\tau) + \boldsymbol{\eta} \\ &= \boldsymbol{s}(\boldsymbol{\theta}) + \boldsymbol{\eta}\end{aligned} \tag{6.78}$$

with $\gamma = \sqrt{\frac{C}{B_r N_0}}$, such that the channel parameters are

$$\boldsymbol{\theta} = \begin{bmatrix}\gamma & \tau\end{bmatrix}^{\mathrm{T}} \tag{6.79}$$

and the noise covariance is normalized to

$$[\boldsymbol{R}_{\boldsymbol{\eta}}]_{ij} = \operatorname{sinc}\left(2B_r T_s \left|i-j\right|\right). \tag{6.80}$$

6.3.2 Oversampling the Analog Receive Signal with 1-bit ADC

First, we consider the effect of oversampling the receive signal by fixing the receive bandwidth to $B_r = 1.023$ MHz and using a sampling rate of $f_s = 2B_r\kappa$ with $\kappa \geq 1$. As a reference we use the ideal receive system having access to $\boldsymbol{y}$ and exhibiting a Fisher information matrix

$$\boldsymbol{F}_{\boldsymbol{y}}(\boldsymbol{\theta}) = \left(\frac{\partial \boldsymbol{s}(\boldsymbol{\theta})}{\partial \boldsymbol{\theta}}\right)^{\mathrm{T}} \boldsymbol{R}_{\boldsymbol{\eta}}^{-1} \frac{\partial \boldsymbol{s}(\boldsymbol{\theta})}{\partial \boldsymbol{\theta}}. \tag{6.81}$$

Note that due to the sampling theorem, (6.81) is independent of the oversampling factor κ. For the 1-bit receive system having exclusively access to a hard-limited version of the receive signal

$$\boldsymbol{z} = \operatorname{sign}(\boldsymbol{y}), \tag{6.82}$$

we calculate a conservative approximation of the FIM by

$$\tilde{\boldsymbol{F}}_{\boldsymbol{z}}(\boldsymbol{\theta}) = \left(\frac{\partial \boldsymbol{\mu}_{\boldsymbol{z}}(\boldsymbol{\theta})}{\partial \boldsymbol{\theta}}\right)^{\mathrm{T}} \boldsymbol{R}_{\boldsymbol{z}}^{-1}(\boldsymbol{\theta}) \frac{\partial \boldsymbol{\mu}_{\boldsymbol{z}}(\boldsymbol{\theta})}{\partial \boldsymbol{\theta}} \tag{6.83}$$

and evaluate the performance gap to the ideal benchmark with respect to the estimation of both channel parameters by

$$\chi_\gamma(\boldsymbol{\theta}) = \frac{\left[\boldsymbol{F}_{\boldsymbol{y}}^{-1}(\boldsymbol{\theta})\right]_{11}}{\left[\tilde{\boldsymbol{F}}_{\boldsymbol{z}}^{-1}(\boldsymbol{\theta})\right]_{11}}, \tag{6.84}$$

$$\chi_\tau(\boldsymbol{\theta}) = \frac{\left[\boldsymbol{F}_{\boldsymbol{y}}^{-1}(\boldsymbol{\theta})\right]_{22}}{\left[\tilde{\boldsymbol{F}}_{\boldsymbol{z}}^{-1}(\boldsymbol{\theta})\right]_{22}}. \tag{6.85}$$

Fig. 6.8 shows the 1-bit quantization loss $\chi_\gamma(\boldsymbol{\theta})$ for the attenuation parameter γ as a function of the oversampling factor κ. It can be observed that the performance gap can be diminished by approximately 1 dB through oversampling. For example, in the low SNR regime where $C/N_0 = 30$ dB-Hz, the loss without oversampling, i.e., $\kappa = 1$, is -1.96 dB and reduces to -1.02 dB for $\kappa = 5$. A similar behavior is observed for medium SNR settings with $C/N_0 = 55$ dB-Hz and $C/N_0 = 60$ dB-Hz where oversampling recovers approximately 1 dB of the loss while the initial loss without oversampling is more pronounced than in the low SNR case. An interesting result is obtained when analyzing the 1-bit quantization loss $\chi_\tau(\boldsymbol{\theta})$ for the delay parameter τ as a function of the oversampling factor κ (see Fig. 6.9). While for the low SNR regime the loss $\chi_\tau(\boldsymbol{\theta})$ shows to be very similar to the performance gap $\chi_\gamma(\boldsymbol{\theta})$, in the medium SNR regime we observe a strong performance improvement through oversampling. In the situation where $C/N_0 = 60$ dB-Hz, the initial loss without oversampling is -3.51 dB while with oversampling with $\kappa = 5$ we reach a gap of only -0.99 dB.

This shows that oversampling is a simple approach in order to compensate the loss introduced by a hard-limiting ADC. While the obtained performance gain for medium SNR scenarios is dependent on the considered parameter, for the low SNR the beneficial effect of oversampling seems to be parameter independent. Besides verifying the classical loss of -1.96 dB for $\kappa = 1$, it is interesting to observe that for $\kappa = 3$ the loss for both parameters is not higher than -1.10 dB. This indicates that when using a fixed receive bandwidth B_r and the same number of comparators the 1-bit system will exhibit a low SNR regime loss which is less than -1.10 dB when comparing to any higher A/D resolution.

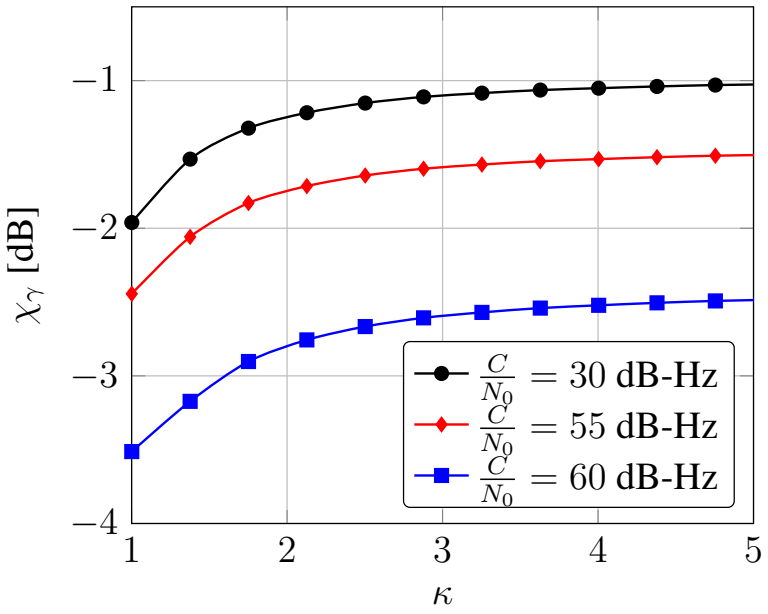

Fig. 6.8. Performance Loss χ_γ vs. Oversampling κ

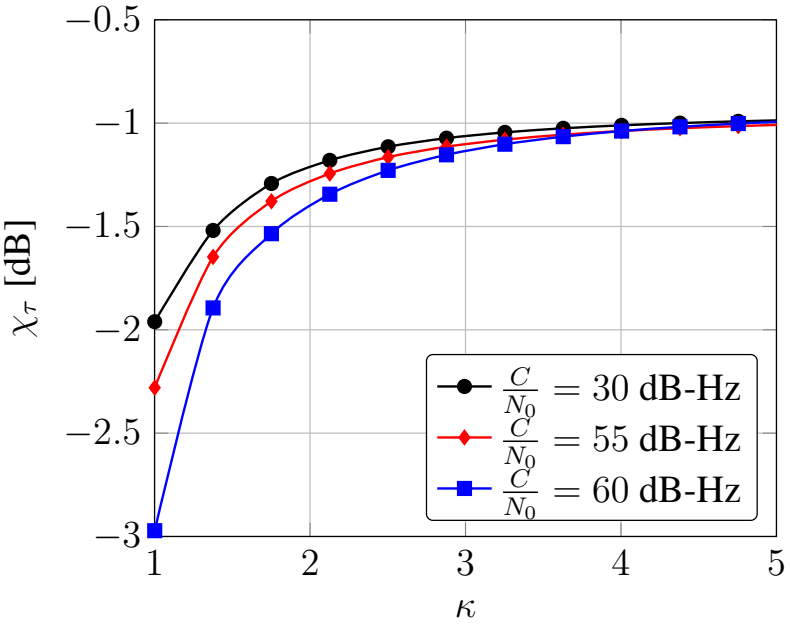

Fig. 6.9. Performance Loss χ_τ vs. Oversampling κ

6.3.3 Adjusting the Analog Pre-Filter with 1-bit ADC

As another possibility to adjust the radio front-end, we discuss the analog pre-filter. To this end, we fix the sampling rate to $f_s = 2.046$ MHz and choose the bandwidth of the ideal analog low-pass filter $B_r = \kappa \frac{f_s}{2}$ with $\kappa \leq 1$. In Fig. 6.10 the performance loss for estimation of the signal strength γ is depicted. While for the medium SNR receive scenario with $C/N_0 = 60$ dB-Hz the information loss constantly increases from -3.69 dB to -4.86 when diminishing κ, for the low SNR regime it is observed that the information loss can be reduced from -1.96 dB ($\kappa = 1$) to -1.60 dB ($\kappa = 0.65$). It is interesting to see that the Fisher information in front of the quantizer becomes significantly smaller for $\kappa < 0.8$ while behind the quantizer the Fisher information in the low SNR regime increases until $\kappa = 0.65$. A similar effect is found for the time-delay parameter τ in Fig. 6.11.

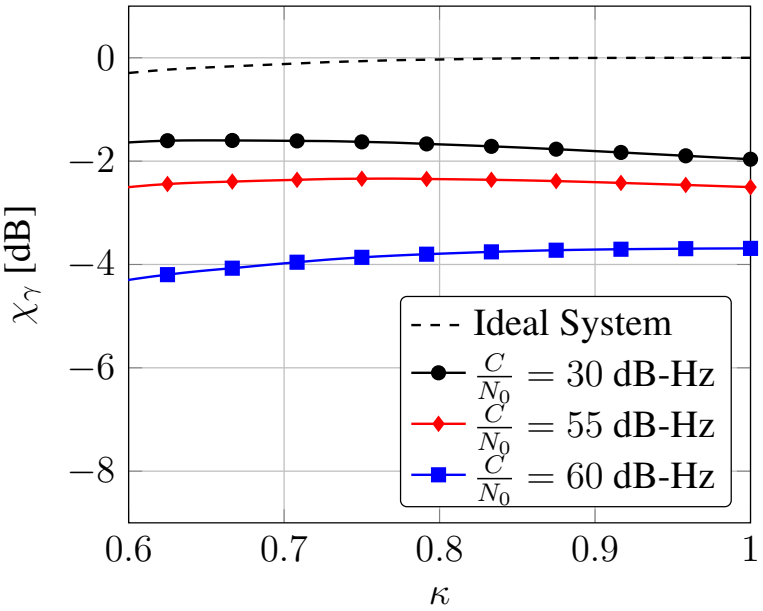

Fig. 6.10. Performance Loss χ_γ vs. Filter Bandwidth κ

Here for the low SNR regime the Fisher information after the quantization operation increases from -1.96 dB ($\kappa = 1$) to -1.80 dB ($\kappa = 0.85$) while for the ideal system the information measure becomes small due to the filter blocking high frequency components. In contrast to the signal strength parameter γ, for the time-delay parameter this effect can also be observed in the medium SNR regime. In the case of $C/N_0 = 60$ dB-Hz the loss diminishes from -2.55 dB ($\kappa = 1$) to -2.41 dB ($\kappa = 0.85$). The results show that the analog pre-filter has a significant impact onto the estimation performance which can be achieved with a 1-bit ADC.

6.3.4 Overdemodulation with 1-bit ADC

Finally, the design of the analog demodulator for receivers with low-resolution ADC is investigated. For infinite ADC resolution, demodulation to baseband with $M = 2$ orthogonal sinusoidal functions (quadrature demodulation) is an optimum design choice with respect to system performance. For receivers which are restricted to ADCs with low amplitude resolution we show here that this classical approach is suboptimal under an estimation theoretic perspective. To this end, we analyze the channel parameter estimation performance when forming $M > 2$ analog demodulation channels prior to low-complexity 1-bit ADCs.

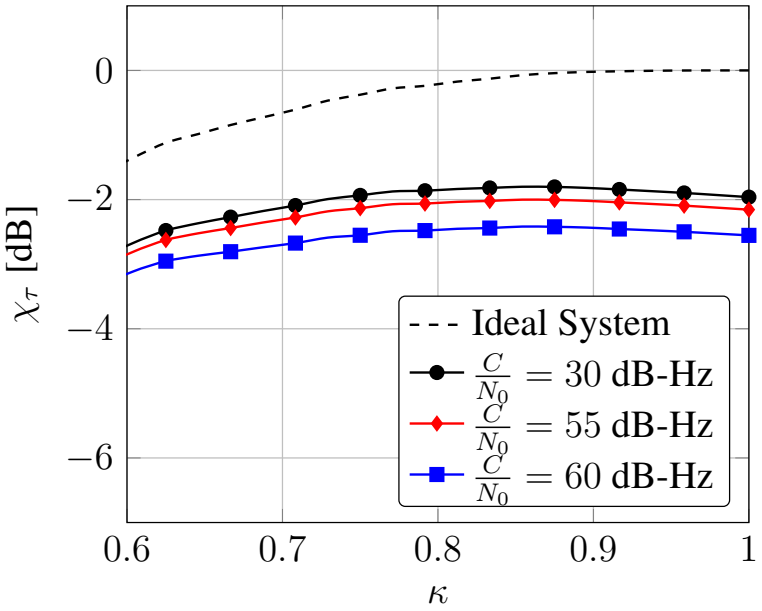

Fig. 6.11. Performance Loss χ_τ vs. Filter Bandwidth κ

In order to demodulate the carrier signal to baseband, classical receivers use a demodulator with in-phase and quadrature channel. Within each channel the receive signal is multiplied with a sinusoid, oscillating at carrier frequency, where the two sinusoids are kept orthogonal by a phase offset of $\frac{\pi}{2}$ [80, p. 582ff.]. While for receivers with infinite A/D resolution this method induces no information-loss during the subsequent transition from the analog to the digital domain, here we show that $M > 2$ demodulation channels allow to significantly reduce the loss due to coarse signal quantization.

For the discussion we assume a single transmitter

$$\breve{x}(t) = \breve{x}_1(t)\sqrt{2}\cos(\omega_c t) - \breve{x}_2(t)\sqrt{2}\sin(\omega_c t), \tag{6.86}$$

where $\omega_c \in \mathbb{R}$ is the carrier frequency and $\breve{x}_{1/2}(t) \in \mathbb{R}$ are two independent input signals. The analog receiver observes

$$\breve{y}(t) = \gamma\breve{x}_1(t-\tau)\sqrt{2}\cos(\omega_c t - \psi) - \gamma\breve{x}_2(t-\tau)\sqrt{2}\sin(\omega_c t - \psi) + \breve{\eta}(t), \tag{6.87}$$

where $\gamma \in \mathbb{R}, \gamma \geq 0$ is the attenuation and $\tau \in \mathbb{R}$ a time-shift due to signal propagation. $\psi \in \mathbb{R}$ characterizes the channel phase offset and $\breve{\eta}(t) \in \mathbb{R}$ is AWGN. For the demodulation to baseband the receiver forms $m = 1, \ldots, M$ channel outputs by performing the multiplications

$$\begin{aligned}\breve{y}_m(t) &= \breve{y}(t) \cdot \sqrt{2}\cos(\omega_c t + \varphi_m) \\ &= \gamma\breve{x}_1(t-\tau)\big(\cos(2\omega_c t - \psi + \varphi_m) + \cos(\psi + \varphi_m)\big) \\ &\quad - \gamma\breve{x}_2(t-\tau)\big(\sin(2\omega_c t - \psi + \varphi_m) - \sin(\psi + \varphi_m)\big) + \breve{\eta}(t)\sqrt{2}\cos(\omega_c t + \varphi_m)\end{aligned} \tag{6.88}$$

with constant demodulation offsets φ_m. Behind a low-pass filter $h(t; B_r)$ of bandwidth B_r, the m-th output channel is

$$\begin{aligned}y_m(t) &= \gamma x_1(t-\tau)\big(\cos(\psi)\cos(\varphi_m) - \sin(\psi)\sin(\varphi_m)\big) \\ &\quad + \gamma x_2(t-\tau)\big(\sin(\psi)\cos(\varphi_m) + \cos(\psi)\sin(\varphi_m)\big) \\ &\quad + \cos(\varphi_m)\eta_1(t) + \sin(\varphi_m)\eta_2(t),\end{aligned} \tag{6.89}$$

where

$$\eta_1(t) = \sqrt{2}\cos(\omega_c t)\big(h(t;B_r) * \breve{\eta}(t)\big), \tag{6.90}$$

$$\eta_2(t) = -\sqrt{2}\sin(\omega_c t)\big(h(t;B_r) * \breve{\eta}(t)\big) \tag{6.91}$$

are independent wide-sense stationary Gaussian random processes with unit power spectral density. The described demodulation operation is depicted in Fig. 6.12. Note that we use the notation $x(t) = h(t;B_r) * \breve{x}(t)$, where $*$ is the convolution operator. Defining the demodulation offset vector

$$\boldsymbol{\varphi} = \begin{bmatrix}\varphi_1 & \varphi_2 & \dots & \varphi_M\end{bmatrix}^{\mathrm{T}}, \tag{6.92}$$

the output signals of the M demodulation channels can be written as

$$\boldsymbol{y}(t) = \boldsymbol{A}(\boldsymbol{\varphi})\big(\gamma\boldsymbol{\Phi}(\psi)\boldsymbol{x}(t-\tau) + \boldsymbol{\eta}(t)\big) \tag{6.93}$$

with the analog signals

$$\boldsymbol{y}(t) = \begin{bmatrix}y_1(t) & y_2(t) & \dots & y_M(t)\end{bmatrix}^{\mathrm{T}}, \tag{6.94}$$

$$\boldsymbol{x}(t-\tau) = \begin{bmatrix}x_1(t-\tau) & x_2(t-\tau)\end{bmatrix}^{\mathrm{T}}, \tag{6.95}$$

$$\boldsymbol{\eta}(t) = \begin{bmatrix}\eta_1(t) & \eta_2(t)\end{bmatrix}^{\mathrm{T}} \tag{6.96}$$

and the matrices

$$\boldsymbol{A}(\boldsymbol{\varphi}) = \begin{bmatrix}\cos(\varphi_1) & \sin(\varphi_1)\\ \cos(\varphi_2) & \sin(\varphi_2)\\ \vdots & \vdots\\ \cos(\varphi_M) & \sin(\varphi_M)\end{bmatrix}, \tag{6.97}$$

$$\boldsymbol{\Phi}(\psi) = \begin{bmatrix}\cos(\psi) & \sin(\psi)\\ -\sin(\psi) & \cos(\psi)\end{bmatrix}. \tag{6.98}$$

Sampling each of the M output channels at a rate of $f_s = \frac{1}{T_s} = 2B_r$ for the duration of $T = NT_s$ and defining the parameter vector $\boldsymbol{\theta} = \begin{bmatrix}\psi & \tau\end{bmatrix}^{\mathrm{T}}$, the digital receive signal is comprised of N temporally white snapshots $\boldsymbol{y}_n \in \mathbb{R}^M$ with

$$\boldsymbol{y}_n = \gamma\boldsymbol{A}(\boldsymbol{\varphi})\boldsymbol{\Phi}(\psi)\boldsymbol{x}_n(\tau) + \boldsymbol{A}(\boldsymbol{\varphi})\boldsymbol{\eta}'_n = \gamma\boldsymbol{s}_n(\boldsymbol{\theta}) + \boldsymbol{\eta}_n. \tag{6.99}$$

The individual digital samples are given by

$$\boldsymbol{y}_n = \begin{bmatrix}y_1\big((n-1)T_s\big) & y_2\big((n-1)T_s\big) & \dots & y_M\big((n-1)T_s\big)\end{bmatrix}^{\mathrm{T}}, \tag{6.100}$$

$$\boldsymbol{x}_n(\tau) = \begin{bmatrix}x_1\big((n-1)T_s-\tau\big) & x_2\big((n-1)T_s-\tau\big)\end{bmatrix}^{\mathrm{T}}, \tag{6.101}$$

$$\boldsymbol{\eta'}_n = \begin{bmatrix}\eta_1\big((n-1)T_s\big) & \eta_2\big((n-1)T_s\big)\end{bmatrix}^{\mathrm{T}}. \tag{6.102}$$

The sampled noise $\boldsymbol{\eta}'_n$ is a zero-mean Gaussian variable with $\mathrm{E}\left[\boldsymbol{\eta'}_n\boldsymbol{\eta'}_n^{\mathrm{T}}\right] = \boldsymbol{I}_2$ while the snapshot noise covariance is

$$\boldsymbol{R}_{\boldsymbol{\eta}} = \mathrm{E}\left[\boldsymbol{\eta}_n\boldsymbol{\eta}_n^{\mathrm{T}}\right] = \boldsymbol{A}(\boldsymbol{\varphi})\boldsymbol{A}^{\mathrm{T}}(\boldsymbol{\varphi}). \tag{6.103}$$

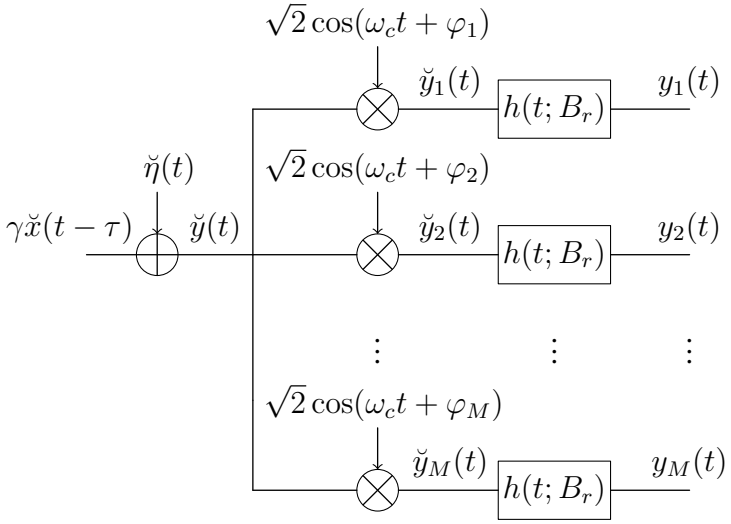

Fig. 6.12. Analog Radio Front-End with Overdemodulation ($M > 2$)

In the following, we assume that the ADC for each of the M output channels is a symmetric hard-limiter, such that the final digital receive data $\boldsymbol{z}_n \in \{-1, 1\}^M$ is given by

$$\boldsymbol{z}_n = \operatorname{sign}\left(\boldsymbol{y}_n\right). \tag{6.104}$$

In order to discuss the benefits of using $M > 2$ demodulation outputs, it is assumed that the receiver infers the deterministic but unknown channel parameters $\boldsymbol{\theta}$ by using the maximum-likelihood estimator (MLE)

$$\hat{\boldsymbol{\theta}}(\boldsymbol{Z}) = \arg\max_{\boldsymbol{\theta}\in\boldsymbol{\Theta}} \ln p(\boldsymbol{Z}; \boldsymbol{\theta}) = \arg\max_{\boldsymbol{\theta}\in\boldsymbol{\Theta}} \sum_{n=1}^{N} \ln p(\boldsymbol{z}_n; \boldsymbol{\theta}), \tag{6.105}$$

where the receive signal with N snapshots has the form

$$\boldsymbol{Z} = \begin{bmatrix} \boldsymbol{z}_1 & \boldsymbol{z}_2 & \dots & \boldsymbol{z}_N \end{bmatrix}. \tag{6.106}$$

The performance analysis can be conducted along the lines (6.36) - (6.38), where the required derivatives are given by

$$\begin{aligned} \frac{\partial \boldsymbol{s}_n(\boldsymbol{\theta})}{\partial \boldsymbol{\theta}} &= \begin{bmatrix} \frac{\partial \boldsymbol{s}_n(\boldsymbol{\theta})}{\partial \psi} & \frac{\partial \boldsymbol{s}_n(\boldsymbol{\theta})}{\partial \tau} \end{bmatrix} \\ &= \begin{bmatrix} \boldsymbol{A}(\boldsymbol{\varphi}) \frac{\partial \boldsymbol{\Phi}(\psi)}{\partial \psi} \boldsymbol{x}_n(\tau) & \boldsymbol{A}(\boldsymbol{\varphi}) \boldsymbol{\Phi}(\psi) \frac{\partial \boldsymbol{x}_n(\tau)}{\partial \tau} \end{bmatrix}, \end{aligned} \tag{6.107}$$

with

$$\frac{\partial \boldsymbol{\Phi}(\psi)}{\partial \psi} = \begin{bmatrix} -\sin(\psi) & \cos(\psi) \\ -\cos(\psi) & -\sin(\psi) \end{bmatrix}, \tag{6.108}$$

$$\frac{\partial \boldsymbol{x}_n(\tau)}{\partial \tau} = -\left[\frac{\mathrm{d}x_1(t)}{\mathrm{d}t} \quad \frac{\mathrm{d}x_2(t)}{\mathrm{d}t} \right]^{\mathrm{T}} \Big|_{t=((n-1)T_s-\tau)}. \tag{6.109}$$

For visualization, we use a GNSS example where the transmitter sends pilot signals

$$x_{1/2}(t) = \sum_{c=-\infty}^{\infty} [\boldsymbol{c}_{1/2}]_{(1+\operatorname{mod}(c,N_c))} g(t - cT_c). \tag{6.110}$$

The signals $\boldsymbol{c}_{1/2} \in \{-1, 1\}^{N_c}$ are binary vectors with $N_c = 1023$ symbols, each of duration $T_c = 977.52$ ns, $g(t)$ is a rectangular transmit pulse and $\mathrm{mod}\,(\cdot)$ is the modulo operator. The receiver bandlimits the signal to $B_r = 1.023$ MHz and samples at a rate of $f_s = 2B_r$ in order to obtain temporally white snapshots. After one signal period $T_o = 1$ ms, the receiver has available $MN = M \cdot 2046$ samples for the estimation task. The unknown channel parameters are assumed to be $\boldsymbol{\theta} = \left[\frac{\pi}{8} \quad 0\right]^{\mathrm{T}}$. The demodulation offsets are equally spaced $\varphi_m = \frac{\pi}{M}(m-1)$ and the performance is normalized with respect to an ideal system with infinite ADC resolution and $M = 2$

$$\chi_{\psi/\tau}(\boldsymbol{\theta}) = \frac{[\boldsymbol{F}_{\boldsymbol{y}}^{-1}(\boldsymbol{\theta})]_{11/22}}{[\tilde{\boldsymbol{F}}_{\boldsymbol{z}}^{-1}(\boldsymbol{\theta})]_{11/22}}, \tag{6.111}$$

where the FIM of the reference system is

$$\boldsymbol{F}_{\boldsymbol{y}}(\boldsymbol{\theta}) = \gamma^2 \sum_{n=1}^{N} \left(\frac{\partial \boldsymbol{s}_n(\boldsymbol{\theta})}{\partial \boldsymbol{\theta}}\right)^{\mathrm{T}} \left(\frac{\partial \boldsymbol{s}_n(\boldsymbol{\theta})}{\partial \boldsymbol{\theta}}\right). \tag{6.112}$$

Note that for $M = 2$ the noise in both channels is independent. Under this condition it holds that the approximated FIM with hard-limiting is exact, i.e., $\tilde{\boldsymbol{F}}_{\boldsymbol{z}}(\boldsymbol{\theta}) = \boldsymbol{F}_{\boldsymbol{z}}(\boldsymbol{\theta})$. Therefore, $\chi_{\psi/\tau}(\boldsymbol{\theta})\big|_{M=2}$ characterizes the 1-bit performance loss with classical I/Q demodulation precisely. For the case $M > 2$ the ratio $\chi_{\psi/\tau}(\boldsymbol{\theta})$ provides a pessimistic approximation.

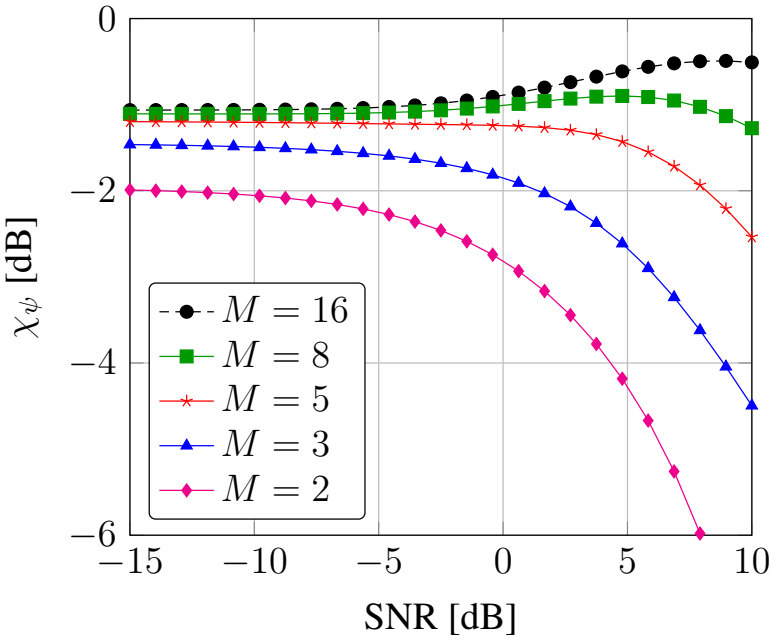

Fig. 6.13. Performance Loss χ_ψ vs. SNR

Fig. 6.13 and 6.14 show the estimation performance $\chi_\psi(\boldsymbol{\theta})$ and $\chi_\tau(\boldsymbol{\theta})$ for different choices of M versus the SNR. For both parameters $M = 16$ allows to diminish the quantization-loss at SNR $= -15.0$ dB from $\chi_{\psi/\tau}(\boldsymbol{\theta}) = -1.99$ dB to $\chi_{\psi/\tau}(\boldsymbol{\theta}) = -1.07$ dB. For high SNR (e.g. SNR $= +10.0$ dB, $M = 16$), the gain is much more pronounced. The loss for phase estimation can be reduced from $\chi_\psi(\boldsymbol{\theta}) = -7.92$ dB to $\chi_\psi(\boldsymbol{\theta}) = -0.51$ dB. For the delay parameter τ, the 1-bit loss changes from $\chi_\tau(\boldsymbol{\theta}) = -6.45$ dB to $\chi_\tau(\boldsymbol{\theta}) = -3.18$ dB.

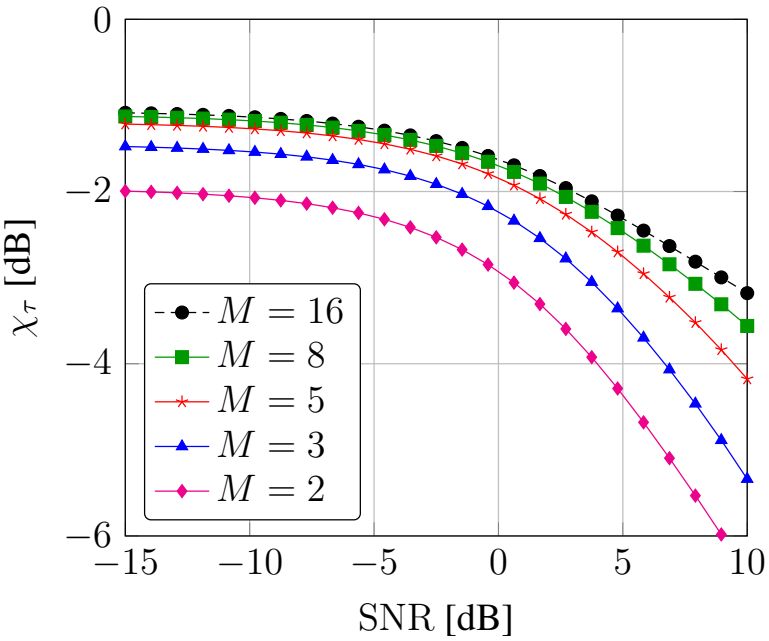

Fig. 6.14. Performance Loss χ_τ vs. SNR

Summarizing this section, a receiver which uses $M > 2$ demodulation channels to map the analog carrier signal to baseband has been analyzed. While with high ADC resolution this approach leads to redundant data, here it was shown by an estimation theoretic investigation, that for receivers which are restricted to low A/D resolution significant performance improvements can be achieved if more than two demodulation channels are used. During system design this opens the possibility to trade-off the A/D resolution (exponential complexity) against the number of demodulation channels (linear complexity).

7. Covariance-Based Parameter Estimation with 1-bit ADC

As discussed in Section 4.6.1, the open problem of a compact expression for the orthant probability makes formulation of the exact likelihood function of a multivariate Gaussian signal model after hard-limiting challenging and therefore hinders optimum 1-bit signal processing. This is in particular the case when covariance-based estimation is considered where the signal parameter of interest modulates the covariance matrix structure of the multivariate Gaussian input distribution to the 1-bit quantizer. Note that in Chapter 6 we have focused on the problem of estimating the location parameter of a hard-limited multivariate Gaussian variable with fixed covariance matrix (4.108). Here we center the discussion around the estimation of a parameter changing the covariance matrix structure of a zero-mean multivariate Gaussian variable (4.116) from 1-bit quantized observations.

Such a signal processing problem arises in wireless applications where the direction-of-arrival (DOA) parameter of a random transmit signal impinging on a receive array with multiple antennas is to be determined. Due to the problem with the representation of the exact 1-bit likelihood under noise correlation, formulation of efficient processing methods for DOA estimation from coarsely quantized data and an analytical performance assessment have, despite their high practical relevance, only found very limited attention in the literature. The main work [39] concerned with efficient 1-bit DOA estimation has to restrict the analytical discussion to $A = 2$ sensors due to the problem outlined in (4.123) and to resort to empirical methods of high computational complexity for cases where $A > 2$.

Here we apply the method of replacing the original system model by an equivalent distribution within the exponential family (exponential replacement) to the blind DOA estimation problem. That way we circumvent calculation of the exact likelihood, obtain a conservative analytic approximation of the system model and can calculate the Fisher information measure for 1-bit DOA estimation under setups with an arbitrary number of sensors. This enables us to formulate a conservative approximation to the Cramér-Rao lower bound (CRLB) and to derive an asymptotically achieving conservative maximum-likelihood estimator (CMLE). The 1-bit DOA performance analysis based on the exponential replacement points out that a low-complexity radio front-end design with 1-bit ADC is in particular suitable for DOA estimation with a large number of array elements operating in the medium SNR regime.

7.1 System Model

For the application of blind DOA parameter estimation with 1-bit ADC, we assume a uniform linear array (ULA) with A sensors, where the spacing between the antennas is equal to half the

wavelength. With a signal source

$$\boldsymbol{x} = \begin{bmatrix} x_I & x_Q \end{bmatrix}^{\mathrm{T}} \in \mathbb{R}^2, \tag{7.1}$$

consisting of independent zero-mean Gaussian in-phase and quadrature components with

$$\mathrm{E}_{\boldsymbol{x}} \left[\boldsymbol{x}\boldsymbol{x}^{\mathrm{T}} \right] = \boldsymbol{I}_2 \tag{7.2}$$

and under a narrowband assumption, the unquantized receive signal of size $M = 2A$

$$\boldsymbol{y} = \begin{bmatrix} \boldsymbol{y}_I^{\mathrm{T}} & \boldsymbol{y}_Q^{\mathrm{T}} \end{bmatrix}^{\mathrm{T}} \in \mathbb{R}^M, \tag{7.3}$$

can be written in a real-valued notation

$$\boldsymbol{y} = \gamma \boldsymbol{A}(\zeta)\boldsymbol{x} + \boldsymbol{\eta}, \tag{7.4}$$

where ζ is the direction under which the transmit signal $\boldsymbol{x}$ impinges on the receive array. Note, that $\boldsymbol{\eta} \in \mathbb{R}^M$ is independent zero-mean AWGN with

$$\mathrm{E}_{\boldsymbol{\eta}} \left[\boldsymbol{\eta}\boldsymbol{\eta}^{\mathrm{T}} \right] = \boldsymbol{I}_M. \tag{7.5}$$

The full array steering matrix

$$\boldsymbol{A}(\zeta) = \begin{bmatrix} \boldsymbol{A}_I^{\mathrm{T}}(\zeta) & \boldsymbol{A}_Q^{\mathrm{T}}(\zeta) \end{bmatrix}^{\mathrm{T}} \in \mathbb{R}^{M \times 2}, \tag{7.6}$$

is modulated by the DOA parameter $\zeta \in \mathbb{R}$ and consists of an in-phase steering matrix and a quadrature steering matrix as given in (6.16)-(6.18). Therefore, with $\theta = \zeta$ the parametric covariance of the unquantized receive signal is

$$\begin{aligned} \mathrm{E}_{\boldsymbol{y};\theta} \left[\boldsymbol{y}\boldsymbol{y}^{\mathrm{T}} \right] &= \boldsymbol{R}_{\boldsymbol{y}}(\theta) \\ &= \gamma^2 \boldsymbol{A}(\theta)\boldsymbol{A}^{\mathrm{T}}(\theta) + \boldsymbol{I}_M \end{aligned} \tag{7.7}$$

and the receive signal of a low-complexity receiver with 1-bit ADC can be modeled

$$\boldsymbol{z} = \operatorname{sign}(\boldsymbol{y}). \tag{7.8}$$

7.2 Performance Analysis for 1-bit Covariance-Based Estimation

In order to apply the pessimistic approximation of the Fisher information (5.230) for DOA estimation with 1-bit hard-limiting, we use the auxiliary statistics

$$\boldsymbol{\phi}(\boldsymbol{z}) = \operatorname{vech}\left(\boldsymbol{z}\boldsymbol{z}^{\mathrm{T}} \right), \tag{7.9}$$

where $\operatorname{vech}(\boldsymbol{B})$ denotes the half-vectorization of the symmetric matrix $\boldsymbol{B}$, i.e., the vectorization of the lower triangular part of $\boldsymbol{B}$. The required mean (5.205) is given by

$$\begin{aligned} \boldsymbol{\mu}_{\boldsymbol{\phi}}(\theta) &= \mathrm{E}_{\boldsymbol{z};\theta} \left[\boldsymbol{\phi}(\boldsymbol{z}) \right] \\ &= \mathrm{E}_{\boldsymbol{z};\theta} \left[\operatorname{vech}\left(\boldsymbol{z}\boldsymbol{z}^{\mathrm{T}} \right) \right] \\ &= \operatorname{vech}\left(\mathrm{E}_{\boldsymbol{z};\theta} \left[\boldsymbol{z}\boldsymbol{z}^{\mathrm{T}} \right] \right) \\ &= \operatorname{vech}\left(\boldsymbol{R}_{\boldsymbol{z}}(\theta) \right), \end{aligned} \tag{7.10}$$

where by the arcsine law [81, pp. 284] the quantized covariance matrix is

$$\boldsymbol{R}_{\boldsymbol{z}}(\theta) = \frac{2}{\pi} \arcsin\left(\frac{1}{\gamma^2+1}\boldsymbol{R}_{\boldsymbol{y}}(\theta)\right). \tag{7.11}$$

For the derivative of the mean (7.10) we find

$$\frac{\partial \boldsymbol{\mu}_{\boldsymbol{\phi}}(\theta)}{\partial \theta} = \operatorname{vech}\left(\frac{\partial \boldsymbol{R}_{\boldsymbol{z}}(\theta)}{\partial \theta}\right), \tag{7.12}$$

where the derivative of the quantized covariance matrix (7.11) is found element-wise

$$\left[\frac{\partial \boldsymbol{R}_{\boldsymbol{z}}(\theta)}{\partial \theta}\right]_{ij} = \frac{2\left[\frac{\partial \boldsymbol{R}_{\boldsymbol{y}}(\theta)}{\partial \theta}\right]_{ij}}{\pi(\gamma^2+1)\sqrt{1-\frac{1}{(\gamma^2+1)^2}\left[\boldsymbol{R}_{\boldsymbol{y}}(\theta)\right]_{ij}^2}} \tag{7.13}$$

with the derivative of the unquantized receive covariance matrix (7.7) being

$$\frac{\partial \boldsymbol{R}_{\boldsymbol{y}}(\theta)}{\partial \theta} = \gamma^2\left(\frac{\partial \boldsymbol{A}(\theta)}{\partial \theta}\boldsymbol{A}^{\mathrm{T}}(\theta) + \boldsymbol{A}(\theta)\frac{\partial \boldsymbol{A}^{\mathrm{T}}(\theta)}{\partial \theta}\right). \tag{7.14}$$

The derivative of the steering matrix is

$$\frac{\partial \boldsymbol{A}(\theta)}{\partial \theta} = \left[\frac{\partial \boldsymbol{A}_I^{\mathrm{T}}(\theta)}{\partial \theta} \quad \frac{\partial \boldsymbol{A}_Q^{\mathrm{T}}(\theta)}{\partial \theta}\right]^{\mathrm{T}} \tag{7.15}$$

with the in-phase component and the quadrature component given by (6.49)-(6.51). For the second moment of the auxiliary statistics (5.206), the expectation

$$\mathrm{E}_{\boldsymbol{z};\theta}\left[\boldsymbol{\phi}(\boldsymbol{z})\boldsymbol{\phi}^{\mathrm{T}}(\boldsymbol{z})\right] = \mathrm{E}_{\boldsymbol{z};\theta}\left[\operatorname{vech}\left(\boldsymbol{z}\boldsymbol{z}^{\mathrm{T}}\right)\operatorname{vech}\left(\boldsymbol{z}\boldsymbol{z}^{\mathrm{T}}\right)^{\mathrm{T}}\right] \tag{7.16}$$

is required. This implies to evaluate all the expected values

$$\mathrm{E}_{\boldsymbol{z};\theta}\left[z_i z_j z_k z_l\right], \qquad i,j,k,l \in \{1,\ldots,M\}. \tag{7.17}$$

For the cases $i=j=k=l$ or $i=j\neq k=l$, we obtain

$$\begin{aligned}\mathrm{E}_{\boldsymbol{z};\theta}\left[z_i z_j z_k z_l\right] &= \mathrm{E}_{\boldsymbol{z};\theta}\left[z_i^4\right] \\ &= \mathrm{E}_{\boldsymbol{z};\theta}\left[z_i^2 z_k^2\right] \\ &= 1.\end{aligned} \tag{7.18}$$

If $i=j=k\neq l$, the arcsine law [81] [82] results in

$$\begin{aligned}\mathrm{E}_{\boldsymbol{z};\theta}\left[z_i z_j z_k z_l\right] &= \mathrm{E}_{\boldsymbol{z};\theta}\left[z_i^3 z_l\right] \\ &= \mathrm{E}_{\boldsymbol{z};\theta}\left[z_i z_l\right] \\ &= \frac{2}{\pi}\arcsin\left(\frac{1}{(\gamma^2+1)^2}\left[\boldsymbol{R}_{\boldsymbol{y}}(\theta)\right]_{il}\right),\end{aligned} \tag{7.19}$$

like in the case $i = j \neq k \neq l$, where

$$\begin{aligned} \mathrm{E}_{\boldsymbol{z};\theta}\left[z_i z_j z_k z_l\right] &= \mathrm{E}_{\boldsymbol{z};\theta}\left[z_i^2 z_k z_l\right] \\ &= \mathrm{E}_{\boldsymbol{z};\theta}\left[z_k z_l\right] \\ &= \frac{2}{\pi}\arcsin\left(\frac{1}{(\gamma^2+1)^2}\left[\boldsymbol{R}_{\boldsymbol{y}}(\theta)\right]_{kl}\right). \end{aligned} \tag{7.20}$$

The case $i \neq j \neq k \neq l$ requires special care, as

$$\mathrm{E}_{\boldsymbol{z};\theta}\left[z_i z_j z_k z_l\right] = \Pr\left\{z_i z_j z_k z_l = 1\right\} - \Pr\left\{z_i z_j z_k z_l = -1\right\} \tag{7.21}$$

involves the evaluation of the $2^4 = 16$ orthant probabilities

$$\Pr\left\{\pm z_i > 0, \pm z_j > 0, \pm z_k > 0, \pm z_l > 0\right\} \tag{7.22}$$

of a quadrivariate zero-mean Gaussian variable with covariance matrix

$$\boldsymbol{R}_{y_i y_j y_k y_l}(\theta) = \begin{bmatrix} 1 & r_{ij}(\theta) & r_{ik}(\theta) & r_{il}(\theta) \\ r_{ij}(\theta) & 1 & r_{jk}(\theta) & r_{jl}(\theta) \\ r_{ik}(\theta) & r_{jk}(\theta) & 1 & r_{kl}(\theta) \\ r_{il}(\theta) & r_{jl}(\theta) & r_{kl}(\theta) & 1 \end{bmatrix}. \tag{7.23}$$

A compact solution for this problem, requiring calculation of four one-dimensional integrals, is given in [57].

7.2.1 Quantization Loss for 1-bit DOA Estimation

Using the information bound (5.230) and the results (7.12) (7.16), we can evaluate the quantization loss for 1-bit DOA parameter estimation with $A > 2$ sensors in a pessimistic manner by forming the information ratio

$$\begin{aligned} \chi(\theta) &= \frac{\tilde{F}_{\boldsymbol{z}}(\theta)}{F_{\boldsymbol{y}}(\theta)} \\ &= \frac{\left(\frac{\partial \boldsymbol{\mu}_{\boldsymbol{\phi}}(\theta)}{\partial \theta}\right)^{\mathrm{T}} \boldsymbol{R}_{\boldsymbol{\phi}}^{-1}(\theta) \frac{\partial \boldsymbol{\mu}_{\boldsymbol{\phi}}(\theta)}{\partial \theta}}{F_{\boldsymbol{y}}(\theta)}. \end{aligned} \tag{7.24}$$

In Fig. 7.1 we plot the performance loss (7.24) versus SNR $= \gamma^2$ for two different DOA setups ($\theta = 10°$ and $\theta = 70°$). It can be observed that the quantization loss with $A = 2$ is $\chi(\theta) = \left(\frac{2}{\pi}\right)^2$ (-3.92 dB) in the low SNR regime. Further, over all SNR values the loss $\chi(\theta)$ becomes smaller for arrays with a larger number of antennas $A = 4$ or $A = 8$. Especially, in the SNR range of -10 to 0 dB, which is a regime of high practical relevance for energy-efficient broadband mobile communication systems, the array size A plays a beneficial role and the gap between the 1-bit receiver and the ideal receive system becomes significantly smaller for the setting $A = 8$. However, for situations where SNR > 5 dB the quantization loss becomes pronounced for all receive scenarios. In Fig. 7.2 the performance loss $\chi(\theta)$ is depicted as a function of the DOA parameter θ for three different array sizes ($A = 2, 4, 8$). It can be seen that while the quantization loss $\chi(\theta)$ decreases with the number of sensors A, it also becomes less dependent on the DOA parameter θ for large arrays. In Fig. 7.3 the quantization loss $\chi(\theta)$ is shown for a large number

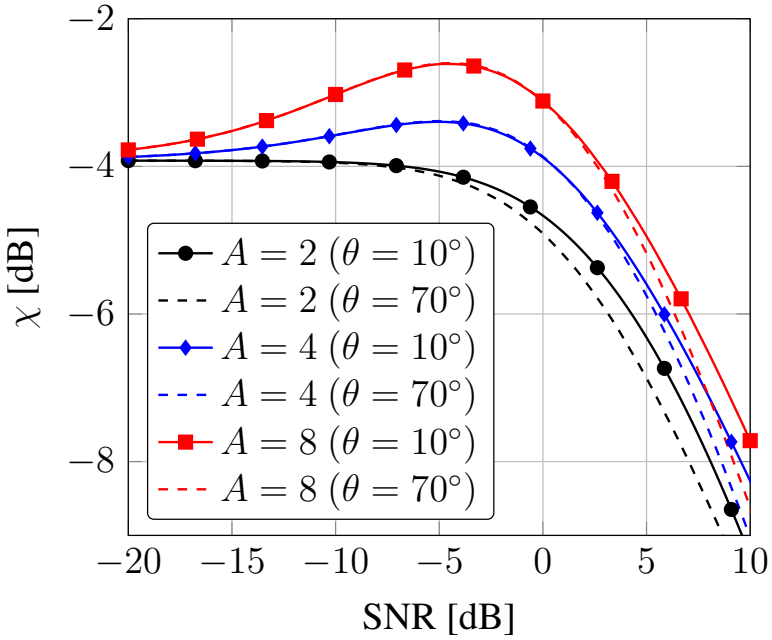

Fig. 7.1. Performance Loss χ vs. SNR (1-bit DOA)

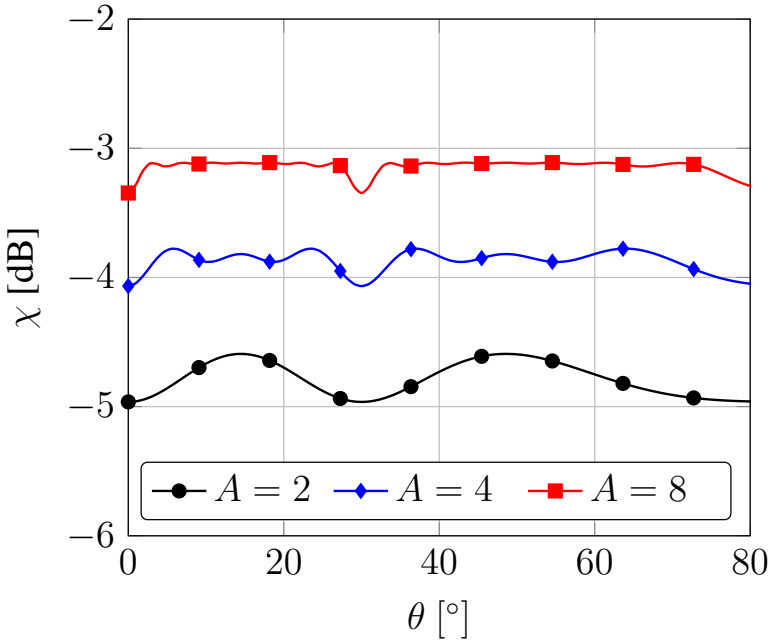

Fig. 7.2. Performance Loss χ vs. DOA (1-bit DOA, SNR= 0 dB)

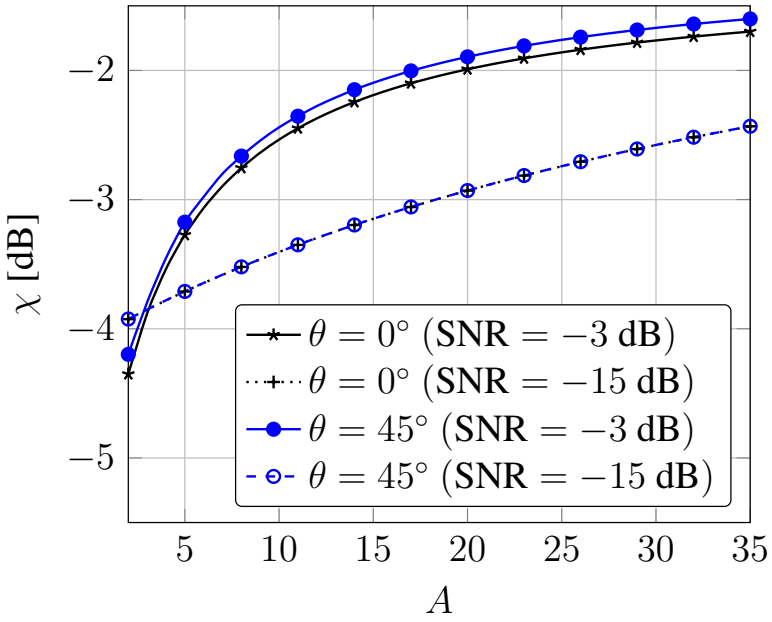

Fig. 7.3. Performance Loss χ vs. Array Elements (1-bit DOA)

of antennas A. For a low SNR receive setup (SNR $= -15$ dB), the gap between the quantized receiver and the unquantized receiver vanishes approximately linear with the array size A, while for a medium SNR scenario (SNR $= -3$ dB), the relative performance of the 1-bit receive system strongly improves by increasing the amount of receive sensors A. Finally, in Fig. 7.4 we compare the performance of the 1-bit receive system for different numbers of antennas A by normalizing to an ideal reference system with $A = 2$. Therefore we depict the quantization loss

$$\begin{aligned}\chi_2(\theta) &= \frac{\tilde{F}_{\boldsymbol{z}}(\theta)}{F_{\boldsymbol{y}}(\theta)|_{A=2}} \\ &= \frac{\left(\frac{\partial \boldsymbol{\mu}_{\boldsymbol{\phi}}(\theta)}{\partial \theta}\right)^{\mathrm{T}} \boldsymbol{R}_{\boldsymbol{\phi}}^{-1}(\theta) \frac{\partial \boldsymbol{\mu}_{\boldsymbol{\phi}}(\theta)}{\partial \theta}}{F_{\boldsymbol{y}}(\theta)|_{A=2}}\end{aligned} \tag{7.25}$$

for three different SNR levels (low, medium and high). It becomes clear that by doubling the numbers of sensors to $A = 4$, the 1-bit system outperforms the ideal system with $A = 2$ in all three considered situations. With $A = 6$ the 1-bit system is significantly better than the ideal receive system with $A = 2$. This shows that for DOA estimation the number of sensors has a much stronger impact onto the performance of the receive system than the resolution of the ADC.

7.2.2 1-bit DOA Estimation with the CMLE Algorithm

In order to demonstrate that the framework of exponential replacement also provides a guideline how to achieve the guaranteed performance

$$\begin{aligned}\mathrm{E}_{\boldsymbol{Z};\theta}\left[\left(\theta - \hat{\theta}(\boldsymbol{Z})\right)^2\right] &\approx \frac{1}{N\left(\frac{\partial \boldsymbol{\mu}_{\boldsymbol{\phi}}(\theta)}{\partial \theta}\right)^{\mathrm{T}} \boldsymbol{R}_{\boldsymbol{\phi}}^{-1}(\theta) \frac{\partial \boldsymbol{\mu}_{\boldsymbol{\phi}}(\theta)}{\partial \theta}} \\ &= \mathrm{PCRLB}(\theta),\end{aligned} \tag{7.26}$$

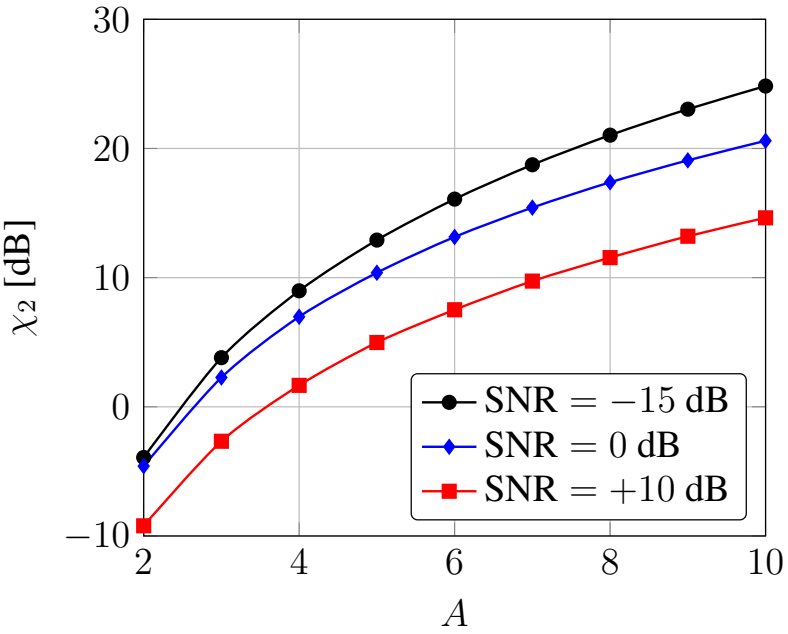

Fig. 7.4. Performance Loss χ_2 vs. Array Elements (1-bit DOA)

in Fig. 7.5 we plot the accuracy (RMSE) of the conservative maximum-likelihood estimation (CMLE) algorithm (5.258) for an array size of $A = 4$, a DOA parameter $\theta = 5°$ and $N = 1000$ samples averaged over 10000 noise realizations. It can be observed that in the considered scenario

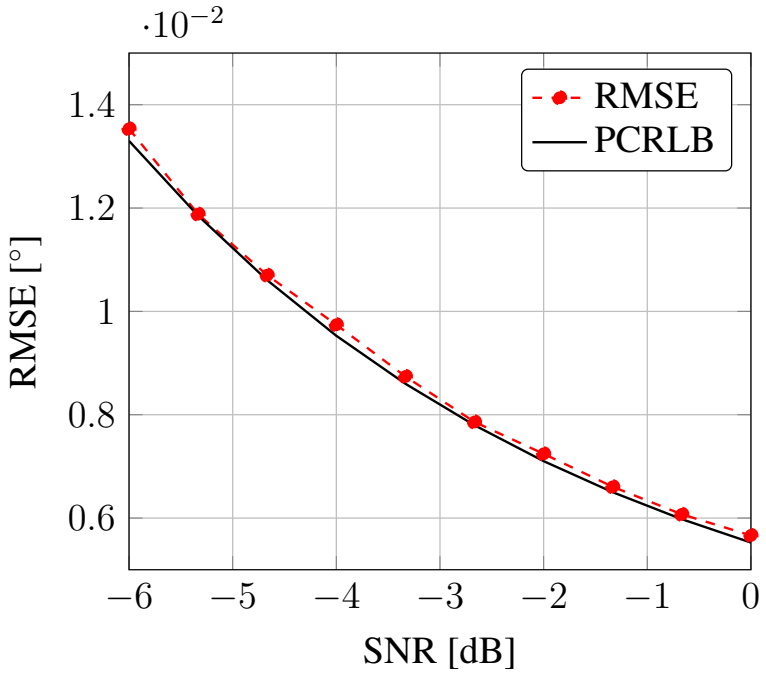

Fig. 7.5. CMLE Performance - 1-bit DOA Estimation ($A = 4$, $\theta = 5°$)

the CMLE performs close to the pessimistic approximation of the CRLB (PCRLB).

Summarizing this chapter, we have discussed the method of exponential replacement in the context of 1-bit DOA estimation with a single signal source and a receive array of A sensors.

The associated pessimistic approximation for the Fisher information measure allows to analyze the achievable DOA estimation accuracy for arrays with $A > 2$ in a conservative manner. Additionally, the exponential replacement provides a guideline how to achieve the accuracy guaranteed by the resulting pessimistic approximation of the CRLB. The performance analysis shows that in the medium SNR regime DOA estimation with 1-bit ADC can be performed at high accuracy if the number of array elements A is large. Further, with respect to the achievable estimation accuracy it is beneficial to trade-off ADC resolution versus the amount of array sensors. These results strongly support the current discussion on future wireless systems which use a large number of low-complexity sensors, i.e., 1-bit massive MIMO wireless systems [83] [84] [85].

8. Concluding Remarks

We have considered the problem of signal parameter estimation with 1-bit ADC. While using an A/D conversion with coarse amplitude resolution allows to obtain an ultra-fast, low-cost and energy-efficient wireless receive system, the nonlinear characteristic of the sampling device causes an information loss with respect to the problem of estimating signal parameters from the noisy receive signal.

Within this thesis we have tried to characterize this loss in an accurate way for various setups. After reviewing the classical loss of $2/\pi$ (-1.96 dB) [26] for location parameter estimation with 1-bit quantizer in the low SNR regime, we have demonstrated that incorporating side-information in the form of state-space models allows to reduce the quantization loss to $\sqrt{2/\pi}$ (-0.98 dB). This result is of high practical relevance as various low SNR signal processing tasks like radar or satellite-based positioning exhibit wireless channels with high temporal correlation among their parameters on sample level.

For the case when the quantization offset of the 1-bit ADC is unknown and has to be estimated during runtime, we have analyzed the additional quantization loss which is introduced by joint estimation of the signal parameter and the quantization level. The results show that a symmetric quantizer is favorable for the estimation of a location parameter while the additional loss due to the unknown offset vanishes in the low SNR regime.

Elaborating on the estimation theoretic analysis of the hard-limiting loss for signal models with correlated noise, we have identified a fundamental problem with implications far beyond the topic of quantized signal processing. When the analytical likelihood function of the system model is intractable (like for multivariate Gaussian models with 1-bit quantization) or unknown (like for many physical signal processing systems) it is not possible to apply strong processing rules like the maximum-likelihood estimator or to conduct an analytic performance analysis based on the Fisher information measure. In order to contribute to the understanding of this problem, we have followed the approach of approximating the classical Fisher information measure in a pessimistic way. For the univariate case we have discussed two compact bounds which are based exclusively on the mean, the variance, the skewness and the kurtosis of the system output. Studying the properties of the Fisher information measure for distributions belonging to the exponential family, we have established the method of exponential replacement. By the exponential replacement we embed an arbitrary stochastic model into the convenient framework of the exponential family by finding the closest (in the sense of Fisher information) equivalent model. This results in a generic lower bound for the Fisher information matrix and a mismatched system model which produces consistent results with a guaranteed performance for the problem of signal parameter estimation with intractable or unknown system models.

Using the exponential replacement framework we have conducted a performance analysis for 1-bit signal processing tasks with a modified wireless radio front-end. For the application of satellite-based synchronization, we have shown that 1-bit systems with slightly higher receive bandwidth or a moderately larger number of receive sensors are capable of outperforming ideal systems with infinite A/D resolution in different receive situations. Also the possibility of oversampling the analog receive signal in the temporal domain or performing overdemodulation in the I/Q domain in conjunction with low-complexity 1-bit ADC has been considered. The results show that it is possible to obtain high signal processing accuracy with low-complexity 1-bit ADC through simple adjustments of the analog radio front-end.

Finally, we have discussed the problem of covariance-based estimation under hard-limiting. For the problem of blind 1-bit DOA estimation, the derived Fisher information lower bound allows to analyze the performance of 1-bit receive systems with a large number of receive sensors. Through the Fisher information lower bound it has been possible to demonstrate that for this particular problem the performance gap between a 1-bit system and a ∞-bit system becomes smaller when the number of antennas increases.

In conclusion the results of this thesis show that low-complexity 1-bit A/D conversion is an attractive design option for systems performing wireless measurement tasks. It allows to significantly reduce the power consumption and the production cost of the system components, while an adjusted analog radio front-end design and advanced model-based statistical signal processing in the digital domain allows to ensure high system performance. Note that, given the exceptional relevance of wireless technology for the modern information society, the conceptual implications of this discussion are far-reaching. Today, wireless systems are mainly designed along a linear paradigm, leading to signal processing systems with few high-quality sensors. In contrast, this thesis indicates that the investigation of performance-oriented system architectures with a massive number of low-complexity sensors may need significantly more attention.

Appendix

A1 Covariance Inequality

Consider two multivariate random variables $\boldsymbol{x} \in \mathbb{R}^M, \boldsymbol{y} \in \mathbb{R}^N$ which follow the joint probability distribution $p(\boldsymbol{x}, \boldsymbol{y})$. Given $\boldsymbol{x}$, construct the auxiliary random variable

$$\hat{\boldsymbol{y}}(\boldsymbol{x}) = \mathrm{E}_{\boldsymbol{x},\boldsymbol{y}}\left[\boldsymbol{y}\boldsymbol{x}^{\mathrm{T}}\right] \mathrm{E}_{\boldsymbol{x}}\left[\boldsymbol{x}\boldsymbol{x}^{\mathrm{T}}\right]^{-1} \boldsymbol{x}. \tag{A1}$$

Observing that by construction

$$\mathrm{E}_{\boldsymbol{x},\boldsymbol{y}}\left[(\boldsymbol{y} - \hat{\boldsymbol{y}}(\boldsymbol{x}))(\boldsymbol{y} - \hat{\boldsymbol{y}}(\boldsymbol{x}))^{\mathrm{T}}\right] \succeq \boldsymbol{0}, \tag{A2}$$

shows that

$$\mathrm{E}_{\boldsymbol{y}}\left[\boldsymbol{y}\boldsymbol{y}^{\mathrm{T}}\right] - \mathrm{E}_{\boldsymbol{x},\boldsymbol{y}}\left[\boldsymbol{y}\boldsymbol{x}^{\mathrm{T}}\right] \mathrm{E}_{\boldsymbol{x}}\left[\boldsymbol{x}\boldsymbol{x}^{\mathrm{T}}\right]^{-1} \mathrm{E}_{\boldsymbol{x},\boldsymbol{y}}\left[\boldsymbol{x}\boldsymbol{y}^{\mathrm{T}}\right] \succeq \boldsymbol{0}, \tag{A3}$$

such that it holds that

$$\mathrm{E}_{\boldsymbol{y}}\left[\boldsymbol{y}\boldsymbol{y}^{\mathrm{T}}\right] \succeq \mathrm{E}_{\boldsymbol{x},\boldsymbol{y}}\left[\boldsymbol{y}\boldsymbol{x}^{\mathrm{T}}\right] \mathrm{E}_{\boldsymbol{x}}\left[\boldsymbol{x}\boldsymbol{x}^{\mathrm{T}}\right]^{-1} \mathrm{E}_{\boldsymbol{x},\boldsymbol{y}}\left[\boldsymbol{x}\boldsymbol{y}^{\mathrm{T}}\right]. \tag{A4}$$

A2 Bayesian Covariance Inequality

For a more general form [8] of the covariance inequality (A4), consider that for two functions $\boldsymbol{f}(\boldsymbol{x}, \boldsymbol{y}) \in \mathbb{R}^M, \boldsymbol{g}(\boldsymbol{x}, \boldsymbol{y}) \in \mathbb{R}^N$ and a matrix $\boldsymbol{A} \in \mathbb{R}^{M \times N}$ it holds that by construction

$$\mathrm{E}_{\boldsymbol{x},\boldsymbol{y}}\left[\big(\boldsymbol{f}(\boldsymbol{x}, \boldsymbol{y}) - \boldsymbol{A}\boldsymbol{g}(\boldsymbol{x}, \boldsymbol{y})\big)\big(\boldsymbol{f}(\boldsymbol{x}, \boldsymbol{y}) - \boldsymbol{A}\boldsymbol{g}(\boldsymbol{x}, \boldsymbol{y})\big)^{\mathrm{T}}\right] \succeq \boldsymbol{0}, \tag{A5}$$

such that we obtain the matrix inequality

$$\begin{aligned}\mathrm{E}_{\boldsymbol{x},\boldsymbol{y}}\left[\boldsymbol{f}(\boldsymbol{x}, \boldsymbol{y})\boldsymbol{f}^{\mathrm{T}}(\boldsymbol{x}, \boldsymbol{y})\right] \succeq\ & \mathrm{E}_{\boldsymbol{x},\boldsymbol{y}}\left[\boldsymbol{f}(\boldsymbol{x}, \boldsymbol{y})\boldsymbol{g}^{\mathrm{T}}(\boldsymbol{x}, \boldsymbol{y})\right] \boldsymbol{A}^{\mathrm{T}} + \boldsymbol{A}\, \mathrm{E}_{\boldsymbol{x},\boldsymbol{y}}\left[\boldsymbol{g}(\boldsymbol{x}, \boldsymbol{y})\boldsymbol{f}^{\mathrm{T}}(\boldsymbol{x}, \boldsymbol{y})\right] \\ & - \boldsymbol{A}\, \mathrm{E}_{\boldsymbol{x},\boldsymbol{y}}\left[\boldsymbol{g}(\boldsymbol{x}, \boldsymbol{y})\boldsymbol{g}^{\mathrm{T}}(\boldsymbol{x}, \boldsymbol{y})\right] \boldsymbol{A}^{\mathrm{T}}.\end{aligned} \tag{A6}$$

Substituting in (A6)

$$\boldsymbol{A} = \mathrm{E}_{\boldsymbol{x},\boldsymbol{y}}\left[\boldsymbol{f}(\boldsymbol{x}, \boldsymbol{y})\boldsymbol{g}^{\mathrm{T}}(\boldsymbol{x}, \boldsymbol{y})\right] \mathrm{E}_{\boldsymbol{x},\boldsymbol{y}}\left[\boldsymbol{g}(\boldsymbol{x}, \boldsymbol{y})\boldsymbol{g}^{\mathrm{T}}(\boldsymbol{x}, \boldsymbol{y})\right]^{-1}, \tag{A7}$$

we obtain

$$\begin{aligned}\mathrm{E}_{\boldsymbol{x},\boldsymbol{y}}\left[\boldsymbol{f}(\boldsymbol{x}, \boldsymbol{y})\boldsymbol{f}^{\mathrm{T}}(\boldsymbol{x}, \boldsymbol{y})\right] \succeq\ & \mathrm{E}_{\boldsymbol{x},\boldsymbol{y}}\left[\boldsymbol{f}(\boldsymbol{x}, \boldsymbol{y})\boldsymbol{g}^{\mathrm{T}}(\boldsymbol{x}, \boldsymbol{y})\right] \mathrm{E}_{\boldsymbol{x},\boldsymbol{y}}\left[\boldsymbol{g}(\boldsymbol{x}, \boldsymbol{y})\boldsymbol{g}^{\mathrm{T}}(\boldsymbol{x}, \boldsymbol{y})\right]^{-1} \\ & \cdot \mathrm{E}_{\boldsymbol{x},\boldsymbol{y}}\left[\boldsymbol{g}(\boldsymbol{x}, \boldsymbol{y})\boldsymbol{f}^{\mathrm{T}}(\boldsymbol{x}, \boldsymbol{y})\right].\end{aligned} \tag{A8}$$

Bibliography

[1] R. H. Walden, "Analog-to-digital converter survey and analysis," *IEEE Journal on Selected Areas in Communications*, vol. 17, no. 4, pp. 539–550, Apr. 1999.

[2] S. M. Kay, *Fundamentals of Statistical Signal Processing: Estimation Theory*. Upper Saddler River, NJ: Prentice Hall, 1993.

[3] R. A. Fisher, "On the mathematical foundations of theoretical statistics," *Philosophical Transactions of the Royal Society*, vol. 222, pp. 309–368, Jan. 1922.

[4] R. A. Fisher, "Theory of statistical estimation," *Proceedings of the Cambridge Philosophical Society*, vol. 22, no. 5, pp. 700–725, Jul. 1925.

[5] H. Luke, "The origins of the sampling theorem," *IEEE Communications Magazine*, vol. 37, no. 4, pp. 106–108, Apr. 1999.

[6] J. Sauerbrey, D. Schmitt-Landsiedel, and R. Thewes, "A 0.5-V 1-μW successive approximation ADC," *IEEE Journal of Solid-State Circuits*, vol. 38, no. 7, pp. 1261–1265, Jul. 2003.

[7] R. Schreier and G. C. Temes, *Understanding Delta-Sigma Data Converters*. Wiley-Interscience/IEEE Press, 2004.

[8] H. L. Van Trees and K. L. Bell, *Bayesian Bounds for Parameter Estimation and Nonlinear Filtering/Tracking*. Wiley-Interscience/IEEE Press, 2007.

[9] E. L. Lehmann and G. Casella, *Theory of Point Estimation*. Springer, 2003.

[10] P. J. Bickel and K. A. Doksum, *Mathematical Statistics: Basic Ideas and Selected Topics*. San Francisco, CA: Holden-Day, 1977.

[11] C. R. Rao, "Information and accuracy attainable in the estimation of statistical parameters," *Bulletin of Calcutta Mathematical Society*, vol. 37, no. 3, pp. 81–91, 1945.

[12] H. Cramér, *Mathematical Methods of Statistics*. Princeton, NJ: Princeton Univ. Press, 1946.

[13] P. Tichavsky, C. H. Muravchik, and A. Nehorai, "Posterior Cramer-Rao bounds for discrete-time nonlinear filtering," *IEEE Transactions on Signal Processing*, vol. 46, no. 5, pp. 1386–1396, May 1998.

[14] M. Šimandl, J. Královec, and P. Tichavský, "Filtering, predictive, and smoothing Cramér-Rao bounds for discrete-time nonlinear dynamic systems", *Automatica*, vol. 37, no. 11, pp. 1703–1716, Nov. 2001.

[15] S. O. Rice, "Mathematical analysis of random noise," *Bell System Technical Journal*, vol. 23, no. 3, pp 282–332, Jul. 1944.

[16] M. Kac and A. J. F. Siegert, "On the theory of noise in radio receivers with square law detectors," *Journal of Applied Physics*, vol. 18, no. 4, pp. 383–397, 1947.

[17] J. J. Bussgang, "Crosscorrelation functions of amplitude-distorted Gaussian signals," *Massachusetts Institute of Technology, Research Laboratory of Electronics*, Technical Report, no. 216, pp. 1–14, 1952.

[18] W. B. Davenport, "Signal-to-noise ratios in band-pass limiters," *Journal of Applied Physics*, vol. 24, no. 6, pp. 720–727, 1953.

[19] M. A. Meyer and David Middleton, "On the distributions of signals and noise after rectification and filtering," *Journal of Applied Physics*, vol. 25, no. 8, pp. 1037–1052, 1954.

[20] R. Price, "A useful theorem for nonlinear devices having Gaussian inputs," *IRE Transactions on Information Theory*, vol. 4, no. 2, pp. 69–72, Jun. 1958.

[21] N. Wiener, *Nonlinear Problems in Random Theory*. New York: Wiley, 1958.

[22] M. B. Brilliant, "Theory of the analysis of nonlinear systems," RLE Tech. Report, No. 345. MIT, Cambride, MA, 1958.

[23] V. Volterra, *Theory of Functionals and of Integral and Integro-differential Equations*. New York: Dover, 1959.

[24] R. Baum, "The correlation function of Gaussian noise passed through nonlinear devices," *IEEE Transactions on Information Theory*, vol. 15, no. 4, pp. 448–456, Jul. 1969.

[25] W. R. Bennett, "Spectra of quantized signals", *Bell System Technical Journal*, vol. 27, pp. 446–472, Jul. 1948.

[26] J. H. Van Vleck and D. Middleton, "The spectrum of clipped noise," *Proceedings of the IEEE*, vol. 54, no. 1, pp. 2–19, Jan. 1966.

[27] M. Hinich, "Estimation of spectra after hard clipping of Gaussian processes," *Technometrics*, vol. 9, no. 3, pp. 391–400, Aug. 1967.

[28] H. M. Hall, "Power spectrum of hard-limited Gaussian processes," *Bell System Technical Journal*, vol. 48, no. 9, pp. 3031–3057, Nov. 1969.

[29] R. M. Gray, "Quantization noise spectra," *IEEE Transactions on Information Theory*, vol. 36, no. 6, pp. 1220–1244, Nov. 1990.

[30] R. E. Curry, *Estimation And Control With Quantized Measurements*. M.I.T. Press, 1970.

[31] B. Kedem, "Exact maximum likelihood estimation of the parameter in the AR(1) process after hard limiting," *IEEE Transactions on Information Theory*, vol. 22, no. 4, pp. 491–493, Jul. 1976.

[32] E. A. Aronson, "Hard-limiter output autocorrelation function: Gaussian and sinusoidal input," *IEEE Transactions on Aerospace and Electronic Systems*, vol. 10, no. 5, pp. 609–614, Sept. 1974.

[33] E. Damsleth and A. H. El-Shaarawi, "Estimation of autocorrelation in a binary time series," *Stochastic Hydrology and Hydraulics*, vol. 2, no. 1, pp. 61–72, Mar. 1988.

[34] E. N. Gilbert, "Increased information rate by oversampling," *IEEE Transactions on Information Theory*, vol. 39, no. 6, pp.1973–1976, Nov. 1993.

[35] S. Shamai, "Information rates by oversampling the sign of a bandlimited process," *IEEE Transactions on Information Theory*, vol. 40, no. 4, pp. 1230–1236, Jul. 1994.

[36] B. Widrow, I. Kollar, and M. C. Liu, "Statistical theory of quantization," *IEEE Transactions on Instrumentation and Measurement*, vol. 45, no. 2, pp. 353–361, Apr. 1996.

[37] A. Host-Madsen and P. Handel, "Effects of sampling and quantization on single-tone frequency estimation," *IEEE Transactions on Signal Processing*, vol. 48, no. 3, pp. 650–662, Mar. 2000.

[38] H.C. Papadopoulos, G. W. Wornell, and A. V. Oppenheim, "Sequential signal encoding from noisy measurements using quantizers with dynamic bias control," *IEEE Transactions on Information Theory*, vol. 47, no. 3, pp. 978–1002, Mar. 2001.

[39] O. Bar-Shalom and A. J. Weiss, "DOA estimation using one-bit quantized measurements," *IEEE Transactions on Aerospace and Electronic Systems*, vol. 38, no. 3, pp. 868–884, Jul. 2002.

[40] D. Rousseau, G. V. Anand, and F. Chapeau-Blondeau, "Nonlinear estimation from quantized signals: Quantizer optimization and stochastic resonance," *International Symposium on Physics in Signal and Image Processing*, pp. 89–92, 2003.

[41] S. Geirhofer, L. Tong, and B.M. Sadler, "Moment estimation and dithered quantization," *IEEE Signal Processing Letters*, vol. 13, no. 12, pp. 752–755, Dec. 2006.

[42] J. W. Betz and N. R. Shnidman "Receiver processing losses with bandlimiting and one-bit sampling," in *Proceedings of the 20th International Technical Meeting of the Satellite Division of The Institute of Navigation (ION GNSS 2007)*, Texas, pp. 1244–1256, 2007.

[43] O. Dabeer and E. Masry, "Multivariate signal parameter estimation under dependent noise from 1-bit dithered quantized data," *IEEE Transaction on Information Theory*, vol. 54, no. 4, pp.1637–1654, Apr. 2008.

[44] G.O. Balkan and S. Gezici, "CRLB based optimal noise enhanced parameter estimation using quantized observations," *IEEE Signal Processing Letters*, vol. 17, no. 5, pp. 477–480, May 2010.

[45] G. Zeitler, G. Kramer, and A. C. Singer, "Bayesian parameter estimation using single-bit dithered quantization," *IEEE Transactions on Signal Processing*, vol. 60, no. 6, pp. 2713–2726, Jun. 2012.

[46] A. Mezghani, F. Antreich, and J. A. Nossek, "Multiple parameter estimation with quantized channel output", *International ITG Workshop on Smart Antennas (WSA)*, pp. 143 –150, 2010.

[47] J. T. Curran, D. Borio, G. Lachapelle, and C. C. Murphy, "Reducing front-end bandwidth may improve digital GNSS receiver performance," *IEEE Transactions on Signal Processing*, vol. 58, no. 4, pp. 2399–2404, Apr. 2010.

[48] O. Dabeer, J. Singh, and U. Madhow, "On the limits of communication performance with one-bit analog-to-digital conversion," *IEEE 7th Workshop on Signal Processing Advances in Wireless Communications, SPAWC '06*, pp.1–5, 2006.

[49] J. Mo and R. W. Heath, "Capacity analysis of one-bit quantized MIMO systems with transmitter channel state information," *Transactions on Signal Processing*, vol. 63, no. 20, pp. 5498-5512, Oct. 2015.

[50] T. Koch and A. Lapidoth, "Increased capacity per unit-cost by oversampling," *IEEE 26th Convention of Electrical and Electronics Engineers in Israel (IEEEI)*, 2010

[51] S. Krone and G. Fettweis, "Capacity of communications channels with 1-bit quantization and oversampling at the receiver," *IEEE Sarnoff Symposium (SARNOFF)*, 2012.

[52] T. Koch and A. Lapidoth, "At low SNR, asymmetric quantizers are better," *IEEE Transactions on Information Theory*, vol. 59, no. 9, pp. 5421–5445, Sept. 2013.

[53] A. Mezghani and J. A. Nossek, "Capacity lower bound of MIMO channels with output quantization and correlated noise," *IEEE International Symposium on Information Theory Proceedings (ISIT)*, 2012.

[54] B. Ristic, S. Arulampalam, and N. Gordon, *Beyond the Kalman Filter*. Artech House Publishers, 2004.

[55] "NAVSTAR GPS Space Segment/Navigation User Interfaces," IS-GPS-200, Rev. D, ARINC Engineering Services, El Segundo, CA, 2004.

[56] B. Kedem, *Binary Time Series (Lecture Notes in Pure and Applied Mathematics)*. New York: Marcel Dekker, 1980.

[57] M. Sinn and K. Keller, "Covariances of zero crossings in Gaussian processes," *Theory of Probability and Its Applications*, vol. 55, no. 3, pp. 485–504, 2011.
[58] A. Mezghani, "Information-theoretic analysis and signal processing techniques for quantized MIMO communications," Ph. D. dissertation, TU München, Munich, Germany, 2015.
[59] M. Sankaran, "On an analogue of Bhattacharya bound," *Biometrika* vol. 51, no. 1/2, pp. 268–270, 1964.
[60] R. G. Jarrett, "Bounds and expansions for Fisher information when the moments are known," *Biometrika* vol. 71, no. 1, pp. 101–113, 1984.
[61] H. Kobayashi, B. L. Mark, and W. Turin, *Probability, Random Processes, and Statistical Analysis*. Cambridge University Press, 2011.
[62] V. Berisha and A. O. Hero, "Empirical non-parametric estimation of the Fisher information," *IEEE Signal Processing Letters*, vol. 22, no. 7, pp. 988–992, Jul. 2015.
[63] P. Stoica and P. Babu, "The Gaussian data assumption leads to the largest Cramèr-Rao bound," *IEEE Signal Processing Magazine*, vol. 28, pp. 132–133, May 2011.
[64] S. Park, E. Serpedin, and K. Qaraqe, "Gaussian assumption: The least favorable but the most useful," *IEEE Signal Processing Magazine*, vol. 30, pp. 183–186, Apr. 2013.
[65] K. Pearson, "Mathematical Contributions to the Theory of Evolution. XIX. Second Supplement to a Memoir on Skew Variation," *Philosophical Transactions of the Royal Society A*, vol. 216, pp. 429–457, 1916.
[66] J. E. Wilkins, "A note on skewness and kurtosis," *Annals of Mathematical Statistics*, vol. 15, no. 3, pp. 333-335, 1944.
[67] A. J. Stam, "Some mathematical properties of quantities of information," Ph.D. dissertation, TU Delft, Delft, Netherlands, 1959.
[68] P. J. Huber, "Robust statistics: a review," *Annals of Mathematical Statistics*, vol. 43, no. 4, pp. 1041–1067, 1972.
[69] D. E. Boekee, "A generalization of the Fisher information measure," Ph. D. dissertation, TU Delft, Delft, Netherlands, 1977.
[70] E. Uhrmann-Klingen, "Minimal Fisher information distributions with compact-supports," *Sankhyā: Indian J. Stat.*, vol. 57, no. 3, pp. 360-374, Oct. 1995.
[71] V. Živojnović, "Minimum Fisher information of moment-constrained distributions with application to robust blind identification," *Elsevier Signal Process.*, vol. 65, no. 2, pp. 297 – 313, Oct. 1998.
[72] J. F. Bercher and C. Vignat, "On minimum Fisher information distributions with restricted support and fixed variance," *Elsevier Information Sciences*, vol. 179, no. 22, Nov. 2009.
[73] C. Rapp, "Effects of HPA-nonlinearity on a 4-DPSK/OFDM-signal for a digital sound broadcasting signal," *Second European Conference on Satellite Communication*, pp. 179–184, Belgium, 1991.
[74] S. Medawar, P. Handel, and P. Zetterberg, "Approximate maximum likelihood estimation of Rician K-factor and investigation of urban wireless measurements," *IEEE Transactions on Wireless Communication*, vol. 12, no. 6, pp. 2545–2555, Jun. 2013.
[75] C. Tepedelenlioglu, A. Abdi, and G. B. Giannakis, "The Ricean K factor: estimation and performance analysis," *IEEE Transactions on Wireless Communication*, vol. 2, no. 4, pp. 799–810, Jul. 2003.
[76] K. Barbé, W. Van Moer, and L. Lauwers, "Functional Magnetic Resonance Imaging: An improved short record signal model," *IEEE Transactions on Instrumentation and Measurement*, vol. 60, no. 5, pp. 1724–1731, May 2011.

[77] L. P. Hansen, "Large sample properties of generalized method of moments estimators," *Econometrica*, vol. 50, no. 4, 1982.

[78] K. Pearson, "Contributions to the mathematical theory of evolution," *Philosophical Transactions of the Royal Society London*, vol. 185, pp. 71-110, 1894.

[79] A. K. Bera and Y. Bilias, "The MM, ME, ML, EL, EF and GMM approaches to estimation: A synthesis," *Elsevier Journal of Econometrics*, vol. 107, no. 1–2, pp. 51–86, 2002.

[80] A. V. Oppenheim, A. S. Willsky, and S. Hamid, *Signals and Systems*, 2nd Edition, *Prentice Hall*, 1996.

[81] J. B. Thomas, *Introduction to Statistical Communication Theory*. Hoboken, NJ: John Wiley & Sons, 1969.

[82] A. Papoulis, *Probability, Random Variables, and Stochastic Processes*. Third edition, *McGraw-Hill*, 1991.

[83] J. Choi, J. Mo, and R. W. Heath, "Near maximum-likelihood detector and channel estimator for uplink multiuser massive MIMO systems with one-bit ADCs," *IEEE Transactions on Communications*, vol. 64, no. 5, pp. 2005–2018, May 2016.

[84] S. Jacobsson, G. Durisi, M. Coldrey, U. Gustavsson, and C. Studer, "One-bit massive MIMO: Channel estimation and high-order modulations," *IEEE International Conference on Communication Workshop (ICCW)*, London , 2015, pp. 1304-1309.

[85] E. Björnson, M. Matthaiou, and M. Debbah, "Massive MIMO with non-ideal arbitrary arrays: Hardware scaling laws and circuit-aware design," *IEEE Transactions on Wireless Communications*, vol. 14, no. 8, pp. 4353–4368, Aug. 2015.